Identifying the mechanisms of antidepressant drug action in mice lacking brain serotonin

D I S S E R T A T I O N

zur Erlangung des akademischen Grades

doctor rerum naturalium

(Dr. rer. nat.)

eingereicht an der

Lebenswissenschaftlichen Fakultät der Humboldt-Universität zu Berlin

von

Markus Petermann

Präsidentin

der Humboldt-Universität zu Berlin

Prof. Dr.-Ing. Dr. Sabine Kunst

Dekan der Lebenswissenschaftlichen Fakultät

der Humboldt-Universität zu Berlin

Prof. Dr. Bernhard Grimm

Gutachter

1. ***Prof. Dr. Michael Bader***
2. ***Prof. Dr. Rüdiger Krahe***
3. ***Prof. Dr. Golo Kronenberg***

Tag der mündlichen Prüfung: 08. Januar 2021

https://doi.org/10.18452/23035

Dedicated to Sven, Rike & Theresa

Eidesstattliche Erklärung zur Selbstständigkeit

Hiermit erkläre ich, dass ich die vorliegende Arbeit selbstständig und nur unter der Verwendung der angegebenen Quellen und Hilfsmittel angefertigt habe. Alle Materialien oder Dienstleistungen, die ich von Dritten erhalten habe, sind als solche gekennzeichnet.

Ich versichere, dass ich mich nicht anderswertig um einen Doktorgrad beworben habe oder einen entsprechenden Doktortitel bereits besitze.

Die Promotionsordnung der Lebenswissenschaftlichen Fakultät (Stand 5. März 2015) der Humboldt-Universität zu Berlin ist mir bekannt.

_____

Markus Petermann Berlin; 01. September 2020

Summary

Serotonin is well-known as the "molecule of happiness" and the most important target for antidepressants. The mainly prescribed drugs in major depression are selective serotonin re-uptake inhibitors (SSRI); but recently, SSR-enhancer (SSRE) have also attracted clinical attention. However, only a quarter of patients responds to treatment and research into the drug mechanisms revives. It needs to be determined, whether SSRI/E act solely via manipulating serotonin levels or whether other pathways are involved, e.g. neurotrophic signaling (brain-derived neurotrophic factor, BDNF) or the hypothalamus-pituitary-adrenal (HPA)-axis. Furthermore, in major depression, dysregulation of central serotonin signaling is accompanied with a decline in hippocampal neurogenesis, as has been observed in rodent models. Therefore, to elucidate the interplay of serotonin, BDNF, adult neurogenesis and the HPA-axis is of importance.

At the center of this thesis is a mouse model deficient in the central serotonin-synthesizing enzyme, tryptophan hydroxylase 2 (*Tph2*$^{-/-}$ mice). Using molecular biology tools, treatment, and behavioral paradigms, I have investigated physiological responses to antidepressant treatment in the absence of brain serotonin, and the possible role of alternative pathways. I observed the typical increase in neurogenesis upon SSRI treatment in WT mice, while it had no effect in *Tph2*$^{-/-}$ mice. In contrast, BDNF levels were significantly decreased in *Tph2*$^{-/-}$ mice after treatment with no effect in WT control mice. Furthermore, my results show a critical role of brain serotonin in the neurobiological effects of electroconvulsive seizure. Surprisingly, in animals lacking central serotonin, increased neurogenesis was observed independently of the treatment. The gathered data indicated an altered stress response; therefore, parameters of the HPA-Axis have been studied, indicating a downregulated HPA system in *Tph2*$^{-/-}$ animals in baseline state, but showed no difference in treatment or feedback control.

This thesis gives insight into the mechanisms of antidepressant action and reveals ideas for novel pathways involved in the process that could be used as targets in therapeutic approaches and further research in major depression.

Zusammenfassung

Serotonin ist bekannt als das "Glückshormon" und gilt als Hauptangriffsstelle der heute gängigsten Antidepressiva. Die am häufigsten verschriebenen Medikamente bei schweren Depressionen sind selektive Serotonin-Wiederaufnahmehemmer (SSRI). Dennoch erzeugten aufgrund guter Verträglichkeit im letzten Jahrzehnt aber auch SSR-Enhancer (SSRE) klinische Aufmerksamkeit. Nur etwa ein Viertel der Patienten sprechen auf therapeutische antidepressive Behandlungen an, weswegen eine große Notwendigkeit des Verständnisses ihrer Wirkungsweisen besteht. Es bleibt offen, ob SSRI / E ausschließlich über die Manipulation des Serotoninspiegels wirken, oder ob alternative Signalwege daran beteiligt sind. Ansatzpunkte hierfür sind beispielsweise die neurotrophen Signalwege (besonders *Brain derived neurotophic factor*, BDNF) oder die Hypothalamus-Hypophysen-Nebennieren- (HPA) – Signalwege des Stressachsensystems. Ebenfalls wurde in Nagetiermodellen beobachtet, dass mit der Dysregulation des zentralen Serotoninsystems bei schweren Depressionen, ein Rückgang der Neurogenese im *Gyrus dentatus* des Hippocampus (HC) einhergeht. Übergeordnetes Ziel dieser Arbeit war, das Zusammenspiel von Serotonin, BDNF, adulter Neurogenese und der Stressachse zu untersuchen und zu verstehen. Zentrum meiner Studien ist ein Mausmodell, mit einer genetischen Depletion des zentralen Serotonin-synthetisierenden Enzyms Tryptophanhydroxylase 2 (sog. *Tph2*$^{-/-}$ Mäuse). Mittels genetischer, molekular- und verhaltensbiologischer Experimente wurden die physiologische Reaktionen auf die Behandlung mit gängigen Antidepressiva abhängig von der Abwesenheit von Serotonin untersucht, um mögliche alternative Signalwege aufzeigen zu können. Die bereits bekannte Zunahme der Neurogenese nach SSRI/SSRE-Behandlung wurde in Wildtyptieren beobachtet, während die Therapie in *Tph2*$^{-/-}$ Mäusen keine direkte kausale Wirkung zeigte. Im Gegensatz dazu waren die BDNF-Spiegel in depressionsrelevanten Hirnregionen in *Tph2*$^{-/-}$ Mäusen nach SSRI Therapie, signifikant verringert, jedoch nicht in ihren WT-Kontroll-Mäusen. Darüber hinaus zeigen meine Ergebnisse eine neurobiologische Relevanz von Serotonin im ZNS, bei den antidepressiven Wirkungsweisen einer Elektrokonvulsiven Krampftherapie (ECT / ECS). Ebenfalls deuten erhöhte Neurogeneseraten bei lebenslanger Abwesenheit von Serotonin im ZNS, unabhängig von der Therapiemethode, möglicherweise auf eine modulierte Stressreaktion hin. Untersuchungen der Parameter des HPA-Stressachsensystems, wiesen auf einen grundlegend veränderten Stresshormonspiegel in *Tph2*$^{-/-}$ Mäusen hin. Somit ermöglicht meine Arbeit weitere Einblicke in Wirkmechanismen gängiger antidepressiver Behandlungen und bietet Ansatzpunkte für weitere therapeutische Ansätze und Forschungen von Depression.

1 Introduction

1.1 Major depressive disorder

> *"In depression this faith in deliverance, in ultimate restoration, is absent. The pain is unrelenting, and what makes the condition intolerable is the foreknowledge that no remedy will come- not in a day, an hour, a month, or a minute. If there is mild relief, one knows that it is only temporary; more pain will follow."*
>
> *– William Styron, Darkness Visible: A Memoir of Madness* [1]

These words written by William Styron, in the 90's of the last century outing himself in his memoir as mentally ill, sound frightening and familiar to many other patients suffering from major depressive disorder (MDD). In his book [1], Styron writes about MDD, a mood disorder that came more and more into clinical focus over the recent years. Not only is it the most common mental health disorder globally, but also the "world's burden of disease" with the most years lost to disability (YLD) in a lifetime per person (76.4 mil. Years / 10.3 % of all total years lost to disabilities and diseases worldwide) – even before the common back and neck pain (Figure 1) [2–5].

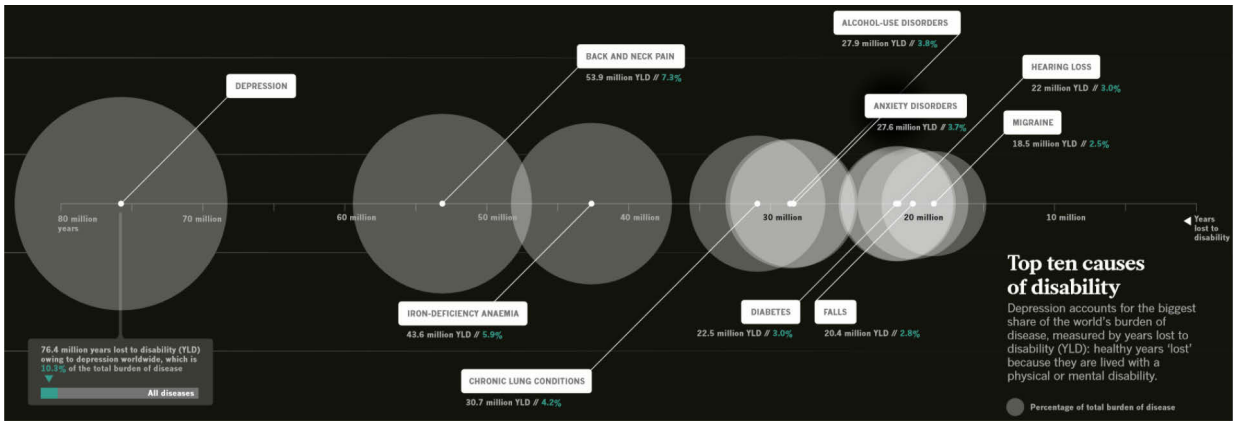

Figure 1 Top ten causes of disability: "Depression accounts for the biggest share of the world's burden of disease, measured by years lost to disability (YLD, white line in the middle): healthy years "lost" because they are lived with a physical or mental disability", taken and modified from "A world of depression" in Nature 2014 [3].

1.1.1 Definition and historical development

Depressive disorders were the fourth leading cause of disability in 2005 and the third leading cause of disability in 2015 and the trend is increasing, as WHO predicts it to be the second leading cause until 2022. The increasing population growth and ageing is stated as a cause for this rise [2,4,6–8]. MDD shows a lifetime risk of 1 in 6 for individuals in all countries worldwide. In 2010, it was accounted to a global prevalence of 298

million cases (4.1-4.7 % disease modeling meta-regression [9]), higher in women with 5.0 %–6.0 % (187 million cases) than in male (3.0 %–3.6 %; 111 million cases) and occurs mostly during working age of 15 to 64 years with a peak in the twenties (Figure 2). The global occurrence of depressive disorders such as MDD but also dysthymia – a milder but more chronic from of depression – has increased by 37.5 % between 1990 and 2010 [2].

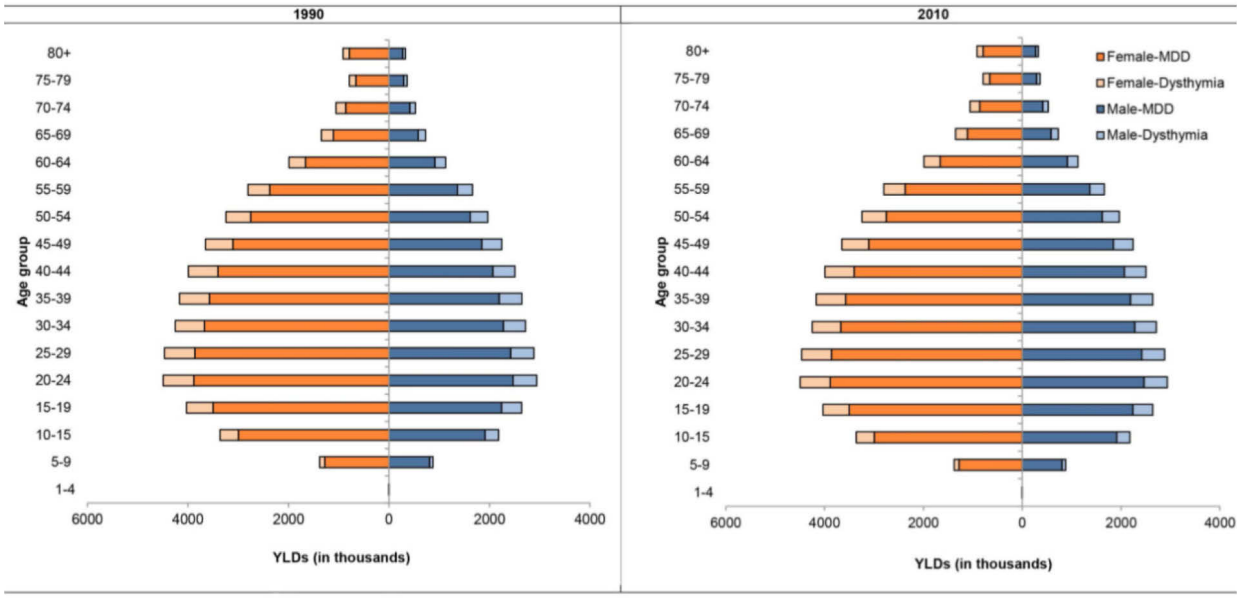

Figure 2 Years lost to disabilities (YLDs) by age and sex for MDD and dysthymia in 1990 and 2010 [2]

An epidemiology study from 2013 across different countries by Kessler and Bromet [10] shows that lifetime rates of depressive episodes, the characteristically course of major depression, are higher in the developed world (15 %) compared to the developing world (11 %), spanning a range from 1.0% (Czech Republic) to 16.9 % (US), with midpoints at 8.3 % (Canada) and 9.0 % (Chile). A respective explanation is that in countries with a higher gross domestic product, the availability of a professional psychiatrist / psychologist is better, so more individuals suffering from mood disorders can be diagnosed, whereas in countries with an obstructed health care system, people suffering from depression might not be declared as such or are not socially accepted and therefore have not been counted [10].

Going one step back in the antique era, today's depression was known as "*Melancholia*" – first defined by Hippocrates. In ancient Greece, patients were diagnosed as melancholic with "*fears and despondencies, if they last a long time*" or as "*dull or stern; dejected or unreasonably torpid, without any manifest cause*". Often it was linked to an excess or deficiency of any of four distinct bodily fluids in a person – the

humors [11,12]. This traditional medical system – *the humoralism* – is one of the pillars of the today's physiology and still lasts until the modern age. Serotonin, a known major player in depression today, was accounted to the neurohumors in the 1950's [13]. In the 11th century, the Persian physician Avicenna described in his book "*The Canon of Medicine*", melancholia as a depressive type of mood and linked it to phobias [14]. A further milestone was the book "*The Anatomy of Melancholy*" by the English scholar Robert Burton in 1621. He brought up first therapy methods to treat melancholia including a healthy diet, sufficient sleep, music, "meaningful work", and sharing the problems with the relatives [15].

The currently used term 'depression' originates from the Latin verb *deprimere*, (pressing down), often linked to an emotional state, and is in use since the 17th and 18th century, when it finally appeared in medical dictionaries (used to describe a mood disorder with a lower emotional state by the French psychiatrist Louis Delasiauve in 1856). The term melancholia was successfully eliminated, since it was "invented by authors, not possessed by the medical field and therefore improper" (Adolf Meyer, 1904) [16].

In the 20th century, Sigmund Freud, inspired by the work of Adolf Meyer, argued that "melancholia could result from a decline or loss of self-perception" [17]. In 1952, depression was included in the Diagnostic and Statistical Manual of Mental Diseases, DSM-I (1952) named as depressive reaction and later in DSM-II (1968) as depressive neurosis. In the latter, depression was defined as an excessive reaction to internal conflicts or an identifiable event [18]. The German psychiatrist Karl Kleist defined the difference between unipolar and bipolar depression, since the term manic-depression refer just to the bipolar disorder before the 1970s [19]. The term MDD today was coined by a group of US clinicians in the mid-1970s as part of proposals for the Research Diagnostic Criteria collection [20], to allow diagnoses to be consistent in psychiatric research between Europe and US and so got incorporated into the DSM-III [21]. MDD was also inserted into the International Classification of Diseases and Related Health Problems, ICD-10, with the same diagnostic threshold as DSM, but declared as a mild depressive episode (MDE), adding higher threshold categories for moderate and severe episodes [22,23].

1.1.2 Hypothesis of Depression

> *"Doctors put drugs of which they know little into bodies of which they know less for diseases of which they know nothing at all."*
>
> *— Voltaire*

This quote reflects the ethical discrepancy we are facing today: mechanisms of mental disorders are not well understood to treat them accordingly and current medications have side effects or insufficient outcome. So, during the times of *melancholia* and *depression* research many hypotheses for depression have been given. Current therapy approaches to target depression are far from optimal, due to lack of understanding the underlaying mechanisms, but also due to missing respective biomarkers. At 1970, the "*monoamine hypothesis"* came up, one of the first concrete hypothesis of depression [24]. It was found that the brain monoamines serotonin, dopamine, and noradrenaline are decreased in their extracellular synaptic concentrations in the depressive states of MDD. Since it was one of the first concrete hypothesis, the most current antidepressants have been developed according to it, e.g. selective serotonin reuptake inhibitor (SSRI) [24,25]. Since then, the monoamine serotonin is known as the "molecule of happiness"; it seems natural that with increased levels of serotonin arises joy – with decreased levels comes depression.

In extension to the monoamine hypothesis of depression, other theories include a deficiency of overall neuroplasticity and cellular resilience. In this "*neurotrophin hypothesis of depression*" antidepressant therapies normalize the impairment of neuroplasticity [26–28], that is functional and structural adaptations of various brain areas, targeting its major player, neurotrophins, especially BDNF. Current theories of depression include impaired regulation of the hypothalamic-pituitary-adrenal (HPA) axis, as part of the endocrine system, and name it: "Neuro-endocrine symptom of depression" [28].

1.2 Monoamine Hypothesis of Depression

1.2.1 The monoamine serotonin and its historical relevance

The existence of serotonin was already hypothesized in the middle of the 19th century as a substance in the blood modulating the cardiovascular system [29]. It took nearly a century until 5-hydroxytryptamine, (5-HT due to the hydroxyl-group at the fifth position within the heterocyclic indole structure of the tryptamine), was found and isolated by scientists from the groups of Page and Green in 1948. It was characterized as hormone from the serum, having a „tonic" vasoconstrictive effect on vessels, being released while the blood is coagulating [30], and therefore called „sero-tonin" (*serum-tonic*). Additionally in 1952, the team of Erspamer and Asero [31] independently identified a substance they called *enteramine* from gastrointestinal enterochromaffin cells (EC), but later found to be structural identical to the serotonin found by Page and Green [31]. In the following decades, research has identified its location, synthesis and the effects in the periphery, while in 1953, Twarog and Page discovered serotonin in the central nervous system (CNS) [32]. This opened an important new chapter in neuroscience, and still challenges a plethora of scientists worldwide [32]. With the discovery of its synthesis and degradation pathways [33,34], the door opened to develop a variety of drugs targeting the serotonin system. In the 1950s, it was shown that lysergic-acid-diethylamide, known as LSD, could antagonize serotonins effects in the rat uterus [35]; unraveling the role of serotonin in certain mental disorders and its neurophysiology could be revealed starting by Wooley and Shawn from 1954 on [36–39]. Furthermore, serotonin was first made visible 1956 via a fluorometric method, enabling the qualitative localization of the monoamine in different brain areas [40]. Later on, the inhibitory action of serotonin on synaptic transmission was revealed; the first step to declare serotonin as neurotransmitter [13]. These are some of the milestones, which led to today's opinion that alterations in brain serotonin cause pathogenic mechanisms leading to mental disorders like MDD [24].

1.2.2 Serotonin biosynthesis and metabolism

The biosynthesis of serotonin starts with L-tryptophan (Trp), an essential α-amino acid that must be obtained with diet [41]. In the serotonin synthesis pathway (Figure 3), Trp is initially hydroxylated by the rate-limiting enzyme Tryptophan-hydroxylase (TPH) to 5-hydroxytryptophan (5-HTP) [42], in the presence of cofactors such as non-heme Fe^{2+} ions, O_2, NADH and tetrahydrobiopterin (BH_4) needed for the hydroxylase reaction.

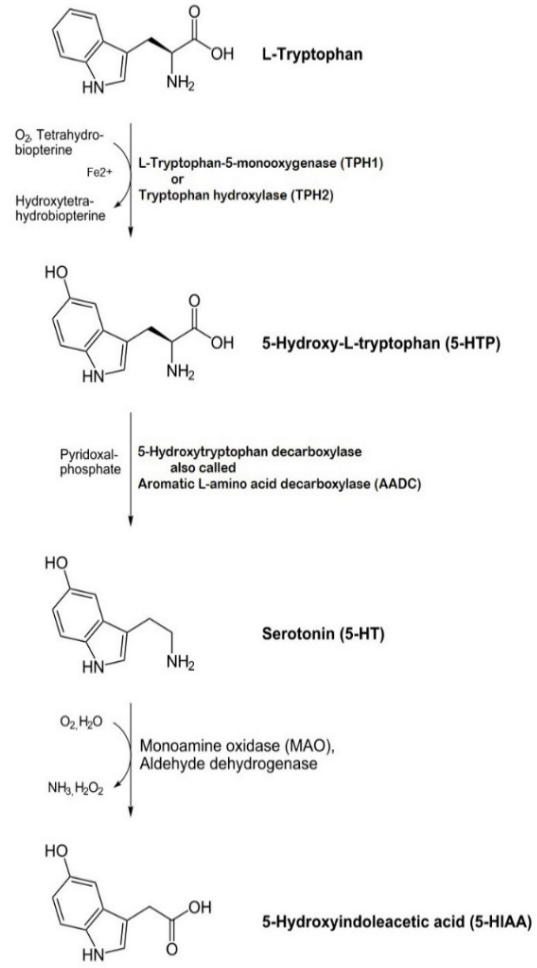

Figure 3 Serotonin biosynthesis and metabolism.

The reaction of TPH can be inhibited by para-chlorophenylalanine (PCPA), being able to penetrate the blood brain barrier (BBB) [43–46]. Serotonin is finally synthesized in a second step by decarboxylation of 5-HTP by Hydroxytryptophan decarboxylase (DDC; also called 5-amino acid decarboxylase, AADC), and its coenzyme Pyridoxal-5-phosphate (P5P / Vitamin B6). AADC is broadly expressed in monoaminergic and other cells, and together with P5P, it decarboxylates other molecules, important for neuromodulation, e.g. L-3,4-dihydroxyphenylalanine (L-dopa) to dopamine [47–49], L-phenylalanine to phenethylamine, L-tyrosine to tyramine, L-histidine to histamine, and L-tryptophan to tryptamine [50]. AADC can be inhibited by 3-hydroxybenzylhydrazine dihydrochloride (NSD), which also crosses the BBB, leading to the accumulation of 5-hydroxytryptophan (5-HTP) and can therefore be used to asses serotonin synthesis rate [51].

Serotonin is degraded intracellularly by a combination of the enzyme monoamine oxidase A (MAO-A), MAO-B and aldehyde dehydrogenase (AD) to 5-hydroxyindole acetic acid (5-HIAA) and is excreted in the urine. 5-HIAA can be monitored as a surrogate of serotonin levels, with 24 hour urinary collection [52]. MAO's two isoforms MAO-A and MAO-B, are flavoproteins expressed ubiquitously in the serotonin systems, as well as endothelial and liver cells at the outer mitochondria membrane [53].

1.2.3 Peripheral serotonin

With the discovery of the two Tph isoforms in 2003 [54], body serotonin systems are distinguished in peripheral and central serotonin signaling. Peripheral serotonin is said to be largely synthesized by Tph1, expressed in enterochromaffin cells in the bowels. These cells within the largest endocrine tissue, the gastrointestinal (GI) epithelium mucosa are specialized enteroendocrine cells (EC) synthesizing and secreting between 90 % and 95 % of total peripheral body serotonin. Tph1 is also expressed in the pineal gland, spleen, and thymus. In humans the *Tph1* and *Tph2* genes, are located on chromosomes 11 and 12, respectively [55]. Even though the spatial separation of Tph2 mostly to the brain, it can be found and expressed in the periphery and takes a minor part in the serotonin production in intestinal neurons, mammary glands [56–59], adipose tissue [60] and pancreatic islets [61]. After serotonin synthesis, its storage happens in secretory granules of blood platelets by the action of vesicular monoamine transporter 2 (VMAT2), which is secreted into extracellular space by exocytosis. Extracellularly, serotonin signals through receptors and is reup-taken by the serotonin transporter (SERT / SLC6A4), in periphery mostly by epithelial cells, smooth muscle cells and platelets [62]. The pleiotropic bioamine serotonin shows a broad range of functions in the body, and all its vast effects are not fully discovered yet. Some peripheral serotonin-dependent functions are:

- Gi / colon motility *[63]*
- Platelet aggregation *[64,65]*
- Vasoactive and cardio-physiological effects *[66–68]*
- Heart development *[67,69]*
- Fetal development *[70]*
- Regulation of bone density *[71,72]*
- Inflammatory cytokine production *[65,73]* (in connection to MDD *[74]*)
- Liver regeneration *[75]*
- Glucose homeostasis *[76]*
- Pain perception and response *[77–79]*
- Lipid metabolism and browning of white adipose tissue *[60,76,80,81]*

1.2.4 The neurotransmitter serotonin

Serotonin is a hormone, neurotransmitter and modulator, signaling a vast amount of effects through 13 G-protein coupled receptors and one ion channel that are distributed throughout the PNS and CNS and the peripheral organs [82]. Physiological function include [83,84]:

- Development
- Eating
- Reward
- Bone mass
- Energy homeostasis
- Thermoregulation
- Circadian rhythm
- Cardiovascular regulation
- Emotion
- Bowel motility and vomiting
- Locomotion
- Pain
- Reproduction
- Memory
- Cognition
- Aggressiveness
- Responses to stressors
- Mood

So impaired serotonin signaling contributes to multiple diseases and disorders [84]:

- Alzheimer's disease [85]
- Irritable bowel syndrome [87]
- Restless legs syndrome [89]
- Sudden infant death syndrome [91]
- Autism [93]
- Anxiety [96–98]
- Affective disorders [100]
- Obsessive-compulsive disorder (OCD) [101]
- Anorexia and bulimia nervosa [86]
- (cluster) Migraine [88]
- Insomnia [90]
- Serotonin syndrome [92]
- Schizophrenia [94,95]
- Parkinson's disease [99]
- Depression

1.2.5 Neuroanatomy of the serotonin system in mouse and human brain

Serotonergic neurons are located in the brain stem raphé nuclei; around 300.000 human and 20.000 rodent serotonergic neurons exist in nine raphé nuclei [102], from where they project via a widespread network with their axonal endings throughout the whole brain [84]. The nuclei are clustered in pairs in rostral and caudal parts of the brain [103–105].

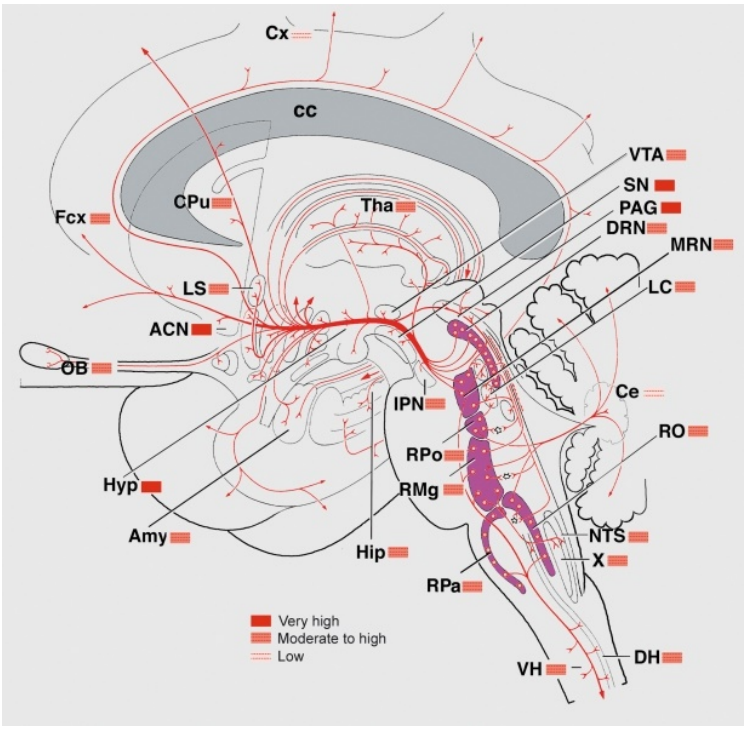

ACN	*Accumbens nucleus*
Amy	*Amygdala*
Cc	*Corpus callosum*
Ce	*Cerebellum*
CPu	*Caudate-putamen*
Cx	*Cortex*
DH	*Dorsal horn spinal cord*
DRN	*Dorsa raphé nucleus*
Fcx	*Frontal cortex*
Hip	*Hippocampus*
Hyp	*Hypothalamus*
IPN	*Interpeduncular nucleus*
LC	*Locus coeruleus*
LS	*Lateral septum*
MRN	*Median raphé nucleus*
NTS	*Nucleus of the solitary tract*
OB	*Olfactory bulb*
PAG	*Periaqueductal gray*
RMg	*Raphé magnus nucleus*
RO	*Raphé obscurus nucleus*
Rpa	*Raphé pallidus*
RPo	*Raphé pontis nucleus*
SN	*Subtantia nigra*
Tha	*Thalamus*
VH	*Ventral horn*
X	*Dorsal motor n of the vagus nerve*
VTA	*Ventral tegmental area*

Figure 4 Schematic sagittal view of the human brain showing the distribution of the serotonergic systems. The raphé nuclei containing most of the serotonergic cell bodies appear in purple, projecting serotonergic axons in red and main terminal nuclei / areas are indicated in red colored innervation density boxes. On the left, a list of areas the serotonergic nerves are projecting in (Figure and text adapted from [84]).

The nuclei are clustered in pairs in rostral and caudal parts of the brain [103–105]: Raphe pallidus (RPa, B1), raphe obscurus (RO, B2), raphe magnus in the ventrolateral medulla (RM, B3), and raphe pontis in the central gray of the medulla oblongata (RPo, B4), with their axons reaching into spinal cord and cerebellum, regulating autonomous somatosensory and motor activity [84,105–107]. The rostral group in pons and midbrain includes the dorsal raphe (DRN, B6 and B7) and median raphe nuclei (MRN, B5, B8 and B9) [106], with fiber projections to the forebrain affecting emotion, perception, cognition and memory. DRN mainly innervate the striatum, amygdala and ventral HC, while MRN project to septum and dorsal HC [105]. (Figure 4 for human, Figure 5 for mouse).

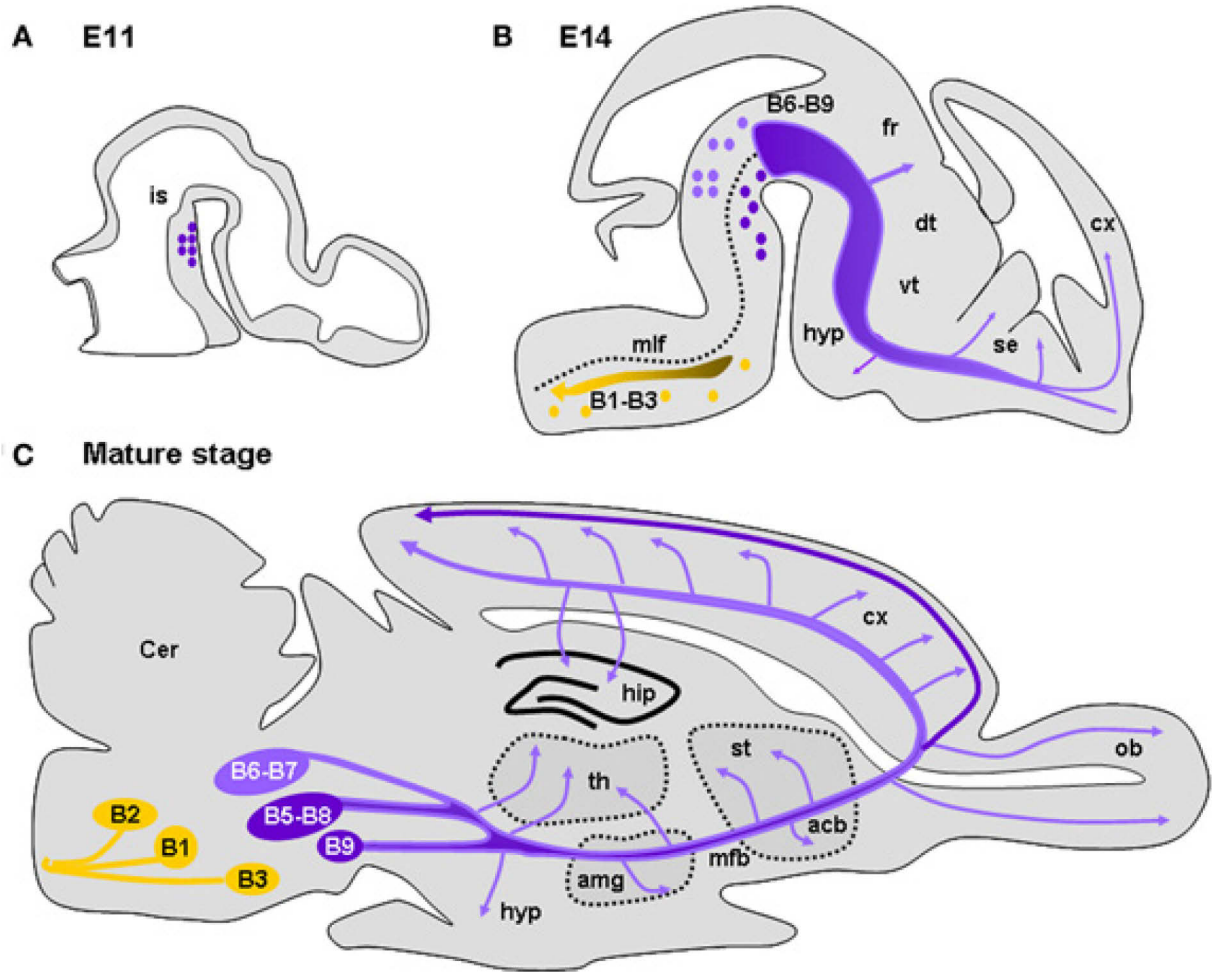

Figure 5 Schematic sagittal view of the developing mouse brain showing the distribution of the serotonergic system and innervation during development. Serotonergic raphé nuclei are indicated from B1-B9. (A) Illustration of a sagittal section of an E11 mouse brain illustrating the position of the developing serotonergic nuclei (purple dots) caudal to the isthmus (is). (B) E15 mouse brain with the nine serotonergic nuclei groups (B1–B9). The caudal group B1-B3 dorsal to the medial longitudinal fasiculus (mlf), sending projections to the medulla, the spinal cord, and the periphery (yellow dots and arrow). The developing rostral group (B6, B7) and the raphé median (B5, B8) send ascending serotonergic innervations destine to the telencephalon and diencephalon (purple dots and arrows). Serotonergic afferents innervating the forebrain travel initially together along the median forebrain bundle (mfb). Arrows indicate regions where axons are seen to deviate from the major ascending pathway: along the fasciculus retroflexus (fr) toward the habenula, in the hypothalamus (hyp), the striatum (st), and the septum (se). (C) Schematic section of the adult mouse brain containing fully developed circuits and nuclei. The caudal group corresponding to raphé magnus (B3), raphé obscurus (B2), raphé pontis (B4) and raphé pallidus (B1) nucleus in the medulla (Yellow dots), innervating the lower brain stem and spinal cord (yellow lines). Rostral group (purple dots) in pons and midbrain including dorsal raphé (B6, B7) and median raphé (B5, B8 and B9), as well as raphé pontis bring their axons to the upper brain stem, accumbens (acc), amygdala (amg) hypothalamus (hip), thalamus (th), striatum (st), olfactory bulb (ob), and cerebral cortex (cx). In the cerebral cortex, layers V and VI receive preferentially afferents arising from the dorsal raphé (light purple) while layer I receives afferents mainly arising from the median raphé (dark purple; Adapted from [104]).

1.2.6 Serotonin-receptors

The TPH2 isoform is the predominant form in the brain [54]. When serotonin is synthesized, it is packed into presynaptic vesicles by mainly the vesicular monoamine transporter (VMAT2) [108] by exploiting a promotor gradient across the vesicular membrane [109]. Serotonin, not stored in vesicles will be degraded by MAO to 5-hydroxyindoleacetic acid (5-HIAA), transported via a unknown mechanism into the cerebrospinal fluid and last secreted via the urine [110].

As soon as a presynaptic action potential arrives, serotonin is released by an exocytotic calcium-dependent mechanism into the synaptic cleft. In the extracellular space, serotonin interacts with the presynaptic auto receptors 5-HT_{1A}, 5-HT_{1B}, and 5-HT_{1D}, causing negative feedback to serotonin vesicle exocytosis [111,112], weakening extracellular serotonin concentration and also further effect stimulation and sensitivity of multiple postsynaptic serotonin receptors: 5-HT_{1A}, 5-HT_{1B}, 5-HT $_{1D,}$ 5-HT_{1E}, 5-HT_{1F}, 5-HT_{2A}, 5-$HT_{2C,}$ 5-HT_{3-7} [113,114]. All but one (5-HT3) are G-protein coupled receptors. 5-$HT1_{A-F}$ and 5-HT_{2A-C} mediate their effects by coupling the Gi/o protein alpha subunit (GNAI) and so inhibiting adenylate cyclase (ADCY) leading to a decrease in cAMP [111]. Another postsynaptic pathway is the activation of phospholipase C (PLC) through coupling to Gq/11 protein alpha (GNAQ), which then catalyzes the formation of myoinositol- 1, 4, 5-trisphosphate (IP3) by cleavage of membrane lipids. IP3 regulates downstream protein kinase C (PKC) activity and diacylglycerol (DAG) [113]. 5-HT_{4-7} are primarily Gs protein α's (GNAS) increasing cAMP by activation of ADCY [115,116]. The amplification of serotonin-dependent second messenger signals, lead downstream to neurotransmitter release from not only serotonergic, but also noradrenergic and dopaminergic neurons causing emotional and behavioral effects. Therefore serotonin receptors are often targets for antidepressants or other pharmaceutical targets of mental disorders [117]. 5-HT_3 is an ionotropic cation-specific ligand-gated ion channel, expressed in PNS and CNS. Its binding of serotonin depolarizes the postsynaptic membrane by sodium influx and potassium efflux. Though 5-HT_3 does not activate a second messenger cascade, its agonistic stimulation leads to decreased synaptic release of acetylcholine (ACh), noradrenaline, and increased the synaptic release of Substance P, GABA and DA [118]. Furthermore, dimerization, chaperone modulation, and different mRNA editing and splicing variants for all serotonin receptors, increase the spectrum of their functionality and effect on the postsynaptic function [82]. A visualized scheme can be seen in Figure 6.

1.2.7 Serotonin transporter

Termination of action of serotonin in the synaptic cleft is task of the serotonin transporter (SERT or 5-HTT), encoding in humans as the solute carrier family 6 (neurotransmitter transporter, serotonin), member 4 (SLC6A4). Released serotonin is transported back into the presynaptic terminals for recycling or degradation via this integral membrane protein. SERT is a member of the sodium-potassium-dependent transporter family where presynaptic re-transport requires a membrane potential created by sodium-potassium adenosine triphosphatase. SERT modulates the ability

of 5-HT_{1A} receptors to inhibit catecholamine release [119]. SERT can be found in the CNS at the axonal synaptic end nodes. The transporter is linked to mental disorders like depression, anxiety, autism and schizophrenia; therefore SERT-targeting pharmaceuticals are often the first treatment choice (e.g. SSRIs, Reviews [93,120,121]). Outside the CNS, SERT is expressed in platelets, pulmonary endothelium, placental epithelia, and other cells that store or transiently release serotonin [122]. (Cyan colored channel in Figure 6)

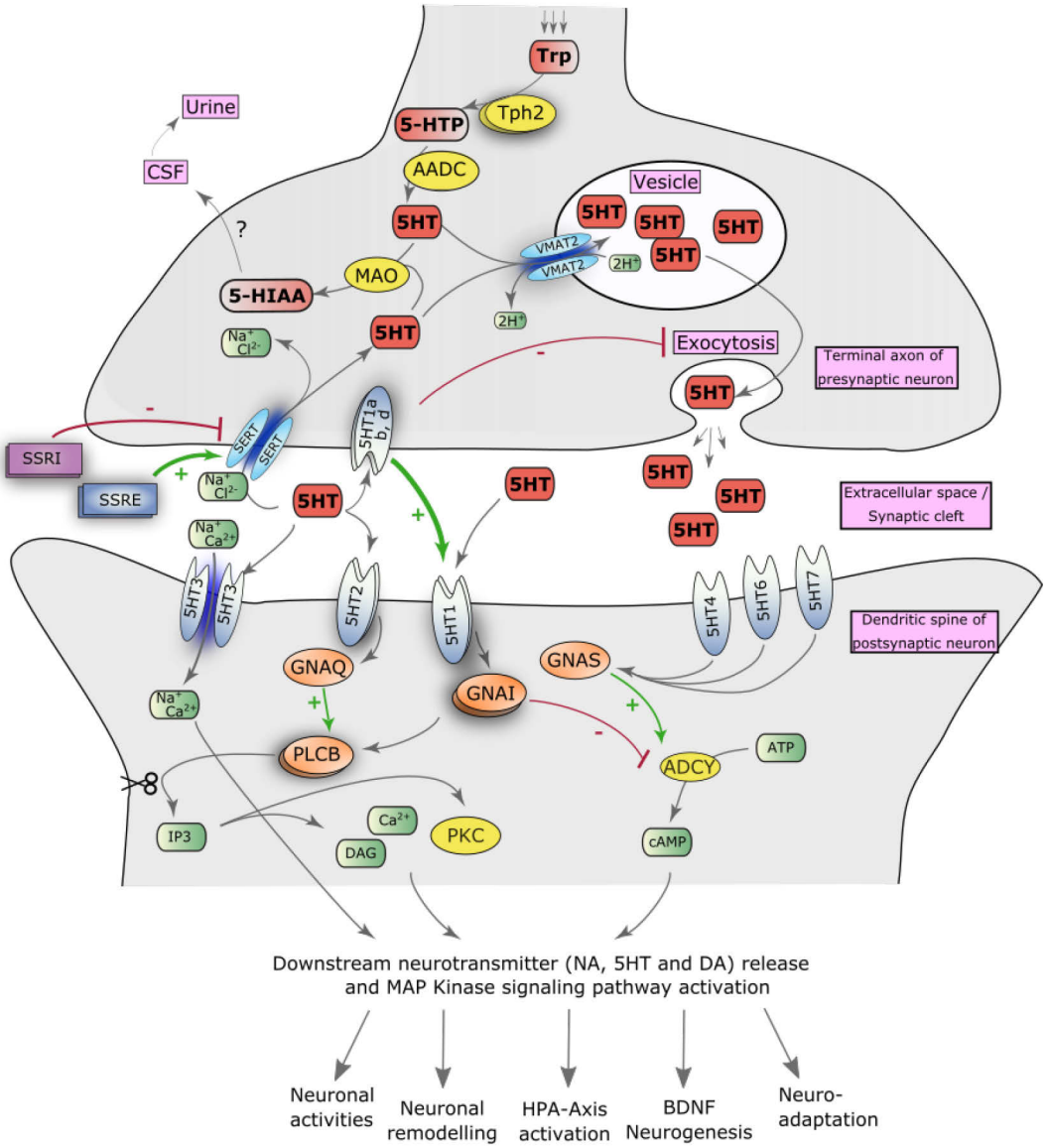

Figure 6 Working mechanisms of the antidepressants SSRI/E in serotonin's synaptic transmission in the CNS. In serotonergic neurons from the raphé nucleus, serotonin (5-HT) is converted from tryptophan (Trp) in the terminal axon, by a 2-step catalytic process by tryptophan hydroxylase 2 (Tph2) and aromatic decarboxylase (AADC). Vesicular monoamine transporter 2 (VMAT2) pumps it into presynaptic storage vesicles, by setting up an electrochemical proton gradient at the vesicle membrane. (Recycled-) Serotonin, not stored in vesicles is degraded by monoamine oxidase (MAO) to 5-hydroxyindoleacetic acid (5-HIAA), transported via an unknown mechanism into the cerebrospinal fluid and last secreted via the urine. Incoming action potentials triggering a calcium dependent exocytotic release of serotonin from presynaptic vesicles into the synaptic cleft. Presynaptic autoreceptors sensitive to serotonin are 5-hydroxytryptamine (serotonin) receptor 1A (5-HT-$_{1A}$), B (5-HT$_{1B}$), and D (5-HT$_{1D}$).Their activation results in a weakening of the 5-HT exocytosis, following lower extracellular serotonin concentrations, further effecting or even sensitizing postsynaptic 5-HT receptor subclasses like 5-HT1 family. Prolonged administration of selective serotonin reuptake inhibitors (SSRI) desensitizes these feedback loops, causing only temporary therapeutic value and delayed onset of action. Postsynaptic dimerized 5-HT $_{1A;B;D,E;F}$ receptors work together with dimerized 5-HT$_{2A,C}$ receptor subtypes in mediating effector signals via activation of second messenger cascades [86] . Postsynaptic 5-HT$_1$ receptor subtypes pathway mainly works via coupling of Gi/o protein alpha subunit (GNAI), resulting in reduced ATP to cyclic AMP (cAMP) turnover by inhibiting adenylate cyclase (ADCY), and activating phospholipase C (PLCB). 5-HT$_2$ receptor subpopulation is sensitizing PLCB through coupling of Gq/11 protein alpha (GNAQ). PLCB which cleaves membrane phospholipids to catalyzes the formation of myoinositol- 1, 4, 5-trisphosphate (IP3) and diacylglycerol (DAG) and mobilizes intracellular calcium and activates PKC. The postsynaptic, ionotropic 5-HT$_3$ receptor is a cation specific ligand-gated ion channel, and this 5-HT activation depolarizes the postsynaptic membrane via Na_2^+ influx and K^+ efflux, influencing the activation of dimerized 5-HT$_2$ receptors. 5-HT$_4$, 5-HT$_6$, and 5-HT$_7$ couple Gs protein alpha (GNAS), which activate ADCY, and therefore raise the cAMP levels. Second messenger signals, like cAMP levels, PKC activation as well as DAG release result in further downstream reactions leading to the mediation of neurotransmitter release from central serotonergic, noradrenergic (NA), and dopaminergic (DA) neurons in the brain by regulating potassium channels, several protein kinases and other calcium dependent signals, as well as transcriptory control by activation of the MAP kinase pathway. The selective serotonin reuptake transporter (SERT) reestablishes homeostasis of serotonergic action in the synaptic cleft, by transporting 5-HT back to the presynaptic terminal axon by Na^+/Cl⁻dependent influx. Selective serotonin reuptake inhibitors (SSRIs) act antidepressant by inhibiting SERT, whereas selective serotonin enhancers (SSRE) promote SERT activity, keeping extracellular 5-HT levels low. Chronic administration of antidepressant treatments have been reported to commonly increase the expression of brain-derived neurotrophic factor (BDNF), an activity-dependent secreted protein that is critical to organization of neuronal networks and synaptic plasticity [93,160]. Second messenger pathways then activate a range of effector systems to change cell behavior; in many cases this includes the regulation of gene transcription. Double layered enzymes and receptors indicate dimers/heteromeres.

1.2.8 Adult Neurogenesis

The monoamine hypothesis of depression–impaired monoamine signaling, mainly of serotonin–has one major issue, which it failed to explain. Antidepressants like SSRI's which increase serotonin concentration have a clinical latency of response of 2-4 weeks; yet, monoamines in the brain are considered to be rapidly effective [123]. Malberg *et al.* [124], showed a possible explanation by increased adult neurogenesis in response to SSRI treatment. In rodents, the generation of new neurons in the HC takes about the same time and is associated with better mood. Furthermore, serotonin plays a role in hippocampal neurogenesis as has been shown by Klempin *et al.* [125,126]. These findings indicate that the rate of adult neurogenesis might be a possible biomarker in depression.

Adult hippocampal neurogenesis occurs in most mammalian brains including humans [127–129]. Adult neurogenesis is the generation of neurons from stem/progenitor cells in restricted regions of the brains, and markedly differs from developmental neurogenesis. It can be made visible by techniques, such as bromodeoxyuridine (BrdU) labeling of DNA- replication in of mitotic cells [130], and immunohistochemistry of certain cell stage markers [131] (Figure 8). The adult rodent brain possesses two main stem cell niches: the sub granular zone (SGZ) of the dentate gyrus (DG) within the HC and the subventricular zone (SVZ) of the lateral ventricle (Figure 7, taken and adapted from [132]).

In the DG neural stem cells (also called radial glia like cells, RGLs and Type 1 cells) give rise to amplified intermediate progenitor cells (Type 2a and b cells) and neuroblasts, which differentiate towards immature neurons, while migrating into the granule cell layer. The last step is the final integration of matured neurons into the existing neural circuits between the CA3 and CA1 region of the trisynaptic circuitry in the HC (Figure

Figure 7 Neurogenic niche microenvironments in the adult organism: In humans the only existing neurogenic niche is the subgranular zone (SGZ) in the hippocampus (left). In mice additionally to the SGZ in the hippocampus, the olfactory bulb (OB) as well as the subventricular zone (SVZ) generate new neurons in adult animals (taken and modified from [132]).

8, adapted from [133] and [134]). Cell proliferation takes two to 24 hours but time for newborn cells to get structurally and functionally integrated takes three to seven weeks [135]. 70–85 % of immature newborn neurons die in the maturation process during the first weeks [136,137]. In adult humans, 700 new neurons/day (with total 1.75 % of annual turnover, measured by ^{14}C method) are generated, but decline during aging [129,138].

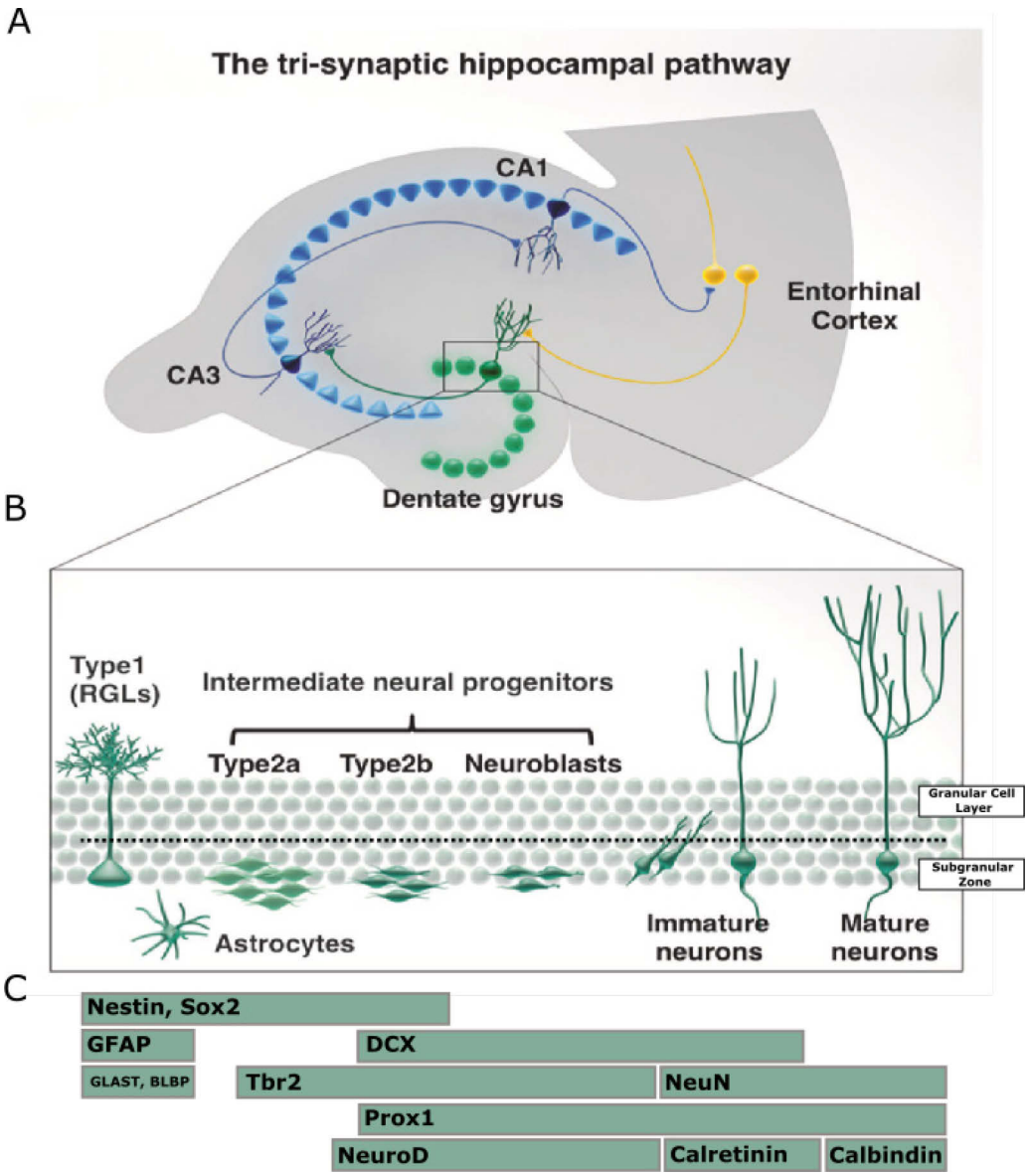

Figure 8 The neurogenic niche microenvironment in humans and mice: Development of adult-born DGCs (b) and the trisynaptic circuitry (a) and their markers (c) in the hippocampus: (a) The trisynaptic neural circuit in the HC from the entorhinal cortex through the DG, CA3 and CA1. (b) Developmental processes of adult hippocampal neurogenesis. Adult neural stem cells in the hippocampus (radial glia-like cells, Type1 cells) differentiate through intermediate progenitors to mature DG neurons, (c) and differ in their marker genes in their intermediate stages: In the radial-glia-like-cells (RGLs, green) or Type1 cells, most dominant markers are glial fibrillary acidic protein (GFAP), the glutamate aspartate transporter (GLAST) and brain lipid binding protein (BLBP). Furthermore, until the Type 2b cell stage of intermediate neural progenitors, RLGs express, the neuroectodermal stem cell marker Nestin, as well as SRY (sex determining region Y)-box 2 (Sox2), which is maintaining self-renewal. In the intermediate neural progenitors, Type 2a cells express eomesodermin also known as T-box brain protein 2 (Tbr2), as well as Nestin and Sox2. Besides Tbr2, in the Type 2b to neuroblast stage, also the neuronal migration protein doublecortin (DCX), the DG-specific Prospero homeobox protein 1 (Prox1), neuronal differentiation transcription factor "Neurogenic differentiation 1" (NeuroD1, β2) are expressed while DCX and Prox 1 are still expressed in immature neurons, firstly neuronal nuclear marker NeuN and calcium binding protein marker calretinin can be used as stage markers. In the final mature stage, most prominent markers are still NeuN and solely for this stage calcium binding protein calbindin-D28k (adapted from [133] and [134]).

In the trisynaptic circuitry, granule cells of the DG are the major source of input of the hippocampal formation, receiving most of their information from the entorhinal cortex (EC). Mossy fiber projections from the granular cells of the DG depolarize downstream cornu ammonis (CA3) pyramidal neurons, which bring information via "Shaffer collaterals" to the CA1 region. From CA1, the trisynaptic circuitry is closed, sending information back to the deep layers of the EC [133] (initially described by Ramón y Cajal [139] and Lorente de No [140]). A major role of the hippocampal trisynaptic formation lies in acquisition and recall of episodic and spatial memories [141]. Adult hippocampal neurogenesis contributes to HC-dependent spatial learning [142], episodic memory [143,144], pattern separation [145–148] and forgetting [149,150]. For learning, forgetting and maintaining a healthy balance in neurogenesis, loss of newborn neurons by programmed cell death helps keeping a self-renewing capacity in the adult brain [151,152].

Adult neurogenesis is stimulated by intrinsic cues [153–156] (steroids and neurotransmitters), and environmental factors [157] and physical exercise [158], but decreases with age [159,160], and is impaired in several pathophysiological conditions, like epilepsy [161] or ischemia [162] and MDD [163] . Promoting adult hippocampal neurogenesis in MDD plays a critical role; with further involvement of the regulation of the hypothalamic-pituitary-adrenal (HPA) axis and corticosterone (CORT) secretion in response to stress [164], in the effects of physical exercise to counter stress [165], and especially in the mechanisms of antidepressant drugs that target the central serotonin system [124].

1.2.9 Serotonin as therapeutic target

Serotonin critically contributes to the SGZ neurogenic niche microenvironment, among other growth factors, hormones, neurotrophins and neurotransmitters regulating cell proliferation and neuronal differentiation. In rodents, the DG has a dense and highly organized serotonergic innervation in hilus (originating from the MRN) and in the molecular layer (originating from the DRN) [126,166–168]. In rats, serotonin modulates excitatory postsynaptic potentials (EPSPs) in dentate granule cells [169]. Studies on initially pharmacological manipulation (injection of 5,7-Dihydroxytryptamine) combined with DG ectomy, gave first modulatory evidence that a decrease in hippocampal serotonin levels correlates with a decline in adult neurogenesis [170,171]. Pharmaceutical inhibition of serotonin synthesis by PCPA, and acute or chronic serotonin depletion also led to a decline in cell proliferation, and the

number of newborn neurons [172]. Still the exact mechanism through which serotonin may affect the neurogenic niches and processes are not yet understood [170,171].

Following serotonin receptor-targeting studies; 5-$HT_{1A + B}$, and 5-$HT_{2A + 2C}$ [182–184] are expressed in the DG niche [185] with 5-HT_{1A} receptor immunoreactivity on type-1 to type-2b cells [186], and 5-HT_{2C} receptors in adult granule cells [187]. While 5-HT_{2C} receptor activation results in an increase in late-stage progenitor cells and early postmitotic neurons, 5-HT_{1A} activation had counteracting effects on DG cell proliferation. Different receptors seem to be necessary to keep homeostasis in the neurogenic niche [187]. 5-HT_4 receptors might also play a role in SSRI-induced adult neurogenesis by reversing the state of maturation in granule cells [188,189]. In 1953 to 1970, important drugs interacting with the serotonin system were discovered (Table 2) [24,33], and summarized into four major classes: tricyclic compounds (TCA), MAO inhibitors (MAOI' s), SSRI, and atypical antidepressant drugs [190]. Invented in the 1950s, tricyclic antidepressants have a broad affinity to receptors, block mainly the re-uptake of both serotonin and noradrenaline [181], with wide side effects. TCAs are approved for treating not only depression, but also obsessive-compulsive disorder, nocturnal enuresis, panic disorder, bulimia, chronic pain, phantom limb pain, chronic itching, and premenstrual symptoms. Although effective, TCAs have largely been replaced by modern antidepressants with less side-effects, like the group of MAOIs that increase levels of monoamines dopamine, noradrenaline, and serotonin by inhibiting their degradation. Still they have plenty of side effects (nausea, dizziness, and sweating) and are toxic in an overdose with some foods and drugs [175]. Prominent commercially atypical drugs are Bupropion (blocks dopamine and noradrenaline reuptake), Mirtazapine (blocks presynaptic adrenergic α2A/C autoreceptor and postsynaptic 5-HT_{2a} receptor) and Trazodone (sedative serotonin reuptake inhibitor and 5-HT_2 receptor antagonist).

Table 1 Commonly used antidepressant drugs manipulating the serotonergic system.

Mechanism of action	Compounds
Vesicular monoamine transporter (VMAT) inhibitor	Reserpine [173], Tetrabenazine [174]
Monoamine oxidase inhibitors (MAOIs) [175]	Pargyline, phenelzine , tranylcypromine, isocarboxazid, hydracarbazine, nialamide
Agonists of 5-$HT_{1A/2A/2C}$ receptors [176]	Lysergic acid diethylamide (LSD)
Aromatic amino acid decarboxylase inhibitor (AADCIs) [177]	Carbidopa, benserazid
Serotonin and norepinephrine reuptake inhibitors(SNRIs) [178]	Venlafaxine, milnacipran, and duloxetine.
Selective serotonin reuptake inhibitors SSRI [179]	Fluoxetine, fluvoxamine, paroxetine, sertraline, vortioxetine and citalopram (escitalopram)
Selective serotonin reuptake enhancers SSRE [180]	Tianeptine
Tricyclic antidepressants [181]	Imipramine, desipramine, amitriptyline, nortriptyline, protriptyline

With the beginning of the new millennium, the anesthetic ketamine provides a promising antidepressant therapy approach, as non-competitive, glutamatergic NMDAR (N-methyl-d-aspartate receptor) antagonist, exerting rapid and sustained antidepressant effects after a single dose, not as usual only after several weeks of treatment. Unfortunately, ketamine is associated with severe side effects up to addiction [191].

1.2.10 Selective serotonin reuptake inhibitors (SSRI)

Current pharmacological therapy of depressive symptoms comprises of SSRIs that attenuate maturation, integration and plasticity of newborn neurons [124,192] and their progenitors [193]. SSRIs are better tolerated and safer in case of an overdose than TCA's and MAOI's, and therefore often considered first-line for treating depression; but also, SSR-enhancer (SSRE) such as tianeptine (commercially Stablon), although challenging the traditional monoaminergic hypotheses, gained more attention in the past few years as they show a high tolerability and efficiency in depression therapy [194]. SSRIs represent the biggest group of serotonin modulating drugs , initially started 1987 with fluoxetine (FLX) [195]. Today, 5 compounds are prescribed: fluoxetine (FLX), fluvoxamine, paroxetine, sertraline, and citalopram (CIT; and its enantiomer escitalopram). With 290 mil. daily dosages in 2016 CIT is the most prescribed antidepressant pharmacotherapy in Germany [196]. SSRI vary in their pharmacological profile resulting in differential efficacy or side-effect profile for particular patients [179]. For instance, sertraline is preferred in the acute phase treatment of major depression but generally associated with a higher rate of participants experiencing diarrhea [197]. Nevertheless, efficacy and acceptability are still higher than in atypical antidepressants. Considering the half-life: CIT, paroxetine, fluvoxamine and sertraline are about 20 hours in the human body, until fully reabsorbed by hepatic pass biotransformation and N-demethylation, whereas FLX is demethylated to norfluoxetine in a similar hepatic pathway and mainly excreted in urine in a long half-life of 2 to 4 days [179].

Pharmaceutical research and development promote SERT as main SSRI target. The antidepressant effect is assumed to be caused by immediate inhibition of serotonin re-uptake into the pre-synaptic cell thus increasing serotonin levels in the synaptic cleft (Figure 6). Some SSRIs like FLX (but not CIT), also exert a transient desensitization of 5-HT_{1A} auto-receptors, subsequently lowering negative feedback inhibition. Therefore, chronic treatment induces a re-establishment of the serotonin system by long-term

downregulation of SERT and 5-HT_{1A} auto-receptor activities. However, the exact molecular mechanism still remains unknown [198].

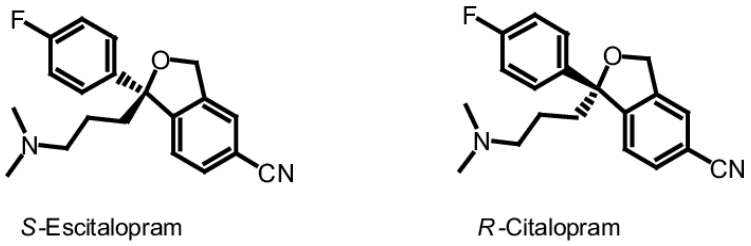

Figure 9 Structures of SSRI enantiomer S-Escitalopram (l) & R-Citalopram (r) [199].

CIT is the flagship therapeutic and first choice in case of certain mental disorders, and clinical research is manifold (>190.000 entries in google.scholar with the search term "citalopram"). With the synthesis of R-Citalopram, comes its eutomer S-Citalopram (mostly known as Escitalopram, Figure 9 [199]). Both act via the typical inhibition of the orthosteric binding site of serotonin in its transporter, and on the allosteric binding site at the residues in the transmembrane domains 10,11, and 12 [200–202], and subsequently decreasing the reuptake of extracellular located "molecule of happiness".

1.2.11 Selective serotonin reuptake enhancer (SSRE)

The SSRE Tianeptine (TIA) is formerly known as the "hypothesis killer", since in contrast to SSRIs, it is enhancing serotonin reuptake, decreasing extracellular serotonin levels in the brain [203,204], and even decreasing number and mRNA expression of SERT sites in the DRN [205]. Clinically, it is nowadays used to treat not only MDD, but also anxiety, asthma, and irritable bowel syndrome. With its racemic, heterocyclic structure, it might be identic to TCAs, but due to its mechanism of action it is considered in the class of the SSREs and has been firstly used in 1960. The drug shows efficacy and tolerability in patients where regular TCA or SSRI do not lead to an response or are not well tolerated [194,206–213]. In rodent stress and depression models, too, efficacy of tianeptine was quantified as good [206,214–219]. Nevertheless, its antidepressant effects cannot be fully described; clinical improvement may depend on

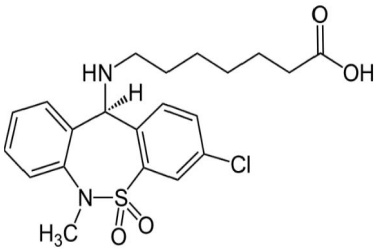

Figure 10 Chemical structure of tianeptine.

other factors, e.g. dopamine, AMPA and NMDA interaction [219]. Glutamate is the major excitatory neurotransmitter, controlling synaptic plasticity, also affecting depressive episodes, stress and anxiety (reviewed in [220–225]). Stress-mediated increases in glutamate efflux in the amygdala can be countered by tianeptine [226], speaking for a glutamatergic-based antidepressant role in stress-induced depression. The SSRE has the capability to oppose the stress and depression induced structural and metabolic changes in the rodent HC [227–232] and amygdala [232–234]. Tianeptine shows no affinity, nor alters concentration and sensitivity/responsiveness for certain neurotransmitter receptors (e.g., 5-HT_1 to 5-HT_7, NMDA, AMPA, kainate, benzodiazepine or GABA-B receptors), except for an increased responsiveness in the α1 adrenergic system [235] (Figure 10).

1.2.12 Electroconvulsive therapy

Becoming widely publicly known from the movie "*one flew over the cuckoo's nest*" (Figure 11), electroconvulsive therapy (ECT, Electro convulsive seizure ECS in rodents) -"Electroshock therapy", has its origin in Europe in the 1930's with focus on therapy in schizophrenia. ECT's value, mechanism of action and research about it, were long neglected since the "Third Reich" used this new shock therapy not only for medical research, but also for "Aktion T4" euthanasia [236,237]. After the end of the second world war up to the 90's, this method was seen controversial and barely used. With this millennium, ECT returns to popularity and is now routinely employed for the efficient therapy of severe and pharmaceutical-resistant MDD, severe catatonia [238], and partly also in severe cases of schizophrenia [239], mania [240], and epilepsy [241]. Efficacy of remission from an uni- and bipolar depression in patients treated with ECT is above 50 % [242,243]. Certain techniques exist; unilateral ECT, with both electrodes on the same side of the patient's head; bilateral ECT, with two electrodes placed on opposite sides. Performed in animals, ECT is called electroconvulsive seizure (ECS).

Figure 11 ECT scene with Jack Nicholson in the movie " One flew over the cuckoo's nest" (1975) directed by Milos Forman / produced by Fantasy Films / distributed by United Artists.

Several hypotheses about the mechanisms of action for an antidepressant effect of ECT exist: Initially, extrinsic seizure was thought to rebalance the number of glial cells in

patients with schizophrenia causing remission from the psychiatric illness [244,245]. In the 1960's, the "Generalized Seizure Theory" claimed, greater generalization of a seizure comes along with stronger brain stem and cortico–thalamic–cortical circuit activation resulting in antidepressant effects [246,247,248]. The antidepressant effect of the "Neuroendocrine–Diencephalic Theory", is restoring neuroendocrine dysfunction of the HPA-axis, stating a disturbed hormonal secretion in MDD [28,249]. ECT reliefs from typical MDD symptoms such as disturbed sleep, appetite, and sexual drive, pointing to a connection to the hypothalamus and endocrine system [250]; ECT induces a release and activation of a plethora of HPA-relevant endocrines and their respective responses [247], such as it elevates plasma concentrations of neuropeptide Y [247,251], corticotropin releasing hormone (CRF) [252,253] and cortisol [254], oxytocin and vasopressin [253,255,256], and prolactin [257]. Still dysregulated in depression, some of these endocrine hormones are debated if really involved in ECT response, nonetheless the endocrine theory is the current most eligible for the mechanisms ECT therapeutic effects [258]. The "Combined Anatomical–Ictal Theory" is similar to the "neurotrophin hypothesis of depression", saying seizure activity in the limbic system induces major neurotrophic pathways crucial for the antidepressant mechanism, e.g. BDNF [259]. Since depression is related to hippocampal volume loss [260–263], increases in both right and left hippocampal volume after ECT have been observed [264], in line with increased neurogenesis in rodents [259,265–270] and primates [271], as well as synaptogenesis [272,273]. In addition, CORT suppressed neurogenesis [156,274] is reversed by ECS [259], even stronger than after pharmaceutical SSRI treatment [124]. ECT induces changes in regional cerebral blood flow and regional glucose metabolism in regions related to MDD [275–277], up-surge in blood pressure resulting in a break in the continuity of the BBB; that leads to certain neuro-chemicals released from circulation to brain parenchyma, inducing increased BDNF levels and changes in angiogenesis and neurogenesis [245,278]. In rodents, ECS experiments have revealed altered expression of various target genes for neuronal plasticity and neurogenesis, e.g. VGEF, NG2, *c-Fos, Egr1, Neuritin 1, BDNF, Gadd45b, Snap29, STEP61, Synapsin I, FGF-1* [245,269,279–283]; and increased neurogenesis in the adult HC itself [124,267,284–288]. Nonetheless ECT/ECS working mechanisms are far from being understood, with a necessity of further research, as depression becomes more and more prevalent in the current epoch.

1.3 Animal models as a tool for researching the serotonin system

In addition to researching on serotonin by pharmacological manipulation of the serotonin system, using agonists and antagonists for different receptors, a variety of mouse models have been generated to study gastrointestinal, cardiovascular, or psychiatric disorders linked to impaired serotonin. Conventional knockout models as well as conditional knock in/out/down models have been developed, e.g., for the 14 serotonin receptors, intracellular transport (VMAT) [289,290], re-uptake (SERT) [290–292], metabolism (MAO) [293,294], and the serotonin neurons development transcription factors *Nkx2.2, PET-1* and *LMX1b* [295] (reviewed [290]). Further tools comprise mouse models with a temporal control of serotonin synthesis by optogenetics [296] (e.g. *Tph2ChR2Yfp-Tg*), inducible *cre*-expression [289,297] or tetracycline-sensitive systems [298,299], relevant for the serotonin system.

1.3.1 Tph2 - deficient mice

After Tph1 and 2 were discovered [54,55], mice depleted in either isoform, or both, have been developed by our group [55,300,301]. *Tph2 KO* mice (*Tph2*$^{-/-}$ mice) are characterized by depletion of serotonin synthesis within the brain [302] (Figure 13 and Figure 12) but the peripheral serotonin system remains unaffected. Serotonin in the brain is absent throughout development; and possible compensatory mechanisms via other neurotransmitter systems cannot be excluded [303]. Earlier characterizations of this model revealed decreased noradrenaline levels [304 305]; in double knockout *Tph1/2* mice, alterations in dopamine levels, and its downstream metabolite homovanillic acid were observed [306]. *Tph2*$^{-/-}$ mice exhibit transient growth retardation during the first six postnatal weeks [302]. Baseline cell proliferation in the dentate gyrus of the HC was unchanged despite serotonin's neuromodulator role [125] (also discussed in results). The full range of physiology and behavior of *Tph2*$^{-/-}$ mice is listed in Table 2 [98,307]. Briefly, in adulthood, *Tph2*$^{-/-}$ mice reveal aggressive behavior, lack of maternal care, and increased despair-like responses [98,307]. This combination of symptoms closely mirrors the clinical features of depressed patients with reduced central serotonin function (i.e., low 5-HIAA levels in cerebrospinal fluid [125,308]).

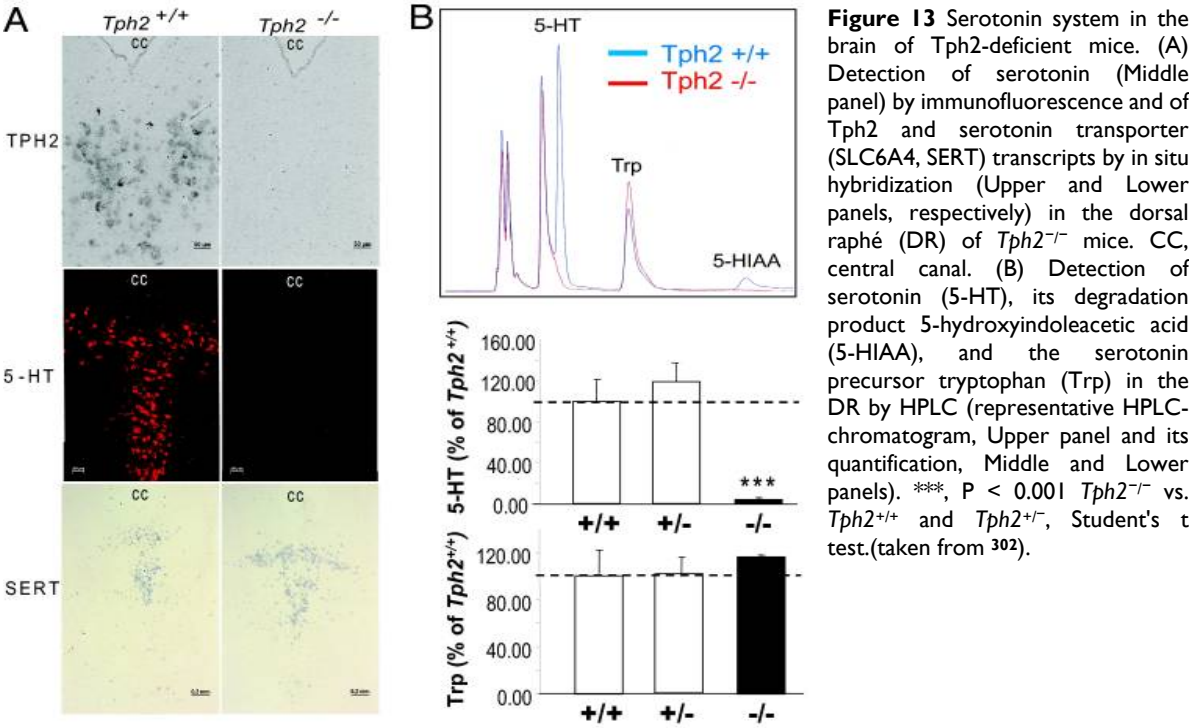

Figure 13 Serotonin system in the brain of Tph2-deficient mice. (A) Detection of serotonin (Middle panel) by immunofluorescence and of Tph2 and serotonin transporter (SLC6A4, SERT) transcripts by in situ hybridization (Upper and Lower panels, respectively) in the dorsal raphé (DR) of *Tph2*$^{-/-}$ mice. CC, central canal. (B) Detection of serotonin (5-HT), its degradation product 5-hydroxyindoleacetic acid (5-HIAA), and the serotonin precursor tryptophan (Trp) in the DR by HPLC (representative HPLC-chromatogram, Upper panel and its quantification, Middle and Lower panels). ***, P < 0.001 *Tph2*$^{-/-}$ vs. *Tph2*$^{+/+}$ and *Tph2*$^{+/-}$, Student's t test.(taken from [302]).

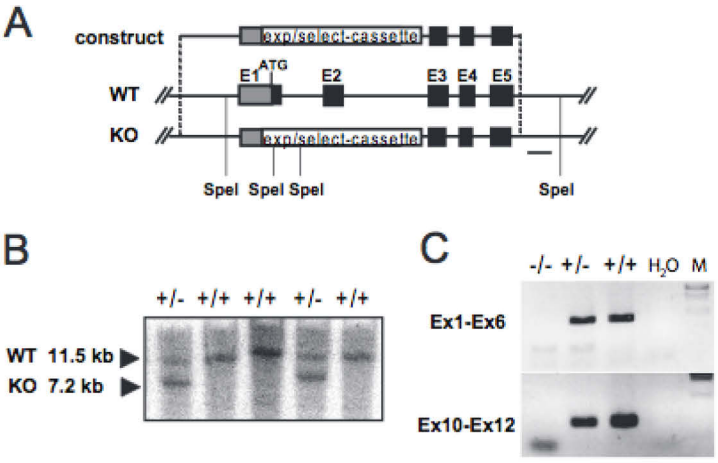

Figure 12 Generation of *Tph2*-deficient mice (A) The coding part of exon1 (E1), including the first ATG and the whole exon 2 (E2) of the mouse Tph2 gene were exchanged with an expression/selection cassette by homologous recombination in embryonic stem (ES) cells. WT, wild type; KO, knockout allele; black boxes, coding sequence; shaded box. 5' UTR; bold line, Southern blot probe. (B) Representative Southern blot analysis of ES cell DNA digested with SpeI. (C) *Tph2* expression in the brain analyzed by RT-PCR. M, marker. (taken from [302]).

Table 2 Physiology and Phenotypic changes in *Tph2* $^{-/-}$ mice. ↑, = increased; ↓ = decreased; → = unchanged, x = failure *C57BL/6* wildtype mice. (?) represents observed but ongoing research. EPm = elevated plus maze, hippocampus = HC, MBT = marble burying test, OF= open field, FST = forced swimming test, PFC = prefrontal cortex, TST = tail suspension test (adapted from Lesch 2012 [304]).

	Changes in *Tph2*$^{-/-}$ compared to WT	Source
Growth/body weight / obesity	↑ / ↓ / →	302,304
Aggression	Male ↑ ↑, Female ↑	98,304, 309
Anxiety-like behavior (EPM, MBT, OF)	EPM, MBT ↓ / OF →	98,304, 306
Conditioned fear response	↑, → ([306])	304, 306
Depression like behavior (FST, TST)	↑	304, 306
Somatosensory sensitivity	Tactile → / thermal → / pain ↑ (?)	304
The sleep-wake cycle	↓	310
USV communication normal / sexual	→ (?) / ↓ sexual	311
BDNF levels HC / PFC	↑ ↑ / ↑	312
mRNA expression of serotonin neuron-specific marker		
5-HTT / SERT	→	304
Vmat2 / Pet1	→ / →	304
Neurotransmitter concentration		
Serotonin / 5-HIAA	↓ ↓ ↓ / ↓ ↓ ↓	304,306, 313
NE	↓	304 306,
DA	→	304, 306
HVA	→	306
DOPAC	→	306
NM	→	306
Glutamate	PFC ↑	314
Neurogenesis		
Overall DG proliferation	→	125
Sox2 / GFAP cells	↓	125
Exercise-induced proliferation	x	125
Monoaminergic neurons		
Serotonin	→	304
NE	↓	304
DA	→	304
Serotonergic neurons		
Fiber density	↑	313, 315
Formation	→	313, 315, 316
Fiber distribution	→	313, 315
Morphology	→	313, 315, 316
GABAergic system (GABA concentration/GABAergic interneurons)		
Frontal cortex	→	304, 314
HC	↑ / →	304, 314
Amygdala	→ / ↓	304, 314
Serotonin receptor expression/function		
5-HT$_{1A}$	↑ ↑	304
5-HT$_{1B}$	↑ ↑	304
Electrophysiology (serotonin neuron firing rate)		
baseline	→	304, 313, 315
Applied Trp	→	304
Applied 5-HTP	↓	304, 313
Applied 8-OH-DPAT	↓ (?)	304

1.3.2 *SERT* - deficient mice

SERT-KO mice (*SERT*$^{-/-}$, also called *SERT* mice, which lack the serotonin reuptake transporter SERT), generated by homologous recombination that replaces the second exon of *SERT* with a neo-cassette, accumulate serotonin in the synaptic cleft 6-fold, yet, with an overall brain serotonin level of only ~40 % [317]. With the lack of *SERT* (Figure 6), a reduced number of serotonin neurons in the DRN was found [318,319]. Therefore, one could also see them as a hypo-serotonergic mouse model. Physiological and phenotypic changes in *SERT* knockouts are: atypical barrel-cortex formation as well as malfunctioning thalamo-cortical connections, resulting in impaired somatosensory feedback and locomotion impairments (reviewed in [320,321]). *SERT*-KO strains also exhibit greater neuronal spine densities in the orbitofrontal cortices and show increased spine density in the basolateral amygdala and PFC [322]. *SERT*$^{-/-}$ mice reveal increased cell proliferation in aged, but not adult mice in dentate gyrus (DG) in HC [323]. Adult, but not early adult *SERT*$^{-/-}$ mice exhibit increased anxiety [324] and are more sensitive to stress [325]. *SERT* is the supposedly main target of SSRIs; therefore, antidepressant action can be studied in this model. However, recent studies show no behavioral effects of escitalopram [326], while using SSRIs (FLX and CIT) and do not show the acute and chronic antidepressant effects [327], like reduced immobility in forced swimming tests (FST) and tail suspension test etc. .

Humans with mental disorders linked to a lower *SERT* expression genotype are comparable with *SERT* KO mice, especially *SERT*$^{+/-}$ mice, in several aspects [304,328–330]. A 50 % reduction in *SERT* expression during early development correlates with the severity and number of episodes of MDD and stressful life events in patients [331–333].

1.4 Neurotrophin Hypothesis of Depression

1.4.1 The Neurotrophins and BDNF

Antidepressants such as the SSRE tianeptine (TIA), or SSRI (FLX, CIT) seem to exert their therapeutic effect also by affecting neuroplasticity in CNS, especially in the HC, where MDD has a degenerative component (reviewed in [334–336]). The major players for central neuro plasticity are neurotrophins, where studies have focused largely on the role of BDNF. Neurotrophins are a family of highly conserved mammalian proteins including the nerve growth factor (NGF), neurotrophin-3 (NT-3) and neurotrophin-4 (NT-4) with major roles in development, and the adult nervous system, although being synthesized in other peripheral organs, too. NGF was the first described between 1950-60's and awarded with the Nobel prize in medicine [337–339]. BDNF was discovered by Barde 1982 [340] and quickly became valuable for research, because it seems to be involved in a variety of neuronal and developmental functions such as cell survival, migration, phenotypic differentiation, axonal plus dendritic growth, cell death, synaptic plasticity, mainly in the HC (reviewed in [341–344]), and is involved in MDD [345,346]. When Nibuya *et al.*, in 1995 reported a first link between adult hippocampal neurogenesis, depression and BDNF, the interest in BDNF as antidepressant target boomed, highly promoting the "neurotrophin theory for depression" [287].

The *BDNF* gene, found in humans on chromosome 11 [347], is controlled by at least eight distinct promoters that initiate transcription of multiple distinct mRNA transcripts, resulting in splicing variants. Each single 5'exon contains the entire open reading frame of the final BDNF protein, but each of the different exons act tissue-specific in different brain regions or non-neural tissues. BDNF is expressed throughout the brain, with the highest levels in neurons of the HC (respective exon II, V and IX) [348,349]. Another is the PFC; here, promoter IV-dependent *transcript* takes major account for the high cortical BDNF expression, induced through local neuronal activity [350,351].

1.4.2 BDNF biosynthesis and pathways

After translation, BDNF protein is sub-categorized in different cleavage-dependent isoforms from the initial proneurotrophin *pre-pro*-BDNF. By translocating into ER, the pre-region is removed, revealing *pro*-BDNF, a 32-kDa precursor, which further undergoes cleavage of the pro-domain by protease PC1 to release mature 14-kDa *m*-BDNF protein as well as a minor truncated form of the precursor (28 kDa; Figure 14). It can be released or packed into vesicles, transported to axonal endings and exocytotic released [352–354]. Secreted *pro*-BDNF or *m*-BDNF activates a heteromeric receptor

complex of p75 neurotrophin receptor and sortilin to initiate a variety of functions ranging from cell- survival to -death [355], but can also bind solely to $p75^{NTR}$, a low-affinity receptor which leads to enhanced long-term depression (LTP) [356]. Studies suggest that *pro*-BDNF accounts for a significant amount of the total neurotrophins secreted extracellularly, particularly in CNS neurons [357,358]. A receptor for *m*-BDNF is the high-affinity tyrosine protein kinase (Trk)B receptor [359], with usually pro-neuronal survival and plasticity effects. The various exact BDNF-receptor interactions and downstream pathways are reviewed elsewhere [342,360]. Hippocampal *m*-BDNF/TrkB signaling is mainly associated with learning [361] and memory [362], and an increase in BDNF endogenous levels induces progenitor cell proliferation in the rat HC [363], while

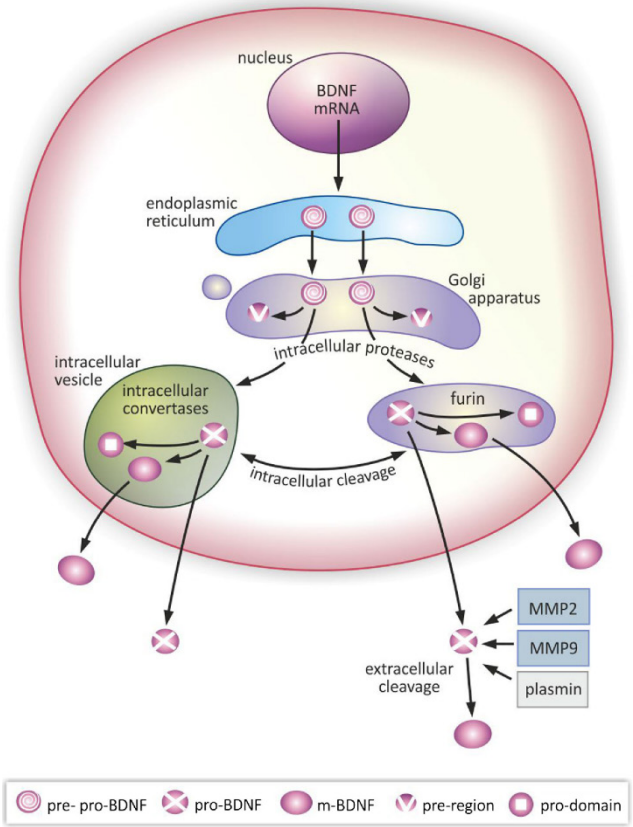

Figure 14 Schematic synthesis and maturation of BDNF. After transcription of the *BDNF* gene in the nucleus the *pre-pro*-BDNF precursor is produced at the endoplasmic reticulum losing it pre-region during membrane translocation resulting in a formation of the immature proneurotrophin isoform of BDNF (*pro*-BDNF). It is transported to the Golgi apparatus, whereby intracellular cleavage, the pro-region sequence is removed and the mature isoform of BDNF (*m*-BDNF) is produced. Intracellular cleavage leading to formation of *m*-BDNF also occurs in intracellular vesicles, allowing transport of this neurotrophin to axonal terminals and subsequent release into the extracellular space, via the presynaptic membrane. Processing of BDNF is accomplished by intracellular proteases. Extracellular cleavage of pro-BDNF also can occur and is dependent on plasmin and matrix metalloproteases 2 and 9 (MMP2 and MMP9; taken and adapted from [360]).

in mice, it influences the survival of newly generated neurons [364]; especially combined with physical exercise [365], or enriched environment [366]. Also a certain ratio of pro-BDNF : *m*-BDNF needs to be set for a healthy brain, since neurons subjected to high level of *pro*-BDNF or low level of *m*-BDNF prevalently undergo elimination [367].

1.4.3 Altered BDNF signaling in disease – antidepressant effects of BDNF

Human BDNF polymorphisms have been linked to anxiety and MDD [368,369]. In MDD, decreased blood BDNF levels have been measured that were later replenished by antidepressant treatment [345,346,370–375]. However, the link between BDNF-polymorphism and depression is currently discussed, based on newer meta-analyses [376–378]. Evidences for the neurotrophin hypothesis help to also track down the antidepressant properties of BDNF to circuitries, e.g. inside the PFC, parts of the HC, the DG and CA regions, but also the ventral tegmental area (VTA) and the nucleus accumbens (NAc) tract (reviewed in [379]). BDNF gene expression is enhanced after SSRI treatment in humans [380]. BDNF's role in adult neurogenesis and depression is further supported by promoted cell proliferation [342,381–384] or survival [382] facilitated by antidepressants. In the HC, serotonin neurotransmission is under the influence of BDNF [385,386]. Also in other brain regions, BDNF administration seems to potentiate antidepressant and anxiolytic effects by increased serotonin transmission [387,388]. In contrast, a BDNF reduction in heterozygous BDNF KO mice leads to SSRI resistance, decreased SERT expression and increased extracellular serotonin levels. In general, chronic administration of SSRIs or ECT increase the expression of BDNF [389–391], and of cAMP response element binding protein (CREB), a transcription factor regulating for BDNF expression in the HC [287,392,393]. In our *Tph2*$^{-/-}$ mice, increased baseline levels of BDNF have been observed suggesting compensatory effects in the absence of serotonin [312], clearly linking serotonin, BDNF signaling and adult neurogenesis.

1.5 Neuro-endocrine symptom of depression and the stress hypothesis

1.5.1 Physiological stress

A historic article from Selye in 1936, defines stress as "a syndrome produced by diverse nocuous agents" [394], describing the response to a distressing situation as adaptations in body physiology to keep homeostasis on a healthy level; for instance in "fight or flight" situations in prehistorian times by boosting glucose metabolism [395]. Today, these "fight or flight" situations are characterized differently, for example distinguishable in early life stress or traumatic events [396], object loss [17,397] or already obtaining a loan. Each stressor is taken separately into a person's stress account (ranked in the social readjustment rating scale [398]). Although stressful events are one of the major phenotypes of MDD, for one-third of the patients, the connection seems

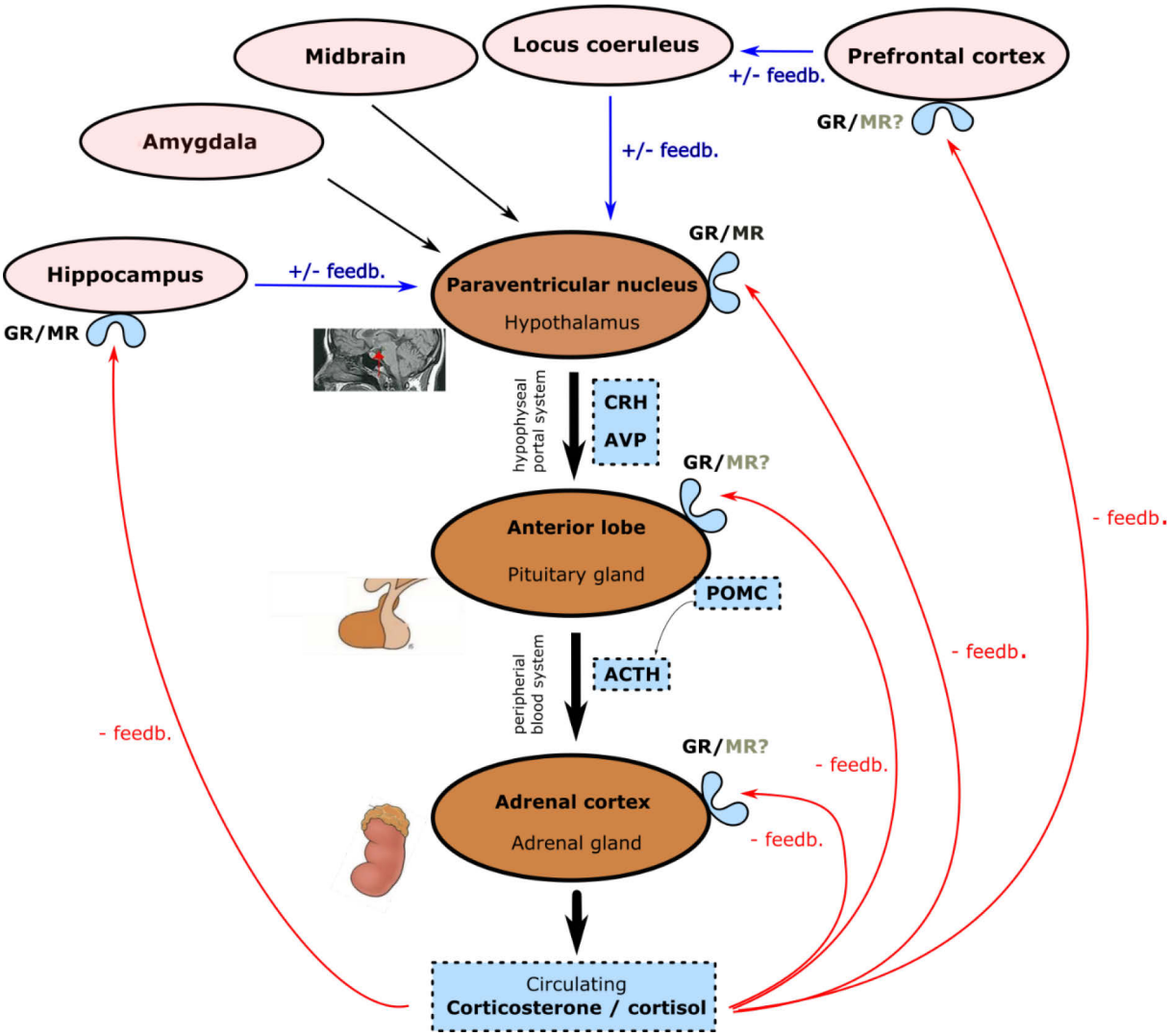

Figure 15 Simplified schematic diagram of the hypothalamic –pituitary-adrenal (HPA, brown) axis, describing regulation and negative feedback (-feedb.,) of cortisol (in humans) and corticosterone (in rodents), via glucocorticoid (GR) and partly mineralocorticoid receptors (MR). Involvement of MR (?) in grey is still under discussion. HPA-axis activity is further regulated by stress sensitive regions (light red) like hippocampus, amygdala, midbrain, and PFC and by the precursor hormones (light blue) circulating between HPA glands and tissues – Arginine vasopressin (AVP), corticotropic releasing hormone (CRH) and adrenocorticotropic hormone (ACTH) / Propiomelanocortin (POMC).

noncausal since MDD selects individuals often only in high risk environmental stress [399]. Negative life events cause distress [400] and activate the HPA-axis leading to the release of glucocorticoid hormones (GC; cortisol in humans, CORT in rodents, Figure 15)–the classical stress hormones– that mediate an response to the challenge not only directly to the brain, but also to the periphery. To maintain the stress response, various signals regulate the synthesis and release of hormones from the adrenal cortex, since long-term exposure to GC leads to noxious effects in certain tissues like the HC [401].

The HPA-axis comprises of three major parts, the hypothalamus, the pituitary and adrenal glands (brown in Figure 15). In response to stress, hypothalamic, paraventricular nucleus (PVN) neurons release corticotropin-releasing hormone (CRF), which subsequently promotes the release of adrenocorticotropic hormone (ACTH) from the pituitary gland (ACTH is metabolized from pro-opiomelanocortin, POMC). This in turn triggers synthesis and release of GC in the adrenal cortex (Figure 15), secretion into the bloodstream and cerebrospinal fluid. CRF and ACTH are not only released upon stimulation of the CNS, but also in response to inflammatory cytokines, such as IL-6 [402] and TNF-α [403] during certain diseases, so this hormonal network system is ideally suited to cope with the immediate demand of the body during emotional, physical, and disease stress. In the last step of the cascade, corticosterone/cortisol activate: mineralocorticoid- (MR) and glucocorticoid receptors (GR) located in the PVN and HC, providing feedback control for stress homeostasis [285] (Figure 15).

1.5.2 Dysregulation of the HPA-axis and the stress receptors

Stressful events can lead to chronic stress that often precedes the onset of depression. Dysregulation or hyperactivation of the HPA-axis is a hallmark of MDD. Not only the HC but also the PVN, is heavily innervated by dorsal raphe serotonin fiber projections [388-391], supporting a linked mechanism of stress, serotonin, and depression. In rodents, administration of high amounts of stress hormones can induce depression-like symptoms. In individuals diagnosed with mood disorders, numerous reports have described increased cortisol and ACTH, indicative of a dysfunctional HPA-axis. Elevated cortisol exposure is associated with elevated 24-hour urinary free cortisol, adrenal gland enlargement, and failure to suppress cortisol in response to the dexamethasone (DEX) suppression test [404–407]. Furthermore, PET imaging showed that the stress hormone response in humans is connected with alterations in central

serotonin transporter levels, which also correlated with the severity of negative mood states [408].

Activation of MR and GR by cortisol/CORT provide feedback control to form an healthy homeostatic state [409,410]; but the receptors form long-term adaptations to stress in the HC and thereby modulate the HPA-axis, often in a negative way in case of a depression [249,411–413]. Studies using selective antagonists demonstrate that MR, but not GR, is crucial for the habituation response to repeated stress from PVN neurons [412,414]. While MR and GR are expressed in many peripheral cell types and tissues (often simultaneously), in CNS MR is mainly present in the HC, hypothalamus and PFC and is responsible for controlling physiological and mild stress-related variation of the HPA-axis [413,415]. MR is expressed in aldosterone target tissues (kidney, colon, salivary, and sweat glands) and in a plethora of non- epithelial/aldosterone target tissues, such as the CNS (cerebral cortex, caudate, cerebellum and HC), mononuclear leukocytes, large blood vessels, macrophages and T-lymphocytes and the heart. Even though MR main known effect is the sodium, potassium and hydrogen ion balance in the nephrons of the kidney, as well as modulation of fluid transport crucial for osmotic and hemodynamic homeostasis [410], it also has functions in the CNS and even in depression [413].

The ubiquitous expression of GRs is essential for energy homeostasis, including gluconeogenesis, and the response to stress and inflammation [395,410]. Excessive and chronic GR activation leads to hippocampal neuron atrophy and eventually death, while MR activation is antiapoptotic and supports neurogenesis [164,416]. Thereby, neuron function and neuronal circuits require an appropriate balance of MR:GR activation [417–419]. The correct balance of MR and GR is known to affect brain serotonin systems and its receptor modulation major depression [420]. Decreased levels of MR over GR expression in the PFC and hypothalamic PVN are implicated in depression and cognitive decline in humans [411,421,422]. Furthermore it was found that MR is quite active in patients with MDD [420].

1.6 Biomarkers for depression

By definition, a biomarker is a measurable indicator to evaluate a biological and physiological status in an organism [423]. In medicine, biomarkers can be used to monitor pathogenic and therapeutic processes. A dominant example is daily blood glucose measurements in patients suffering from diabetes.

The causes for a depressive episode can be manifold. An early childhood trauma, burnout syndrome, depression due to social neglect or object loss etc. might each have another neurobiological cause. Since this heterogeneity of depression, research still lacks clear biomarkers to diagnose and evaluate the depressive symptoms, severity, and pathologic process more precisely. To evaluate the presence and severity of symptoms consistent with the DSM-V or the ICD- 10 diagnostic criteria [22], so far, a wide range of rating scales based on a physician-patient consultation exist. Examples are *Hamilton Depression Rating Scale* or the *Montgomery-Åsberg Depression Rating Scale* [424,425]. Even self-screening is possible for the patients, by subjection to *Patient Health Questionnaire (PHQ)-9* [426].

Unfortunately, these screening rating scales are still limited to accurate subjective statements by the patients and restricted to humans only. Researchers are still striving to find suitable and objective indicators, especially for animal experiments and test a plethora of potential biomarkers for depression (e.g. for inflammation, growth factors, neurotransmitters, the endocrine system, metabolic factors, cell morphology and genetics (Table 3); yet most are not fully understood in their mechanism or following downstream pathways. The appearance of new biomarkers and their heterogeneity slightly masks how biological information can be used to enhance diagnosis, treatment, and prognosis of depression. Furthermore, lack of consensus for a precise classification of depression and ongoing disparity of esteem between physical and mental health in medicine and society, results in only a third of patients diagnosed with MDD receive state-of-the-art treatment with noticeable remission [427,428]. A dominant and replicable cellular effect of antidepressant therapies is the induction or modulation of adult hippocampal neurogenesis [124,126,183,187,249]. Although underlying mechanisms that enhance the generation of new neurons are still unknown, they involve the stress axis, serotonin and neurotrophin signaling [7,126,249,429]. The main goal of this thesis is to unravel the mechanisms and to define new biomarkers or to confirm the ones suggested below. The following table (Table 3) summarizes current literature and markers suitable for the various hypotheses of depression, that might act as biomarkers

in the treatment of MDD. Table 3 can also be expanded even beyond the neurobiological level by including (epi-) genomic, transcriptomic, proteomic, metabolomic and even exogenic microbiome areas for possible sources of biomarkers for depression. This high volume of potential biomarkers represents the complexity and heterogeneity of a depressive phenotype. (reviewed in R. Strawbridge, A.H. Young, A. J. Cleare, in 2017 [428]).

Table 3 Possible biomarkers for depression (Table adapted and updated from [428]).

System	Marker
Inflammation	IL-6 [430–432], CRP [430,431], TNFα [430,432], IL-1β [430,431,433], IL-2 + sIL-2R [432,434] , IL-4 [435], IL-10 [434,436,437], C-C chemokine ligand 2 [434],INFγ [434,438],IL-8 [439], MCP1 [439], IL-1a [440] , IFNα, IL-5 [438], IL-7 [439], IL-12 [434], IL-12p70 [439], IL-13 [434,439], IL-15 [439], IL-16 [441] ,IL-18 [434], IL-17 [442], IL-33 [443],TNF receptor 2 [434],TNFβ, macrophage-derived chemokine [444],MCP1 [445], MCP4 [445], Mip1α [440], Mip1β [443,445,445], SAA [440], sICAM1 [446], sVCAM1 [446], eotaxin [445,447], eotaxin3 [447], TARC, IP-10 [445,447], GM-CSF [438]
Growth factors	(m-)BDNF [7,345,346,355,356,375,380,389,448–451] (pro-BDNF [452,453]), VEGF [454–457] (VEGF-C [451] and VEGF-D[451]), NGF [458,459] , GDNF [460], IGF-1 [461,462], bFGF [463,464], Tie2 [451], NT-3 [459]
Neurotransmitters	Serotonin (5-HIAA, 5-HTP, SERT and Serotonin receptors), NA [465,466], DA [466–469], glutamate/glutamine [465], GABA[470], histamine [465], MHPG [465], HvA [465]
Endocrine system	HPA-System/Pathways [164,249,471,472] (Glucocorticoids/Cortisol levels and receptors, FKBP5 [473], ACTH [472,474], CRF [422,475],Dehydroepiandrosterone [476], vasopressin [475,477]), ACE [478], TSH [479], fT3 [479], fT4 [479], melatonin [459]
Metabolic factors	HOMX [443], Leptin [480,481], Insulin [482], Ghrelin [483], Albumin [484], Glucose [485], Lipids [486], Lipoproteins [487]
Cell morphology	Dendritic spine density [453,488]; Neurogenesis [164,249]
Anatomical morphology	Structural changes [489–492] (PFC volume [490], hippocampal volume [260,490,493], gray/white matter volume [490,491]), Functional changes [492] (BOLD-MRT, PET ligands assessing various sources)
Genetic	Genome-wide association studies/polygenic risks [494,495], Telomere length [496], Chaperones [473,497], Gene polymorphisms [478], epigenetic changes [498], histone modification [498], gene expression assessments [498]

1.7 Aims

The specific aims of this thesis were designed to elucidate the mode of serotonin action in the adult mouse brain to clarify whether known antidepressants work by targeting the serotonin system or whether other biological mechanisms are involved.

1.7.1 Comparison of the physiological effects mediated by SSRI and SSRE treatment

Pharmacological manipulation of serotonin leads to clinical improvement associated with a delayed increase in hippocampal neurogenesis, as shown in rodents [124,183,187]. This thesis is determined to shed light on, how serotonin and neurogenesis are linked to the antidepressant effects for certain therapies like SSRI / SSRE. This aim was developed to examine the role of a novel downstream mediator of serotonin action - BDNF. Altered BDNF signaling could be relevant to mechanisms of serotonin therapy; and previous data revealed increased levels of hippocampal BDNF in *Tph2*$^{-/-}$ mice [312]. Specifically, the known antidepressants CIT (SSRI) and TIA (SSRE) were tested for their effects on adult hippocampal neurogenesis in wild type animals compared to *Tph2*$^{-/-}$ mice after treatment over 21 days. BDNF signaling might be involved in the action [7,499,500], and so BDNF protein levels were determined.

1.7.2 Test electroconvulsive therapy (ECT) in a model with serotonin depletion

Most of the patients do not respond to SSRIs. Instead ECT is used, as highly effective in the treatment of major depression. In animal models, a series of ECS leads to increased neurogenesis and increased BDNF signaling, that might contribute to the mood stabilizing action of ECT in patients [124,267,284–288]. This aim examined whether serotonin signaling is essential for the well-established effects of ECT, namely the induction of hippocampal neurogenesis and BDNF. *Tph2*$^{-/-}$ mice were subjected to a series of 5 daily seizure sessions, and BDNF, behavior and the generation of new neurons in the HC were determined in the absence of serotonin.

1.7.3 Elucidating the role of serotonin on the HPA-axis

This aim addressed specifically the effects of life-long serotonin deficiency on novel adaptive mechanisms. *Tph2*$^{-/-}$ and *SERT*$^{-/-}$ mice were tested in response to chronic stress. A study of Jabbi *et al.* in 2007 reported that psychological stress in human patients with low SERT expression significantly increases plasma ACTH and cortisol levels [501], suggesting a link between the HPA-axis and the serotonin system. Increased activity of the HPA-axis is a major player in the pathophysiology of MDD, and HPA-hyper-sensitivity in response to stress might be a long term trigger for depression [249].

Here the physiological parameters of the HPA-axis – ACTH and CORT plasma levels at baseline and after mimicking a chronic stressful event by daily i.p. injections of different drugs, were determined. The results will contribute to our understanding of the etiology of MDD and may lead to develop better therapy approaches.

1.7.4 Alterations in daily life activities as a behavior biomarker for depression

To address the psychological challenge - whether depression is a mankind-specific mental disorder or whether a comparable depressive-like performance can be observed in animal models, a behavioral approach was set according to the "Activities of daily living" (ADL) paradigm [502,503]. This aim was developed to determine alterations in the rodent CNS, that are linked to less structured ADL, as seen in patients [24,25]. A typical ADL for mice is nest building behavior. Mice in nature build nests that provide thermoregulation, protection and shelter from sexual competitors and for the offspring [504], nest building behavior is altered in disease [505]. A standardized nesting setup adapted from Deacon in 2006 [502] was used here to test several transgenic animal models altered in serotonin signaling. Another behavior test is “Burrowing and Hoarding”, first developed for Alzheimer’s disease research. Hoarding paradigms require a distant food source to be linked to the home cage by a connecting passage and display the natural behavior of rodents craving for food [503]. While establishing the hoarding paradigm, mice were performing digging ("burrowing") movements, further evolving a burrowing paradigm as an ADL for mice.

2 Methods

2.1 Animals and housing conditions

2.1.1 *Tph2*$^{-/-}$

Generating transgenic *Tph2*$^{-/-}$ mice is described elsewhere in detail [300,302] (see also Figure 12). To obtain *Tph2* gene-deleted mice on a pure genetic background, heterozygous *Tph2*-deficient animals (*Tph2*$^{+/-}$) on *C57BL/6N* background (after at least 6th generation backcross) were bred for at least four further generations to *C57BL/6N* mice (Charles River, Germany) [302].

2.1.2 *SERT*$^{-/-}$

SERT$^{-/-}$ mice (also called *SERT* mice) have been commercially purchased from Jackson laboratory. To keep *SERT* gene-deleted mice on a pure genetic background, *SERT*$^{-/-}$ mice were bred for at least 10 generations to *C57BL/6J* mice.

2.1.3 *ACE2*$^{-/-}$

ACE2$^{-/-}$ deficient female mice used in this study were backcrossed to *C57BL/6N* for more than 7 generations. *ACE2*$^{-/-}$ mice are generated as described elsewhere [506–508].

2.1.4 Housing conditions

All animal procedures and experiments were performed according to national and institutional guidelines and were approved by the official Berlin committee (LAGeSo, Berlin, Germany) and in accordance with the Animal Welfare Act and the European Communities Council Directive 2010/63/EU). Husbandry and breeding were performed at MDC Berlin. Mice are kept in an individually ventilated cage (IVC) rack system, cage size 35x20x13 cm (max. 5 animals), at room temperature and light/dark cycle of 12h/12h. Animals had access to standard chow and drinking water *ad libitum*. Supplies and cages are minimum changed once per week, same day, and time. Litter removal, cage and equipment cleaning was automatized by the core facility; therefore, a standardized odor removal can be anticipated. When showing of signs of any health limitations, an animal was excluded from any experiment. If the health status did not normalize within a day the responsible veterinary/experimental leader was informed and/or the animal was terminally anaesthetized. Offspring were weaned at around PND 21 and genotyped by toe cut or ear-mark biopsies.

Besides for stress experiments when mice of both sexes were used, studies on adult neurogenesis, serotonin and antidepressants are performed in 8 to 15-week-old female

mice. Most of the times, littermates were used as control group; however, in cases when animal numbers per experimental groups were not appropriate, *C57BL/6* mice were used/purchased from Charles River (*C57BL/6N*) / Jackson Laboratory (*C57BL/6J*) as wild type control animals (WT).

2.2 BrdU and drug treatment

2.2.1 BrdU treatment

To analyze cell proliferation in the HC, animals received three intraperitoneal injections (i.p.) of the thymidine analog BrdU (5-Bromo-2'-deoxyuridine; SIGMA, Germany) in a dose of 50 mg/kg (dissolved in 0.9 % NaCl, and filtered before use) 6 hours apart on day 1 of the experiments.

2.2.2 SSRI, SSRE treatment

To analyze the effects of antidepressants, from day one on for 21 days, animals received one i.p. injection of either drug at 5 pm (start of dark/active phase is at 6 pm): SSRI FLX (Tocris, Bristol UK; Fluoxetine hydrochloride; 10 mg/kg body weight dissolved in 0.9 % NaCl), SSRI CIT (Lundbeck, Hamburg GER; Citalopram hydrochloride; 10 mg/kg body weight dissolved in 0.9 % NaCl), SSRE TIA (Tocris, Bristol UK; Tianeptine sodium chloride; 10 mg/kg body weight dissolved in 0.9 % NaCl); 0.9 % NaCl (Carl Roth, Karlsruhe Germany). In addition, one group was held non-treated and unhandled for 20 days. At day 21, animals were perfused in the morning, and brains were collected.

For analysis of BDNF levels in HC and PFC animals were subjected to the same antidepressant treatment protocol for 20 days as described for the immunohistochemistry analysis, without prior BrdU treatment. At day 21 animals were sacrificed by cervical dislocation, PFC and HC were collected in liquid nitrogen, transported on dry ice, and stored at -80°C until further procedures.

2.3 Experimental designs

2.3.1 Comparison of the physiological effects mediated by SSRI and SSRE treatment

This experiment was designed to address the effects of long-term serotonin deficiency on novel adaptive mechanisms. First, known antidepressants CIT (SSRI), and TIA (SSRE) were given to female wild type (control, CTR) and *Tph2*$^{-/-}$ mice to determine their effects on adult hippocampal neurogenesis upon treatment over 21 days; and to test whether the drugs also act in the absence of serotonin. In this approach, the role of a novel downstream mediator of serotonin action was examined, BDNF. Neurotrophic signaling might be involved in drug action, and BDNF protein levels of the HC and PFC will be determined by ELISA. Further analysis comprises phenotypes of the neuronal lineage of newly generated, BrdU+ cells, with and without treatment (Figure 16).

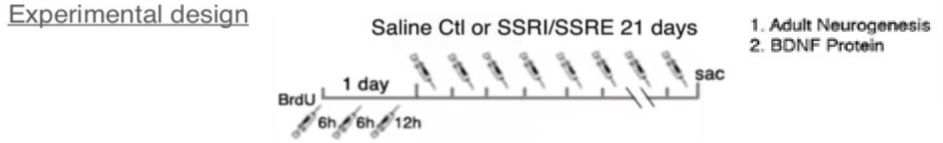

Figure 16 Experimental design for chronic treatment studies over 21 days in *Tph2*$^{-/-}$ and CTR mice. 3x i.p. BrdU on day 1 was followed by daily i.p. injection of either SSRI, SSRE or Saline to evaluate adult neurogenesis and BDNF protein. One group of mice was left unhandled as survival group. All groups were sacrificed at day 21.

Specifically, eight-weeks old female mice, randomly assigned into groups (saline, SSRI, SSRE), received daily intraperitoneally (i.p.) injections with either drug (SSRI/SSRE) or saline (SAL) vehicle for 21 days. One group of mice ('survival') remained unhandled for 21 days. For immunohistochemistry analysis of adult neurogenesis, mice received three i.p. injections of BrdU at day 1 of the experiment.

2.3.2 Test electroconvulsive therapy (ECT) in a model with serotonin depletion

In another approach, female *Tph2*$^{-/-}$ and CTR mice have been tested upon a series of 5 daily ECS sessions. Experimental readout is 1) adult neurogenesis, 2) BDNF signaling, and 3) behavior. Mice, 13-15 weeks old at the beginning of the experiment, randomly assigned to experimental groups, received, or not received, respectively, ECS for 5 days. Seizures followed an established protocol with pentobarbital pretreatment and unilateral electrode placement, as described in detail elsewhere [509]. ECS treatment was performed with the help of Prof. Dr. Peter Gass and Christof Dormann from the Central Institute for Mental Health Mannheim, Germany. Seizure threshold was adjusted on day 1. The stimulation dose was increased, when seizures were insufficient during the ECS course [510]; for WT: a reliably tonic-clonic convulsive seizure motor response was

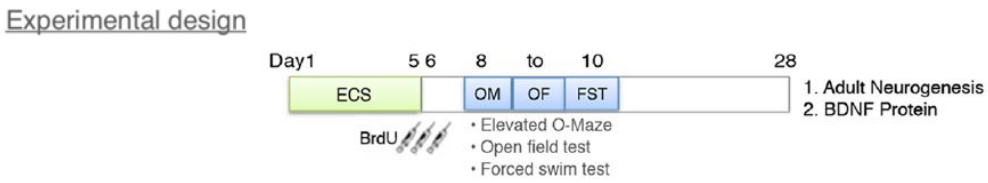

Figure 17 Experimental design for ECS treatment in WT and *Tph2*$^{-/-}$ mice. Initial daily electro convulsive treatment for 5 days, followed by 3x BrdU injections (in 6h rotation) at day 6. After 2 days habituation behavior assays for depressive phenotype are set from day 8 to 10 (OM-Elevated O-Maze; OF-Open field test; OF-Forced swim test). Sacrifice was performed at day 28 with experimental readout of adult neurogenesis and BDNF protein measurements.

observed between 35 and 39 mA on day 5, while all *Tph2*$^{-/-}$ mice had a threshold seizure response of 35 mA (frequency 80 Hz, duration 1.2 s, pulse width 0.5 ms). Subsequently on day 6, all animals receive three injections of BrdU followed by behavioral tests on day 8 to 10. Animals were sacrificed by perfusion with NaCl on day 28, whereas one brain hemisphere was taken for the histological neurogenesis readout (left), the other (right) for the BDNF tissue protein level measurements of PFC and HC by ELISA (Figure 17).

2.3.3 Elucidating the role of serotonin on the HPA-axis

Here, the treatment paradigm from 2.3.1. was repeated (SAL and SSRI) to determine a possible stress outcome due to the injections. Analysis comprises mRNA expression levels of MR, GR, CRF and POMC; as well as CORT plus ACTH hormone levels, to investigate and compare CTR and *Tph2*$^{-/-}$ mice (13-15 weeks old) in their response to stress and baseline levels of the HPA-system (Figure 18). The baseline group

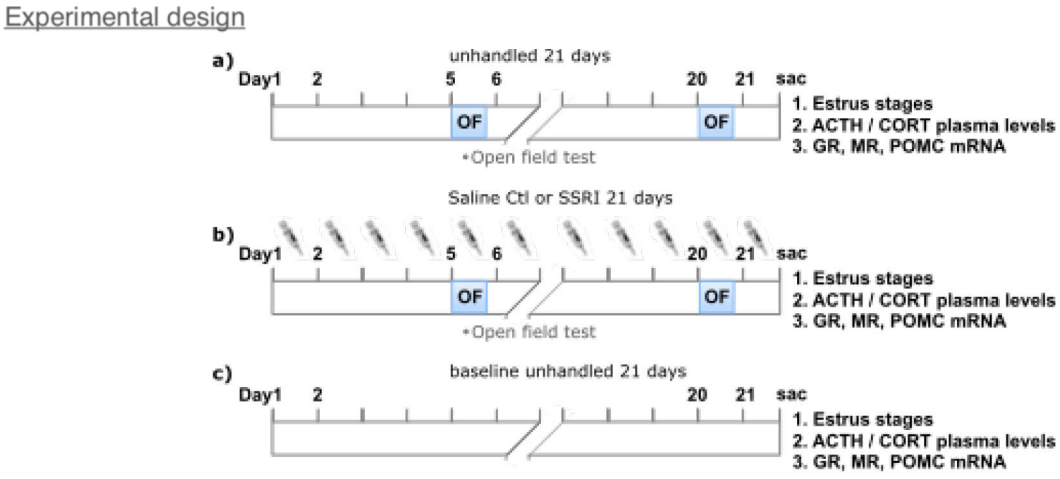

Figure 18 Experimental design for chronic treatment studies over 21 days in female *Tph2*$^{-/-}$ mice. SSRI or saline have been injected i.p. to mimic a chronic stressful event (b), and to evaluate the interplay of serotonin and HPA-axis. Subsequently plasma was taken to determine ACTH and CORT levels, compared with estrus stages, and brain areas for gene expression of GR, MR. Obtained values are compared with unhandled animals (a). In addition, baseline values for ACTH and CORT plasma levels have been created for male and female *SERT*$^{-/-}$, *Tph2*$^{-/-}$ animals (c).

(untreated and unhandled) was completed by *SERT*$^{-/-}$ mice (13-15 weeks old). Trunk blood was collected by decapitation from male and female, treated and untreated mice. Female CORT and ACTH plasma levels were also measured in correlation to the estrus cycle stage, which was determined right after sacrificing the animals. This helped to exclude misleading female sexual hormone influence on CORT levels [511]. In addition, SAL and SSRI female treated female mice were tested for anxiety in the open field test; performed at day 5 and 20.

2.3.4 Alterations in daily life activities as a behavior biomarker for depression

To elaborate daily life activities as a behavior biomarker for depression, nesting paradigm was performed and different animal models (male vs. female) with altered serotonin system were tested (8-11 weeks old): *Tph2*$^{-/-}$, *SERT*$^{-/-}$, *ACE2*$^{-/-}$ with their respective controls *Tph2*$^{+/+}$, *C57BL/6J* and *C57BL/6N* (8-11 weeks old). Burrowing and hoarding paradigm were established (performed as stated in 2.9.), due to availability, only for female *Tph2*$^{-/-}$ *and C57BL/6N* mice (12 weeks old). All animals were habituated during the day (3 weeks to the room, 2 days to the new material), tested o.N. (1 day) and evaluated and groups in a close succession of days. Each animal was tested only once for each paradigm, to exclude memorization. Nesting was performed single housed for better scoring, whereas nesting and burrowing paradigms were performed in pairs to keep social conditions and isolation effects.

2.4 Genotyping

2.4.1 gDNA Isolation

For genotyping, biopsies of toenail (until p7), ear and tail (after experiment to re-genotype) were collected from the sedated animal. Samples were stored at -20°C until further use. To isolate genomic DNA (gDNA), biopsies were mixed with “Ear” buffer containing 1 mg/ml Proteinase K (Table 4) in a micro tube and incubated o.N. at 55°C in a thermomixer, whilst shaking at 150 rpm. Proteinase K activity was inactivated by incubation at 95°C for 10 min, whilst shaking at 150 rpm. For RNA degradation, 1x TE buffer, containing 20 µg/ml RNase A was added and afterwards stored at 4°C until further usage. Genotyping of transgenic mouse lines was then performed by Polymerase chain reaction (PCR).

Table 4 Buffers for genotyping of transgenic mouse lines.

Buffer/Solution	Component	Final concentration
"Ear buffer"	NaCl	200 mM
pH 7.0	Tris-HCl	100 mM
	EDTA	0.1 M
	SDS	1 %
	H20	Fill to X Volume
	Proteinase K	1mg/ml
1x TE buffer	Tris-HCl	10 mM
pH 8.0	EDTA	1 mM
	H20	Fill to X Volume
1x TAE Buffer	Tris-HCl	242 g/l
	Sodium Acetate	68 g/l
	EDTA	18.5 g/l
	H20	Fill to X Volume
10x DNA Loading Dye	Sucrose	40 %
	Bromophenol Blue	250 mg/l
	1xTE Buffer	Fill to X Volume
1-3 % Agarose Gel	Agarose Powder	1-3 %
	Ethidium Bromide	0.5 µg/ml
	1xTAE	Fill to X Volume

2.4.2 PCR-Amplification of the template DNA

After gDNA isolation, a specific primer pairs for the transgenic line (Table 49) was chosen and a PCR reaction mix was prepared according to Table 6 . Reaction mix was prepared in 50 µl PCR tubes on ice. Before set to the thermocycler, the liquid inside the tubes was briefly vortexed and spun down. The machine was set accordingly to Table 5. An optimized primer annealing temperature had to be chosen by the help of the "Tm – Calculator" from NEB (http://tmcalculator.neb.com) and established beforehand. PCR samples were run on PeqSTAR PCR Thermocyclers (PeqLab VWR, Germany) and afterwards stored at 4°C until further processed.

Table 5 PCR program for genotyping PCRs.

PCR Step	Time (s)	Temp. (C°)	Cycles
Heating Lid	∞	To 110	Until End
Initial denaturation	180	95	1x
Denaturation	30	95	
Primer Annealing	30	55-65	35x
Elongation	30	69	
Finish Elongation	300	69	1x
Storage	∞	4	Until End

Table 6 Reaction mix for PCR.

Reagent (Stock)	Volume (µl)
10x ThermoPol Reaction Buffer	2,5
dNTP's (5mM)	1
Primer Fwd (7,15 µM)	0.5
Primer Rev (7,15 µM)	0.5
Taq DNA ThermoPolymerase (5,000 units/ml)	0.125 (0.25 U/µl)
Isolated gDNA template	2
Nuclease-free dH20	To 25

2.4.3 Gel electrophoresis for DNA separation

Products from PCR were separated by size (in bp) and were visualized by agarose gel electrophoresis. Therefore 1-3 % agarose gel (Table 7) was prepared with 1x TAE buffer containing 0.5 µg/ml ethidium bromide (Roche, Germany) in an appropriate electrophoresis gel chamber. PCR samples were mixed with loading buffer. PCR-Products were mixed 6:1 with DNA- Loading dye and loaded to the solidified agarose gel, then subjected to electrophoretic separation according to size of PCR products for 20 - 40 min at 120 V in a chamber. Gel was placed in an electrophoresis gel UV imaging system/Transilluminator, illuminated with 300 nm UV light, and observed with Azure software to take a picture for further analysis. The size and the approximate concentration of the DNA bands was determined by comparison with standardized molecular weight markers (DNA ladder; NEB, England). Genotype was evaluated according to expected band size and DNA size marker loaded together with biopsy samples.

Table 7 Agarose gel concentration.

Agarose content in gel	Suitable for PCR-Product size
1.0 %	500–10.000bp
2.0 %	50–2.000bp
3.0 %	20-500bp

2.5 Tissue preparation

2.5.1 Anesthesia of animals

Mice were anaesthetized via isoflurane-inhalation or i.p. by Ketavet/Rompun mixture. For short treatments mice were narcotized only briefly in a semi-isolated chamber. For longer treatments (e.g., repeated blood sampling from the tail) a Univentor 410 anesthesia unit was used assuring a permanent supply of 3.0 - 4.5 % isoflurane (adjusted to the size of the respective animals). Animals were always under permanent

observation and if necessary, the mouse was subjected to additional inhalation of isoflurane. Before any treatment, the level of anesthesia was validated by pain and reflex tests on tail, hind and front paws, by pinch with sharp forceps. In case of total loss of response to pinching, treatment was started. For terminal anesthesia, animals were left under the respective isoflurane concentration and an overdose of Ketavet/Rompun mixture was applied. As soon as breathing stopped and cardiovascular failure occurred, mice received a cervical dislocation by hand to ensure a final death.

2.5.2 Animal perfusion

For immunohistochemistry and -fluorescence, mice were anaesthetized by an overdose of isoflurane-inhalation or i.p. injection of Ketavet/Rompun mixture. First, the thorax was opened laterally, the heart punctured at the right atrium, to release pressure induced by perfusion. Infusion needle was injected in the left ventricle, then blood was removed by 50 ml 0.9 % NaCl, infused via a tube-pump (2.5ml/min). In a second step, 50 ml ice-cold 4 % paraformaldehyde (PFA) was infused for permanent fixation of the tissue.

2.5.3 Organ sectioning and cryoprotection

Brains of sacrificed animals were isolated and transferred to 4 % PFA for 24 hours at 4°C. Afterwards, brains were transferred into 30 % sucrose. After a few days, brains were tagged onto a small bed of TissueTek® O.C.T Compound and cut into 40 µm sections on a Leica Cryostat/Leica-Microtome at -22°C surface temperature. Slices were stored in cryoprotection solution (25 % ethylene glycol, 25 % glycerin, and 0.05M phosphate buffer) in 96-well plates at 4°C, before organ slices were stained via immunohistochemistry free floating in 12-well dishes.

2.5.4 Trunk blood collection and plasma isolation

Before sample collection, mice were habituated to the room at least 3 weeks to prevent stress effects originating from habituation events. Blood was collected in another room to prevent body fluid odors distracting the mice and leading to CORT masking effects. Mice were decapitated two to three hours after the dark phase. Trunk blood was collected in MiniCollect® EDTA-coated tubes and stored on ice. Samples were centrifuged at 1000 xg for 15min at 4°C to separate plasma from cell bodies and lipid layer. The upper plasma phase was taken and stored at -80°C for later use.

2.6 Histology / Immunofluorescence

Table 8 Self-made buffers and solutions for histology.

Buffer/Solution	Component	Final concentration
0.1 M Borate Buffer pH 8,5	Boric Acid 5N NaOH ddH20	3.08 g 5N NaOH to pH 8.5 Fill to 500 ml Volume
Cryoprotection solution (CPS)	Glycerol Ethylenglycol PO4	25 % 25 % 0.1 M
0.1 M Phosphate Buffer	NaH2PO4 x 2H2O Na2HPO4 x 1H2O ddH2O	3.18 g 13.73 g Fill to 1 l Volume
Saccharose 30 %	Saccharose 0.1 M PO4	150 g 400 ml
10x Tris buffer solution (TBS)	Trizma HCl Trizma Base NaCl ddH20	264,40 g 38,80 g 180 2 l
1x TBS	10x TBS ddH20	100 ml 900 ml
1x TBS+	1x TBS Triton X-100 (10 %) Donkey serum	96 ml 1 ml (0.1 %) 3 ml (3 %)
0.6 % H_2O_2	1x TBS 30 % H_2O_2	40 ml 0.8 ml
2N HCl	12N or 37 % HCl ddH20	41.25 ml 8.25 ml

2.6.1 DAB-labeling of BrdU-positive cells

All incubation steps, except for HCl, were performed on an orbital shaker at 150 rotations/minute. Organ slices were moved by brush from CPS-filled wells to a Corning® Netwells® net inserts-equipped 12 well plates filled with Tris-buffered saline (TBS) solution. Slices were washed 2 times for 5 min each. TBS was replaced by 0.6 % H202 for 30 min to block endogenous peroxidase activity within the cells, with light protection. Slices were then washed 3 times for 5 min each in TBS. Afterwards, the nucleus was permeabilized and DNA was hydrolyzed with 2N HCl for 20 min inside a water bath at 37°C. Net inserts were dried on paper towel to remove remaining HCl, before placing them in 0.1 M borate buffer, pH 8.5 at RT for 10 min, followed by

washing 6 times in TBS for 7 min each. Blocking in TBS+ for 30 min was subsequently followed by the 1st AB incubation with BrdU anti-rat at 4°C, o.N. , shaking, dilution 1:500 in TBS+ in 24-well plates (300-400 µl volume).Brain slices were moved the following day into 12-well plates with nets and washed 2 times for 15 min with TBS. Next, slides were blocked 15 min with TBS+ and 2nd AB, biotinylated anti-rat (1:250), was applied for 2 hours at RT. Samples were washed three times 5 min in TBS and transferred into 30 min before prepared ABC-solution (Vectastain, according to manual) for 1 hour at RT. After avidin biotin complex intercalation, samples were washed three times 5 min and DAB-solution (Vectastain, prepared according to manual) was added quickly to all samples and incubated until a brownish staining was detectable on slices, 3-7 minutes. Reaction was stopped immediately with tap water followed up by 3 times washing and shaking with tap water for 5 min each, subsequently two times by TBS for 5 min each. Samples were stored in 0.1M PO4 and mounted onto glass-slides; briefly drying, and incubation in 200 µl Neo-Clear on Xylene basis (Roche, Germany) per slide for 10 min and coverslipped with Neo-Mount (Roche, Germany).

2.6.2 Immunofluorescence of BrdU-positive cells for phenotypic analysis

Brain slices for immunofluorescence labeling were washed 2 times á 5 min in TBS solution. Permeabilization and blocking of tissue was done in TBS+ for 30 min at RT, while orbital shaking at 100 turns/min. Afterwards TBS+ diluted primary antibodies (Table 8 and Table 47) were added onto the tissue and incubated at 4°C o.N. The next day, tissues are washed three times for 5 min and blocked in TBS+ for 15 min at RT on a shaker. Secondary antibodies were applied, light protected and incubated at RT for four hours. Finally, slices were washed three times in TBS, stored in 1 M PO_4 and mounted on glass slides with self-made PVA-DABCO (polyvinyl alcohol with diazabicyclooctane) or Vectashield hardset medium without DAPI.

Primary antibodies were applied in the following concentrations: anti-BrdU (rat, 1:500; Biozol), anti-doublecortin (DCX; goat, 1:250; Santa Cruz Biotechnology), anti-GFAP (rabbit, 1:2000; Acris Antibodies), anti-GFAP (mouse, 1:1000; Sigma-Aldrich), anti-Sox2 (goat, 1:500; Santa Cruz Biotechnology), anti-iba1 (rabbit, 1:500; Wako), anti-Caspase3 (rabbit, 1:500; Cell Signaling Technology, see also Table 47). For immunofluorescence, Alexa488-conjugated, Cy3-conjugated, Cy5-conjugated, or Alexa647-conjugated secondary antibodies (Jackson ImmunoResearch Laboratories) were used at a concentration of 1:250 (Table 48).

2.6.3 Quantification of cell proliferation and survival

BrdU-positive cells of the granular cell layer between hilus and molecular layer were counted in every sixth section along the rostral-caudal axis of the DG. Numbers of BrdU-labeled cells per hemisphere were multiplied by 6 to obtain the total number per DG. If sections were not analyzable, due to damage, or missing, the average number of BrdU+ cells per counted slides was filled in. Images were obtained at Keyence Biorevo fluorescence microscope with a PlanApo 40X NA 0.95 (width 0.14 mm) or PlanApo 20x NA 0.75 (width 1.00 mm) objective lenses and quantification was done manually using the of Keyence BioAnalyzer software.

2.6.4 Tunnel cell death staining

Protocol was adapted from the manual of the In-Situ Cell Death Detection Kit, TMR red or TMR green, provided by Sigma-Aldrich (Germany).

Free floating sections were additionally fixated with 4 % PFA for 20 min at RT. Remaining fixation solution was washed off 3 times 10 min with TBS and then permeabilized in TBS+ solution for 5 min on ice (+2 to +8°C). A fixed and permeabilized negative control section was incubated, in Label Solution (without terminal transferase) instead of TUNEL reaction mixture. Furthermore, an incubated fixed and permeabilized positive control treated with recombinant DNase I was generated to induce DNA strand breaks prior to labeling procedures. 50 µl TUNEL reaction mixture (from Kit 1:10, 50µl of enzyme solution to 450 µl label solution) was applied on samples and covered with parafilm for 1h of incubation in a humidified incubation chamber at +37°C in the dark. Sections were rinsed 3 times with TBS. Samples were either embedded in anti-fade Vectashield Hardset without DAPI and directly analyzed under a fluorescence microscope by use of excitation wavelength in the range of 520-560 nm (maximum 540 nm; green) or subjected to additional follow up immunohistochemistry as described earlier.

2.7 ELISA

2.7.1 Standard curve calculation for endocrine HPA-parameters

CORT and ACTH values were taken from plasma from trunk blood using IBL CORT ELISA kit (Human, Rat, Mouse), and IBL ACTH ELISA kit (Human, Mouse). All reagents were unfrozen on ice and then acclimatized to RT at least 10 min before usage. Tissues of all experimental groups were always measured in the same respective assay to minimize the influence of unavoidable inter-assay variances between experiments. Each plasma / tissue sample, standard and control was validated in duplicates, if possible, in triplicates. To generate a calibration curve, the 4th order polynomial regression

$$Y=B0 + B1*X + B2*X^2 + B3*X^3 + B4*X^4$$

was used for at least 5 standard-values (GraphPad Prism 5). Regression curves always needed to have a significance ($p<0.050$) R2-value above 0.90. If R2-value had not reached the significant value, a polynomial regression of the next lower order was chosen, until a significant R2-value could be obtained. Coeffecients (B) were automatically determined by Prism for a good curve fit.

2.7.2 BDNF

BDNF values were measured in liquid-nitrogen shock-frozen wet tissues of dissected PFC and HC with the adapted version of BDNF Emax® ImmunoAssay System (Promega). The BDNF-ELISA was performed according to the kit's manual but the manufacturer's instructions were adapted to a highly sensitive fluorometric technique as described in Hellweg *et al.* [512,513] at Charité, Berlin in the laboratory of Prof. Dr. Rainer Hellweg. BDNF content was expressed as equivalents of recombinant human BDNF.

2.7.3 CORT / Glucocorticoids

The corticosterone ELISA was performed according to the kit's manual. Appropriate dilutions in blank / 0 nmol/l standard were prepared 1:5 up to 1:10. Capture antibody pre-coated wells were filled with 20 µl of either sample, standards (0, 5, 15, 30, 60, 120, 240 nmol/l), or control-solutions. After adding 200 µl enzyme-conjugate to the solution plates were orbital shaken at 150 turns/min for 30 sec and incubated for 60 min at RT, followed by three washing steps. Afterwards, 100 µl substrate (TMB) was incubated in the well for 10 min at RT. The reactions were terminated by adding a 50 µl stop-solution and spectrometric measurement was done with 15 detection flashes

per well at 450 nm in a micro-plate reader (TECAN, Germany). With prior horizontal shaking at 3.5 mm amplitude for 1.5 sec. Measurement was performed three times and the mean was calculated.

2.7.4 ACTH

The ACTH ELISA was performed according to the kit's manual. Appropriate dilutions in conjugate diluent were 1:3 up to 1:10. Capture antibody pre-coated wells are filled with 200 µl of either samples, standards (0, 11, 28, 69, 172, 431 pg/ml) or control-solutions. After adding 25 µl enzyme-conjugate to the solution plates were incubated for 60 min at RT while being shaken at 150 turns/min, followed by 5 washing steps. Afterwards 200 µl substrate (TMB) was incubated in the well for 20 min at RT. The reactions were terminated by additional 50 µl stop-solution and spectrometric measurement was done with 15 detection flashes per well at 450 nm with a reference filter of 620 nm or 650 nm, in a micro-plate reader (TECAN). With prior horizontal shaking at 3.5 mm amplitude for 1.5 sec. Measurement was performed three times and mean was calculated.

2.8 qPCR for mRNA expression of HPA-Axis parameters

2.8.1 Complementary DNA (first strand) synthesis

For complementary DNA (cDNA) synthesis, 1 µg of RNA was used in a reverse transcription with a prior DNA digestion by DNAseI treatment. 1 µg RNA was first digested with a mixture of 1 U/µg DNAseI, 20 U/µg RNAsin RNAse inhibitor and 10x DNAseI reaction buffer (Table 9). A PCR-thermocycler was used to incubate at 25°C for 30 min, to digest remaining DNA and reaction was stopped at 75°C for 5 min (Table 10). The needed amount of treated RNA (default 1 µg) was mixed with 0.5 µg Random Hexamer Primers (Thermo Fischer, USA) for each µg used RNA, filled up to 20 µl H20 and incubated 5 min at 70°C to melt down RNA secondary structures, subsequently cooled at 0°C minimum of 5 min to prevent reformation of secondary structures (Table 11). Reverse transcription was done in a final volume of 20 µl reaction mix (Table 13) by Moloney Murine Leukemia Virus Reverse Transcriptase (M-MLV RT, Promega, USA) in a thermocycler with the program for cDNA synthesis shown in Table 12. Samples were stored in -20°C for later use.

Table 9 Reagents for DNAse treatment.

Reagent (Stock)	Volume (µl)
10x DNAseI Reaction Buffer	1.5
DNAseI recombinant 10 U/µl	0.5 (5 U)
Recombinant RNasin® Ribonuclease Inhibitor 25 units 50 U/µl	0.5 (25 U)
H20	to 20

Table 10 Cycler program for DNAse treatment.

PCR Step	Time (s)	Temp. (C°)	Cycles
Heating Lid	∞	To 110	Until End
Incubation/ DNA denaturation	1800	25	1x
DNAse Inactivation	300	75	1x

Table 11 Cycler program for breaking secondary RNA structures.

PCR Step	Time (s)	Temp. (C°)	Cycles
Heating Lid	∞	To 110	Until End
Melting secondary structures	300	70	1x
Cooling	300	0	Until End

Table 12 Cycler program for reverse transcriptase.

PCR Step	Time (s)	Temp. (C°)	Cycles
Heating Lid	∞	To 110	Until End
Priming	900	25	1x
Reverse transcription	3600	37	1x
M-MLV inactivation	900	70	1x

Table 13 Reaction mix for reverse transcriptase.

Reagent (Stock)	Volume (µl)
M-MLV 5X Reaction Buffer 5 µl	4
dNTPs 10 mM	1.25
M-MLV (10.000 U)	0.8 (200 U)
Recombinant RNasin® Ribonuclease Inhibitor 50 U/µl	0.5 (25 U)
H20	to 20

2.8.2 Quantitative Real-Time PCR (qRT-PCR / qPCR)

qRT-PCR was performed in order to quantify mRNA levels of genes of interest in diverse brain regions and organs. cDNA was diluted to 2 ng/µl with ddH20, and the qRT-PCR reaction Mix was prepared with GoTaq® qPCR Master Mix and CXR reference dye solution (Table 14). Reactions were prepared in duplicates for each gene of interest. qRT-PCR reaction was performed in a MicroAmp® Optical 384-Well Reaction Plate and measured at QuantStudio 5 Thermocycler (Table 15). Primer annealing temperatures between 55°C and 65°C had to be tested and established in advance by the use of the help of the "Tm – Calculator" from NEB

(http://tmcalculator.neb.com). QuantStudio™ Design & Analysis Software v1.4.3 was used to set Ct values for the respective genes. Threshold was determined automatically by QuantStudio™ software. If done manually, the threshold was set in the steepest exponential phase of amplification (using log scale for fluorescence). Relative gene expression of target genes, Knockout normalized to WT, was calculated by using the common 2^{-ddCt} method [514]; with *28S, GAPDH* and *tbp1* as reference genes (Table 49).

Table 14 Reaction mix for quantitative RT -PCR.

Reagent (Stock)	Volume (µl)
GoTaq® qPCR Master Mix	5
Forward Primer 5 µM	0.2
Reverse Primer 5 µM	0.2
CXR Reference Dye	0.1
cDNA (1 ng/µl)	4.5

Table 15 qRT-PCR program for gene expression analysis.

qPCR Step	Time (s)	Temp. (C°)	Cycles
Priming	120	50	1x
Initial denaturation	600	95	1x
Denaturation	30	95	35x
Primer Annealing	60	55-65	
Melt Curve			
Step 1	15	95	1x
Step 2	60	60	1,6C/s decline
Step 3 (Dissociation)	15	95	0,075C/s increase

2.8.3 Spectrometric measurement of nucleic acid concentration

Genomic DNA and genomic RNA concentration and purity were measured using a NanoDrop 1000 microvolume spectrophotometer. 1 µl of the respective nucleic acid solution in ddH2O was positioned at the sensor and optical densities (OD) at 230, 260 and 280 nm were measured. ddH2O was used to initialize and re-blank the instrument. Nucleotide concentrations were calculated with the modified Beer-Lambert Equation, with a focus on a 260/280 and 260/230 nm ratio, close to 2, which declares purity of the sample.

$$c=(A*e)/b•$$

- ***c*** is the nucleic acid concentration in ng/µl
- ***A*** is the absorbance in AU (260 for concentration, nm)
- ***e*** is the wavelength-dependent extinction coefficient in ng-cm/µl
  dsDNA:50ng-cm/µl; ssDNA:33ng-cm/µl, gRNA:40ng-cm/µ
- ***b*** is the path length in cm

2.9 Behavioral testing

All animals have been habituated to the experimental rooms for at least one week before the test was performed. Cage interior and enrichment was standardized in location and order, one week before. Amount of bedding per cage was standardized to 0.5 cm height. Water, food, and cage renewal was limited to one time per week on the same day and time. During all experiments animals were under (indirect) visual observation to terminate tests in case of emergency. Videos/Pictures were recorded with a Sony α37 and an Ø=55mm objective on a mount from min. 45 cm distance or a Sony CCD IRIS with 55 cm, Audio recordings were done with Ultrasound Sonoplus microphones with a distance of maximum 20 cm.

2.9.1 Elevated O-Maze

Elevated plus maze is a common method to indicate anxiety in rodents [515]; subjecting them to open spaces (as opposed to closed arms) to trigger inherent fear to be accessible to predators. A grey plastic annular runway (width 6 cm, outer diameter 46 cm, 50 cm above ground level, illuminated with 25 Lux) was covered with black cardboard paper to prevent animals slipping off the maze. Two opposing sectors were protected by inner and outer walls with a height of 10 cm. With beginning of each trial, animals were placed in one of the protected sectors facing the exit of the sector. Latency to first exit, number of exits and total time spent in the open compartments were measured over 5 min as described earlier [516,517]. Explorative stretching into an arm was not counted as an entry. After each trial, the experimental setup was cleaned with 70% EtOH to prevent odor marks, which could distract the following mouse. Activity monitoring was conducted 5 min via a video camera (Sony CCD IRIS). The resulting data were analyzed using the image processing system Etho-Vison 1.96 (Noldus Information Technology, Netherlands).

2.9.2 Open field

A large arena made of white non-transparent acrylic glass (50x50x15 cm) under dimmed light conditions (25 Lux) was used as an open field to measure locomotor activity and anxiety levels [518,519]. The middle (20 cm diameter, 15 cm off walls) was marked with a cross. At the start of each trial, the mouse was placed into one corner, and activity and crossing were measured. Time spent in the center and close to the walls was monitored. After each trial, the experimental setup was cleaned with 70 % EtOH to prevent odor marks for the next mouse that could mask following results. Activity monitoring was conducted for 10 min for the ECT experiment, and over 5 min

when SSRI was administered. Activity monitoring was conducted by video camera (Sony CCD IRIS, Japan). The resulting data was analyzed using the image processing system Etho-Vison 1.96 (Noldus Information Technology, Netherlands).

2.9.3 Forced swim test

The Forced swim test was applied to measure depressive-like behavior by assessing the tendency to give up the attempt to escape from an unpleasant or threatening environment, as originally described by Porsolt (Porsolt forced swim test) [520]. For this purpose, mice were placed into a glass cylinder (23 cm height, 13 cm diameter) filled with water (21°C) up to a height of 8 cm. Within a period of 6 min onset and time of floating ("giving up") was determined as immobility time in seconds. Mice floating motionless in water or performing only faint movements to keep the respiratory tract beyond reach of the water. Activity monitoring was conducted 5 min via a video camera (Sony CCD IRIS, Japan). The resulting data were analyzed using the image processing system Etho-Vison 1.96 (Noldus Information Technology, Netherlands)

2.9.4 Nesting behavior

Nesting is a standardized experimental behavior setup according to Deacon 2006 [502]. Empty cages (35x20x13 cm, max. 5 animals) were filled with 80 g of bedding, water and chow *ad libitum* and a lid. Mice were habituated to the room at least for one week in group housed conditions at the same spot, where the nesting experiment was going to be done. After habituation to the room, mice were separated into single housed condition (smaller cages, 20x20x13 cm; 20 g of litter) and a fresh 5x5 cm nestlet (Ancare, USA), beginning 6 hours before dark phase, was introduced for 3 hours per day for two consecutive days during light phase. On day 3, a new nestlet was introduced into the cage, and after the last day of nestlet habituation, one hour before dark phase, a new nestlet was positioned in the upper right corner and kept with the mice o.N. (single housed). Nests were analyzed the next morning; weighed and rated according to nesting score 1-5 (a-e) shown below (Table 16 & Figure 19; half points were added if a nest hollow was spotted next to the nestled in the bedding, or subtracted if a criteria of a score was just failed; i.e.: clearly round nest with high walls but less than 90 % material was used = 4.5 instead of 5). Pictures were taken with the use of a Sony α37 camera (Sony, Japan).

Table 16 Nesting Scores according to Deacon[502,503].

Score 1 (a) Nestlet not noticeably touched (more than 90 % intact).
Score 2 (b) Nestlet partly torn (50-90 % intact).
Score 3 (c) Nestlet mostly shredded but not identifiable as a nest site: less than 50 % remain intact, but less than 90 % is within a quarter of the cage floor area, i.e., spread around the cage
Score 4 (d) An identifiable but flat nest: 90 % of the Nestlet is torn and material is gathered into a nest within a quarter of the cage floor are, but nest is flat with walls higher than mouse body height (if a mouse curled up on its side) for less than 50 % of its circumference
Score 5 (e) A (almost) perfect nest: more than 90 % of the Nestlet is torn and the nest is a crater, with fluffy walls higher than mouse body height for more than 50 % of its circumference. Mostly in a round and clear shape and mouse can be spotted most of the time inside the nest.

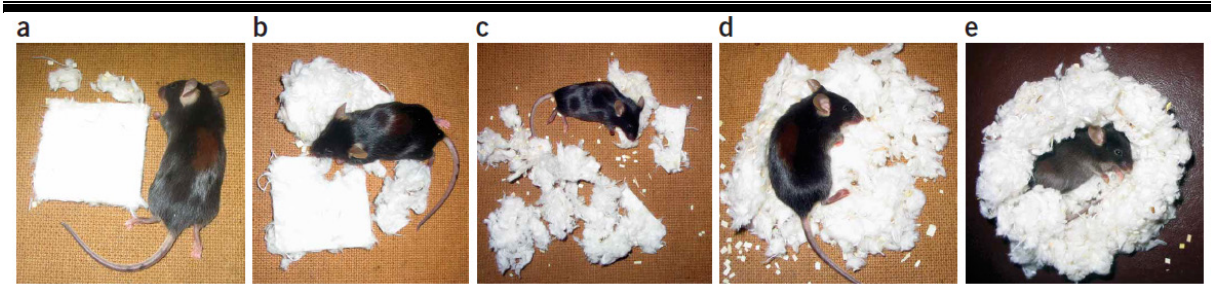

Figure 19 Nesting scores: Nesting scores according to Deacon (2006) [502,503]. Pictures show the score range shown in Table 16 from (a): defines the lowest score of 1 with least nest behavior visible; to (e) defines the highest score of 5 with a clear visible nest structure.

2.9.5 Hoarding

Hoarding method has been adapted from Deacon 2012 [503]. Initially mice were habituated to the testing cage 1 week in advance to make them feel home (Hoarding cage, Figure 51) , transparent 40 cm x 22 cm x 15 cm, with a hole on the broadside 1 cm above ground Ø = 4.3 cm, hole median 11 cm to both sidewalls). Cages were filled with typical environment the mice are familiar with (red house, paper roll, soiled hemp nest material and wooden piece from their previous cages). The amount of grain bedding is 90g with a filling height of 5mm. The hole as blocked with a plastic bung during the habituation phase. Water and food were provided *ad libitum* in this week. Two mice were set per cage and run. 100 g food pellets (a mixture of small and large) was placed at the distal end of the hoarding tube. To make sure the mouse is mildly hungry before testing begins, the *ad libitum* chow, but not water was removed 2h before actual test. 2 hours before the start of the dark phase, the bung is removed, to give the two mice per cage access to the hoarding tube. The next morning, 2h after dark phase ends (14h testing), a picture of the cage situation was taken, the remaining food pellets in the tube and the ones hoarded in the cage were weighted separately. Pellets outside the mesh and cage are not counted. Mice were placed back to their original home cages. Pictures were taken with a Sony α37 camera.

2.9.6 Burrowing

Burrowing method was adapted from Deacon 2012 [503]. First mice were habituated to the burrowing tube (Figure 20; Grey plastic tube Ø = 7 cm, l=20 cm with one side open and elevated for 3 cm with metallic screws) two days before experiment, 2h a day starting 4 hours before dark phase, in transparent 40 cm x 22 cm x 15 cm cages with 90g grain bedding (height 5 mm). During test and habituation burrowing tube was filled with 200 g of chow pellets normally used in diet. Alternative housing was not provided. Animals were kept in social groups of three during habituation time inside of the cages and then placed back in their home cage. Tube and cage were cleaned sensitively with 70 % EtOH to extinguish remaining odors. Baseline run was performed two times with 48h in-between, 4h before dark phase with 200 g of chow in the tube. Mice were tested in randomized social group of 3 per genotype/cage. Snapshot views were not taken, to not disturb the mice in their "daily abilities", but mice were observed for the first 30 min in their behavior. Testing with 200g of chow in the tube happened during the dark phase + 2h of light phase, then a picture of the cage was taken and the amount of pellets left in the burrowing tube was measured and mice were placed back to their original home cages. Pictures were taken with a Sony α37 camera (Sony, Japan).

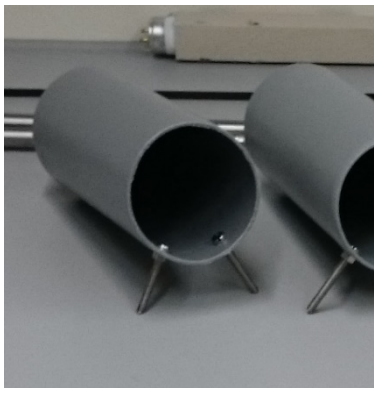

Figure 20 Burrowing tube

2.10 Vaginal smear analysis to determine estrus cycle stages

Method was adapted from Shannon *et al.* 2012 [521] .To evaluate the estrus cycle in C57 BL6/N and *Tph2*$^{-/-}$ females 5 min post mortem, vaginal smear was taken. Vaginal smear analysis can distinguish between cycle stages (proestrus, estrus, metestrus, and diestrus) based on cell composition [311] (Figure 21). A pipette with 10 µl PBS was used to rinse the outer part of the vagina. PBS was pipetted up and down 3 times. The solution was thereafter transferred on a super frost glass slide and stained with a Quick Stain Kit (Kwik-Diff, Thermo Scientific, USA) after brief drying. This method was performed in collaboration with Dr. Elena Popova (Bader research team at MDC).

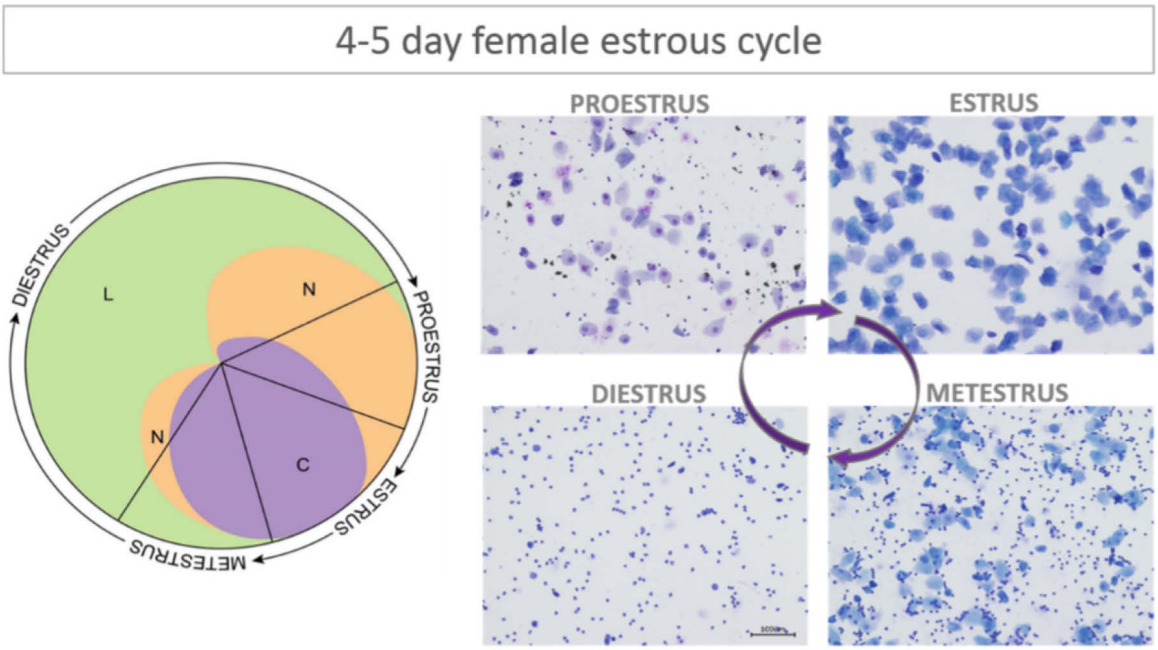

Figure 21 Cell composition in vaginal smears during the 4 different estrous cycle stages of WT female mice: (l) cake diagram of the 4-5 days estrous cycle with all different estrous stages. Colored area indicates approx. timeframe, certain cell type typical for the stage are occurring. (r) Cell types marked with a quick stain kit: Nucleated epithelial cells in proestrus (N, orange), cornified cells in estrus (C, violet), leukocytes mainly in diestrus (L, green), and metestrus showing all 3 type of cells. Figure taken from PhD-Thesis of Cornelia Hainer [311,521].

2.11 Statistical analysis

> "*Everybody believes in the [Gaussian distribution]: the experimenters, because they think it can be proved by mathematics; and the mathematicians, because they believe it has been established by observation.*"
>
> -W. Lippmann

Statistical analysis was performed using Prism 6 (GraphPad) software. Results are presented as mean ± SEM, to quantify the precision of the mean, as representation of the variance of the used mice models. For all tests, the rejection threshold of the null hypothesis, p-values were set as described in Table 17.

Since different groups within one experimental data set happen to be both: Gaussian and non-Gaussian distributed, non-parametric tests were applied first, then if the majority in the group follows normality, a respective parametric test was applied.

Table 17 p-Value significance levels.

Indication p-value	Significance term
ns > 0.05	not significant
* ≤ 0.05	significant
** ≤ 0.01	highly significant
*** ≤ 0.001	extremely significant

Data-sets were assumed to be non-parametric with a small sample size, unless analyzed for a proper Gaussian-distribution by using D'Agostino & Pearson omnibus normality test (by default), Shapiro-Wilk, and Kolmogorov-Smirnov-test (For small n<4) [522]. For numerical identification of outliers, the mean of an experimental group, e.g., the number of proliferating cells per DG for n>5 animals, was calculated and two times the interquartile range was added (standard deviation, outliers above third quartile), as well as subtracted (outliers below third quartile). The data point outside this calculated range or the animal, respectively, is excluded from the analysis. Moreover, since non-parametric tests, especially in low group sample sizes (n<10) indicate a low power, to exclude false negative interpretation and according to the Central Limit Theorem, the distribution within an experimental group can also be expected to follow biological Gaussian distribution, since mice come from the same background, age and husbandry and in larger populations, results are expected to come closer to a normal distribution. Therefore, statistics indicated in plotted figures represent, (if not stated differently in legend) parametric statistical tests. If groups of small sample sizes in biomedical experiments are considered to be statistically or biologically normally distributed, both non- and parametric statistics are calculated and compared to detect statistical misinterpretation. Analyses of two groups is performed using Student's *t*-test (parametrical test for unpaired data), after checking for homologous or heterologous variance using previous indicated test. A Mann-Whitney U-Test (for non-parametric data) was used when no Gaussian distribution is given (and Student's *t*-test is not applicable). For comparison of the mean involving more than two groups (e.g., interaction, genotype x condition), Analysis of variance (ANOVA, One-way or two-way) was performed. ANOVA was followed by *post hoc* tests, e.g. Tukey's *post hoc* for parametric, Bonferroni for non-parametric data groups, or Dunnett's, when groups would be compared with one control.

2.12 Miscellaneous software

Photos were taken with a private α37 DSLR - Sony with default stock Ø = 55mm objective. For illustration and graphics, Prism 6 (GraphPad) and open-source software Inkscape V 0.94 were used, to create figures in the final .png format. Post picture processing as done with the open source software GIMP 2.4, to convert to the final .png/ .tiff format for embedding.

3 Results

3.1 Comparison of the physiological effects mediated by SSRI vs. SSRE treatment

3.1.1 The effects of the SSRI CIT on adult neurogenesis in *Tph2*$^{-/-}$ mice and control

To evaluate whether serotonin plays a role in the SSRI-related effects on adult neurogenesis, as has been shown by Malberg in 2000 [124], 6-week-old female *Tph2*$^{-/-}$ mice and their *Tph2*$^{+/+}$ littermates were subjected to 21 days of CIT treatment; 0.9 % saline for control groups, respectively. Prior treatment, animals were injected with 50 mg/kg BrdU to label dividing cells, and to detect their survival during the treatment period. Surprisingly, after daily saline injection, the number of BrdU-positive cells in the SGZ of the DG was significantly higher in *Tph2*$^{-/-}$ mice compared with control (n = 5, *Tph2*$^{-/-}$ 496 ± 55 cells vs. *Tph2*$^{+/+}$ 185 ± 27 cells; One-way ANOVA $F(3,14)=7{,}827$, $p = 0.0026$ followed by Tukey's *post hoc* test $p<0.01$, if values are considered as biologically normally distributed (Figure 22 + Table 18)). SSRI CIT resulted in an increase in the survival of BrdU-positive cells in *Tph2*$^{+/+}$ mice (n = 5, 279 ± 13 cells vs. 185 ± 27 cells; Student's *t* test $p = 0.0177$); no difference was seen between *Tph2*$^{-/-}$ mice compared to saline injections (n = 6, 416 ± 64 cells; Figure 22 + Table 18). Since

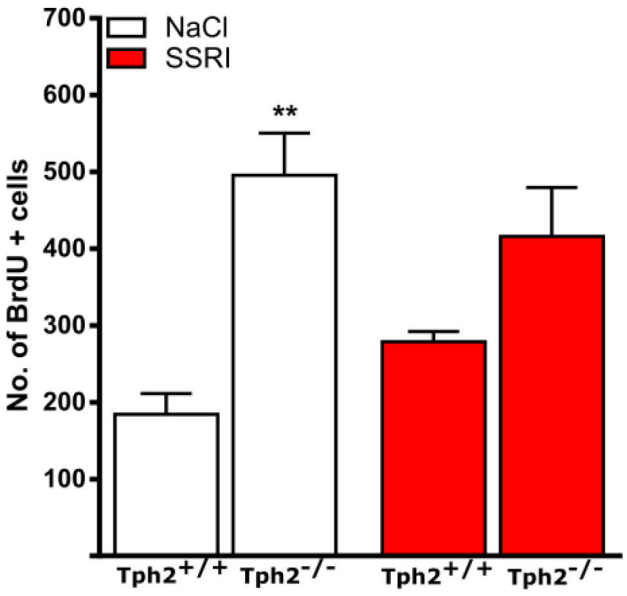

Figure 22 Survival of BrdU-labeled cells in the SGZ of the DG in the hippocampus after 21 days of SSRI CIT or saline treatment in *Tph2*$^{+/+}$ and *Tph2*$^{-/-}$ mice. After daily saline injection, a significant increase in the number of surviving cells was observed in *Tph2*$^{-/-}$ mice compared to littermates; SSRI treated *Tph2*$^{-/-}$ animals showed an insignificant trend for increased BrdU+ cell levels. One-way Anova with Tukey's-*post hoc* test, **p < 0.01.

Table 18 Mean + SEM + n: No. of average BrdU+ cells in a SGZ of the DG in HC after 21days i.p. treatment

Group	No. BrdU positive cells	SEM	n
Tph2$^{+/+}$ NaCl	185	27	5
Tph2$^{-/-}$ NaCl	496	55	5
Tph2$^{+/+}$ CIT/SSRI	279	13	5
Tph2$^{-/-}$ CIT/SSRI	416	64	6

Tph2$^{+/+}$ control mice are supposed to be comparable with regular WT *C57BL/6N* mice, a more pronounced effect of the SSRI on adult neurogenesis was expected (based on earlier studies using FLX) [124,126,183,187]. Furthermore, testing for normally distributed data, the Kolmogorov-Smirnov test failed to reject the null hypothesis for knockout mice while the null hypothesis was rejected for littermates. In addition, the increase in neurogenesis in *Tph2*$^{-/-}$ animals after saline treatment compared to *Tph2*$^{+/+}$ was unexpected; our own previous studies had not shown any effect on baseline neurogenesis in *Tph2*$^{-/-}$ mice [125]. The daily treatment of the animals (with saline or SSRI) may have triggered chronic stress mechanisms and thereby caused alterations in neurogenesis in particular in *Tph2*$^{-/-}$ animals. The experiment was repeated in addition to treatment with SSRE (see 3.1.3).

3.1.2 Cell survival w/o treatment

In an attempt to address the increased number of cells after saline treatment, another group of 6-week-old female *Tph2*$^{+/+}$ and *Tph2*$^{-/-}$ mice were kept for 21 days unhandled (except for initial BrdU injection and regular animal husbandry; Figure 23 + Table 19). Here, data show that daily i.p. saline injection increased the number of surviving cells in the SGZ of the DG of *Tph2*$^{-/-}$ mice (227 ± 43 vs. 512 ± 100 cells) while unhandled

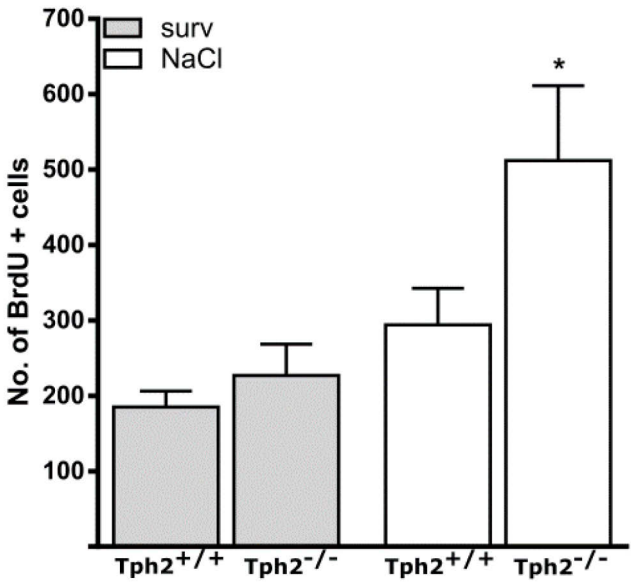

Figure 23 Baseline survival of BrdU-labeled cells in the SGZ in the DG after 21 weeks in unhandled and saline-treated female *Tph2*$^{+/+}$ and *Tph2*$^{-/-}$ animals: In *Tph2*$^{-/-}$ mice, daily i.p. saline injection showed a significant increase in surviving cells compared to unhandled controls (surv.); *p<0,05 in One-way ANOVA with Tukey's-*post hoc*-test).

Table 19 Mean + SEM + n: No. of average BrdU+ cells in a SGZ of the DG in HC after 21days i.p. treatment / no treatment

Group	No. BrdU positive cells	SEM	n
Tph2$^{+/+}$ survival / baseline	185	21	6
Tph2$^{-/-}$ survival / baseline	227	42.58	3
Tph2$^{+/+}$ NaCl	294	85	3
Tph2$^{-/-}$ NaCl	512	100	7

animals had cell numbers comparable with littermates (One-way ANOVA F (3, 18) = 4.263 followed by Tukey's *post hoc* test, *p = 0.0193)*. For both experiments, ANOVA followed by Tukey's *post hoc* test is used based on parametric distribution.

3.1.3 The effects of the SSRE TIA on adult neurogenesis in *Tph2*$^{-/-}$ mice and control

In a third experiment, the CIT injection paradigm was repeated, in addition to testing the new clinically used drug TIA, a SSRE. 6-week-old female *C57BL/6N* (WT) mice were used as control animals, due to unavailability of appropriate littermates. Mice were treated according to the approaches above, with 21 daily i.p. injections of 0.9 % saline, SSRI or SSRE. Since not enough *Tph2*$^{-/-}$ animals were available, SSRI treatment was only repeated for wild type mice, whereas SSRE treatment was subjected to both groups.

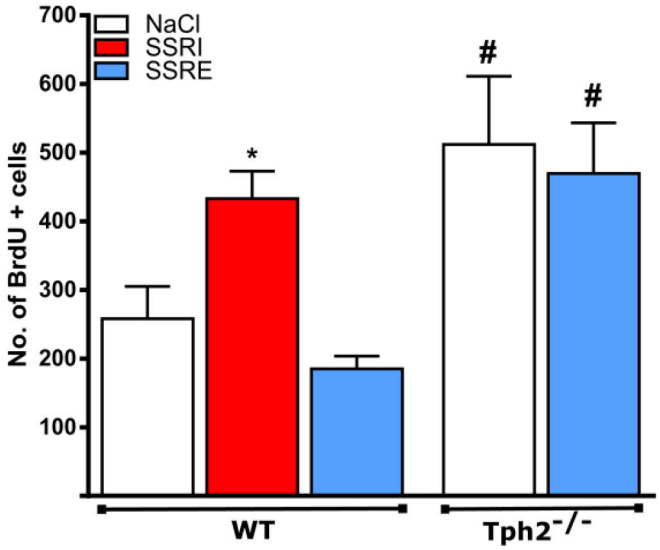

Figure 24 Survival of BrdU labeled cells in the SGZ in the DG after 21 days of treatment with saline (white), SSRI (red), or SSRE (blue) in female WT and *Tph2*$^{-/-}$ mice: SSRI increased the number of surviving cells in WT, while SSRE had no effect. In *Tph2*$^{-/-}$ groups, higher cell survival than WT saline control was observed. One-way ANOVA $F(5,27)=5.018$, $p = 0.0022$ followed by Tukey's post hoc test *p<0,05 to saline control and #p<0.05 to saline WT and SSRE WT, respectively.

Table 20 Mean + SEM + n: No. of average BrdU+ cells in a SGZ of the DG in HC after 21days i.p. treatment.

Group	No. BrdU positive cells	SEM	n
C57BL/6N WT NaCl	258	47	6
Tph2$^{-/-}$ NaCl	513	100	7
C57BL/6N WT CIT/SSRI	433	40	5
C57BL/6N WT TIA/SSRE	185	19	6
Tph2$^{-/-}$ TIA/SSRI	470	73	6

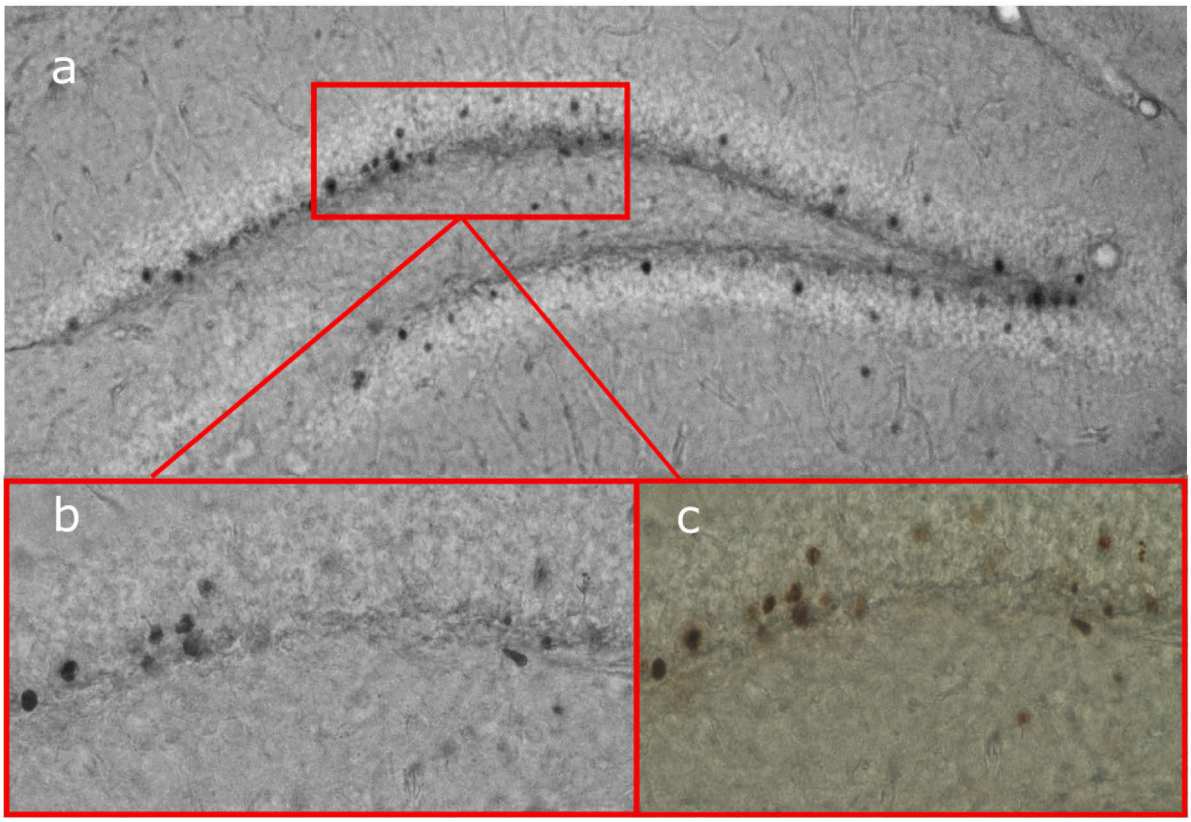

Figure 25 Dentate gyrus of a saline treated *Tph2*$^{-/-}$ mouse. (a) Full focus monochromatic 200x magnification of a representative dentate gyrus in 40 µm hippocampus section of a *Tph2*$^{-/-}$ mouse treated with 21-day saline i.p. injections, stained are BrdU+ by DAB-Peroxidase staining in the SGZ. (b) Monochromatic and (c) polychromatic 600x magnification of (a), representing BrdU+ clustering of 3-5 cells, indicating the origin from the same radial glia cell, but also showing granular cell morphology with no clear cell boundaries.

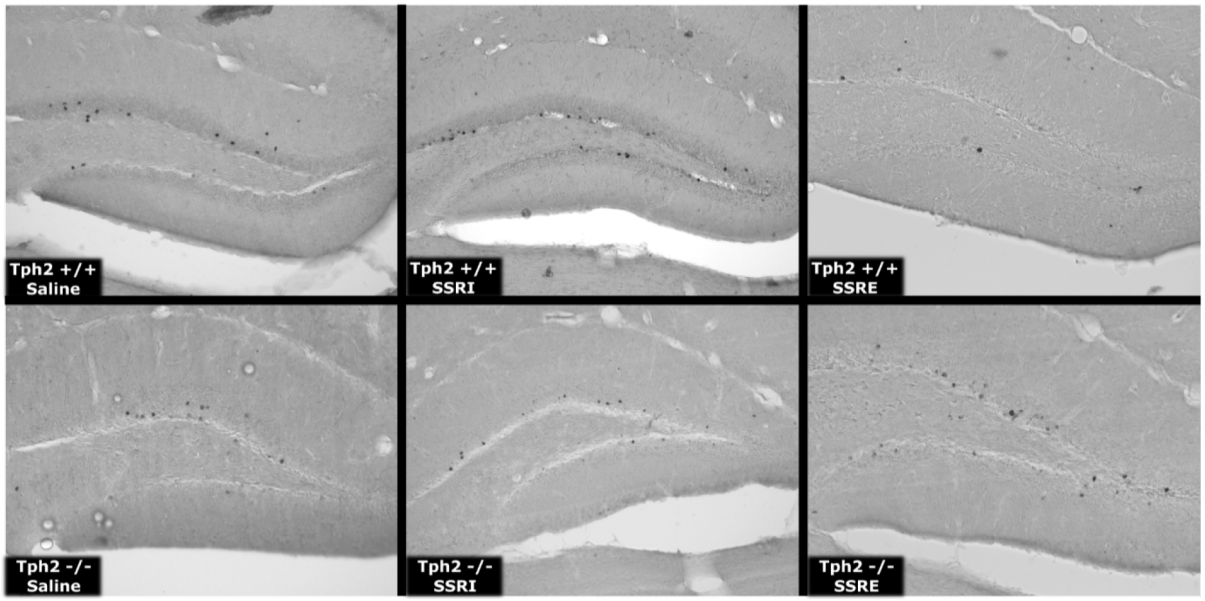

Figure 26 Coronal sections , with DAB-stained DG of the HC (200x magnification) of 21 days i.p. treated mice: (left) Saline, (middle) SSRI CIT and (right) SSRE Tianeptine. Upper row represents *Tph2*$^{+/+}$ animals, the lower *Tph2*$^{-/-}$ groups. The figures exemplify the results stated in Figure 22 to Figure 24. Each black dot inside the SGZ of the DG sections represent a BrdU+ cell.

The results are shown in Figure 24 + Table 20. WT animals treated 21 days with the SSRI CIT showed the typical increase in survival of proliferating cells compared to saline (*n=6, 433 ± 40 cells vs 258* ± 47 cells;). The previously demonstrated increase in

surviving BrdU+ cells in *Tph2*$^{-/-}$ saline treated animals *(n= 7, 512 ± 100 cells)* compared to WT saline treated *C57BL/6N* animals *(n=6, 258 ± 47 cells)*, could be reproduced (Determining for normality for knockout groups revealed normal distribution). The SSRE TIA group showed also a significant increase in cell survival in *Tph2*$^{-/-}$ animals treated for 21 days with TIA (*n=6, 470 ± 73 cells;* One-way ANOVA F (4, 23) = 6.055, *p = 0.0018* followed by *Tukey's post hoc* test *p<0.05 to saline control and #p<0.05 to saline WT and SSRE WT, respectively; Figure 24 and Table 20). SSRE TIA-treated WT animals (*n=6, mean =185 ± 19 cells*) did not show an increase in BrdU+ cells, there was even a trend towards a decrease. Representative pictures of DAB stained BrdU+ cells in the DG of the HC of the above treated animals are stated in Figure 26.

3.1.4 Phenotypic analysis and apoptosis

BrdU-labeled cells generally occurred singly or in small clusters of three to five cells in knockout mice, indicating their origin from the same local radial glia cell (Figure 25) [523]. In a next step, the functional integration and state of neuronal development of these "newborn" cells needed to be determined. Therefore, IHC was done for different markers. Before, TUNEL assay (*TdT-mediated dUTP-biotin nick end labeling)* was

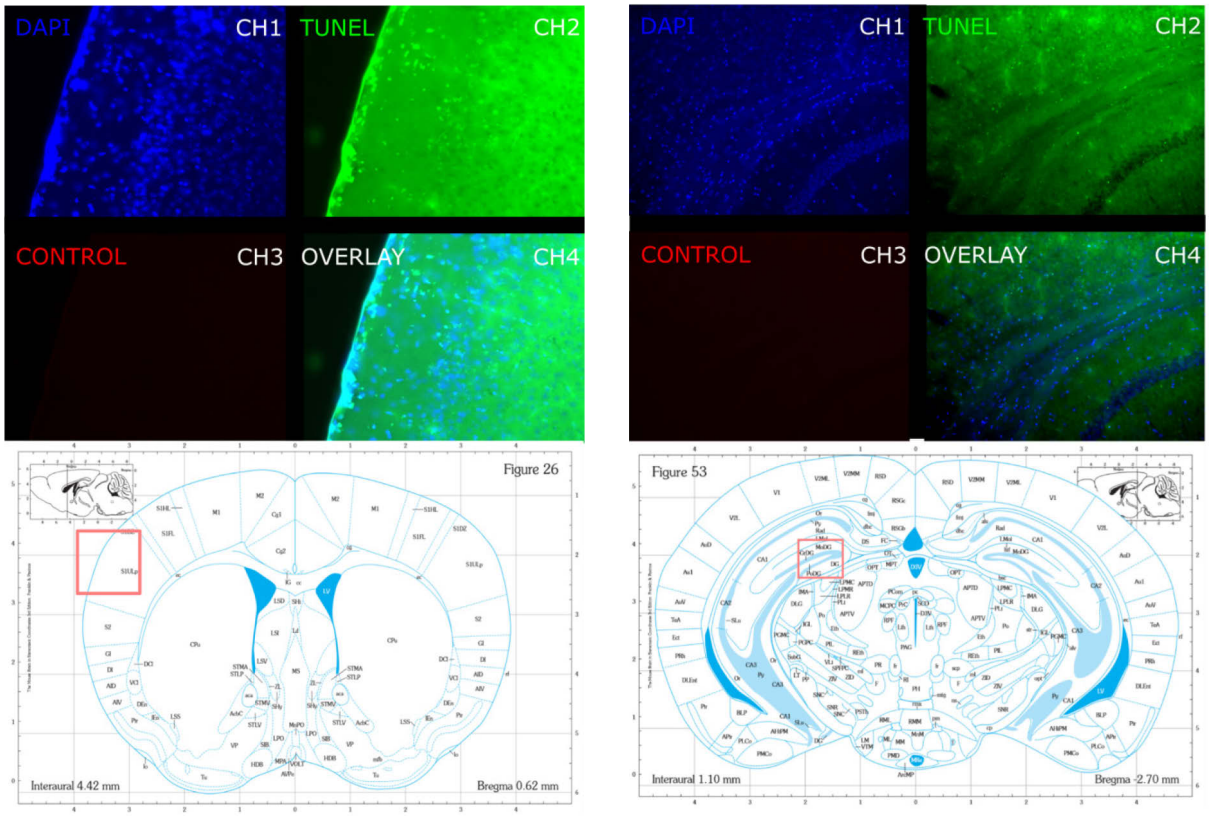

Figure 27 Coronal sections, TUNEL and DNAseI-treated DG of the HC, right (200x magnification), and control cortex section, left (300x magnification). Channel (CH1) represents cell nuclei dyed with DAPI, (CH2) represents TUNEL staining, and (CH3) control channel for fluorescence artifacts. (CH4) represents an overlay of 1-3. No TUNEL+ or apoptotic cells were observed for the DG. DNAseI treatment allowed the induction of dsDNA breaks in the mouse brain, confirming that the TUNEL method detects apoptotic processes in the brain. Bottom: Location of the coronal section in the mouse brain is indicated by red box in the brain atlas [524].

done to examine cell apoptosis in *Tph2*$^{-/-}$ mice since cell structure seemed atypically granular and inhomogeneous, nearly necrotic. Unfortunately, in none of the stained brain sections of any treatment, apoptosis, or Caspase 3 (data not shown) staining co-localized with BrdU+ cells (Figure 28). In general, only rarely apoptotic cells could be detected in the DG, in contrast to DNAse I treated primary somatosensory cortex used as TUNEL control (Figure 27, area marked in the brain atlas [524]) and liver samples (highly regenerative tissue) for caspase activity [525].

To determine the cell types affected by the treatments, BrdU+ cells were evaluated for co-labeling with neural stem cells biomarker Sox2 (SRY-related HMG-box gene 2), and markers of the neuronal lineage (Figure 8): the transient immature neuronal marker DCX, the transient post-mitotic marker Calretinin, a calcium-binding protein involved in calcium signaling, and NeuN as common neuronal nucleus marker. Respective sample stainings for the markers are presented in Figure 29. The increase in total BrdU numbers following SSRI in WT control (Figure 22 to Figure 24) was reflected by increased numbers of BrdU/Sox2+ cells (One-way ANOVA for WT treatment groups

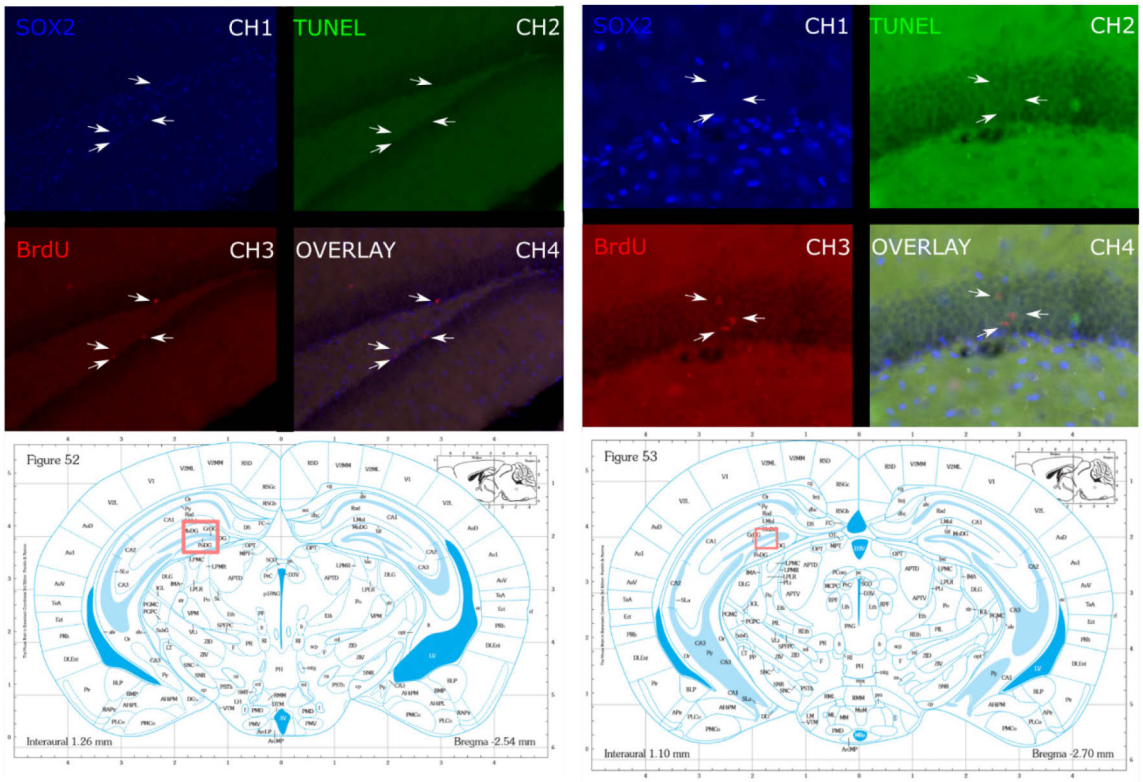

Figure 28 Coronal sections, TUNEL stained DG of the HC of a 21-day i.p. saline treated WT mouse, right (400x magnification), and 21-day i.p. saline treated *Tph2*$^{-/-}$ mouse control cortex section, left (290x magnification). Channel (CH1) represents cell nuclei dyed with the precursor marker Sox2, (CH2) represents TUNEL staining, and (CH3) as control channel for fluorescence artifacts. (CH4) represents an overlay of 1-3. Whereas the newly generated BrdU+ cells, show a SOX 2 double staining, not a single TUNEL event in BrdU+ cells could be seen in any of the 21, day i.p. treated *Tph2*$^{-/-}$ animals, neither for saline, nor CIT, nor tianeptine treatment. The white arrows help with identification of the location of the BrdU+ cells in the other Channels. Bottom: Location of the coronal section in the mouse brain is indicated by red box in the brain atlas [524].

followed by *Dunnett's post hoc* test, p =*0.0015*; Table 21 b), BrdU/DCX+ cells (p = *0.0018*; Table 21 b) and BrdU/NeuN+ cells (p = *0.0046*; Table 21 b). In contrast, a significant decrease in the distribution of BrdU/Calretinin-labeled cells in response to SSRI was found in WT mice. (p = *0.0113*; Table 21 a; as has been published earlier; Klempin 2010 [187]). Surprisingly, while SSRE treatment had no effect on total BrdU numbers in WT, a significant decrease in number and distribution of BrdU/DCX-expressing cells was observed (p =0.0015; Table 21). The *Tph2*$^{-/-}$ phenotype overall resembles CTR mice upon CIT treatment. The number of BrdU+ cells expressing Sox2 is increased in SAL and SSRE groups compared with the appropriate WT control, while the proportion of Calretinin is low in response to any compound and similar to WT SSRI (Table 21a). Within *Tph2*$^{-/-}$ groups, the number or distribution of the various phenotypes was not affected, with one exception, SSRI treatment slightly increased the proportion of BrdU/DCX-positive cells relative to SAL (p = 0.048; Table 21).

Table 21: Proportion and number of BrdU+ cell phenotypes, to investigate their neurogenetic cell stages in SGZ of the DG in HC after 21days i.p. treatment of saline, SSRI, or SSRE. The arrows indicate a decrease (↓) or increase (↑) compared to their respective controls. Phenotype of BrdU+ cells in different states of neurogenetic development, expressing the stage specific, respective postmitotic marker, as described in Figure 8.
a) Proportion (%, SEM, in brackets) of BrdU+ cells. One-way ANOVA followed by *Dunnett's' post hoc* test, *p<0-05; **p< *0.01; $p*<0.05; $$$p$< *0.01* compared to treatment control.
b) Total number (#, SEM in brackets) of cells One-way ANOVA followed by *Dunnett's' post hoc* test, *p<0.05; **p< *0.01* compared to WT control, $p<0.05; $$$p$< *0.01* compared to treatment control.

a)

Group	BrdU+ cell count	Sox2 (%)	DCX (%)	Calretinin (%)	NeuN (%)
Saline					
C57BL/6N WT	261 (34)	19.8 (2.3)	46.8 (3.8)	24.3 (6.2)	22.4 (1.0)
Tph2$^{-/-}$	**455 (69)*↑**	22.2 (2.0)	34.4 (3.9)	**7.6 (3.5)* ↓**	20.0 (3.9)
SSRI					
C57BL/6N WT	408 (50)	23.4 (2.2)	43.4 (5.4)	**5.4 (2.3)$^{\$}$ ↓**	27.0 (1.3)
Tph2$^{-/-}$	416 (64)	27.4 (5.0)	**49.7 (4.8)$^{\$}$ ↑**	8.3 (1.9)	17.3 (5.4)
SSRE					
C57BL/6N WT	204 (21)	23.1 (6.6)	**20.6 (3.4)$^{\$\$}$↓**	25.0 (2.4)	22.5 (9.6)
Tph2$^{-/-}$	**481 (62)**↑**	22.2 (4.5)	29.8 (7.6)	**5.7 (3.0)** ↓**	11.1 (11.1)

b)

Group	BrdU+ cell count	Sox2 (#)	DCX (#)	Calretinin (#)	NeuN (#)
Saline					
C57BL/6N WT	261 (34)	55 (7)	115 (11)	58 (13)	55 (2)
Tph2$^{-/-}$	**455 (69)*↑**	**110 (10)**↑**	172 (27)	43 (20)	**96 (14)*↑**
SSRI					
C57BL/6N WT	408 (50)	**110 (10)$^{\$\$}$↑**	**212 (35)$^{\$}$↑**	26 (12)	**131 (7)$^{\$\$}$↑**
Tph2$^{-/-}$	416 (64)	117 (26)	215 (38)	38 (13)	82 (34)
SSRE					
C57BL/6N WT	204 (21)	50 (11)	**46 (8)$^{\$\$}$↓**	57 (9)	49 (22)
Tph2$^{-/-}$	**481 (62)**↑**	**127 (37)**↑**	**141 (25)**↑**	31 (18)	65 (65)

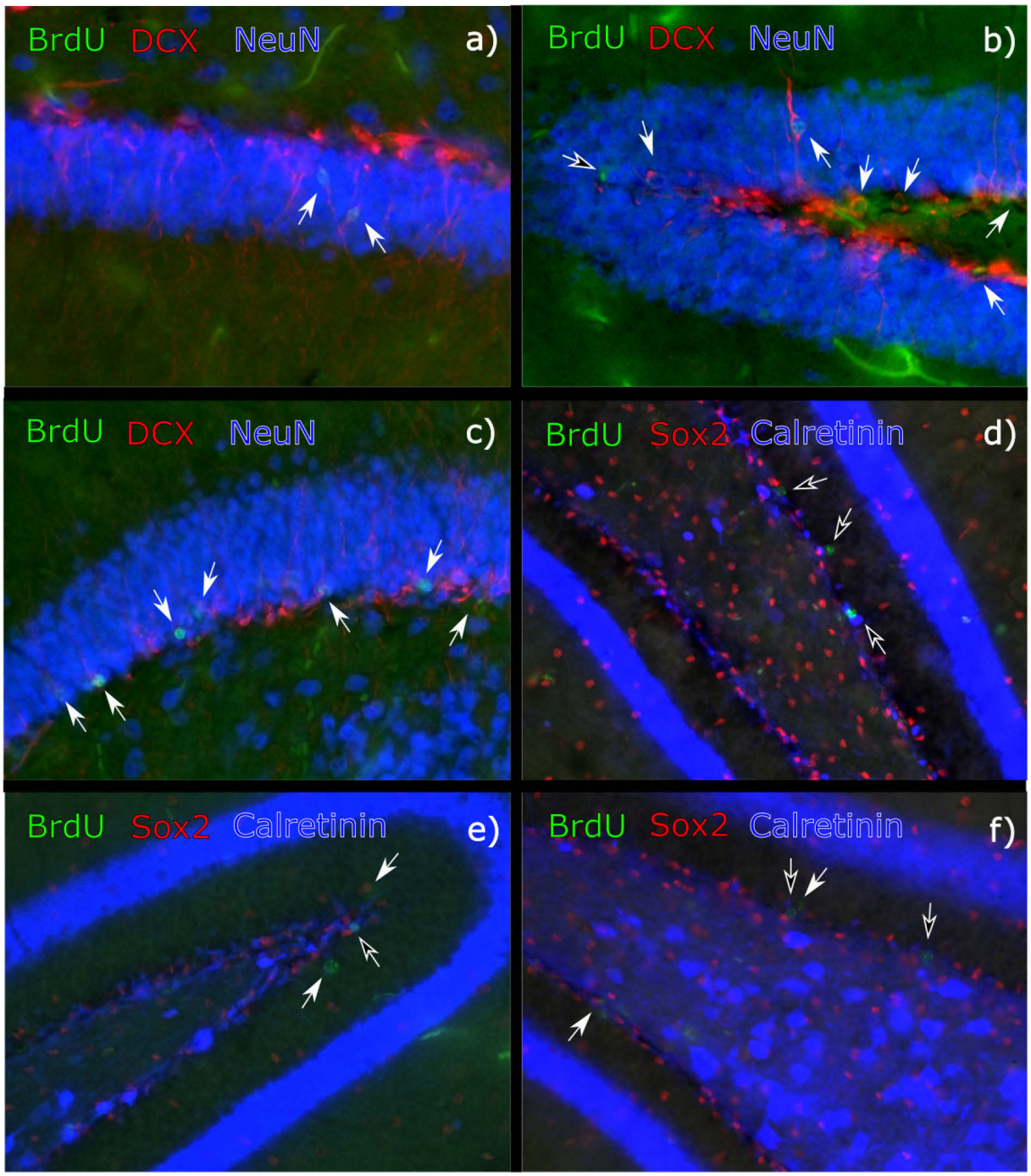

Figure 29 Expression pattern *in vivo* of the transcription factors and neurogenesis cell stage markers DCX, Sox2, NeuN and Calretinin in immunohistochemical stained coronal sections of the DG of the HC. Arrows indicate BrdU+ cell included in the morphological analysis in Table 21, expressing these cell stage markers and indicating the current neurogenetic stage of the cells. A-c) Anti-BrdU (green), anti-doublecortin (DCX, red) and anti-NeuN (blue) staining (400x magnification). White arrows show colocalized expression of DCX in BrdU+ cells, branching and migrating from SGZ to GZL in the DG, indicating a neurogenetic maturation in between type 2b and immature neuron cell stage (white arrows, see also Figure 8). BrdU+ cells expressing additionally Calretinin, show cells in a more mature neuronal stage in neurogenesis after the treatment (Black arrows, see also Figure 8). D-f) Anti-BrdU (green), anti-Sox2 (red) and anti-Calretinin (blue) staining (300x magnification) shows colocalized expression of BrdU+/Sox2 (white arrows) revealing earlier neurogenesis precursor cells stages (RGL to Type 2a) and BrdU+/Calretinin (black arrows) representing cells of an immature neuron stage , in the SGZ in the DG (see also Figure 8). Pictures represent all genotypes and treatments.

3.1.5 CIT treatment decreases BDNF protein levels in *Tph2*$^{-/-}$ mice

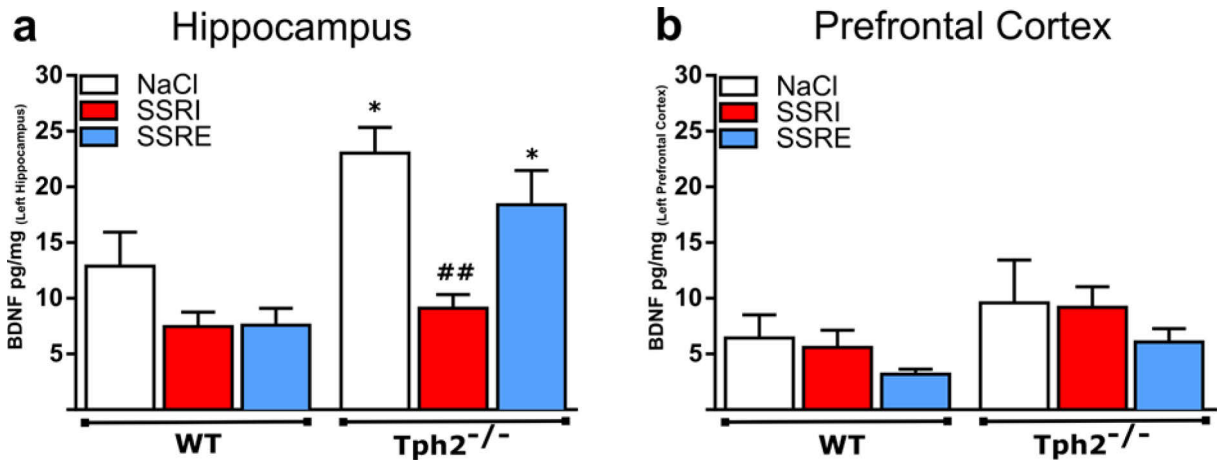

Figure 30 BDNF levels after antidepressant treatment: Chronic treatment of the SSRI CIT (10 mg/kg/day; red) shows a significant decrease in BDNF protein levels in the hippocampal tissue in CIT treated *Tph2*$^{-/-}$ animals, when compared to saline (0.9% 100 µl/20 g ,white) treated animals (left), but not in the PFC (right) of *Tph2*$^{-/-}$ mice. In line with literature, saline treatment itself in *Tph2*$^{-/-}$ showed an increased BDNF tissue levels in hippocampus compared to WT, but not in PFC. After SSRE Tianeptine (10 mg/kg/day; blue) and saline treatment itself, an increase in *Tph2*$^{-/-}$ animals compared to WT is observed in HC (in PFC only trend), whereas one could not observe SSRI-induced increased BDNF levels in the brain of either genotype. Data are presented as mean ± SEM; Two-way Anova with Tukey posthoc-test *p<0.05 to WT Ctl; ##p<0.01 to *Tph2*$^{-/-}$ saline CTR.

A possible mechanism by which serotonin influences neurogenesis includes alterations in the signaling of the neurotrophin BDNF, a major player in MDD - "neurotrophin hypothesis of depression" [345,346,429]. A previous study of our group revealed increased baseline levels of BDNF in the HC of both genders in *Tph2*$^{-/-}$ mice and in the PFC [312]. Here, I was aiming to investigate the correlation of serotonin and BDNF following SSRI and SSRE, by subjecting another cohort of *Tph2*$^{-/-}$ and littermates to 21-day pharmaceutical treatment. BDNF levels were determined in the HC and PFC versus saline as control. In response to either SSRI CIT or SSRE TIA, BDNF levels were not

Table 22 Mean + SEM + n: BDNF levels in HC and PFC of left hemisphere after antidepressant treatment.

Group	Mean (pg/mg)	SEM	n
Hippocampus			
C57BL/6N WT Saline	12.88	3.060	6
Tph2$^{-/-}$ Saline	23.05	2.280	6
C57BL/6N WT CIT/SSRI	7.460	1.307	5
Tph2$^{-/-}$ CIT/SSRI	9.105	1.239	6
C57BL/6N WT TIA/SSRE	7.644	1.525	5
Tph2$^{-/-}$ TIA/SSRE	18.52	3.098	5
Prefrontal Cortex			
C57BL/6N WT NaCl	6.445	2.059	6
Tph2$^{-/-}$ NaCl	9.585	3.851	6
C57BL/6N WT CIT/SSRI	5.580	1.569	5
Tph2$^{-/-}$ CIT/SSRI	9.197	1.843	6
C57BL/6N WT TIA/SSRE	3.175	0.453	6
Tph2$^{-/-}$ TIA/SSRI	5.960	1.169	5

affected in control animals (Figure 30). However, a treatment and genotype effect were observed for *Tph2*$^{-/-}$ mice (Two-way ANOVA $F(2,26) = 9.449$, $p_{(treatment)} = 0.0008$; $F(1,26) = 16.78$, $p_{(genotype)} = 0.0004$; left + Table 22). BDNF protein levels were significantly increased in saline (61 %) and SSRE (73 %) groups relative to WT mice confirming the increased, baseline BDNF expression in *Tph2*$^{-/-}$ mice [312], while 21 days of SSRI decreased BDNF signaling to the level of control mice ($p = 0.0004$; Figure 30a + Table 22). This result reveals SSRI reduces BDNF levels in the absence of brain serotonin and therefore might act serotonin independent. In PFC, no difference in neither treatment could be seen. (Two-way ANOVA $F(2,28) = 1.398$, $p_{(treatment)} = 0.9826$; $F(1,28) = 16.78$, $p_{(genotype)} = 0.0864$; Figure 30b +Table 22).

3.2 Dysregulation of the HPA-Axis in the absence of serotonin

3.2.1 CORT and ACTH plasma levels

To elaborate on the role of serotonin in the "Stress Hypothesis of Depression", certain factors of the HPA-axis were tested. The daily i.p. injection routine in these experiments may have created some sort of chronic or acute stress syndrome. To evaluate genotype-specific HPA alterations, baseline CORT blood plasma levels (ng/ml) were measured in 14-week-old, unhandled, *Tph2*$^{-/-}$ and *Tph2*$^{+/+}$ littermates. Since sex difference in the HPA-axis exists, both genders were tested [526,527] (Figure 31). Female *Tph2*$^{-/-}$ mice revealed a decreased CORT plasma level compared to their *Tph2*$^{+/+}$ littermates (*Student's t*-test p=0.005) whereas respective male mice only showed a slight trend for a decrease (*Student's t*-test p=0.112, Figure 31a). This indicates the involvement of serotonin in CORT secretion in the HPA-axis, subsequently baseline levels of 14-week-old, unhandled, male, and female *SERT*$^{-/-}$ mice were tested and *C57BL/6J* mice as control. As expected, with their higher synaptic serotonin levels, female *SERT*$^{-/-}$ mice showed a trend towards increased CORT plasma

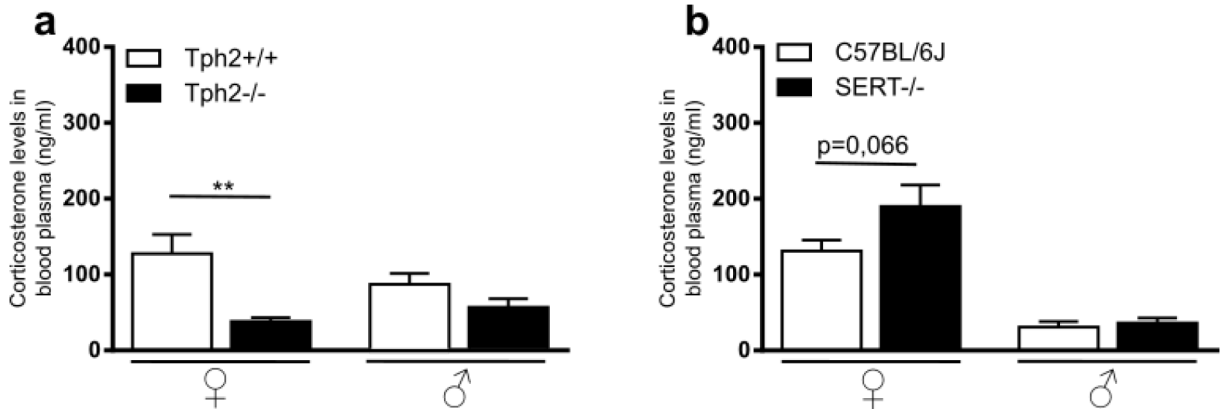

Figure 31 Baseline CORT plasma levels in 14-week-old (a) *Tph2*$^{-/-}$ (black bars) and their *Tph2*$^{+/+}$ littermates (white bars); (b) *SERT*$^{-/-}$ mice (black bars) with *C57BL/6J* (white bars) controls. Both sexes have been tested (a) Female *Tph2*$^{-/-}$ mice revealed a decreased CORT plasma level compared to their *Tph2*$^{+/+}$ littermates whereas male mice only showed a slight trend for decrease. (b) Female but not male *SERT*$^{-/-}$ mice showed a trend towards increased CORT plasma values compared to their *C57BL/6J* control. Student's t-test, **=p<0.01.

Table 23 Mean + SEM + n: Baseline CORT plasma levels in 14-week-old untreated animals (ng/ml).

Group	Mean (ng/ml)	SEM	n
Tph2$^{+/+}$♀	127.50	25.40	12
Tph2$^{-/-}$♀	38.05	5.269	10
Tph2$^{+/+}$♂	85.23	14.31	6
Tph2$^{-/-}$♂	54.82	11.31	8
C57BL/6J♀	131.2	14.31	11
SERT$^{-/-}$♀	190.0	28.36	9
C57BL/6J♂	30.83	7.204	6
SERT$^{-/-}$♂	36.21	6.627	12

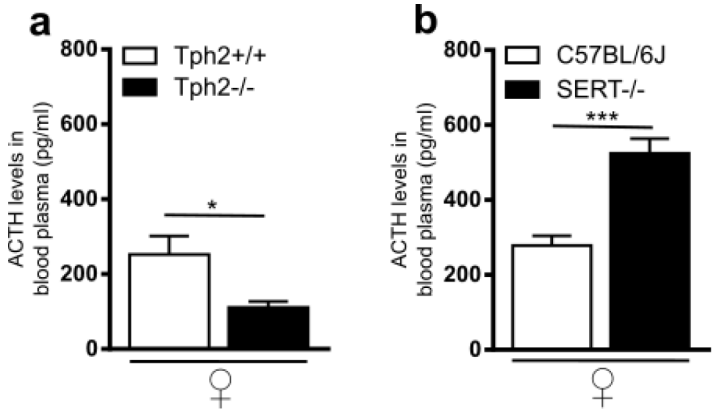

Figure 32 Baseline ACTH blood plasma levels (pg/ml), in female 14 week old (a) *Tph2*$^{-/-}$ (black bars) and their *Tph2*$^{+/+}$ littermates (white bars); (b) *SERT*$^{-/-}$ mice (black bars) with their *C57BL/6J* (white bars) mice as control. Mice have been tested after 3 weeks of no treatment, except husbandry. (a) Female *Tph2*$^{-/-}$ mice revealed a decreased ACTH plasma level compared to their *Tph2*$^{+/+}$ littermates. (b) Female *SERT*$^{-/-}$ mice showed high increase of ACTH plasma levels compared to their *C57BL/6J* control. Student's t-test, *p<0.05; ***p<0.001.

Table 24 Mean + SEM + n: Baseline ACTH plasma levels in (pg/ml).

Group	Mean (pg/ml)	SEM	n
Tph2$^{+/+}$ ♀	252.3	49.35	9
Tph2$^{-/-}$ ♀	110.8	110.8	9
C57BL/6J ♀	278.4	25.95	10
SERT$^{-/-}$ ♀	524.0	39.47	9

compared to their *C57BL/6J* control but fell short of significance (*Student's t*-test p=0.066, Figure 31b + Table 23); male had no difference (*Student's t*-test p=0.622, Figure 31b + Table 23).

Next, ACTH levels were measured. In line with CORT, *Tph2*$^{-/-}$ mice had a lower baseline ACTH release than their *Tph2*$^{+/+}$ controls *(Student's t-test* p=0.0151, Figure 32a + Table 25). In addition, female *SERT*$^{-/-}$ mice revealed a highly increased baseline ACTH blood plasma level compared to *C57BL/6J* (Student's t-test p<0.0001; Figure 32b + Table 25). These results support the hypothesis that serotonin plays a role in the HPA-axis acting upstream of the pituitary gland (Figure 31), where the PVN of the hypothalamus is highly innervated by serotonergic fibers [528].

The results were repeated in an additional experiment. Results from Figure 35, showing a higher CORT baseline blood plasma level range in untreated animals (200 - 300 ng/ml ;Table 27 + Figure 35, grey bars), than the baseline blood plasma levels, determined in *Tph2*$^{-/-}$ *and Tph*$^{+/+}$ animals in earlier experiments (50-200 ng/ml; Table 23 and Table 24). To reevaluate these results, 15-week-old female *Tph2*$^{-/-}$ with their *Tph2*$^{+/+}$ littermates were left unhandled for 3 weeks, except regular husbandry and baseline ACTH and CORT plasma levels of collected trunk blood were determined. The *Tph2*$^{-/-}$ genotype specific relation in baseline animals, as seen in earlier experiments could be reproduced. Unhandled *Tph2*$^{-/-}$ mice showed lower baseline CORT and ACTH plasma levels with Student's *t*-test with $p_{(CORT)}$=0.0287 and $p_{(ACTH)}$= 0.0015. (*Tph2*$^{+/+}$

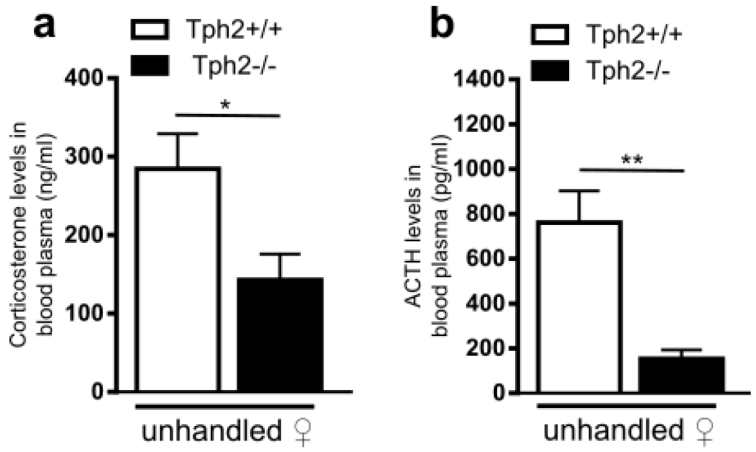

Figure 34: Baseline CORT (ng/ml, a) and ACTH (pg/ml; b) blood plasma levels in 15 week old female *Tph2*$^{-/-}$ mice (white bars), after 3 weeks of no treatment or handling, except husbandry, revealed a similar relation in decrease, compared to their *Tph2*$^{+/+}$ littermates (black bars), as found in previous results (Figure 35, Figure 32 and Figure 31). Student's t-test, *=p<0.05, **=p<0.01.

Table 25 Mean + SEM + n: Female CORT and ACTH plasma levels of 15-week-old animals.

Group	Mean (s)	SEM	n
CORT plasma levels (ng/ml)			
Tph2$^{+/+}$ ♀ unhandled	284.40	44.72	5
Tph2$^{-/-}$ ♀unhandled	142.80	33.05	6
ACTH plasma levels (pg/ml)			
Tph2$^{+/+}$ ♀ unhandled	760.70	141.30	5
Tph2$^{-/-}$ ♀ unhandled	153.80	38.87	6

group failed tests for normality, and so, if the experiment is considered as non-parametric; Mann Whitney test showed similar results with $p_{(CORT)=}$ 0.0303 and $p_{(ACTH)=}$ 0.0087). Noticeably, overall plasma values of this replication, appear to be higher for CORT (Student's t-test, $p_{(Tph2+/+)}$=0.0056; p $_{(Tph2-/-)}$=0.0012) and ACTH (Student's t-test, $p_{(Tph2+/+)}$=0.0013 ;p $_{(Tph2-/-)}$=0.2667) than in the earlier tested female, unhandled, baseline *Tph2*$^{-/-}$ and *Tph2*$^{+/+}$ animals (Table 23 and Table 24 vs Table 25), but in a similar range (150-300 ng/ml for CORT and 200 - 1000 pg/ml, as those tested in the chronic stress tests Figure 35 and Table 27.

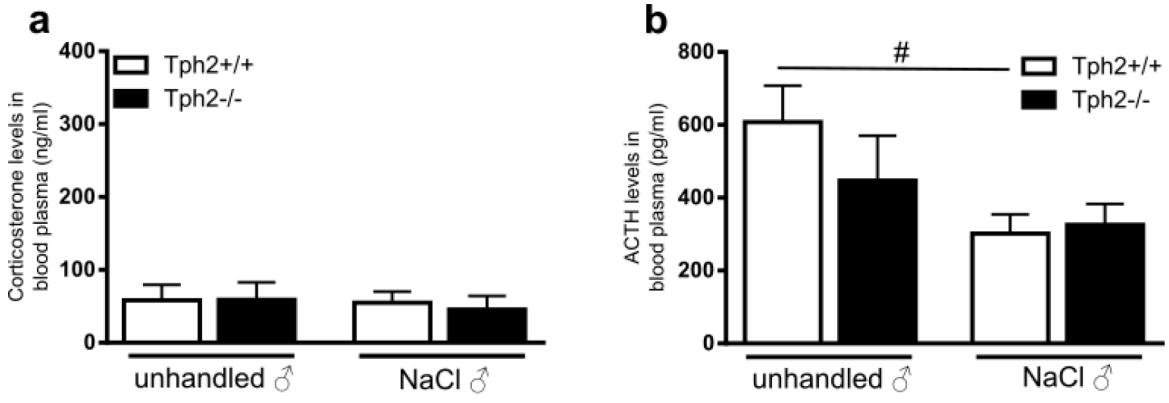

Figure 33 CORT (ng/ml, a) and ACTH (pg/ml, b) blood plasma levels in 14-15 week old, male *Tph2*$^{-/-}$ (black bars) and *Tph2*$^{+/+}$ littermates (white bars) mice, after 21 day daily i.p. saline injection, to mimic a chronic stress event (rear), and after 21 days of no handling (front), except husbandry. Saline treatment revealed no difference in CORT plasma levels, neither in genotype, nor compared to baseline values (a). However, 21-day saline injection decreased ACTH plasma levels in *Tph2*$^{-/-}$ compared to the unhandled CTL (b, white bars), whereas no treatment vs. unhandled difference could be spotted in *Tph2*$^{-/-}$. Two-way ANOVA followed by Tukey's *post hoc* test, #p<0.05.

Table 26 Mean + SEM + n: Male CORT and ACTH plasma levels after 21-day i.p. injection of NaCl.

Group	Mean	SEM	n
CORT plasma levels (ng/ml)			
Tph2$^{+/+}$ ♂ unhandled	58.50	21.30	4
Tph2$^{-/-}$ ♂ unhandled	59.06	24.18	6
Tph2$^{+/+}$ ♂ NaCl	55.14	15.33	4
Tph2$^{-/-}$ ♂ NaCl	45.73	18.91	4
ACTH plasma levels (pg/ml)			
Tph2$^{+/+}$♂ unhandled	607.50	100.40	6
Tph2$^{-/-}$ ♂ unhandled	447.30	123.20	5
Tph2$^{+/+}$♂ NaCl	301.60	52.38	7
Tph2$^{-/-}$ ♂ NaCl	326.00	56.84	6

The data on neurogenesis after 21 days of drug injections suggested an increased stress sensitivity of *Tph2*$^{-/-}$ mice (Figure 22 to Figure 24), also recognizable vocally while injecting. Therefore, in an additional experiment, 14-15-week-old male mice received saline i.p. injections daily for 21 days, and CORT and ACTH were measured by ELISA (Figure 33 + Table 26). No difference in CORT plasma levels were detected between *Tph2*$^{-/-}$ and *Tph2*$^{+/+}$ mice (Figure 33a). However, 21-days of saline injection decreased ACTH plasma levels in *Tph2*$^{+/+}$ compared to the non-treated group (white bars) whereas no difference occurred for the *Tph2*$^{-/-}$ genotype (black bars) (Two-way ANOVA followed by Tukey's *post hoc* test F (1, 20) = 6.598, $p_{(treatment)} = 0.0183$; Figure 33b + Table 26). Noticeable, neither in male *Tph2*$^{-/-}$ nor in male *Tph2*$^{+/+}$ mice the baseline CORT plasma levels of female mice could be replicated, such as the genotype difference (Figure 31a), as in both male genotypes the CORT plasma levels stay on similarly low levels at 54 ng/ml. Also, in contrast to females (Figure 33a and Figure 34) there was no significant difference in ACTH values between male *Tph2*$^{-/-}$ and *Tph2*$^{+/+}$ mice.

3.2.2 CORT and ACTH levels upon treatment paradigms

As a chronic stress-dependent over-activation of the HPA-Axis can impact neurogenesis [249], certain parameters of the HPA-axis were investigated following 21 days of saline, and CIT. Surprisingly, CORT plasma levels were not affected at genotype level, but showed a treatment effect (Two-way ANOVA with Tukey *post hoc* test, F (2, 24) = 3.489, $p_{(treatment)}$ = 0.0468; F (1, 24) = 2.818, $p_{genotype}$ = 0.1062 Figure 35a +Table 27). Nevertheless, *Tph2*$^{-/-}$ CORT levels for all groups show the same trend for a decrease, as the previous experiments. ACTH plasma levels are decreased in *Tph2*$^{-/-}$ mice compared with *Tph2*$^{+/+}$ controls at baseline and following CIT (Two-way ANOVA with Tukey *post hoc* test, F (2, 22) = 3,382, $p_{(treatment)}$ = 0.0524; F (1, 22) = 12.98, $p_{(genotype)}$ = 0.0016 Figure 35b +Table 27).

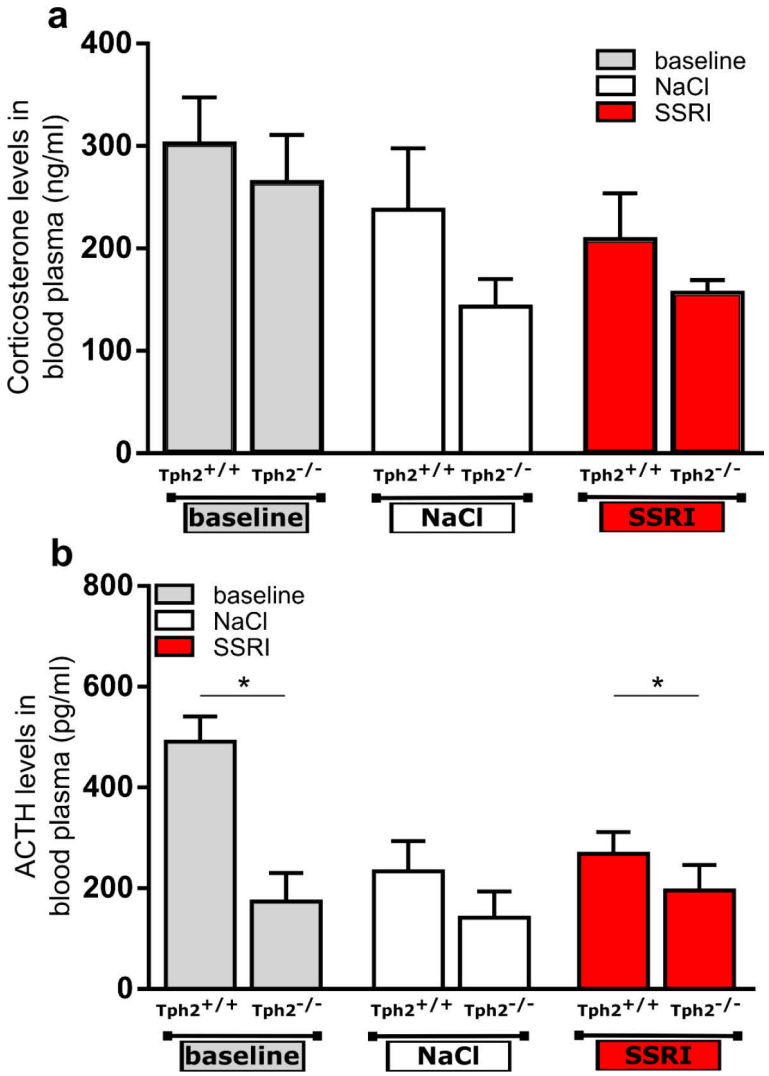

Figure 35 CORT a) and ACTH b) plasma levels in 14-week old female *Tph2*$^{-/-}$ and *Tph2*$^{+/+}$ control mice, after 21 day daily saline (NaCl, white bar/box), CIT (SSRI, red bar/box), or 21 days no handling, except husbandry (baseline, grey bar/box). In (a) no significant difference could be seen in CORT plasma levels of neither genotype, nor treatment. Nevertheless, *Tph2*$^{-/-}$ CORT values in treatment groups show the same trend for a decrease, as in the previous experiments. In (b), ACTH plasma values are decreased genotype for *Tph2*$^{-/-}$ mice, compared to *Tph2*$^{+/+}$ littermates in baseline and CIT conditions. Saline treatment revealed no difference in ACTH plasma levels. Two-way ANOVA followed by Tukey's *post hoc* test, *p<0.05.

Table 27 Mean + SEM + n: Female CORT and ACTH plasma levels after 21-day i.p. injection of NaCl or SSRI.

Group	Mean	SEM	n
CORT plasma levels (ng/ml)			
Tph2$^{+/+}$ ♀ unhandled	304.0	44.92	5
Tph2$^{-/-}$ ♀ unhandled	266.1	45.93	5
Tph2$^{+/+}$ ♀ NaCl	236.4	60.09	5
Tph2$^{-/-}$ ♀ NaCl	141.9	26.81	5
Tph2$^{+/+}$ ♀ CIT / SSRI	209.0	44.86	6
Tph2$^{-/-}$ ♀ CIT / SSRI	156.7	12.40	5
ACTH plasma levels (pg/ml)			
Tph2$^{+/+}$ ♀ unhandled	488.1	50.15	3
Tph2$^{-/-}$ ♀ unhandled	170.8	56.73	5
Tph2$^{+/+}$ ♀ NaCl	231.0	60.29	5
Tph2$^{-/-}$ ♀ NaCl	139.1	51.83	5
Tph2$^{+/+}$ ♀ CIT / SSRI	268.3	43.47	5
Tph2$^{-/-}$ ♀ CIT / SSRI	195.4	50.88	5

3.2.3 CRF and POMC levels in hypothalamus

In addition to CORT and ACTH, CRF, the main initiator for HPA-axis activity, has been measured by real time PCR. CRF mRNA was validated for the hypothalamus of 14-week old female *Tph2*$^{-/-}$ mice and their *Tph2*$^{+/+}$ littermates, after 21-days treatment vs. baseline control paradigm. No significant changes in the CRF mRNA expression (fold change as 2^-ΔΔct) between genotypes and upon treatment was detected; yet a decrease tendency was seen for *Tph2*$^{-/-}$ mice with CIT group short off significance (Student's *t* test for individual comparison between genotypes per treatment group; p = 0.069; Figure 36a + Table 28). Figure 36b shows mRNA data relative to baseline mRNA levels per genotype that was not significantly different (One-Way ANOVA for *Tph2*+/+ F(2,14)=1.805; p=0.2007).

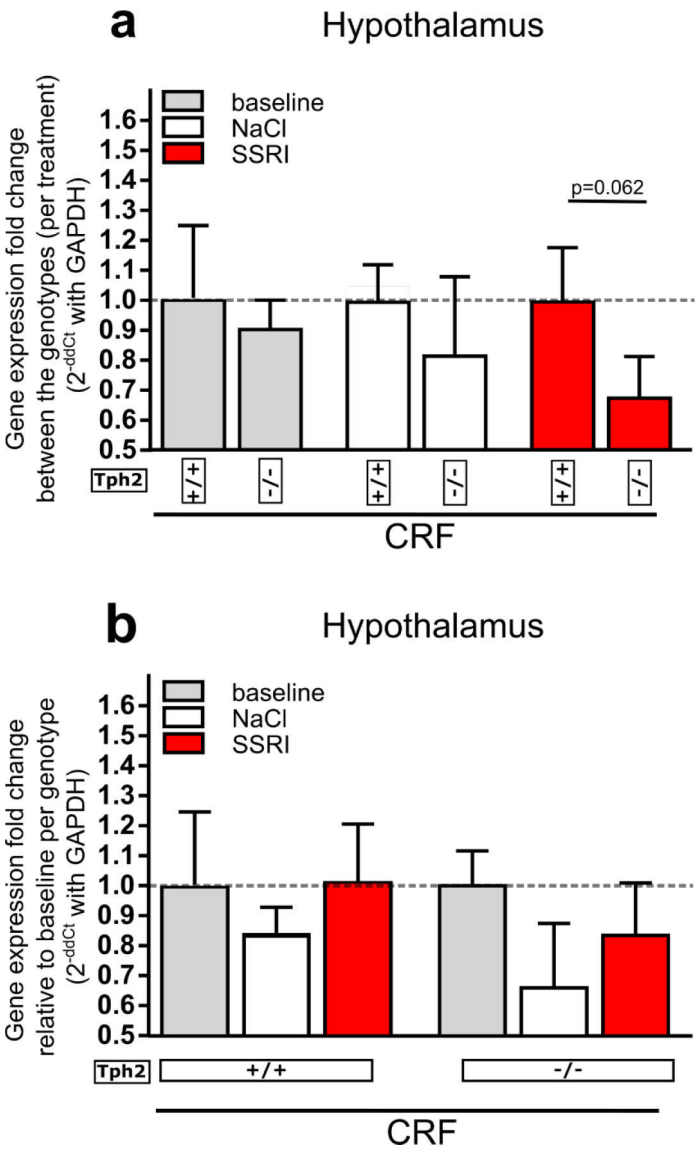

Figure 36 Expression fold change (2^-ΔΔct) of CRF in the hypothalamus of 14-week old *Tph2*$^{-/-}$ mice and their *Tph2*$^{+/+}$ littermates. Bars in grey, untreated baseline, white bars, 21-days of NaCl, red bars, 21-days of CIT treatment. a) fold change reveals no significant changes in CRF expression, but a decreased tendency for *Tph2*$^{-/-}$ compared with *Tph2*$^{+/+}$ control for all groups. b) no changes in CRF mRNA expression were detected when treatments were compared per genotype. GAPDH was used as housekeeping gene.

Table 28 Mean CRF mRNA expression level in the hypothalamus of 14-week-old animals subjected to 21-days of treatment compared to baseline control. Δct levels are stated as cycles, ΔΔct levels are calculated based on GAPDH housekeeping gene; *Tph2*$^{-/-}$ compared with *Tph2*$^{+/+}$, as well as treatment effects of NaCl vs. SSRI CIT.

Group	Mean Δct	ΔΔct
Hypothalamus		
Relative to genotype		
Tph2$^{+/+}$♀ baseline CRF	9.321	0.000
Tph2$^{-/-}$♀ baseline CRF	9.516	0.1951
Tph2$^{+/+}$♀ NaCl CRF	9.815	0.000
Tph2$^{-/-}$ ♀ NaCl CRF	10.43	0.6193
Tph2$^{+/+}$♀ CIT CRF	9.196	0.000
Tph2$^{-/-}$ ♀ CIT CRF	9.946	0.7499
Relative to baseline treatment		
Tph2$^{+/+}$♀ baseline CRF	9.321	0.000
Tph2$^{+/+}$♀ NaCl CRF	9.815	0.494
Tph2$^{+/+}$♀ CIT CRF	9.196	-0.124
Tph2$^{-/}$ ♀ baseline CRF	9.516	0.000
Tph2$^{-/-}$♀ NaCl CRF	10.43	0.9181
Tph2$^{-/-}$ ♀ CIT CRF	9.946	0.431

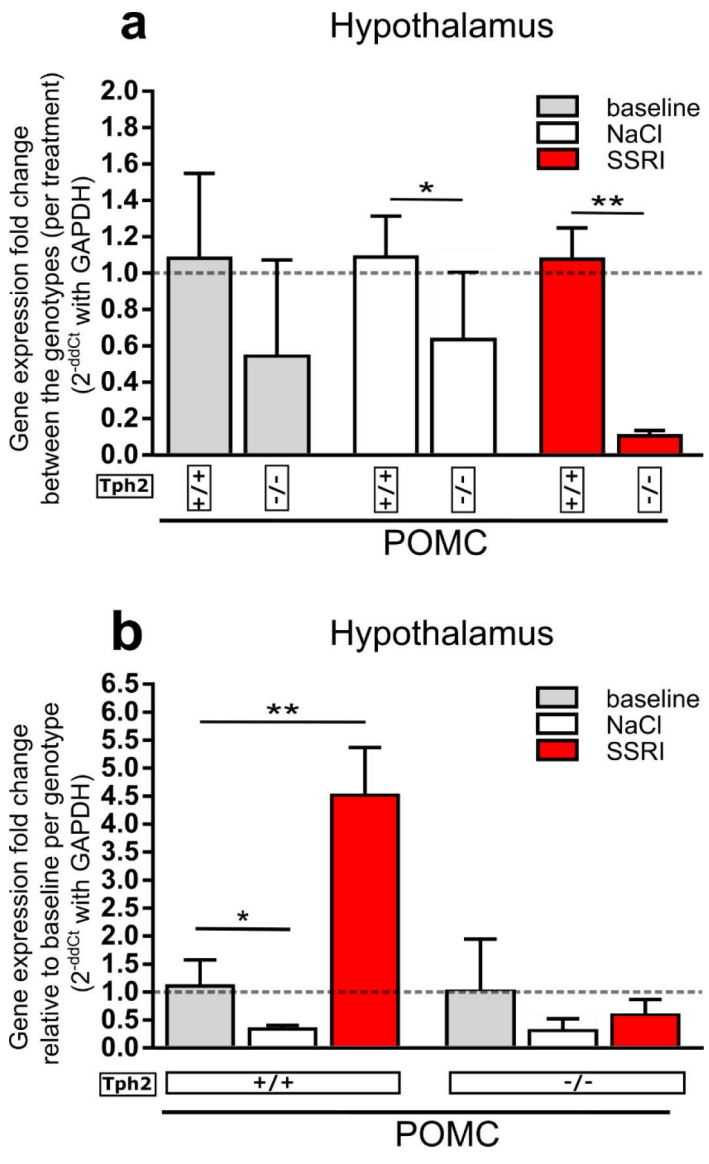

Figure 37 mRNA expression (fold change (2-ΔΔct) of POMC in the hypothalamus of 14-week old female *Tph2*$^{-/-}$ mice compared with *Tph2*$^{+/+}$. Bars in grey, baseline control, white bars 21-days of NaCl and red bars 21-days of CIT. a) *Tph2*$^{-/-}$ animals have a decrease in POMC mRNA expression, and highly significantly upon CIT. *p<0.01, ***p<0.0001 Student's *t* tests between genotypes; b) data shown in relation to baseline per genotype; upon CIT, a 4.5-fold increase in POMC expression was observed in *Tph2*$^{+/+}$ control mice, while treatment negatively affected POMC levels in *Tph2*$^{-/-}$ mice. One-Way ANOVA *p=0.05, ***p<0.0001.

Furthermore, POMC, a precursor polypeptide synthesized in corticotropic cells of the anterior pituitary gland, cleaved into ACTH or vasopressin and relevant for the HPA-axis [529], was measured in the hypothalamus of 14-week old female *Tph2*$^{-/-}$ mice. POMC mRNA was significantly reduced in *Tph2*$^{-/-}$ animals upon saline and CIT treatment (Students' *t* test *p*(saline) = 0.035; *p*(CIT) = <0.0001; Figure 37a+Table 29), with a tendency also seen at baseline. When treatment effects within genotypes were looked at, CIT strongly enhanced POMC levels 4.5-fold in *Tph2*$^{+/+}$ animals (while it in saline was decreased; One-Way ANOVA F(2,13)=9.496 p = 0.0029 Figure 37b + Table 29), while POMC levels were reduced in *Tph2*$^{-/-}$ animals upon any treatment (One-Way ANOVA F(2,11)=1.146 p = 0.3531).

Table 29 POMC mRNA expression level in the hypothalamus of 14-week-old animals, subjected to 21-days of either or no treatment. Δct levels are stated as cycles, ΔΔct levels are calculation based on GAPDH housekeeping genes, with their respective relative fold changes of mRNA expression *Tph2*$^{-/-}$ compared to *Tph2*$^{+/+}$ littermates, as well as treatment effect fold changes compared to unhandled baseline control animals within the respective genotype groups**.**

Group	Mean Δct	ΔΔct
Hypothalamus		
Relative to genotype		
Tph2$^{+/+}$♀ baseline POMC	3.914	0.000
Tph2$^{-/-}$♀ baseline POMC	4.785	0.871
Tph2$^{+/+}$♀ NaCl POMC	5.822	0.000
Tph2$^{-/-}$♀ NaCl POMC	6.460	0.638
Tph2$^{+/+}$♀ CIT POMC	1.739	0.000
Tph2$^{-/-}$ ♀ CIT POMC	5.490	3.751
Relative to baseline treatment		
Tph2$^{+/+}$♀ baseline POMC	3.914	0.000
Tph2$^{+/+}$♀ NaCl POMC	5.822	1.908
Tph2$^{+/+}$♀ CIT POMC	1.739	-2.174
Tph2$^{-/-}$♀ baseline POMC	4.785	0.000
Tph2$^{-/-}$ ♀ NaCl POMC	6.460	1.675
Tph2$^{-/-}$ ♀ CIT POMC	5.490	0.705

3.2.4 No influence of estrous cycle on CORT and ACTH levels

To exclude any impact of the mice's estrus cycle on CORT and ACTH levels [511,530] at the time of trunk blood collection, another set of *C57BL/6N* WT mice (25 week old)- unhandled for 3 weeks was examined. Plasma CORT levels, collected 2 h after dark phase had ended, were correlated to the cycle stage of mice (see referenced cycle stages in Figure 21). No difference in CORT plasma levels were detected in between animals of different estrus cycle stages (one-way ANOVA followed by Tukey's *post hoc* test F (5, 27) = 3.150, *p= 0.9316;* Figure 38 + Table 30). Also, no estrus cycle stage synchronization could be seen among WT mice, kept grouped housed in the same cage. This result helps to exclude major effects of the estrus cycle stages for previous experiments.

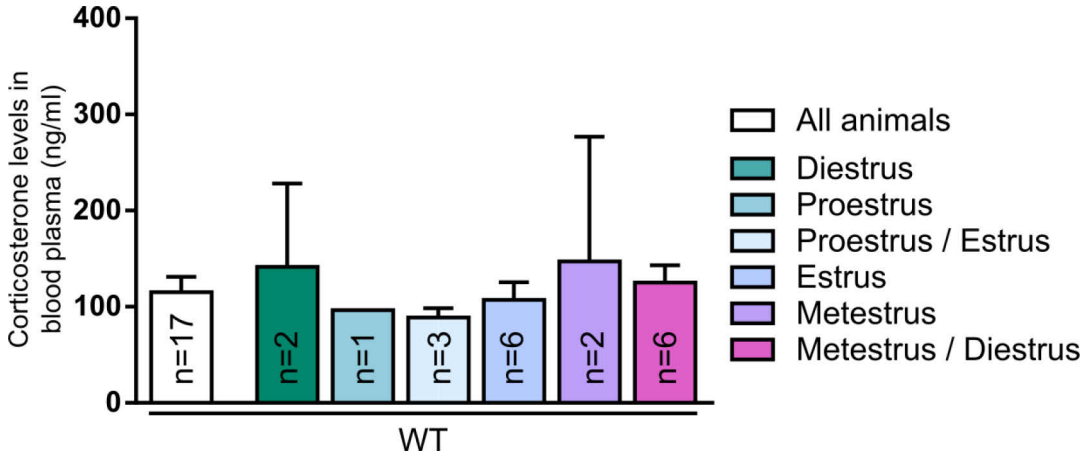

Figure 38 CORT plasma levels in ng/ml of female WT (*C57BL/6N*, 25 - 32 weeks old, unhandled, female) distributed by estrus cycle stage. Cycle stages are color coded and bars show respective number (n) of animals in this cycle stage with their mean CORT levels. CORT baseline blood values did not show an estrus cycle stage-dependent increase or decrease in sham WT mice, if sacrificed 2h after dark phase. Also, no cage-dependent synchronization of the estrus stages was spotted. One-way ANOVA followed by Tukey's post hoc test, p>0.05.

Table 30 Mean + SEM + n: Female CORT plasma levels of WT *C57BL/6N* distributed by estrus cycle stage

Group	Mean	SEM	n
CORT plasma levels (ng/ml)			
Average of all animals	115,3	15.76	17
Diestrus	141.3	86.71	2
Proestrus	96.56	x	1
Proestrus / Estrus	88.94	9.522	3
Estrus	107.2	18.26	6
Metestrus	147.2	129.6	2
Metestrus / Diestrus	125.3	17.73	6

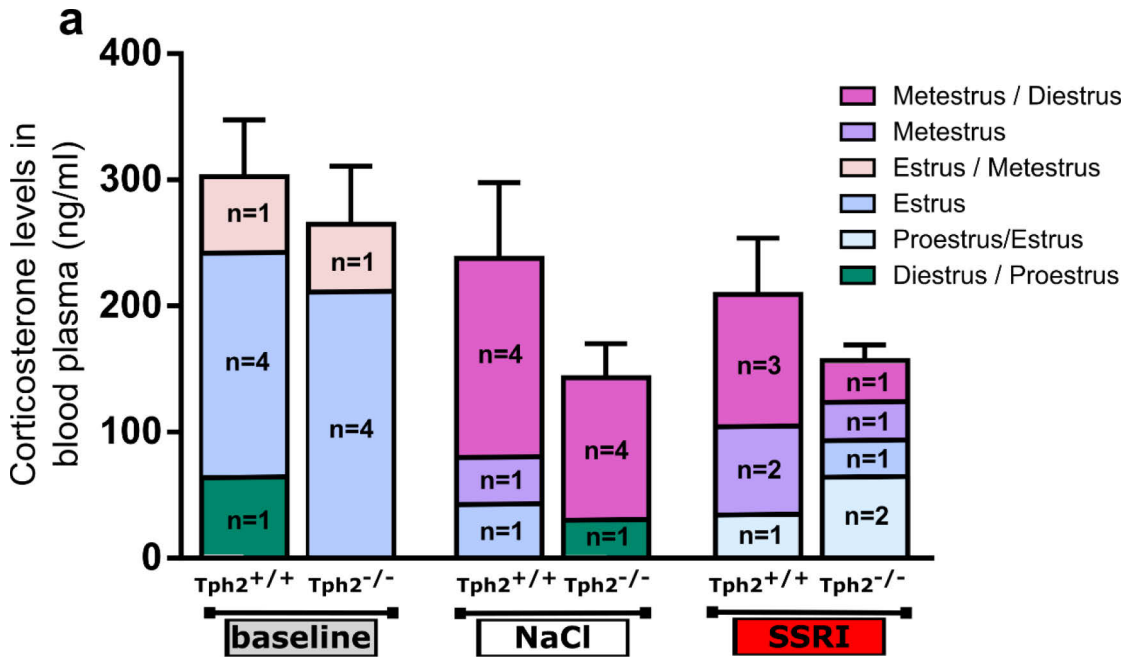

Figure 39 CORT plasma levels in 14-week old, female *Tph2*$^{-/-}$ and *Tph2*$^{+/+}$ control mice, after 21-day daily i.p. saline (NaCl, white bar/box , middle group), i.p. CIT (SSRI, red bar/box, most right group) or 21 days no handling, except husbandry (baseline, grey bar/box, most left group). The idea was, to mimic a chronic stress event and similar experimental conditions as set in Figure 24. The estrus cycle stage of each mouse is stated within each group bar. n represents number of mice in the respective cycle stage per group. No significant difference could be seen in CORT plasma levels of neither genotype, nor treatment, with no correlation for estrus cycle stage. Picture represents the same CORT values as in Figure 35a. A cycle stage synchronization of mice of the same cage is visible in treatment groups for estrus (n=4) in baseline, and metestrus / diestrus (n=4) in saline treatment.

The experiments were repeated according to a shift in estrous cycles stages in *Tph2*$^{-/-}$ mice, reported earlier in our lab [311]. Certain parameters of the HPA-axis were investigated following 21 days of saline, and CIT, and in dependence of the cycle stage. A cycle stage synchronization of mice in the same cage is visible in treatment groups for estrus (n=4) at baseline, and metestrus / diestrus (n=4) for saline treatment, but also here no clear estrus cycle correlation for CORT levels has been seen (Figure 39).

3.2.5 Open field test upon treatment

The same group of animals was used to investigate CIT's anxiolytic effect and to test if daily injection can be rated as a chronic or acute stress paradigm. Open field experiments were performed after 5 days and 20 days of treatment, with 300 s length of total recording. Time spend in the center (in %) is measured (Figure 40 + Table 31). *Tph2*$^{-/-}$ mice were less anxious as previously reported [510].While SSRI treatment decreased anxiety levels initially at 5 days (increased time spent in the center) in WT, no changes were observed in *Tph2*$^{-/-}$ mice at 5 days (Two-way ANOVA followed by Tukey's / post hoc test $F(2, 25) = 4.835$, $p_{(treatment)} = 0.0168$; $F(1, 25) = 6.603$, $p_{(genotype)} = 0.0165$), but seemed to increase anxiety at 20 days (Two-way ANOVA followed by Tukey's post hoc test $F(2, 22) = 6{,}621$, $p_{(treatment)} = 0.0056$, $F(1, 22) =$

20,84, p (genotype) = 0.0002). Further surprisingly, saline-treatment for 5 days increased anxiety in *Tph2*$^{-/-}$ mice which was abolished at 20 days (Two-way ANOVA followed by Sidak's post hoc test F (2, 19) = 7,687, p (interaction) = 0.0036; F (2, 19) = 2.408, p (treatment) = 0.1170, F (1, 19) = 2.809, p (genotype) = 0.1101)

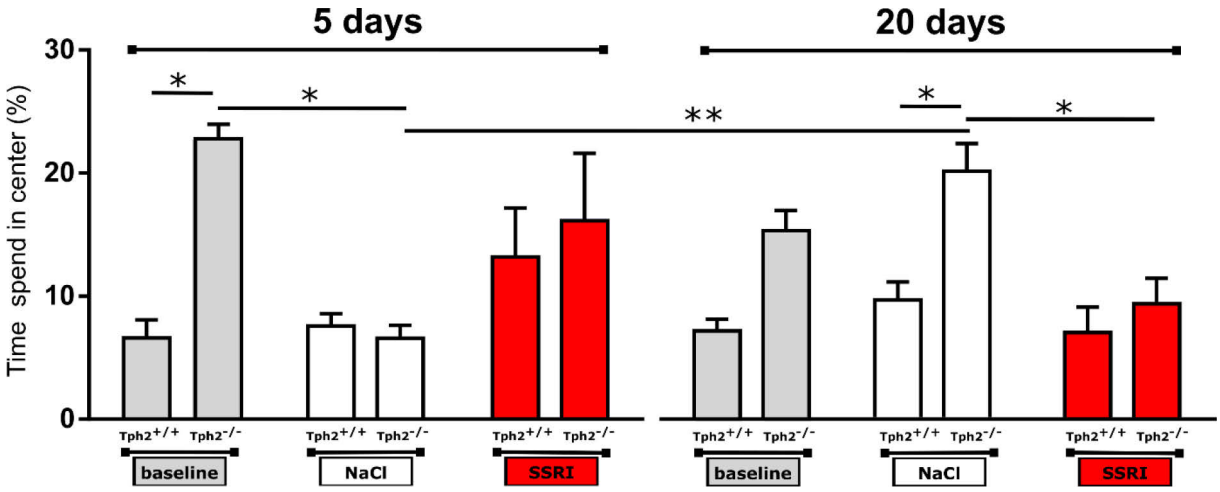

Figure 40 Open field experiment after 5 days or 20 days of treatment, with 300s of total recording. Time spent in the center in percentage (%) of the 300s recording time. Continuous injection of saline resulted in a longer center time of *Tph2*$^{-/-}$ at day 20 compared to day 5 (white bars). *Tph2*$^{-/-}$ mice were less anxious at baseline. While SSRI treatment decreased anxiety levels initially at 5 days (increased time spent in the center) in WT, no changes were observed in *Tph2*$^{-/-}$ mice at 5 days but seemed to increase anxiety at 20 days. Saline-treatment for 5 days increased anxiety after 5 days in *Tph2*$^{-/-}$ mice which was abolished at 20 days (white bars). Two-way ANOVA followed by Tukey's / Sidak's post hoc test, *p < 0.05 significant genotype specific difference, §p < 0.05 and §§p < 0.01 significant timepoint difference between day 5 and 20, #p < 0.05, significant difference between treatment; data are presented as mean ± SEM.

Table 31 Mean + SEM + n: Time spent in the center (%) in 300s Open Field test, after 21-day i.p. injections of NaCl or SSRI or unhandled, at day 5 and 20.

Group	Mean	SEM	n
After 5 days of treatment			
Tph2$^{+/+}$♀ unhandled	6.62	1.48	6
Tph2$^{-/-}$♀ unhandled	22.75	1.19	4
Tph2$^{+/+}$♀ NaCl	7.60	0.98	6
Tph2$^{-/-}$♀ NaCl	6.58	1.06	5
Tph2$^{+/+}$♀ CIT / SSRI	13.20	3.95	5
Tph2$^{-/-}$♀ CIT / SSRI	16.14	5.46	5
After 20 days of treatment			
Tph2$^{+/+}$♀ unhandled	9.52	1.28	6
Tph2$^{-/-}$♀ unhandled	20.43	2.18	3
Tph2$^{+/+}$♀ NaCl	12.72	1.97	6
Tph2$^{-/-}$♀ NaCl	26.70	3.00	3
Tph2$^{+/+}$♀ CIT / SSRI	9.22	2.75	6
Tph2$^{-/-}$♀ CIT / SSRI	12.34	2.79	5

3.2.6 Glucocorticoid-, and Mineralocorticoid receptor gene expression

As ACTH and CORT levels are significantly lower in female *Tph2*$^{-/-}$ mice at baseline, underlying HPA-feedback control mechanism were evaluated in more depth. Possible differences in gene expression levels of the CORT sensitive stress receptors, GR (Nr3C1) and MR (Nr3C2), in certain brain areas of 15-week old female *Tph2*$^{-/-}$ and *Tph2*$^{+/+}$, were determined at baseline level and with SSRI / CIT treatment. PFC and HC brain areas are mostly involved in neurogenesis and related to depression, and susceptible to stress are PFC and HC [249].

Baseline GR and MR gene expression in PFC and HC

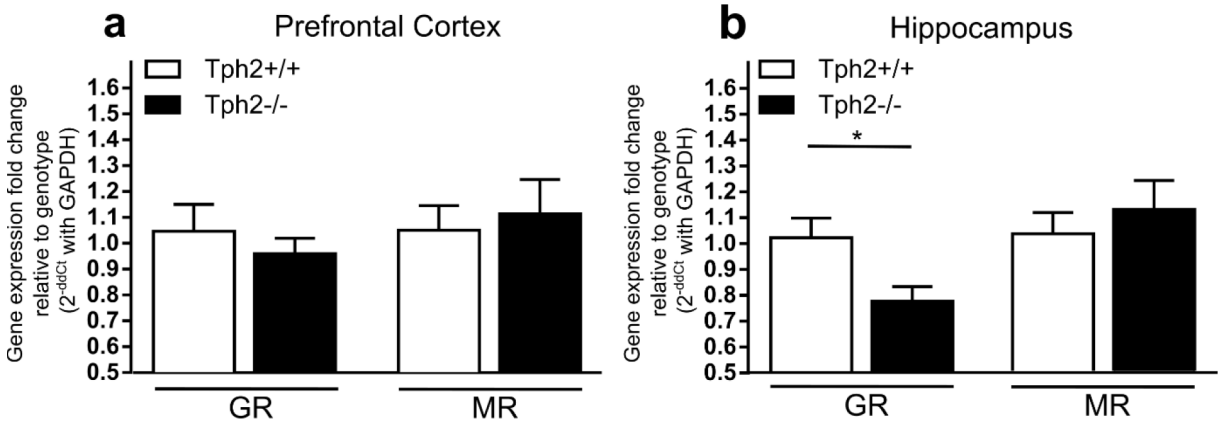

Figure 41 Gene mRNA expression (fold change as $2^{-\Delta\Delta ct\ of\ mean}$ method) of glucocorticoid receptor (Nr3C1, GR) and mineralocorticoid receptor (Nr3C2, MR) in PFC (a) and HC (b) tissue (pooled hemispheres) of 15-week old, untreated, female mice at baseline, of *Tph2*$^{-/-}$ (black bars) compared to their *Tph2*$^{+/+}$ littermates (white bars). GR gene mRNA expression is significantly lowered in the HC of untreated *Tph2*$^{-/-}$ mice, compared to their *Tph2*$^{+/+}$ littermates. Statistics are based on the Δct values, calculated by the use of the GAPDH housekeeping gene (Table 32). Student's t-test, *p<0.05. Data presents mean + SEM.

Table 32 Mean Δct + ΔΔct: Female GR and MR mRNA expression levels in PFC and HC tissue (both hemispheres pooled). of 15-week-old untreated animals**.** Δct levels are stated as cycles, ΔΔct calculation based on GAPDH housekeeping genes, relatively compared *Tph2*$^{-/-}$ to *Tph2*$^{+/+}$ littermates.

Group	Mean Δct	ΔΔct
Prefrontal cortex		
Tph2$^{+/+}$GR	6.177	0.1451
Tph2$^{-/-}$GR	6.267	0.08960
Tph2$^{+/+}$MR	7.936	0.1613
Tph2$^{-/-}$MR	7.890	0.1805
Hippocampus		
Tph2$^{+/+}$GR	5.903	0.1055
Tph2$^{-/-}$GR	6.308	0.1152
Tph2$^{+/+}$MR	5.102	0.1301
Tph2$^{-/-}$MR	4.994	0.1376

The baseline mRNA expression fold change (2-ΔΔct method, Figure 41 and Table 32) of glucocorticoid receptor (Nr3C1, GR) and mineralocorticoid receptor (Nr3C2, MR) in PFC (Figure 41a) and HC (Figure 41b) tissue in *Tph2*$^{-/-}$ compared to their *Tph2*$^{+/+}$ littermates was measured. Both hemispheres were pooled. Subjects were 15-week old, untreated, female mice of *Tph2*$^{-/-}$ genotype (black bars) compared to their *Tph2*$^{+/+}$ littermates (white bars). Real-time qPCR data revealed no differences in neither GR nor MR receptor mRNA expression for the PFC for both genotypes (fold change as 2^-ΔΔct of mean, Figure 41a + Table 32 with GAPDH as housekeeping gene). However the qPCR data run for the HC tissue revealed that GR mRNA expression is significantly lowered in the HC of untreated female *Tph2*$^{-/-}$ mice, compared to their *Tph2*$^{+/+}$ littermates with (Student's t-test p(GR)=0.00197), whereas for MR there was no difference seen (Figure 41b + Table 32).

GR and MR gene expression in PFC after 21-day CIT treatment

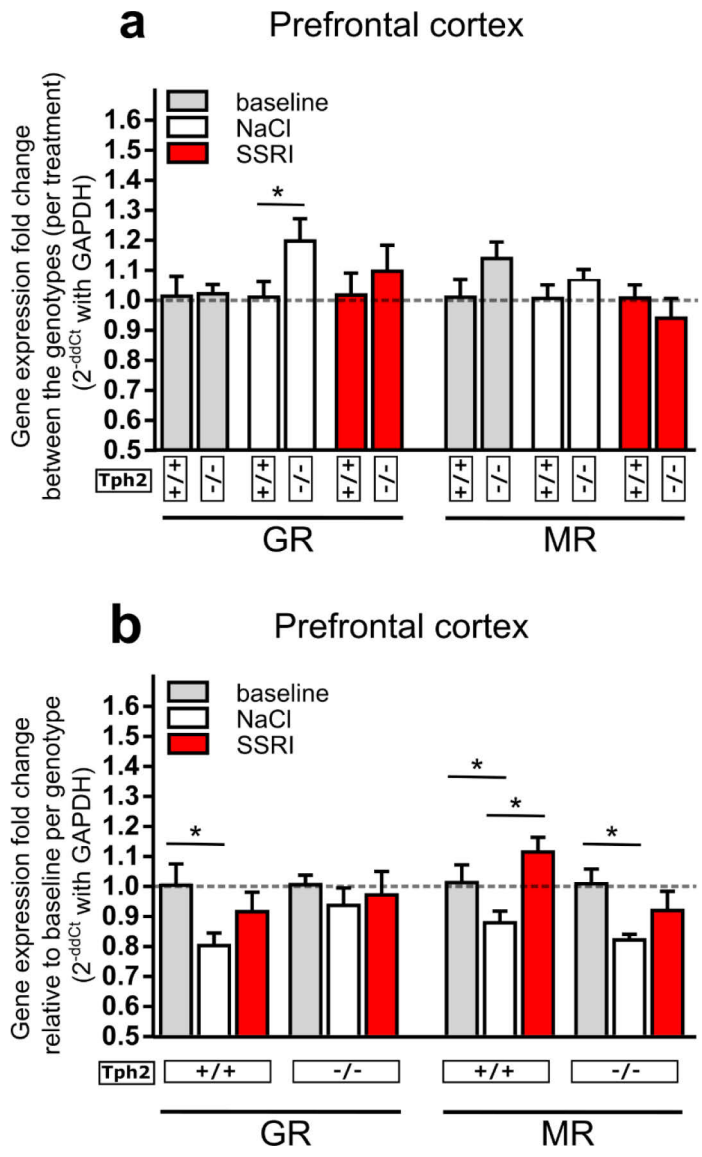

Figure 42 mRNA expression (fold change as $2^{-\Delta\Delta ct\ of\ mean}$ method) of GR and MR in PFC (pooled hemispheres) of 14-week old female *Tph2*$^{-/-}$ mice compared to *Tph2*$^{+/+}$ littermates. Bars in grey represent untreated baseline groups, white bars 21-day NaCl, and red CIT. (a) fold change in the PFC of *Tph2*$^{-/-}$ shows a significant increase in GR mRNA expression after saline treatment. Student's t test *p<0.05 (b) treatment groups compared relative to the untreated baseline show *Tph2*$^{+/+}$ mice treated with saline have decreased GR levels (Dunnett's post hoc test). For MR levels, saline treatment reduced the expression in *Tph2*$^{+/+}$ and also *Tph2*$^{-/-}$ mice, *p<0.05.

Table 33 GR and MR mRNA expression levels in the PFC. Animals were subjected to 21-days of either no treatment or control. Δct and , i.p. saline (0,9 % NaCl) or i.p. CIT (10mg/kg SSRI) treatment. ΔΔct values per treatment between genotypes (a) and per genotype for different treatments (calculated based on GAPDH; *Tph2*$^{-/-}$ vs. *Tph2*$^{+/+}$).

Group	Mean Δct	ΔΔct
Prefrontal cortex Relative to genotype		
Tph2$^{+/+}$ baseline GR	4.701	0.000
Tph2$^{-/-}$ baseline GR	4.68	-0.021
Tph2$^{+/+}$ NaCl GR	5.035	0.000
Tph2$^{-/-}$ NaCl GR	4.790	-0.2449
Tph2$^{+/+}$ CIT GR	4.855	0.000
Tph2$^{-/-}$ CIT GR	4.745	0.1094
Tph2$^{+/+}$ baseline MR	7.402	0.000
Tph2$^{-/-}$ baseline MR	7.223	-0.1794
Tph2$^{+/+}$ NaCl MR	1.005	0.000
Tph2$^{-/-}$ NaCl MR	7.515	-0.0869
Tph2$^{+/+}$ CIT MR	7.259	0.000
Tph2$^{-/-}$ CIT MR	7.365	0.1059
Relative to baseline treatment		
Tph2$^{+/+}$ baseline GR	4.701	0.000
Tph2$^{+/+}$ NaCl GR	5.035	0.3339
Tph2$^{+/+}$ CIT GR	4.855	0.1553
Tph2$^{-/-}$ baseline GR	4.68	0.000
Tph2$^{-/-}$ NaCl GR	4.790	0.1106
Tph2$^{-/-}$ CIT GR	4.745	0.0655
Tph2$^{+/+}$ baseline MR	7.402	0.000
Tph2$^{+/+}$ NaCl MR	1.005	0.2000
Tph2$^{+/+}$ CIT MR	7.259	-0.1433
Tph2$^{-/-}$ baseline MR	7.223	0.000
Tph2$^{-/-}$NaCl MR	7.515	0.2925
Tph2$^{-/-}$ CIT MR	7.365	0.1419

Real-time PCR of receptor expression patterns following saline treatment and long term 21-day CIT (same animal groups as for Neurogenesis and OF, Figure 42 +Table 33), revealed that saline treated *Tph2*$^{-/-}$ mice had a significantly higher GR mRNA expression level in the PFC compared with *Tph2*$^{+/+}$ (Student's *t*-test between genotypes per treatment group, $p_{(GR)}$ =0.0402, Figure 42a). Levels at baseline and following CIT were unaffected. Figure 42b describes mRNA expression with focus on treatment effects per genotype; in *Tph2*$^{+/+}$ animals treated with saline, the amount of GR levels was significantly decreased (One-way ANOVA F(2,15)=3.344 p =0.0629, Dunnett's *post hoc* test p=0.0379. For MR levels, saline treatment reduced the expression in

Tph2$^{+/+}$ mice (F(2,15)=5.677 p =0.0146), and also in *Tph2*$^{-/-}$ mice (F(2,12)=3.709 p =0.0557, Dunnett's post hoc test p=0.0336).

GR and MR gene expression in HC after 21-day CIT treatment

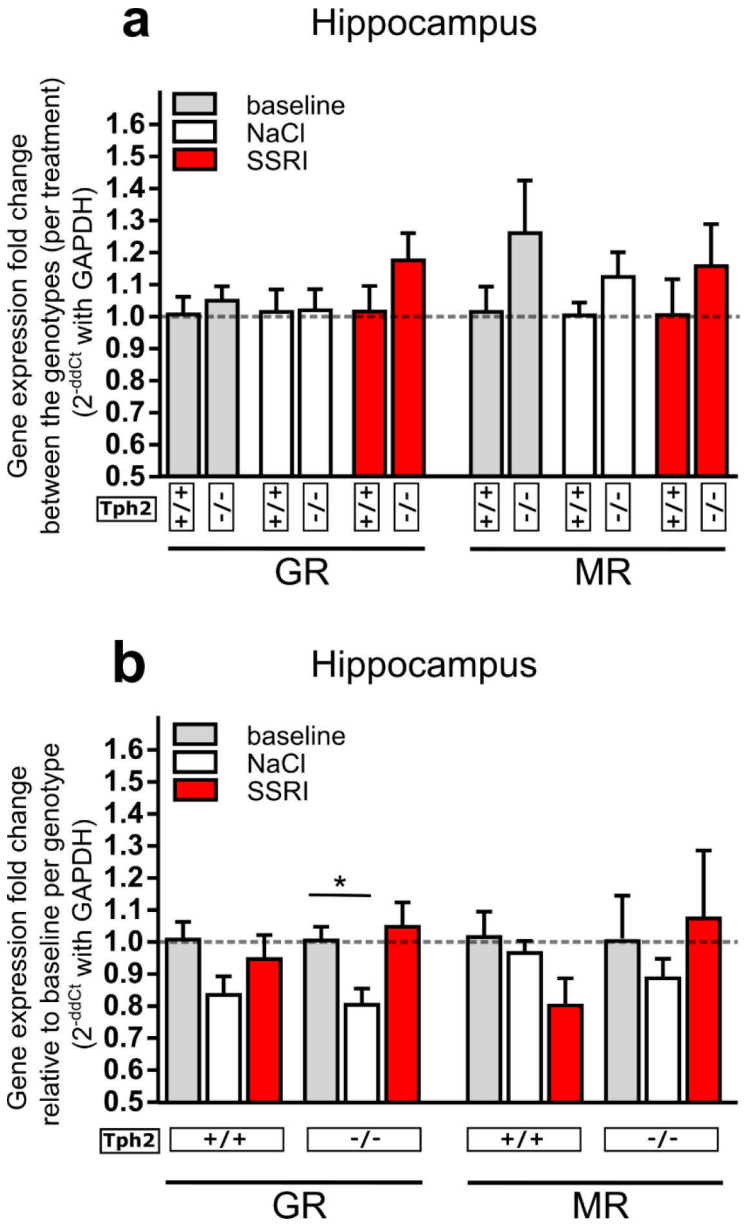

Figure 43 mRNA expression (fold change as $2^{-\Delta\Delta ct\ of\ mean}$ method) of GR and MR in HC (pooled hemispheres) of 14-week old, female *Tph2*$^{-/-}$ mice compared to *Tph2*$^{+/+}$. Bars in grey, baseline control, white bars 21-day NaCl and red bars 21-day SSRI CIT. a) *Tph2*$^{-/-}$ animals tend to higher MR levels in the HC at baseline. b) upon saline treatment GR mRNA expression was decreased in Tph2$^{-/-}$ animals, *p<0.05.

Real-time PCR data in the HC of 14-week old, female *Tph2*$^{-/-}$ mice, and their *Tph2*$^{+/+}$ littermates reveal no changes in mRNA expression of MR and GR for any treatment group between genotypes (Figure 43a + Table 34). When calculated per treatment group, GR mRNA expression was decreased in *Tph2*$^{-/-}$ animals upon saline (One-way ANOVA F (2, 12) = 4.575 p = 0.0033; Figure 43b + Table 34).

Table 34 GR and MR mRNA expression levels in the HC. Animals were subjected to 21-days of treatment or control. Δct and ΔΔct values per treatment between genotypes (a) and per genotype for different treatments (calculated based on GAPDH; *Tph2*$^{-/-}$ vs. *Tph2*$^{+/+}$).

Group	Mean Δct	ΔΔct
Hippocampus		
Relative to genotype		
Tph2$^{+/+}$ baseline GR	5.057	0.0.00
Tph2$^{-/-}$ baseline GR	4.993	-0.0645
Tph2$^{+/+}$ NaCl GR	5.339	0.000
Tph2$^{-/-}$ NaCl GR	5.323	-0.01559
Tph2$^{+/+}$ CIT GR	5.160	0.000
Tph2$^{-/-}$ CIT GR	4.675	-0.4853
Tph2$^{+/+}$ baseline MR	5.773	0.000
Tph2$^{-/-}$ baseline MR	5.488	-0.2853
Tph2$^{+/+}$ NaCl MR	5.832	0.000
Tph2$^{-/-}$ NaCl MR	5.678	-0.1535
Tph2$^{+/+}$ CIT MR	6.139	0.000
Tph2$^{-/-}$ CIT MR	5.501	0.2883
Relative to baseline treatment		
Tph2$^{+/+}$ baseline GR	5.057	0.000
Tph2$^{+/+}$ NaCl GR	5.339	0.2815
Tph2$^{+/+}$ CIT GR	5.160	0.1031
Tph2$^{-/-}$ baseline GR	4.993	0.000
Tph2$^{-/-}$ NaCl GR	5.323	0.0585
Tph2$^{-/-}$ CIT GR	4.675	0.3659
Tph2$^{+/+}$ baseline MR	5.773	0.000
Tph2$^{+/+}$ NaCl MR	5.832	0.3304
Tph2$^{+/+}$ CIT MR	6.139	-0.3176
Tph2$^{-/-}$ baseline MR	5.488	0.000
Tph2$^{-/-}$ NaCl MR	5.678	0.1904
Tph2$^{-/-}$ CIT MR	5.501	0.1275

GR and MR gene expression in hypothalamus after 21-day CIT treatment

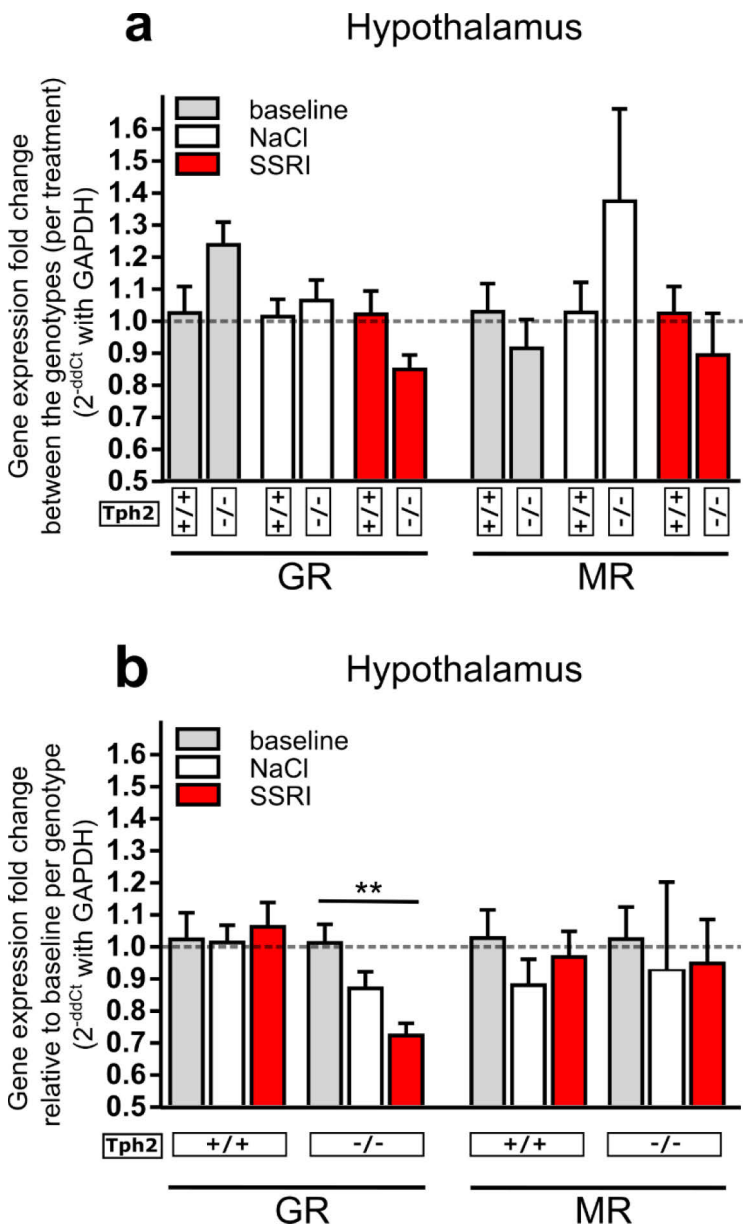

Figure 44 mRNA expression (fold change as $2^{-\Delta\Delta ct\ of\ mean}$ method) of GR and MR in the hypothalamus of 14-week old, female *Tph2*$^{-/-}$ mice compared to *Tph2*$^{+/+}$. Bars in grey, baseline control, white bars 21-day NaCl and red bars 21-day SSRI CIT. a) *Tph2*$^{-/-}$ animals trend to increased GR levels at baseline. b) treatment effects reveal reduced GR expression upon CIT within *Tph2*$^{-/-}$ mice groups *p<0.05.

With the hypothalamus being one of the main coordinators of the HPA-axis containing neurons that react strongly to glucocorticoids within a regulatory feedback system, MR and GR expression was investigated in *Tph2*$^{-/-}$ after certain treatments in hypothalamic tissue of 14-week old female mice. Data revealed no significant differences in GR and MR mRNA expression between genotypes (Figure 44a+ Table 35). However, based on treatment effects (Figure 44b), within *Tph2*$^{-/-}$ groups, GR was significantly reduced upon CIT compared with baseline (One-Way ANOVA $F(2,12)=8.848$ $p=0.0044$, followed by Dunnett's *post hoc* test p=0.0023).

Table 35 GR and MR mRNA expression levels in the hypothalamus. Animals were subjected to 21-days of treatment or control. Δct and ΔΔct values per treatment between genotypes (a) and per genotype for different treatments (calculated based on GAPDH; *Tph2*$^{-/-}$ vs. *Tph2*$^{+/+}$).

Group	Mean Δct	ΔΔct
Hypothalamus		
Relative to genotype		
Tph2$^{+/+}$ baseline GR	5.794	0.000
Tph2$^{-/-}$ baseline GR	5.504	-0.2904
Tph2$^{+/+}$ NaCl GR	5.793	0.000
Tph2$^{-/-}$ NaCl GR	5.724	-0.0688
Tph2$^{+/+}$ CIT GR	5.735	0.000
Tph2$^{-/-}$ CIT GR	5.991	0.2567
Tph2$^{+/+}$ baseline MR	8.120	0.000
Tph2$^{-/-}$ baseline MR	8.285	0.1656
Tph2$^{+/+}$ NaCl MR	8.341	0.000
Tph2$^{-/-}$ NaCl MR	7.990	-0.709
Tph2$^{+/+}$ CIT MR	8.198	0.000
Tph2$^{-/-}$ CIT MR	8.446	0.2485
Relative to baseline treatment		
Tph2$^{+/+}$ baseline GR	5.794	0.000
Tph2$^{+/+}$ NaCl GR	5.793	-0.00108
Tph2$^{+/+}$ CIT GR	5.735	-0.0595
Tph2$^{-/-}$ baseline GR	5.504	0.000
Tph2$^{-/-}$ NaCl GR	5.724	0.2206
Tph2$^{-/-}$ CIT GR	5.991	0.4877
Tph2$^{+/+}$ baseline MR	8.120	0.000
Tph2$^{+/+}$ NaCl MR	8.341	0.2211
Tph2$^{+/+}$ CIT MR	8.198	0.0782
Tph2$^{-/-}$ baseline MR	8.285	<0.000
Tph2$^{-/-}$ NaCl MR	7.990	-0.6535
Tph2$^{-/-}$ CIT MR	8.446	0.1611

GR and MR mRNA gene expression in adrenal gland after 21-day CIT treatment

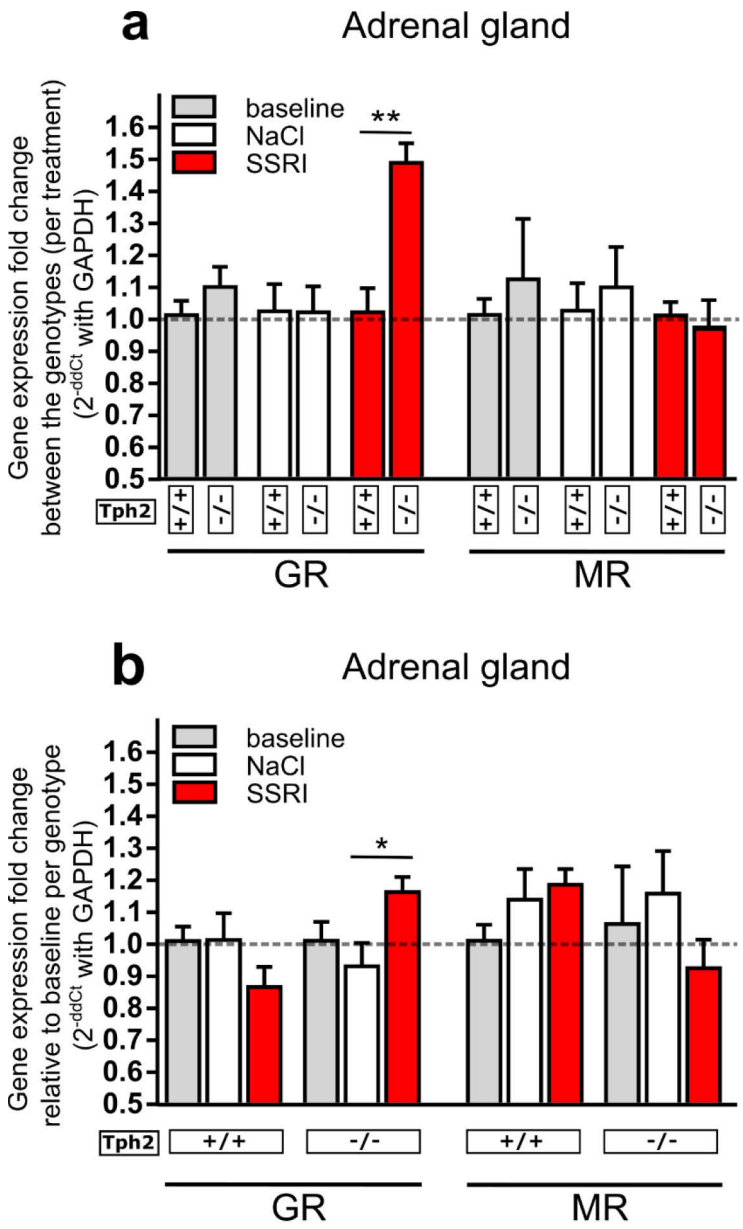

Figure 45 mRNA expression (fold change as $2^{-\Delta\Delta ct\ of\ mean}$ method) of GR and MR in the Adrenal gland of 14-week old, female *Tph2*$^{-/-}$ mice compared to *Tph2*$^{+/+}$. Bars in grey, baseline control, white bars 21-day NaCl and red bars 21-day SSRI CIT. a) *Tph2*$^{-/-}$ animals have significant higher levels of GR upon CIT treatment. *p<0.05 b) a treatment effect was observed for *Tph2*$^{-/-}$ mice' with increased GR expression levels upon CIT, *p<0.05.

At last, the adrenal gland is finally releasing the glucocorticoids form the zona fasciculata of its adrenal cortex [531]. A possible effect on GR and MR expression at adrenal gland level is quantified by qPCR. Data in Figure 45a + Table 36 reveal *Tph2*$^{-/-}$ animals have significant higher adrenergic GR levels when treated with CIT (Students *t* test p = 0.0072; Figure 45a, + Table 36). No changes were seen for MR. When treatment is compared (Figure 45b), a treatment effect was observed for *Tph2*$^{-/-}$ mice GR expression with increased levels upon CIT ($F(2,12)=4.115$ p= 0.0436).

Table 36 GR and MR mRNA expression levels in the Adrenal gland. Animals were subjected to 21-days of treatment or control. Δct and ΔΔct values per treatment between genotypes (a) and per genotype for different treatments (calculated based on GAPDH; *Tph2*$^{-/-}$ vs. *Tph2*$^{+/+}$).

Group	Mean Δct	ΔΔct
Adrenal gland		
Relative to genotype		
Tph2$^{+/+}$ baseline GR	5.874	0.000
Tph2$^{-/-}$ baseline GR	5.755	-0.1192
Tph2$^{+/+}$ NaCl GR	5.886	0.000
Tph2$^{-/-}$ NaCl GR	5.884	-0.00194
Tph2$^{+/+}$ CIT GR	6.110	0.000
Tph2$^{-/-}$ CIT GR	5.547	-0.7582
Tph2$^{+/+}$ baseline MR	8.641	0.000
Tph2$^{-/-}$ baseline MR	8.563	-0.0779
Tph2$^{+/+}$ NaCl MR	8.486	0.000
Tph2$^{-/-}$ NaCl MR	8.395	-0.09143
Tph2$^{+/+}$ CIT MR	8.407	0.000
Tph2$^{-/-}$ CIT MR	8.702	0.0585
Relative to baseline treatment		
Tph2$^{+/+}$ baseline GR	5.874	0.000
Tph2$^{+/+}$ NaCl GR	5.886	0.01268
Tph2$^{+/+}$ CIT GR	6.110	0.2362
Tph2$^{-/-}$ baseline GR	5.755	0.000
Tph2$^{-/-}$ NaCl GR	5.884	-0.1553
Tph2$^{-/-}$ CIT GR	5.547	-0.2341
Tph2$^{+/+}$ baseline MR	8.641	0.000
Tph2$^{+/+}$ NaCl MR	8.486	0.1299
Tph2$^{+/+}$ CIT MR	8.407	-0.4027
Tph2$^{-/-}$ baseline MR	8.563	0.000
Tph2$^{-/-}$ NaCl MR	8.395	-0.1688
Tph2$^{-/-}$ CIT MR	8.702	-0.09754

3.3 Electroconvulsive seizure (ECS)

3.3.1 ECS does not affect anxiety levels but attenuates the highly active phenotype of *Tph2*$^{-/-}$ mice

Results and respective discussion of the following section 3.3 have been published in Kronenberg, Petermann *et al.*, 2018 [510], and were created with the help of Prof. Dr. Peter Gass and Christof Dormann from the Central Institute for Mental Health Mannheim, Germany. 12-weeks-old *Tph2*$^{-/-}$ and *C57BL/6N* (WT) control female mice were randomly assigned into groups for ECS ("treatment") and control (CTR). To elicit ECS, pentobarbital pretreatment was followed by unilateral electrode placement for 5 days in treatment group, whereas control (CTR) groups did not receive ECSs (Figure 46a). In treatment group, at **day 1** *Tph2*$^{-/-}$ mice showed with 30 ± 0 mA a significantly higher seizure threshold compared to WT animals 23.8 ± 1.4 mA ($p < 0.001$);

at **day 2** for *Tph2*$^{-/-}$ 31.2 ± 1.4 mA vs. WT 31.0 ± .0.33 mA ($p > 0.01$)

at **day 3** for *Tph2*$^{-/-}$ 34.9 ± 0.1 mA vs. WT 33.4 ± .0.42 mA ($p < 0.01$);

at **day 4** for *Tph2*$^{-/-}$ with 35 ± 0 mA vs. WT with. 35.9 ± .0.31 mA ($p < 0.05$);

at **day 5** for *Tph2*$^{-/-}$ with 35 ± 0 mA vs. WT with 37 ± 0.4 mA, $p = 0.0001$;).

Notably, *Tph2*$^{-/-}$ mice already reached their final seizure response of 35 ± 0 mA on day 3 of the ECS course (Figure 46b).

All animals were subjected to behavior tests on days 8–10 to test for locomotor activity, stress, and antidepressant response to ECS (Figure 46a). In the elevated O-Maze test, a robust treatment and genotype effect was observed in WT and start latency to exit

Table 37 Mean + SEM + n: Time spend in open arms (O-Maze) after ECS treatment.

Group	Mean (s)	SEM	n
C57BL/6N WT CTR	59,50	8.89	8
Tph2$^{-/-}$ CTR	98,80	13.09	5
C57BL/6N WT ECS	59,90	6.740	10
Tph2$^{-/-}$ ECS	116.20	23.85	9

Table 38 Mean + SEM + n: Time spend in the center (%) of the open field after ECS treatment.

Group	Mean (%)	SEM	n
C57BL/6N WT CTR	11.46	1.59	8
Tph2$^{-/-}$ CTR	24.18	4.28	5
C57BL/6N WT ECS	10.20	0.70	10
Tph2$^{-/-}$ ECS	17.07	3.71	9

Table 39 Mean + SEM + n: Distance to the wall in open field after ECS treatment.

Group	Mean (cm)	SEM	n
C57BL/6N WT CTR	6.26	0.37	8
Tph2$^{-/-}$ CTR	8.74	0.50	5
C57BL/6N WT ECS	5.97	0.14	10
Tph2$^{-/-}$ ECS	7.78	0.58	9

into open arms was increased three fold in ECS treated WT mice (Two-way ANOVA followed by Tukey's *post hoc* test $F(1,24) = 7.175$, $p_{(\text{interaction})} = 0.0131$; $F(1,24) = 13.21$, $p_{(\text{treatment})} = 0.0233$; $F(1,24) = 5.870$, $p_{(\text{genotype})} = 0.0013$;Figure 46c and Table 37). In *Tph2*$^{-/-}$ mice, start latency was not affected (Figure 46c), and mice spent more time in the open arms of the O-Maze independently of treatment ($F(1,28) = 9.004$,$p = 0.0056$; Figure 46d + Table 37). When assessing exploratory behavior in the open field test, a genotype effect was observed ($F(1,28) = 12.99$, $p = 0.0012$; Figure 46e + Table 38). *Tph2*$^{-/-}$ mice spent significantly more time in the center of the arena, an effect diminished by treatment (Figure 46e). This is consistent with *Tph2*$^{-/-}$ mice staying in greater distances to walls ($F(1,28) = 24.60$, $p < 0.0001$; Figure 46f + Table 38 and Table 39).

In *Tph2*$^{-/-}$ mice, latency to immobility was significantly shorter regardless of treatment ($F(1,27) = 75.04$, $p < 0.0001$; Figure 46h + Table 41). *Tph2*$^{-/-}$ mice revealed an increased immobility time that was abolished upon ECS ($F(1,26) = 5.037$, $p_{(\text{treatment})} = 0.0335$; $F(1,27) = 16.59$, $p_{(\text{genotype})} = 0.0004$; Figure 46I + Table 40).

Table 40 Mean + SEM + n: Immobility time (s) in FST after ECS treatment.

Group	Mean (s)	SEM	n
C57BL/6N WT CTR	206.2	10.74	8
Tph2$^{-/-}$ CTR	271.1	16.87	5
C57BL/6N WT ECS	191.1	8.70	10
Tph2$^{-/-}$ ECS	229.4	11.96	7

Table 41 Mean + SEM + n: Latency to immobility (s) in FST after ECS treatment.

Group	Mean (s)	SEM	n
C57BL/6 N WT CTR	68.11	3.32	8
Tph2$^{-/-}$ CTR	36.24	4.54	5
C57BL/6N WT ECS	66.24	3.05	10
Tph2$^{-/-}$ ECS	38.53	2.85	8

Table 42 Mean + SEM + n: Total distance travelled in FST after ECS treatment.

Group	Mean (cm)	SEM	n
C57BL/6N WT CTR	63.65	4.87	8
Tph2$^{-/-}$ CTR	54.60	4.10	5
C57BL/6N WT ECS	67.80	3.45	10
Tph2$^{-/-}$ ECS	47.78	2.91	9

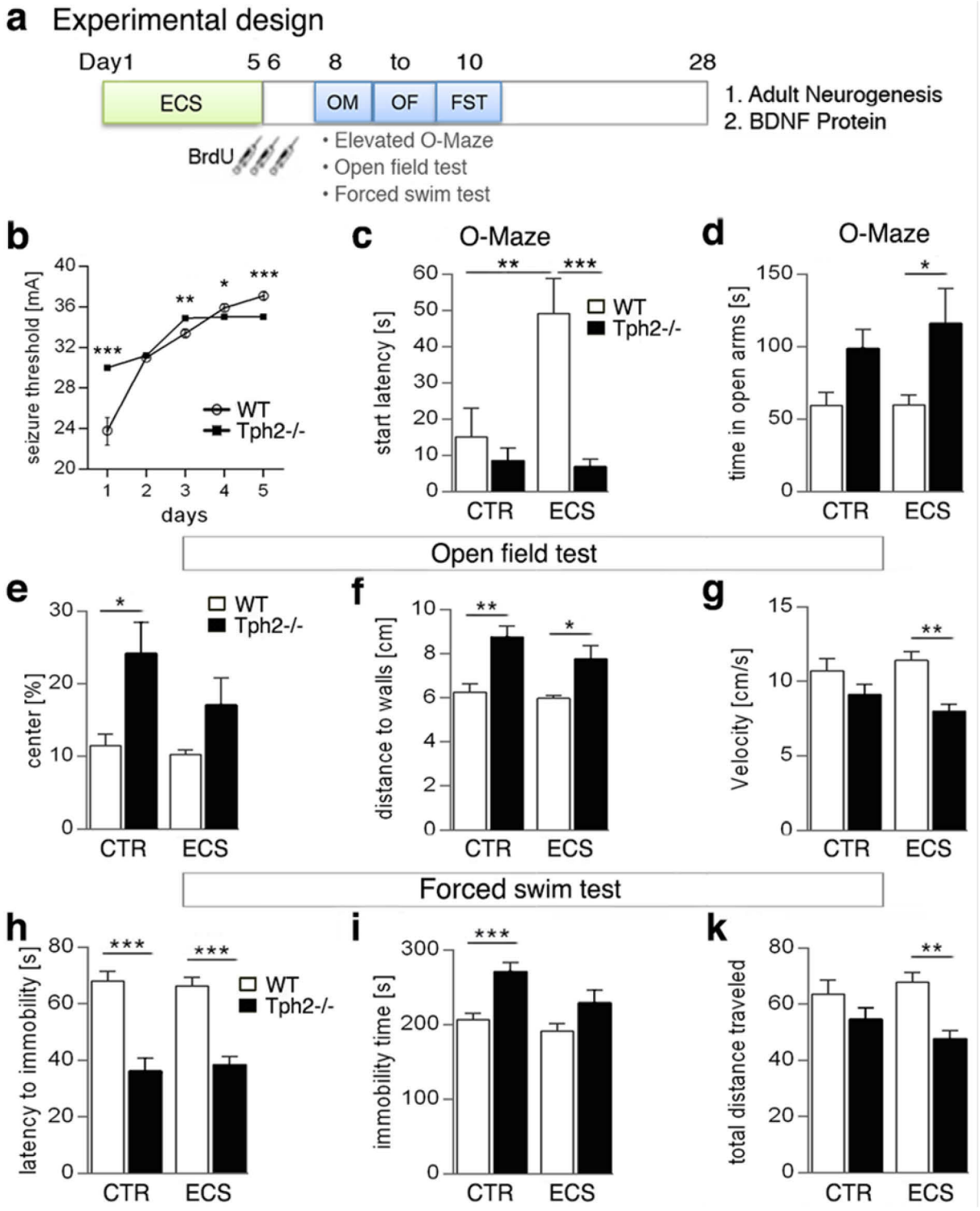

Figure 46 Physiology and behavior responses to ECS. (a) Experimental design. (b) Mean seizure thresholds for 5 days of *Tph2*$^{-/-}$ and WT mice. (c) Start latency in the elevated O-Maze test was increased in WT animals upon ECS. (d) *Tph2*$^{-/-}$ mice spent more time in open arms independently of treatment. (e–g) Open field test: *Tph2*$^{-/-}$ mice spent more time in the center (e, percentage) and off the walls (f) which was diminished in response to ECS, as was the activity index (mean velocity, g). (h–k) Forced swim test: latency to immobility time was significantly shorter in *Tph2*$^{-/-}$ mice and unaffected by ECS (h). However, the longer immobility time of *Tph2*$^{-/-}$ mice was abolished after treatment (i), and mice traveled shorter distances (k). CTR control sham w/o seizure; two-way ANOVA followed by Tukey's post hoc test, *p < 0.05, **p < 0.01, ***p < 0.001, ****p < 0.0001, data are presented as mean ± SEM; Published in 2018 in European Archives of Psychiatry and Clinical Neuroscience volume 268 [510].

The activity level of *Tph2*$^{-/-}$ mice upon ECS was decreased as shown by total velocity ($F(1,28) = 13.73$, $p_{(genotype)} = 0.0009$; Figure 46g). No effect of ECS was observed for WT in the forced swim test. Furthermore, ECS therapy attenuates the highly active phenotype of *Tph2*$^{-/-}$ mice as shown by shorter distances traveled ($F(1,28) = 13.20$, $p = 0.0011$; Figure 46k +Table 42). Tail suspension test was performed but, due to their impulsiveness, the *Tph2*$^{-/-}$ mice either managed to free their tail or lift up from hanging state, already after a short time.

3.3.2 Reduced neurobiological responses to ECS in *Tph2*$^{-/-}$ mice

On day 28, the survival of BrdU-labeled cells, and BDNF protein levels in the HC were assessed by separating the hemispheres for each method (right for BDNF-ELISA, left for histology). In response to ECS, the number of newly generated cells in the DG was significantly increased 21 days after BrdU injections (Two-Way-ANOVA $F(1,26) = 55.26$, $p_{(treatment)} < 0.0001$; Figure 47a + Table 44), which led to the characteristic boost in WT mice (CTR 190 ± 32 cells vs. ECS 695 ± 73 cells, $p = 0.0001$; Figure 47a), and a significantly attenuated increase in *Tph2*$^{-/-}$ mice (CTR 179 ± 48 cells vs. ECS 496 ± 50 cells, $p < 0.01$ Figure 47a). Likewise, a treatment as well as genotype effect for BDNF protein levels was observed in the HC in response to ECS ($F(1,26) = 6.120$, $p_{(treatment)} = 0.0202$; $F(1,26) = 10.83$, $p_{(genotype)} = 0.0029$; Figure 47b + Table 45) revealing an increase by 66 % in WT mice. In *Tph2*$^{-/-}$ mice, BDNF protein levels increased by 43 % upon treatment but reached only 50 % of WT in HC

Table 43 Mean + SEM + n: BDNF PFC levels after ECS treatment.

Group	Mean (pg/mg)	SEM	n
C57BL/6N WT CTR	2.86	0.57	8
Tph2$^{-/-}$ CTR	3.53	1.00	6
C57BL/6N WT ECS	11.46	3.63	9
Tph2$^{-/-}$ ECS	12.87	3.77	8

Table 44 Mean + SEM + n: BrdU+ cells in HC after ECS treatment.

Group	No. BrdU positive cells	SEM	n
C57BL/6N WT CTR	173	33	7
Tph2$^{-/-}$ CTR	163	44	6
C57BL/6N WT ECS	623	99	9
Tph2$^{-/-}$ ECS	496	50	9

Table 45 Mean + SEM + n: BDNF HC levels after ECS treatment.

Group	Mean (pg/mg)	SEM	n
C57BL/6N WT CTR	30.25	3.74	8
Tph2$^{-/-}$ CTR	18.01	2.73	6
C57BL/6N WT ECS	49.76	10.34	7
Tph2$^{-/-}$ ECS	25.75	2.03	9

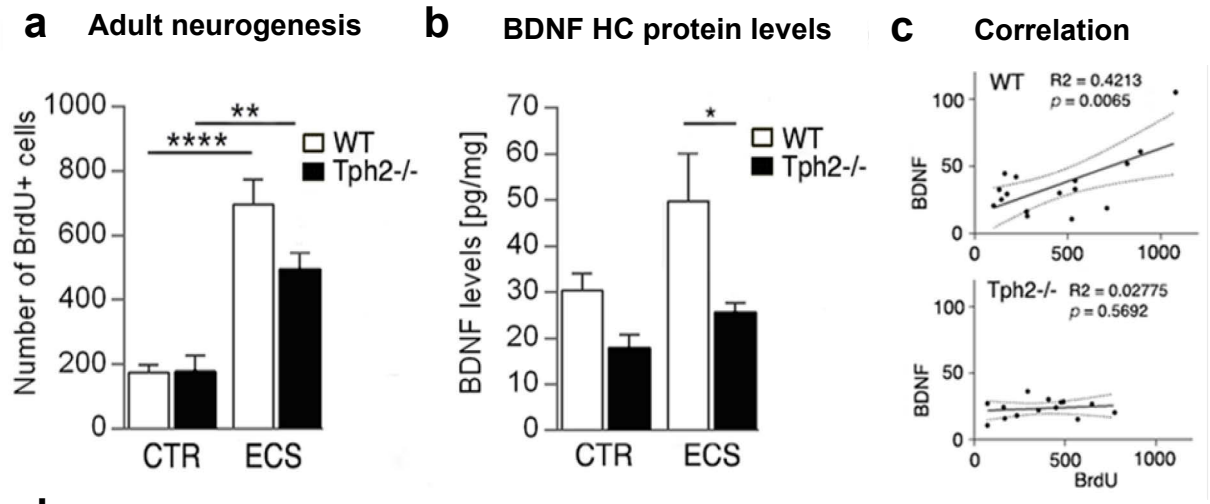

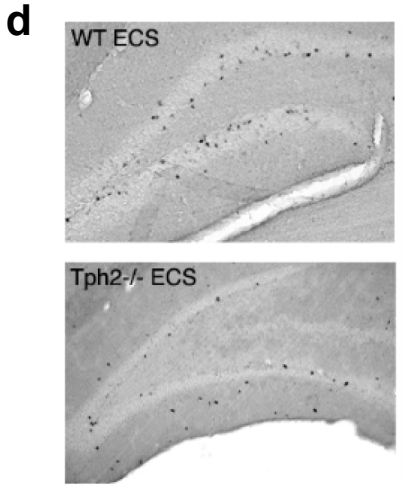

Figure 47 Physiology and behavior responses to ECS: (a) In response to ECS, the survival of newly generated cells was robustly increased 21 days following BrdU in WT mice, with an attenuated increase in *Tph2*$^{-/-}$ animals. (b) At 28 days, BDNF protein levels were increased in the hippocampus of WT mice, with a markedly attenuated response in *Tph2*$^{-/-}$ animals. (c) The positive correlation of BDNF levels with adult neurogenesis in WT mice was absent in *Tph2*$^{-/-}$ mice. (d) Representative staining of DG with DAB stained BrdU+ cells, black dots, in ECS treated WT compared to *Tph2*$^{-/-}$, CTR control sham, w/o seizure; Two-way ANOVA followed by Tukey's post hoc test, *p < 0.05, **p < 0.01, ****p < 0.0001, data are presented as mean ± SEM.

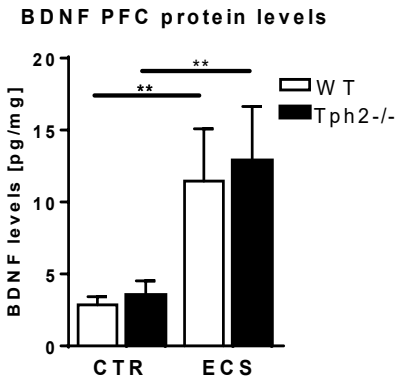

Figure 48 ECS treatment increased BDNF levels, serotonin independent in both genotypes in the left PFC hemisphere. ECS electro convulsive seizure treatment, CTR control sham, w/o seizure; two-way ANOVA followed by Tukey's post hoc test, **p < 0.01. Data are presented as mean ± SEM.

(Tukey's post hoc test p = 0.0219; Figure 47b + Table 45). Notably, our data reveal a positive correlation between the number of newly generated cells in the DG and BDNF protein levels in HC (not in PFC) in WT mice (R_2 = 0.4213, p = 0.0065; Figure 47c) that was absent in *Tph2*$^{-/-}$ mice (Figure 47c). In the PFC, BDNF levels were significantly increased for both genotypes (Two-way ANOVA, F (1, 28) = 9.855, p (treatment) = 0.0040, Figure 48 + Table 43) after ECS treatment.

3.4 Behavioral setups as a biomarker for depression

3.4.1 Reduced nesting behavior in the lack of serotonin

During the antidepressant application studies, an altered behavior of *Tph2*$^{-/-}$ mice compared with WT was observed. Keeping the cage clean, intact, and building a nest seemed less structured in *Tph2*$^{-/-}$ mice, with excreting in all areas of the cage and often no nest built. Based on these observations, a standardized experimental setup for nesting behavior was established, according to Deacon [502], which was also described as test for a depressive-like behavior (Figure 49). Different transgenic mouse strains with altered levels of serotonin were tested in both genders, and littermate controls.

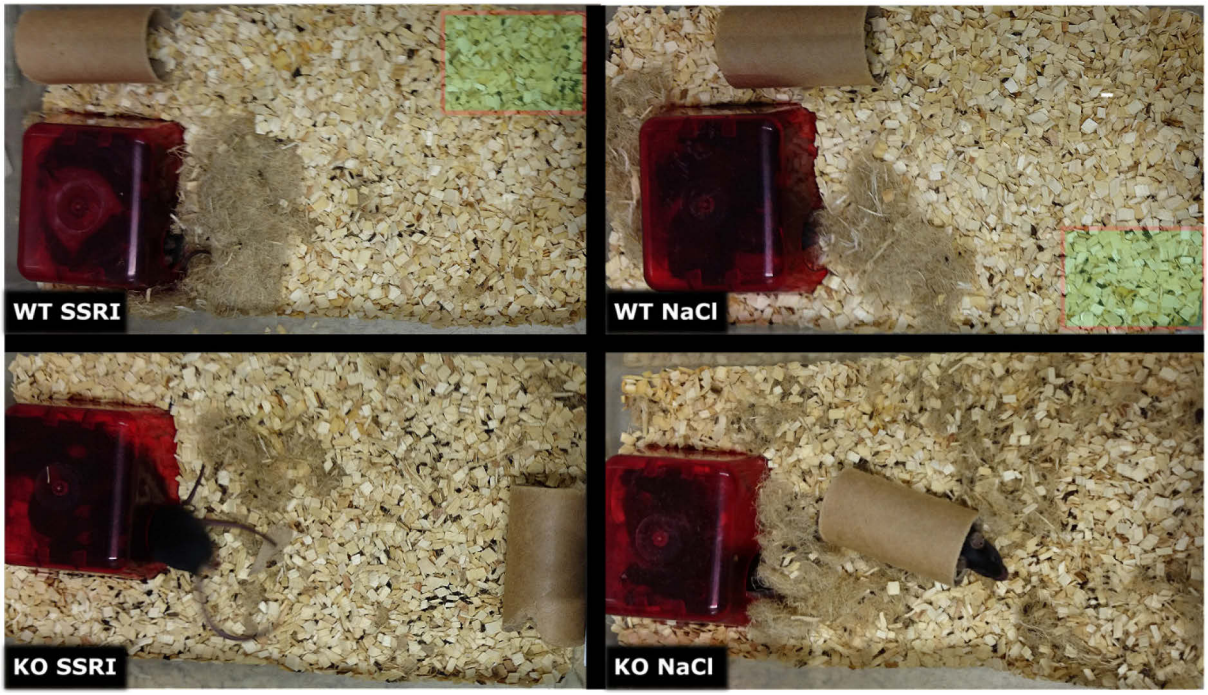

Figure 49 Representative cage behavior in female *C57BL/6N* (WT) and *Tph2*$^{-/-}$ (KO) after 20 days of CIT (SSRI 10mg/kg/day) and Saline (NaCl, 0,9 %/day) treatment. The four pictures indicate the status of a fresh cage after keeping the treated mice for 7 days in it, where environment is positioned at standardized positions at day 1 (House- lower left corner, paper roll – upper right corner, nest material – opposite corners to housing). WT mice show more structured cage behavior than *Tph2*$^{-/-}$, concerning defecation area (indicated by greenish area in WT, in *Tph2*$^{-/-}$ no such distinct area detectable), nest material hoarding, interaction with environment (e.g. paper roll) and overall cage hygiene.

Mice with altered serotonin system, SERT$^{-/-}$ (n=11), *Tph2*$^{-/-}$ (n=10) and *ACE2*$^{-/-}$ (n=10), failed to build appropriate nests (Figure 50) out of a square cotton nestlet introduced for one night (*ACE2*-deficient mice were added as another model with reduced serotonin levels in the brain [506,507]). SERT$^{-/-}$ mice tend to show fear to the novel object in their cage and sometimes bury it, which comes in line with their known anxious phenotype [532]. *Tph2*$^{-/-}$ mice show active behavior, often tear the cotton nestlet apart and spreading it all over their cage, failing to produce a proper nest in the end. (Figure 50) This is in line with their active and aggressive behavior. Surprisingly, *Tph2*$^{+/+}$ (n=12) littermates also show a trend for an impaired nesting behavior, leaving the

nesting material partly intact, when compared with BL/6N mice (similar genetic background) but not being anxious like SERT$^{-/-}$. Proper nests with a score of 4+ could only be spotted in the control groups of *C57BL/6* mice from both Charles River (N, n=9) and Jackson laboratories (J, n=10, Figure 50).

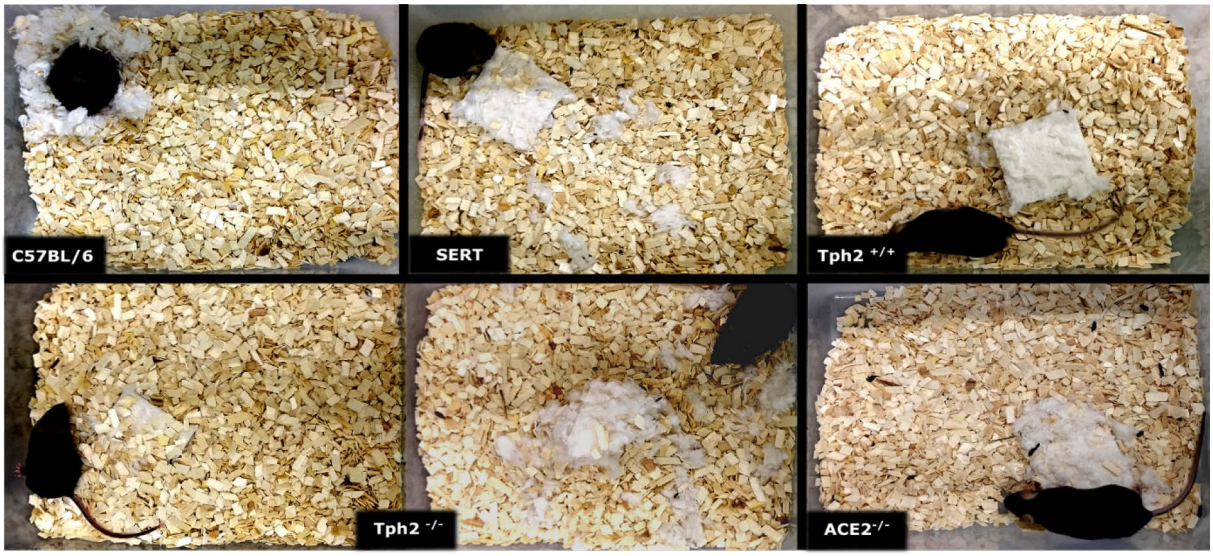

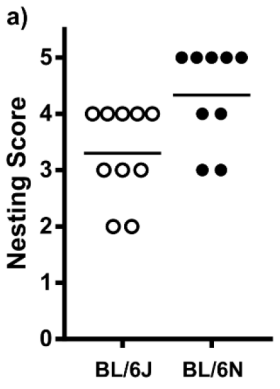

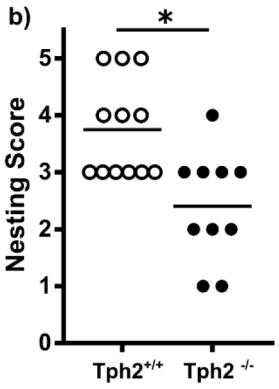

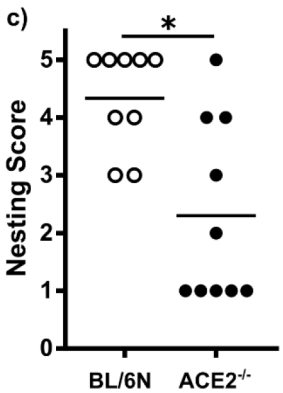

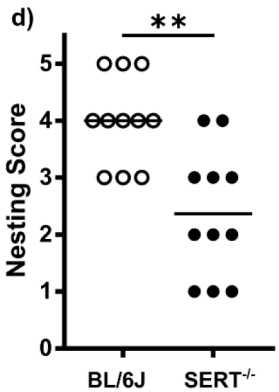

Figure 50 Assessing scores to nests (Scoresheet Figure 19) in different female transgenic mouse strains compared to their controls. (Top) Sample pictures of nesting after exposure to the nestlet o.N.. (a-d) Nesting scores. Each dot represents a nesting score of one mouse, being exposed to nesting material during its active phase. Mice with altered serotonin system showed a lower score in b to e, whereas a slight difference can already be spotted between the control inbred strains *BL/6J* deriving from Jackson and *BL/6N* from NIH Laboratories in (a). The bar represents the average nest score per group. One-way ANOVA followed by Tukey's post hoc test *p<0.05 Tph2; **p<0.01 SERT KO to C57BL/6J control.

3.4.2 Hoarding and Burrowing

To assess further if the absence of brain serotonin lead to a deterioration in behavior for activities of daily living in a rodent, *Tph2*$^{-/-}$ mice have been subjected to burrowing and hoarding paradigms as biomarkers for depression [503]. Female *C57BL/6N* mice (n=6; 27 weeks old) and female *Tph2*$^{-/-}$ mice (n=6; 19-weeks-old) were tested in a group of 2 for hoarding and a group of 3 for burrowing with habituation time of 2 days to ensure unobstructed behavior to novel objects. The weight of the hoarded / burrowed food pellets was measured.

Whereas *C57BL/6N* (n=3) mice hoarded nearly all provided pellets to their home cage after 14 h test (Figure 51; 80.67 g ± 10.87 g chow hoarded in cage; chow leftovers in tube 11.00 g ± 11.00 g), the *Tph2*$^{-/-}$ (n=3) mice showed a trend for decreased hoarding behavior. (56.00 g ± 8.718 g chow hoarded in cage; chow leftovers in tube 38.67 g ± 8.110 g). Since the number of trials (n=3) was low, no statistics were applied. In all three rounds of experiments, it could be observed that in *C57BL/6N* mice, the pellets were moved into the cage but positioned next to the junction site between tube and

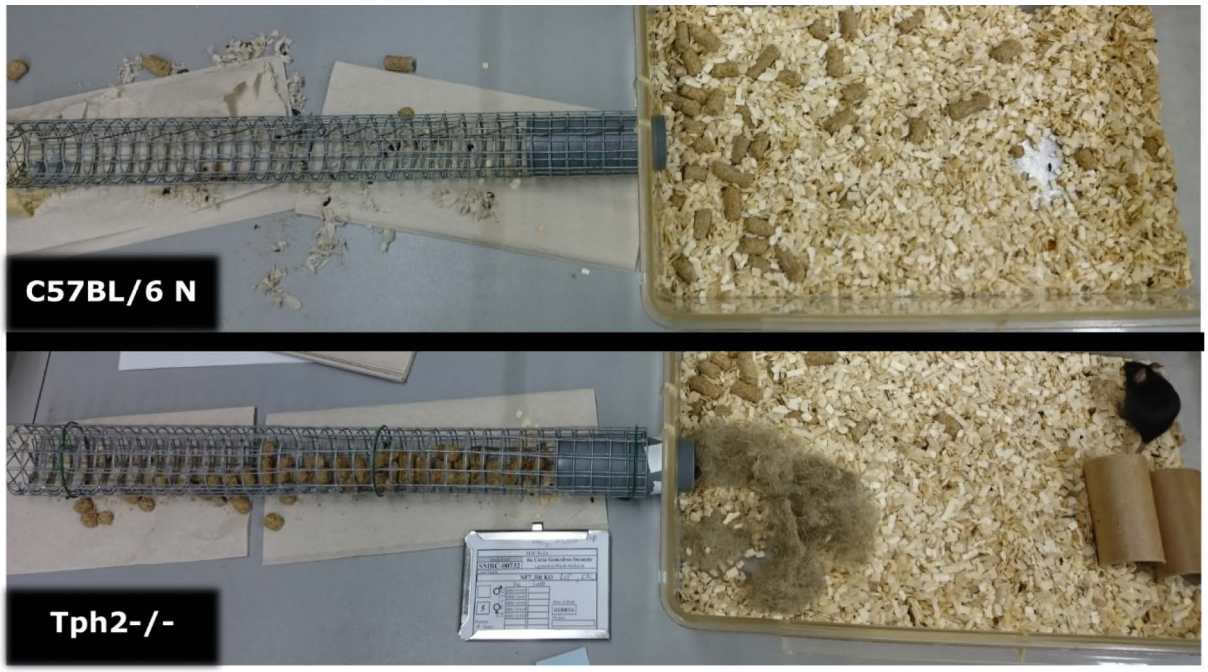

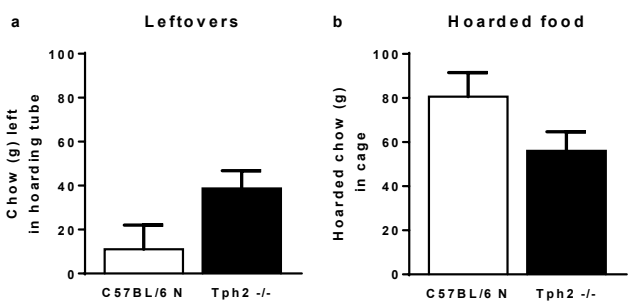

Figure 51 Hoarding behavior of in WT (n=3) and *Tph2*$^{-/-}$ mice (n=3). (Top) Sample pictures of experimental setup and outcome after 14h test. (Left a+b) Mice lacking brain serotonin show a trend towards decreased chow hoarding (b). All tested *C57BL/6N* mice (white bars, top picture) collected nearly all provided pellets from the attached mesh (a) into their home cage (b), whereas *Tph2*$^{-/-}$ only hoarded part of it (a).

cage, whereas in *Tph2*$^{-/-}$, hoarded pellets were spread over the whole cage (Figure 51). Also, the number of pellets and litter outside around the mesh tube was obviously more than in WT mice.

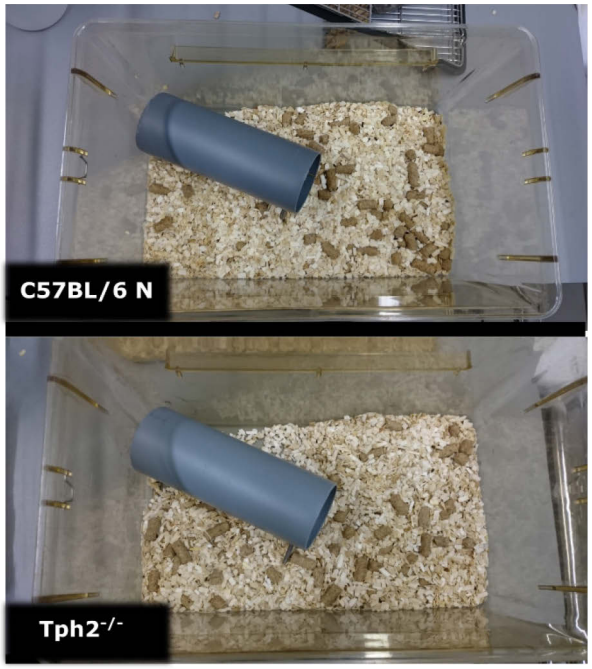

Figure 52 Sample cages after 14h of burrowing test paradigm. WT (n=3) and *Tph2*$^{-/-}$ (n=3) removed the complete 200g chow from the tube after 14h of testing in the dark phase, and spread it in the whole cage.

In the tested burrowing paradigm, WT (n=3) and *Tph2*$^{-/-}$ (n=3), both groups showed a low burrowing behavior during habituation, while light phase, but in the 14h dark phase testing all groups emptied the burrowing tube completely and spread the chow non-systematically and non-burrowed in the cage (Figure 52). During the observation of the first half of an hour of the test, both groups investigated the tube right after placing it chow filled in the cage, but no burrowing behavior was noticeable in the beginning for both groups. In the end not a single piece of chow was left in the tube.

4 Discussion

In my thesis, I have identified "mechanisms of antidepressant action" in rodents and compared my results with mice that lack brain serotonin – *Tph2*$^{-/-}$. As the link between depression, neurogenesis, and stress had been reported [164,28,249,533], I specifically tested the current pharmaceutical theories that are of clinical relevance and made use of the antidepressants drugs citalopram (CIT) and tianeptine (TIA), as well as of electro convulsive seizure (ECS). I determined their effects on neurobiological systems, e.g., cell survival in the HC, adult neurogenesis, BDNF signaling, and the stress axis. During the process of my thesis, I concluded that the various systems interplay, and that, although largely separable, mostly involve serotonin signaling.

4.1 Monoamine hypothesis – serotonin is target in SSRI but not SSRE function

Impaired serotonin transmission has long been implicated in the pathogenesis of depression - in the so called "Monoamine hypothesis of depression" [25]. Compounds targeting serotonin, like the SSRI CIT shown in this study, are widely used as flagship antidepressants. Yet only 25 % of patients respond to the drug, and mechanisms still need to be determined. The classically used antidepressant drug, Prozac, a SSRI, in form as fluoxetine (FLX) for rodents, showed that its chronic administration increases neurogenesis in the adult rat and mouse HC [124,187].

My thesis determined the pro-neurogenic effects of CIT and TIA on adult neurogenesis, BDNF signaling and various parameters of the HPA-axis.

The first experiments in Figure 22 - Figure 24, showed differential effects of CIT vs. TIA. The rate of cell survival of newborn neurons in the HC is an important factor in drug action. 21 days of CIT treatment significantly increases the number of BrdU-positive cells in the DG in WT animals, while SSRE TIA has no effect (Figure 24) with a trend for a decrease in BrdU+ cell numbers. The results obtained by the SSRI fit to the theory that serotonin is beneficial for neurogenesis in the DG [124,125]. Surprisingly, in *Tph2*$^{-/-}$ mice, administration of all three compounds increases BrdU number. Notably, survival of BrdU+ cells for 21 days was not affected without treatment, Figure 23. Nonetheless, in *Tph2*$^{-/-}$ mice, adult neurogenesis was consistently increased, and one has to distinguish drug effect from *Tph2*$^{-/-}$ phenotype. Given high BrdU+ cell numbers in all *Tph2*$^{-/-}$ treatment groups including SAL (Figure 22-Figure 24), my

results suggest that no drug effect occurs in the absence of brain serotonin; arguing serotonin is a prerequisite in antidepressant action, namely the increase in cell survival [124,187]. For survival (untreated, unhandled), the amount of BrdU+ cells is not increased. However, enhanced survival of newly generated cells at baseline had been described earlier in other models of serotonin depletion, *Pet1*$^{-/-}$ and *VMAT2 SERT*-Cre mice [186]. These findings could not be reproduced in several independent experiments as show here; e.g. baseline ECS, no difference in BrdU numbers (Figure 47) [510], and additional studies on unhandled mice (Figure 23). The increase in neurogenesis may be a result of daily treatment, or injection-stress, independent of the used compound – that had been determined separately in the experiment of Figure 35 and following.

Song *et al.* showed in 2016 that in adulthood, an acutely induced depletion of serotonergic neurons and serotonin neurotransmission by using a tamoxifen-induced *Cre* (*Pet1-CreERT2* mice) goes along with an increase in precursor proliferation and net neurogenesis. The increase can be diminished by chronic treatment with an agonist for 5-HT$_{2C}$ receptor [534]. It needs to be seen whether targeting of 5-HT$_2$ receptor subtypes in *Tph2*$^{-/-}$ mice will have an effect. Furthermore, CIT has been shown to desensitizes 5-HT$_{1a}$ auto-receptors allowing higher levels of serotonin in the synaptic cleft [535]. Therefore, applying a 5-HT$_{1A}$ receptor agonist to our *Tph2*$^{-/-}$ mice may also result in increased neurogenesis. Constitutive depletion models, as stated above, and as shown by Diaz et al in 2013, show increased BrdU+ cell number [186]. However, we have seen this difference in cell numbers only after daily treatment.

Second notably is the use of C57BL/6N as wild type mice versus *Tph2*$^{+/+}$ littermates as control "WT" mice in comparison with our *Tph2*$^{-/-}$. Due to availability, some experiments used one group, some the other as control. The transgenic *Tph2* knockout strain is originally generated on *BL/6/129Sv* genetic background [302]; later *Tph2*$^{-/-}$ mice were backcrossed for multiple generations to the C57BL/6N strain (min. of 10 generations), thus a similar phenotype of *Tph2*$^{+/+}$ and C57BL/6N is to be expected. Nonetheless, a complete absence of strain specific physiological differences cannot be taken as granted and is not fully proven, as multiple strain differences in physiology occur often in research literature [536].

No effect of chronic TIA treatment on cell survival was observed. An earlier study on male tree shrews has shown that orally given TIA, although reversing stress-induced reductions in BrdU+ cell numbers, had no effect under baseline conditions [227,537,538], which is in line with the results here. TIA has been identified for its modulation of

glutamate transmission and neurotransmitter interplay [219]. Since transient DCX-expressing cells in the SGZ first display GABA receptors acting excitatory [539], TIA administration might act on that population explaining the observed decrease in BrdU/DCX-positive cells. CIT-treated mice have an increased DCX population due to increased BrdU+ cell numbers. Further experiments should characterize the ratio of cell survival and cell death of newly born neurons in the DG at the transcriptional level, as immunohistochemistry did not show any results. Possible readouts can be also obtained by single cell sequencing / RNAseq, focusing on fluorescence-BrdU labeled cells, of animals treated with SSRI / SSRE, and at different times (short-time treatment for several days up to 21-day treatments) in *Tph2* (conditional) knockouts.

In addition, antidepressant therapies enhancing extracellular serotonin levels like SSRIs, affecting the 5-HT1 receptor feedback loop, only show temporary effects and delayed onset of action in patients [540]. This does not account *vice versa* for SSREs [541]. Maybe after 21 days of treatment with the SSRI CIT, we see already an attenuation of the extracellular serotonin levels, induced by the 5-HT1a receptor, leading to a similar phenotype as in our *Tph2*$^{-/-}$ mice, whereas TIA treatment stays unaffected. Supportive HPLC of serotonin levels during treatment can help here.

In addition, the half-life of the drugs plays a role. CIT's is about 35 hours in humans. Half-lives in mouse were tested with 24 mg/kg body weight and resulted in 1½ hours and systemic plasma clearance in male mouse was 87 ml/min/kg BW, and female mouse 116 ml/min/kg BW [542]. Experiments here were performed with 10 mg/kg body weight, as the most commonly applied concentrations in research, so the plasma clearance might be faster in our experiments. Also, since *Tph2*$^{-/-}$ mice show already changes in HPA-Axis and glucocorticoid levels, a different plasma clearance of the administered antidepressants is expected, as with differences in glucocorticoids come differences in several metabolisms in the organism [316]. Maybe SSRI concentrations for *Tph2*$^{-/-}$ mice were set too low. TIA pharmacokinetics also differ between adult mice and men. The primary metabolite of TIA (MC5) has a longer half-life in brain and plasma (>8h in mice) than TIA (<1h in mice, when given in higher doses of 30 mg/kg). TIA's metabolite MC5 mimics the behavioral effects of TIA in a mu-opioid receptor (MOR)-dependent fashion [543]. Pain or stressful conditions can activate opioid neurons (i.e. by MOR) in the ventral portion of periaqueductal gray next to the DRN, which in turn may modulate the activity of serotonergic neurons in the DRN [544–548]. Especially activation of MOR has been shown to differentially modulate serotonin efflux in the rat central

nervous system via the DRN [549]. TIA is a full agonist on MOR, (for G-protein activation and inhibition of cAMP accumulation) - that is a prerequisite for anxiolytic, acute and chronic antidepressant-like behavioral effects of the SSRE, as shown in mice [543,550]. In another mouse study, loss of MOR lead to increased BrdU-labeling after repeated i.p. injections of BrdU [551]. As MOR affects serotonin efflux, in our *Tph2*$^{-/-}$ mice TIA cannot exert its MOR-driven antidepressant effect, leading to the increased injection-based cell proliferation in the DG, as seen in previous research by the other groups [551]. This speaks for an indirect serotonin-dependence of one antidepressant mechanism of TIA.

4.1.1 Stress effects on adult neurogenesis

To pin down depression to a simple deficiency of serotonin or monoamines would be naive. SSRI such as CIT or SSRE like TIA have the pharmacologic abilities to quickly increase monoamine transmission [552], whereas the therapeutic approach and mood stabilization takes several weeks. The complexity of an intact brain is proven by tests, where monoamines have been depleted in unmedicated depression patients, resulting in drop in mood, but in healthy subjects this depletion did not result in a mood change, speaking for several downstream modulators, directly modulated by serotonin [553]. Neurogenesis seems to be a relevant modulator, as shown here (Figure 22 - Figure 24 + Table 18-Table 20), all *Tph2*$^{-/-}$, receiving a hypothetical "stressful" injection over 21 days results in a high increase in neurogenesis, masking the cell survival promoting effects of SSRI. Chronic stress and CORT administration in rodents reduce hippocampal volume [554–558]. 21-days of injection may not be considered chronic stress, as the data here rather reveal lowered CORT / glucocorticoid and ACTH plasma levels in treated mice, when compared with non-treated mice (Figure 35). Furthermore, the lowered CORT and ACTH plasma levels in *Tph2*$^{-/-}$ mice fit the high glucocorticoid - low neurogenesis observation, as we also see elevated cell survival number in all treatment. Hippocampus, amygdala, PFC and the hypothalamic PVN, are not only connected to each other, but are also heavily innervated by dorsal raphe serotonin fiber projections [166,528,559,560] supporting a highly linked interplay mechanism of stress and serotonin in depression [166]. The increase in BrdU+ cell numbers seem to be independent of CORT, fitting to the low CORT levels observed in *Tph2*$^{-/-}$ mice.

Increased neurogenesis confers resilience to chronic stress by balancing cell proliferation to cell death = homeostasis. When neurogenesis is impeded, mice show a slower glucocorticoid recovery after stress exposure, attributing to the HC an important role for the regulation of the HPA-axis [561,562]. Furthermore neurogenesis-

deficient mice showed increased stress-induced depressive like behavior in a novel environment test, increased behavioral despair in FST, and decreased anhedonia as measured by sucrose preference [164]. *Vice versa* neurogenesis can be attenuated by glucocorticoid hormones [563–565], representing the tight interplay between HC and the HPA-axis. Another study showed that GR in the DRN inhibited tph2 gene expression upon CORT activation [566] [125,170,182,187,311].

Adult neurogenesis may maintain a homeostatic hippocampal volume, that however, is not connected to a stress-induced volume loss [274]. A detailed revision on behavioral tests conventionally used to evaluate a depressive-like state or phenotype in rodents, clearly demonstrates that simply decreased neurogenesis is not enough to directly induce a depressive-like state [567]. Rather chronic stress-produced volume loss in the HC in humans by, i.e., atrophy of CA3 pyramidal cells suppresses adult neurogenesis in rodents [274]. Chronic stress might go along with the decline of neurogenesis in depressed patients [249], and antidepressant treatment with SSRI or ECT can rescue the hippocampal volume loss in depression and partly release from depressive symptoms [260,274,557,568]. In contrary, studies found no significant differences in hippocampal volume between depressed and non-depressed-, but risk factor patients [569], and no age-dependent decline of neurogenesis in the DG. Furthermore a decline in hippocampal neurogenesis does not necessarily come with a decrease in hippocampal volume [570]. Together with Prof. LiPing Wang from the Chinese Academy of Science (SIAT, in Shenzhen) and Dr. Naozumi Araragi (AG Bader / MDC Berlin), we have been collaborating on another model, *Tph2ChR2-YfpTg* mice, to investigate hippocampal long-term potentiation (LTP), and to see whether optical stimulation of serotonergic neurons in raphe nuclei may directly affect cell proliferation in the DG. The mouse model expresses a photosensitive-gated ion channel (Channel rhodopsin 2, ChR2), activated by laser light [296,571]. The channel is only expressed in Tph2-positive, serotonergic neurons; visualized by yellow-fluorescent protein (YFP, Figure 53). An activation

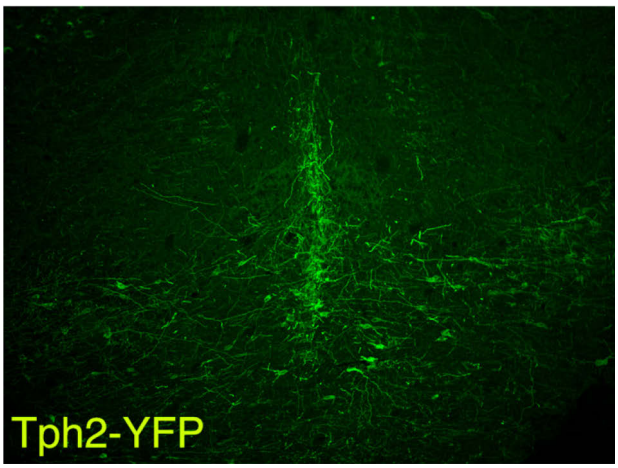

Figure 53 Coronal section (40 µm) of the DRN of a female Tph2ChR2-Yfp mouse, showing expression of the autofluorescence YFP-protein in Tph2 expressing neurons and therefore expression of the ChR2 channel in serotonergic neurons (x300 magnification).

of the channel would lead to a release of serotonin into the synaptic cleft. Briefly, an optical fiber is transplanted via stereotactic injection into the raphe nuclei, or the HC, respectively. The mouse is stimulated for 1-5 days overnight with blue laser light. At the day of the last stimulation the mouse is injected with BrdU, and newly generated cells in the DG were analyzed. The idea was to establish an optogenetic setup, to study the effect of induced serotonin release on neurogenesis and maybe use it further for research in antidepressant mechanism. Preliminary data showed a lateral decrease of BrdU-labeled cells when serotonergic neurons were acutely stimulated overnight (Araragi *et al. unpublished*). These data suggest a direct effect of serotonin fiber stimulation on cells in the DG. Ongoing experiments focus on electrophysiological recordings of hippocampal neurons. Targeting of HC directly allows for analyzing alterations in LTP or LTD.

Since a correlation of serotonin and neurogenesis was confirmed, the link for the behavioral effects following chronic antidepressant treatment mediated by the stimulation of hippocampal neurogenesis is needed. Interestingly, X-irradiation of mouse hippocampi prevented the neurogenic and behavioral effects of SSRIs (FLX) [183] indicating SSRIs' working mechanisms to act via neurogenesis, whereas several types of stress that reduced cell proliferation does not itself lead to depression [249,567]. For example, rodents in which hippocampal neurogenesis has been ablated (i.e. by irradiation [164,183]) do not show anxiety or stress-related depression-and respective behaviors. So, the results are still contradictory and further investigation on a molecular level is definitely needed.

4.1.2 The SSRE TIA – A doubtful "hypothesis-killer" !

SSRIs promoting an extracellular serotonin release affect SERT and 5-HT1 receptor feedback inhibition; which therefore contributes to temporary effects and a delayed onset of action [540]. SSRIs have high affinity to SERT [117]; as was shown in SERT knockout mice where the common SSRIs (FLX and CIT) did not show the acute and chronic antidepressant effects [327]. This further confirms the monoamine hypothesis of depression but speak for a possible compensatory pathway to maintain brain functionality if a lifelong serotonin depletion exists. This does not account for SSREs [541]. TIA is enhancing serotonin reuptake, decreasing extracellular serotonin levels in the brain [203,204], and even decreasing number and mRNA expression of SERT sites in the DRN [205]. Clinically, it is nowadays used to treat not only MDD, but also anxiety, asthma, and irritable bowel syndrome. The drug shows efficacy and tolerability in

patients where regular TCA or SSRI do not lead to an response or are not well tolerated [194,206–213]. In rodent stress and depression models, efficacy of TIA was quantified as good, too [206,214–219]. Nevertheless, its antidepressant effects cannot be fully described; clinical improvement may depend on other factors, e.g. dopamine, AMPA and NMDA interaction [219]. Glutamate is the major excitatory neurotransmitter, controlling synaptic plasticity, also affecting depressive episodes, stress and anxiety (reviewed in [220–225]). Stress-mediated increases in glutamate efflux in the amygdala can be countered by TIA [226], speaking for a glutamatergic-based antidepressant role in stress-induced depression. The SSRE has the capability to oppose the stress- and depression-induced structural and metabolic changes in the rodent hippocampus [219,227–232] and amygdala [232–234], often glutamate mediated. TIA shows no affinity, nor alters concentration and sensitivity/responsiveness for certain neurotransmitter receptors (e.g., dopaminergic receptors, 5-HT1 to 5-HT7, NMDA, AMPA, kainate, benzodiazepine or GABA-B receptors), except for an increased responsiveness in the α1 adrenergic system, but does not block or decrease the uptake or degradation of NA in the CNS [180,219,572]. Further it has been shown that TIA increases extracellular DA in the NAc in a serotonin independent manner [573], but how remains unclear.

Further, it is known that TIA triggers a cellular cascade of adaptions, leading to its efficiency as an antidepressant. One of the adaptions is the increased phosphorylation of AMPA/glutamate receptor subtypes in the frontal and cingulate cortex, as wells as in the CA1 and CA3 region of hippocampus, and reverses stress induced down-regulation of the putative BDNF/MEK/MAPK signaling cascade in the frontal cortex [572,574]. This thesis' task is to see, if TIA's antidepressant effects are serotonin plus neurogenesis based and / or BDNF-related. In my experiments, neither alteration of BDNF levels in hippocampus nor in PFC could be seen in WT mice after chronic TIA treatment, when compared to saline treatment. The earlier described increased BDNF protein tissue levels in the hippocampus of *Tph2*$^{-/-}$ mice were reproduced [312], and were not altered by TIA treatment, but CIT. Besides serotonin, glutamate and GABA signaling can increase BDNF expression in the HC [575,576] and increases the motility of neuronal progenitor cells in hippocampus [577], bringing another evidence for TIA's antidepressant effects since its main working mechanism goes via glutamatergic pathway. A further testing of the glutamatergic activity in these brain regions would be a suitable follow up experiment to proof the findings.

Summarized, TIA's antidepressant mechanism maybe the modulation of the glutamatergic system, located upstream before it is mediating serotonin release in the DG [578], but still serotonin is relevant for healthy homeostatic neurogenesis in the hippocampus. This might be a reason, why an increase in DG cell survival in *Tph2*$^{-/-}$ animals was observed, but not in WT. Serotonin regulates neurogenesis, stress or depression alter the glutamatergic systems, subsequently alter correct serotonin homeostasis, and further deregulate the neurogenesis process. TIA might indirectly act via serotonin in depressed patients, by directly affecting the glutamatergic system, with the support of other brain metabolites, such as NA. Therefore, a combination of glutamate receptor antagonists, as well as measurements of extracellular serotonin level measurements in the DG might be helpful, with a closer look on the effect on neurogenesis. Combinational therapeutic drug treatment targeting both neurotransmitters might be more efficient for mood stabilizing effects but must be extensively studied since glutamate and serotonin play an ubiquitous role in a plethora of physiological and psychological functionalities.

4.2 Neurotrophin Hypothesis – BDNF is involved in brain plasticity in the absence of serotonin

In extension to the monoamine hypothesis of depression, the "neurotrophin hypothesis of depression" was added. BDNF has been implicated in the pro-neurogenic effect of SSRIs. In line with the neurotrophin theory, HC, amygdala and PFC [579] undergo volume and structural changes in depressive patients [261,490,580]; based on neurobiology of dendrite shrinkage, glial cell loss, and/or impairments in neuroplasticity and cellular resilience [581]. Often the "Neurotrophin hypothesis of depression" is denoted as "BDNF hypothesis, and bases on the antagonistic effects of stress, affecting cell survival or morphology on the HC [429].

In this thesis, I have tested both hypothesis in ECS, and following SSRI and SSRE. Upon ECS, serotonin was identified as prerequisite in mediating key neurobiological effects, an increase in adult neurogenesis and BDNF signaling. In *Tph2*$^{-/-}$ mice, diminished treatment-induced increase in cell survival and BDNF concentrations in the HC was observed. 21 days of CIT and TIA had no effects on BDNF protein levels in WT mice. Yet, increased levels upon SSRI is central in the BDNF hypothesis of depression [365], and had been described in rodents [393] and similarly in depressed

patients [449]. However, to ensure an effect, data from BDNF protein vs. mRNA expression, blood vs. brain tissue levels need to be distinguished. The study by Jacobsen and Mark 2004 reveals no effects of SSRI on BDNF mRNA expression but decreased BDNF protein levels in the HC; arguing, antidepressant-induced modulations of mRNA and protein may not correspond [582]. Balu *et al.* 2009 showed chronic (21 days) but not acute (1 day) antidepressant treatment with TCAs, SSRIs (FLX 10 mg/kg/day) and MAOIs increased BDNF levels in the frontal cortex of rats by 10-30 %, while CIT in our study had no effect. Duman *et al.*, demonstrated an increase in BDNF mRNA in the HC of rats chronically treated with different antidepressants, suggesting that its induction promotes neuronal survival to overcome the damaging effects of stress [249,287,583].

Tph2$^{-/-}$ mice, where adult neurogenesis was consistently increased after injection / antidepressant treatment, showed increased BDNF protein levels, which were reduced by CIT. Increased BDNF protein in *Tph2*$^{-/-}$ mice was also shown in Kronenberg *et al.* in 2015 [312]. Serotonin and BDNF signaling are intertwined. For example, some characteristics of *BDNF*$^{+/-}$ mice are increased extracellular serotonin levels and reduced SERT expression. When BDNF is administered into the ventral HC of these mice, it correlates with anxiolysis, increased serotonin transmission and therefore with a potentiation of anti-depressant-like effects [387], supporting the role of serotonin in the "monoamine hypothesis of depression", and a tight interplay of BDNF and serotonin in antidepressant action (reviewed in [499,584]). In response to stress, BDNF expression is reduced in the HC [585,586], whereas long-term administration of antidepressant therapies such as ECT and SSRI/E increase BDNF levels, followed by increasing stress resilience, often due to neurogenesis [247,249,587]. Accordingly, enhanced BDNF function might contribute to recovery of nerve cells in the HC from stress-induced damage and protection against new stress-related damage [584]. Nonetheless, the involvement of neurotrophins in stressful events needs to be revisited. First, not only have direct BDNF changes in response to either stress or antidepressant treatment lead to similar reproducible results [588–590], also secondly, respective BDNF-polymorphisms (such as *BDNF-Val66Met* impairing the release of BDNF [591] and shrinking hippocampal volume [592,593]) seem to not be directly involved in depression, when clinical trials are run with larger sample sizes [376,377]. Third, an elimination of BDNF or the receptors TrkB and p75 from the frontal lobe of male mice did not produce behavior similar to depression [7]. Last but not least, increased BDNF levels in the VTA and NAc somewhat

induced depression, and a selective knockout of the gene encoding BDNF from this circuit has antidepressant-like effects (reviewed in [123,379]).

TIA, as was seen for neurogenesis, has no effects on BDNF signaling. This is somewhat unexpected but may possibly be due to the fact that the mechanism of action of TIA differs significantly from that of other antidepressants. Studies suggest a pro-neuroplasticity role of TIA, by increasing gene expression of BDNF and NGF in HC [594] and amygdala [595]. In this thesis, the BDNF assay shows contrary results of TIA in WT animals, as chronic antidepressant treatment does not affect BDNF in HC tissue. Therefore, investigating if TIA upregulates BDNF only on gene but not protein expression is required in future research projects. After translation, BDNF protein is sub-categorized in different cleavage-related isoforms from the initial pro-neurotrophin *pre-pro*-BDNF; Secreted *pro*-BDNF or *m*-BDNF activates a heteromeric receptor complex of 75 neurotrophin receptors and sortilin as stated above. The antibody used in the ELISA assays here, may be too unspecific, and therefore only targets *m*-BDNF, whereas *pro*-BDNF remains undetected. It is definitely of interest to check the neurotrophin's active metabolic isoforms [349]: The precursor form *pro*-BDNF that induces neuronal apoptosis [355,596]; the well-studied *m*-BDNF promotes cell proliferation, survival, and plasticity; and the proteolytic cleaved *truncated*-BDNF isoform, which is related to schizophrenia, when occurring in low levels to *pro*-BDNF [597]. An imbalance of these isoforms cannot be excluded in depression when serotonin is pathology-wise altered by antidepressant therapy. Therefore, follow up data of BDNF signaling compounds such as TrkB and p75 and detecting changes in their isoform expression (*pro*-BDNF vs. *m*-BDNF) is thinkable.

In HC, serotonin, glutamate and GABA signaling can increase BDNF expression [126,575,576], which then increases the motility of neuronal progenitor cells [577]. Moreover, treatment with antidepressants, actions of CREB and other transcriptional regulators linked to BDNF [123,598], increases the amounts of growth factors beneficial for neurogenesis (BDNF, VEGF and VGF) in the HC. Also chronic SSRI treatment [287,393] and ECS [287] have been shown to increase the expression of CREB in the HC [392]. Conversely serotonin neurotransmission in the HC is under the influence of BDNF, but also in other brain regions [385,386], where BDNF administration into the ventral HC seems to potentiate antidepressant and anxiolytic effects plus increases-serotonin transmission [387,388]. In our *Tph2*$^{-/-}$ mice, increased baseline levels of BDNF have been observed suggesting compensatory effects in the absence of serotonin [312]; clearly

linking serotonin, BDNF signaling and adult neurogenesis, but levels of other neurotransmitters such as glutamate and GABA signaling leave open questions in these mice and might be altered, to compensate the lifelong loss of serotonin and keep the brain in a functional state. Therefore, investigating these transmitters by HPLC and BDNF-neurogenesis linked transcription factors such as CREB in combination with SSRI or SSRE injections in our *Tph2*$^{-/-}$ mice, would help to unravel possible serotonin replacing pathways and further antidepressant relevant mechanisms upstream of BDNF and serotonin.

Taken together, my results on the serotonin and BDNF interplay point out that the "neurotrophin-" and "monoamine hypotheses of depression" show correlation to each other, by i.e. stating increased neurogenesis is responsible for the therapeutic effects of chronic treatment with antidepressant drugs. Yet, they might independently act on new-born neurons.

4.3 Serotonin affects the HPA-Axis

Stressful events can lead to chronic stress that often precedes the onset of depression. Dysregulation or hyperactivation of the HPA-axis is a hallmark of MDD. Not only the HC, amygdala, and the PFC but also, the PVN are heavily innervated by dorsal raphe serotonin fiber projections [166,528,559,560] supporting a linked mechanism of stress, serotonin and depression. In rodents, administration of high amounts of stress hormones can induce depression-like symptoms. In individuals diagnosed with mood disorders, numerous reports have described increased cortisol and ACTH, indicative of a dysfunctional HPA-axis. Elevated cortisol exposure is associated with elevated 24-hour urinary cortisol, adrenal gland enlargement, and failure to suppress cortisol in response to the DEX suppression test [406,407,599]. Furthermore, PET imaging showed that the stress hormone response in humans is connected with alterations in central serotonin transporter levels, which also correlated with the severity of negative mood states [408]. In rodents, increased levels of CORT have been shown to decrease neurogenesis in the DG [565]. Furthermore, studies reveal that chronic CIT administration attenuates the HPA-axis that is negatively affected in depression. I here tested whether a daily injection routine might alter CORT values in WT, and *Tph2*$^{-/-}$ mice, as explanation for the high BrdU+ cell survival rates following multiple injections.

The results on CORT and ACTH plasma levels support serotonins involvement in the stress axis. Female *Tph2*$^{-/-}$ mice revealed a decreased CORT plasma level compared to their *Tph2*$^{+/+}$ littermates; in turn, female *SERT*$^{-/-}$ mice showed a trend towards increased CORT plasma levels compared to their control. ACTH upstream levels revealed, in line with CORT, decreased levels in *Tph2*$^{-/-}$ mice, whereas female *SERT*$^{-/-}$ mice have increased ACTH plasma levels. Upon treatment, CORT levels for all groups show the same trend for a decrease in *Tph2*$^{-/-}$ mice, as shown at baseline. ACTH plasma levels were significantly decreased in *Tph2*$^{-/-}$ mice following CIT.

Low CORT levels maybe the reason why no depressive-like behavior, but instead an exaggerated aggressive behavior, is seen in *Tph2*$^{-/-}$ mice [98,316]. Of further interest is, that there is a phenotype difference between males and females, since they differentially react to chronic injection (stress) or chronic mild stress paradigms, as male show different CORT levels (Figure 33) compared to female mice (Figure 31). In further attempts, the capability of stress compensation in *Tph2*$^{-/-}$ will be determined by measuring CORT levels in blood, feces, and hair at the beginning of an experiment, after injections and handling. In addition, animals treated with CORT synthesis inhibitors (i.e. Metyrapone [600]) / or GR agonists such as DEX [405] prior (antidepressant) injection could help to determine stress-dependent influence of animal handling on neurogenesis and serotonin's role as "stress buffer". Elucidation of resilience in a chronic stress model [601] and the response to antidepressant treatment in *Tph2*$^{-/-}$ mice. The relation between chronical stress, depression and neurogenesis is well known and reviewed [164,28,249,533].

In addition to CORT and ACTH, CRF was measured by real time PCR. The neuropeptide CRF is crucially involved in the pathogenesis of depression based on hyperactivity of the HPA-axis [249,409,413]. The role of serotonin is still unclear in this interplay, but since serotonergic neurons innervate areas closely related to the HPA/CRF system involving the HC, locus coeruleus, and PFC, a dominant role is assumed. With a stressful event, CRF is produced by parvocellular neuroendocrine cells within the paraventricular nucleus (PVN) of the hypothalamus and is released at the median eminence from neurosecretory terminals of these neurons into the primary capillary plexus of the hypothalamic-hypophyseal portal system, being transported right to the anterior lobe of the pituitary gland. Main function: the stimulation of the pituitary synthesis of ACTH, as part of the HPA-axis and also being relevant for depressive disorders [475]. As the PVN of the hypothalamus is strongly innervated by

serotonergic fibers [528], and there have been low levels of ACTH present already at baseline in *Tph2*$^{-/-}$ (Figure 32 etc.), a change already at the CRF expression level was thinkable. Here, the data revealed no significant changes in the CRF mRNA expression between genotypes and upon treatment; yet a decreased tendency was seen for *Tph2*$^{-/-}$ mice with citalopram that corresponds to CORT and ACTH levels.

Along with CRF, arginine vasopressin (AVP) mediates a stress response [410,602]. Both synergistically modulate POMC-related peptide release in the hypothalamus and the anterior pituitary gland (here as ACTH's precursor metabolite) [603,604]. Serotonin stimulates the release of AVP from the posterior pituitary gland [605] and increases vasopressin levels in plasma, which is followed by increased glucocorticoid levels [606]. In my thesis, POMC mRNA levels were significantly reduced in *Tph2*$^{-/-}$ animals upon saline and CIT treatment, in line with decreased baseline ACTH plasma levels. However, CIT strongly enhanced POMC levels 4.5-fold in *Tph2*$^{+/+}$ animal despite decreased (though not significant) levels of CORT and ACTH (unfortunately for the treatment experiment, no anterior pituitary gland could be isolated, to check POMC mRNA here). SSRIs might affect AVP release, followed by POMC expression, since in early studies it was shown that an i.c.v. injection of serotonin produced a rapid transient increase in plasma vasopressin levels, which were followed up by increased glucocorticoid levels [606]. A possible mediator could be the activity of POMC neurons, which is regulated by serotonin and its 5-HT_{2C} receptor; responsible also for the leptin pathway, playing a role in depression and obesity [607,608]. The leptin pathway and its relation to depression are not going to be discussed here, but the involvement of 5-HT_{2C} receptors could be tested by pharmacologically targeting the receptor in *Tph2*$^{+/+}$ and *Tph2*$^{-/-}$ mice, to possibly rescue the SSRI-POMC- phenotype observed in Tph2$^{+/+}$. This has to be done with animals being also tested for vasopressin parameters and in addition subjected to distinct chronic or acute stress models such as restraint stress, foot shock etc. and respective tests for depressive or anxious behavior (Glucose preference test, FST, TST etc.).

Further studies on CIT in rats reveal that chronic administration attenuates ACTH plasma levels, but not CRF mRNA levels, and additionally elevate vasopressin mRNA levels in the PVN [609,610]. SSRIs attenuating ACTH levels are supposed to be regulated by the vasopressin-containing subset of CRF neurons in the PVN, giving vasopressin a possible important role in antidepressant mechanism of CIT. My data can partly confirm this in mice, as a remarkable increase in POMC mRNA was observed in

Tph2$^{+/+}$ mice (Figure 37); whereas CRF level remains unaffected (Figure 36). The vasopressin-effect of CIT seems serotonin-dependent, as I neitherdo not see this elevation of POMC mRNA in *Tph2*$^{-/-}$ nor following SSRI treatment. The results so far give an idea for a vasopressin involvement in SSRI-antidepressant mechanism, independent of the SSRI-mediated modulations on CRF, ACTH or CORT.

CRF and ACTH are not only released upon stress-stimulation of the CNS, but also in response to inflammatory cytokines, such as IL-6 [402] and TNF-α [403] during certain diseases, so this hormonal network system is ideally suited to cope with the immediate demand of the body during emotional, physical, and disease stress. As no increased CRF mRNA, CORT or ACTH plasma levels and attenuated GR mRNA levels in adrenal gland or hypothalamus are visible in injected mice independent of genotype (Figure 33 - Figure 45), possible inflammatory effects of the daily i.p. injection might be excluded. Anyway, to exclude an inflammatory effect due to daily injections, all drugs and soluble treatments were filtered sterile. Still, due to daily treatment, inflammatory responses are possible. Therefore, injection sites are checked for swelling or redness, but could not be spotted for any treatment. Even though, it is known, that multiple daily i.p. injections are a safe method to administer pharmaceutical reagents into female mice, without generating any signs of illness [611], an additional group, only subjected to needle injection could be tested, when more animals would be available. This might have helped to exclude any side effects of liquid-dependent inflammatory, stress or pain responses, to the by injection of extra liquid volume increased pressure in the bowels.

4.3.1 Receptors of the stress axis

Overall, parameters of the stress axis are decreased in *Tph2*$^{-/-}$ mice; CIT also affects stress levels, yet only in the absence of serotonin. When looking at the receptor's expression, GR mRNA expression is significantly lower in the HC of untreated *Tph2*$^{-/-}$ mice, while treatment had no effect (for both, MR and GR expression levels in the HC, and also hypothalamus). However, within *Tph2*$^{-/-}$ groups, GR expression in the hypothalamus was significantly reduced upon citalopram, and significantly higher in the adrenal gland.

Measuring HPA-axis parameters, e.g., the activation of GRs in the HC is of importance [249]. MR and GR are expressed in numerous cell types and tissues, where they interact at both, the molecular and functional levels, to mediate and modulate diverse functions via binding of their ligands. Neuronal effects are membrane excitability in neurons and muscle cells, trophic and adaptive responses to injury, and neuronal responses critical

for learning, memory, and early response to stress [410]. MR is mainly expressed in the HC and is responsible for controlling physiological and mild stress-related variation of the HPA-axis [415]. The ubiquitous expressed GRs are essential for energy homeostasis, including gluconeogenesis, and the response to stress and inflammation [395,410]. The MR response to the diurnal fluctuations in cortisol levels, i.e. by the circadian rhythm and thus provides, together with the GR, the regulatory feedback system for stress and glucocorticoid homeostasis [612,613]. Although it is still not clear whether the stress-response of the central serotonin system is mediated through GR, as downstream negative feedback regulatory mechanisms of the HPA-axis are unbalanced due to lifelong serotonin deficiency, which show decreased stress hormone releases already at baseline levels and to injection stressors (Figure 31 and following).

In this study, primers were designed to cover most transcript variants and exclude isoform specific changes firsthand, since an expression of the beta variants of GR and MR in the brain is still discussed. In general, excessive and chronic GR activation leads to hippocampal neuron atrophy; MR activation is antiapoptotic and supports neurogenesis [164,416]. So one can say both MR and GR are important for the long-term adaptation of the hippocampus to stress and its downstream modulation of the HPA [411,614]. Excessive and enduring GR activation increases the expression of the tumor suppressor protein p53 and so induces hippocampal granule cell apoptosis, while MR activation suppresses p53 transcription in developing and mature hippocampal neurons and is protective [410,615,616]. Also the ratio of MR:GR plays a role in function and malfunction and balanced activation of MR and GR provides optimal cognitive performance [417–419]. Decreases in MR or the ratio of MR:GR expression in the PFC and hypothalamic paraventricular nucleus are implicated in depression and cognitive decline in humans [411,421,422]. Furthermore MR proper function is essential to keep up learning and memory under stressful situations [410,617,618]. MR is crucial for proper differentiation, migration, and function of neurons in adult neurogenic niche [583] and the developing brain [619,620].

Expression of MR in the adrenal gland as part of the HPA feedback system is still under discussion but mRNA expression can be found for both receptors, MR and GR [621]. Nevertheless, the numbers for the MR expression in Nishimura's work are quite small, so MR expression patterns from the qPCR data in this thesis must be taken with caution. In addition, it is not completely clear if the MR expression in the adrenal gland is responsible for HPA-feedback control. The binding of ACTH to its specific

melanocortin 2 receptor (MC2R) in the zona fasciculata of the adrenal cortex results in CORT / cortisol synthesis and release.

Activation of MR and GR inside the HPA-axis by cortisol/CORT regulates feedback control [409]; the receptors form long-term adaptations to stress in the HC and thereby modulate the HPA-axis [411]. Antagonist studies demonstrate MR's role, but not GR for the habituation response to repeated stress from PVN neurons [412,414] .While MR and GR are expressed in many cell types and tissues (often simultaneously), MR is mainly present in the HC and responsible for controlling physiological and mild stress-related variation of the HPA-axis [415]. The ubiquitous expression of GRs is essential for energy homeostasis, including gluconeogenesis, and the response to stress and inflammation [395,410]. Besides CORT, MR can also bind the cardio-vascular active mineralocorticoid aldosterone, while GR only binds cortisol or corticosterone, stating a role of MR for the renin-angiotensin system [410]. MR mRNA was detected in the adrenal gland in humans [409,621], but never stated elsewhere. Protein expression of MR is doubtful and needs to be confirmed by protein analysis in adrenal gland tissue (i.e. by western blot, immunohistochemistry). Furthermore, it is stated that miRNAs regulate the GR expression in the adrenal gland, controlled by ACTH [622], maybe a downstream silencing for the mRNA for MR might be possible, too.

In addition to the quantitative gene expression analysis of the stress receptors and hypothalamic hormones applied here in this study, supportive protein expression studies were planned in the tested mouse strains, to reveal post-transcription modulations of the antidepressant therapies and serotonin to the HPA-system. An attempt tried here by semi-dry western blotting. To determine RNA and proteins from same tissue was done to keep the three Rs in animal welfare (Replacement, Reduction and Refinement). Several protein/RNA isolation approaches have been tried with respective antibodies for MR, GR, and POMC, as well as respective ELISAs were conducted. Unfortunately, only RNA in sufficient quality could be obtained. Extracted proteins could not be detected in a sufficient qualitative or quantitative outcome to be suitable for a scientific result in this thesis. GR and MR protein expression will be targeted in future experiments, to give a statement about impact of stress receptors on antidepressant mechanisms, when serotonin is absent or not. One other approach could be protein measurements using liquid chromatography. At this, different isoforms and splicing variants of the receptors should also be considered, since β-GR can act as an inhibitor for the more abundantly expressed α-GR and MR receptor by

hetero dimerization with GR [623–626] or interfering with MR [417,612]. Even α-, β- and γ - MR have regulatory functions in the developing HC, so interplay in the adult neurogenetic niche has to be excluded first [620].

Further systems and neurotransmitters that react to acute stress, such as the catecholamines pathways are also altered in in *Tph2*$^{-/-}$ animals with no brain serotonin (reviewed in [316]), but not in *Tph2 knock-in* animals with reduced brain serotonin [627]. Brain norepinephrine (NE)-levels are mostly reduced and GABA levels are highly increased in the HC region; Glutamate levels are increased in the PFC region in *Tph2*$^{-/-}$ mice [314]. Especially relevant for acute stress homeostasis, are projections from the NE-system into the HC and cortex, which can also affect the glucocorticoid response [553,628,629]. Early life stress boosts the NE receptor sensitivity in the PVN of the hypothalamus in the serotonin controlled median eminence [630,631], and also increases its GR expression. Follow up these increases, CRF synthesis expression is downregulated by the negative feedback mechanism to return to a normal stress homeostasis [631–633]. This is in line with the results obtained from unhandled *Tph2*$^{-/-}$ mice, as they show already low CORT and ACTH plasma levels and a trend for lower CRF mRNA levels in the hypothalamus (Figure 31 and following), when compared with their littermates. This speaks for a totally deregulated HPA-axis already at baseline level, mediated by the missing serotonin and possibly even by the altered NE levels [316,634]. GR receptors mRNA in the hypothalamus, necessary for the feedback control show a trend for an increase in the *Tph2*$^{-/-}$ animals, supporting the phenotype, whereas the MR receptor levels remain unaffected (Figure 44).

A useful supportive approach can be to map fiber connections in *Tph2*$^{-/-}$ mice in 3D, between dorsal / median raphé and the HC, hypothalamus etc. using "*CLARITY*", originally invented by Deisseroth and Chung in 2013 [635]. The idea is to get a *clear* insight of the spatial alignment and the connection of serotonergic and CRH neuronal networks, between DG, PVN and raphé in a whole mouse brain, when the brain might develop an alternative HPA-axis system as in our *Tph2*$^{-/-}$ mice.

4.3.2 Sex-specific physiological functions of serotonin

In rodents, sex-specific physiological functions of serotonin have been reported early in literature [636–638]. In *Tph2*$^{+/+}$, females show higher CORT levels than males (Figure 33 + Figure 31), but in *Tph2*$^{-/-}$ mice with no brain serotonin, both sexes exhibit similar low CORT values. Especially relevant for my thesis is a study showing that restraint or chronic mild stress leads to higher plasma CORT levels in female mice which can be

normalized by ovariectomy and testosterone administration. In contrast to my results (10 mg/kg), 15 mg/kg of CIT independent of stress resulted in a greater CORT response in females, which can also be normalized by testosterone. The higher CIT concentration might explain the difference in results. Furthermore, sex differences along the serotonin - HPA-axis are greater pituitary serotonin receptors expression and adrenal weights in females. Moreover, in stress-regulatory regions, sex-specific differences in GR and glutamic acid decarboxylase expression is found in males, promoting their negative stress feedback regulation [526,527,639]. A possible reason for this could be the increased testosterone levels in *Tph2*$^{-/-}$ mice [640], changing the female HPA-axis phenotype to a male one, if brain serotonin is absent. Gutknecht *et al.* suggested in 2015 [307], that the serotonin-dependent alteration of the HPA system activity such as decreased brain GR and CRF expression [639,641,642] and the decreased CORT release (as also confirmed in my studies) in *Tph2*$^{-/-}$ females is likely due to a cumulative effect of the lifelong serotonin depletion in the brain and the endogenous effects of the gonadal steroids 7β-estradiol and progesterone in females, manipulating the adaptive mechanisms to stress in females vs. males. Paradoxically, I could not reproduce the decreased GR and CRF mRNA levels in *Tph2*$^{+/+}$, which has been previously reported for female *C57BL/6* mice after treated with the SSRI FLX [641]. No alteration in GR and CRF in *Tph2*$^{+/+}$ animals treated with SSRI CIT, but (trend for) a decrease in CRF and GR mRNA in hypothalamus was observed here.

Based on Gutknecht's hypothesis and to exclude any impact of the mice's estrus cycle on the CORT and ACTH levels [511,530], at the timepoint of the trunk blood collection, 17 C57BL/6N WT mice (25 week old) have been kept unhandled for 3 weeks in group housed conditions. Trunk blood was collected at similar times as in previous experiments (Figure 38*),* and plasma CORT levels of trunk blood were compared with their cycle stage at timepoint of sacrifice (Figure 21). Data revealed no difference in CORT plasma levels between animals of different estrus cycle stages (Figure 38*)*. Also, in the subsequent SSRI and saline treatment experiments (Figure 39) no cycle stage influence was seen. Furthermore, no estrus cycle stage synchronization could be seen among the mice kept grouped-housed in the same cage [643]. This result helps to exclude major effects of the estrus cycle stages for previous experiments. Nonetheless, a continuation of gender specific research in depression is required, especially as major depression shows a higher prevalence in women than in men [9].

4.3.3 *SERT*$^{-/-}$ mice are perfect counterparts for the stress-result from *Tph2*$^{-/-}$ mice

Here, *SERT*$^{-/-}$ mice display a perfect counterpart to *Tph2*$^{-/-}$ mice. I have determined the serotonin-dependent activation of the HPA-axis, transmitted by serotonergic innervation of the hypothalamus and possible interactions of the serotonin receptors. High CORT / ACTH levels were found in *SERT*$^{-/-}$ mice, that have increased extracellular serotonin (Figure 31 + Figure 32), which is opposed to the decrease in *Tph2*$^{-/-}$ mice with a total brain serotonin depletion (Figure 34 + Figure 34). *SERT*$^{-/-}$ mice are considered as a hypo-serotonergic mouse model, with elevated extracellular serotonin levels in the synaptic cleft. SERT can be found in the CNS at the axonal synaptic end nodes and in PNS, and is peripherally expressed mainly in platelets, pulmonary endothelium, placental epithelia, and adrenal chromaffin cells (ACCs) [532]. Although ACCs do not synthesize serotonin, they express SERT, and mainly secrete catecholamines (Adrenalin, NA and DA) to mediate the physiological short-term response to stress. Adrenal glands from WT mice contained a serotonin:adrenaline abundance ratio of 1:750. In *SERT*$^{-/-}$ mice, this ratio is reduced by ~80 % without a change in adrenal gland levels of catecholamines, since SERT promotes the ability of 5-HT$_{1A}$ receptors to inhibit catecholamine exocytosis [119]. This increased catecholamine-dependent stress response might be one of the reasons for higher CORT and ACTH plasma levels found in *SERT*$^{-/-}$ mice. Catecholamines are known to stimulate ACTH synthesis when circulating in the body [644]. Looking at CRF hypothalamic mRNA levels in *Tph2*$^{-/-}$ mice (Figure 36) with no difference found in comparison to *Tph2*$^{+/+}$ (a trend towards a decrease*),* the involvement of the catecholamines and their stimulating effect on ACTH are revealed. It could be shown that changes in catecholamines decrease noradrenaline levels (as seen in *Tph2*$^{-/-}$ mice in previous experiments [634]), and therefore directly affect the HPA-axis and hippocampal cell proliferation and survival in the DG. It is even more conceivable that a combination of both mechanism is a reason for the phenotypic change of the CORT and ACTH release in *Tph2*$^{-/-}$ mice, but this has to be confirmed by further measurements of the catecholamines and vasopressin in *Tph2*$^{-/-}$*, Tph2*$^{+/+}$ *and SERT*$^{-/-}$ mice subjected to acute / chronic stress and /or subjected to CIT, as its antidepressant mechanism seems not be exerted by the CRF-ACTH-CORT pathway of the HPA-axis, but maybe by the CRF-vasopressin track.

Mild stress, such as handling and saline injection, significantly increases ACTH secretion in *SERT*$^{+/-}$ and *SERT*$^{-/-}$ mice [325], that supports my findings. Stress seems to affect *SERT*$^{-/-}$ mice more than WT, e.g. in response to an acute swim stress [325]. This is

accompanied by hypo-activation of medial (m)PFC' cFos expression, due to the enhanced capacity of 5-HT_{1A} receptors inhibiting neurons in the mPFC as well as to exert feedback inhibition of DRN serotonin neurons [645]. Also human studies revealed a correlation between the quantity of stressful life events and the severity and number of episodes of MDD in individuals carrying lower SERT expression genotypes [331–333]. Furthermore, PET imaging shows that the stress hormone response is connected with alterations in central SERT expression, which also correlated with the severity of negative mood states [408]. Together with my findings of increased ACTH and CORT baseline levels, these data suggest that a lifelong absence of SERT function, beginning already early in development, also may disturb a correct HPA-axis development, resulting in increased sensitivity to stress by a possible dysregulated feedback system. This indicates the importance of serotonin and its system for a healthy stress homeostasis. Studying the mechanisms by which the reduction in SERT function during development influences the sensitivity and regulatory feedback mechanisms of HPA-axis response to stress, for instance by evaluating MR and GR levels in combination with 5-HT_{1A} receptor antagonists, could provide significant insight for our understanding of the involvement of serotonin and stress hormone effects in MDD. *SERT*$^{-/-}$ mice reveal increased cell proliferation in aged and adult mice in DG [323], and a similar increase also after 21-days of chronic injections of saline / or SSRI (unpublished data from our group). As previously reviewed by Mahar et al. in 2014 [249], acute stress increases cell proliferation in the DG, maybe mediated by catecholamine / a CORT-based stress response. This might be the case in *SERT*$^{-/-}$ mice, in combination with activation of the 5-HT_{1A} receptor, if the initial injection is seen as an acute stressor. Whether increased cell proliferation and survival is beneficial, needs to be shown by further cell morphological studies.

Using mouse models developmentally altered such as *Tph2* or *SERT*, one cannot discriminate between compensatory processes provoked by life-long alterations in serotonin levels, and phenotypes induced by serotonin *per se*. New genetic models where serotonin can be acutely altered might recapitulate the human condition of depressive episodes more adequately, i.e. *Tph2*$^{Tph2\text{-}iCre}$–conditional Tph2-knockout mouse line dependent on inducible Cre-recombinase. This transgenic line has been generated by *Tph2*$^{flox/flox}$*/TPH2-CreER*(T2) in the Bader research team (reviewed in [290]). Tph2 will be depleted in serotonergic neurons of the brain stem raphe nuclei upon TMX treatment, which causes persistent absence of brain serotonin. Studying this

mouse will yield further important insights into the role of serotonin in the etiology and pathogenesis of MDD.

4.4 Electroconvulsive therapy (ECT) in a model with serotonin depletion

A large amount of patients do not respond efficiently enough to SSRI medication, to achieve a successful therapy from MDD [646,647]. Therefore, ECT is used as highly effective in the treatment of major depression. In animal models, a series of ECS leads to increased neurogenesis and increased BDNF signaling, that might contribute to the mood stabilizing action of ECT in patients [124,267,284–288]. My thesis examined whether serotonin signaling is essential for the well-established effects of ECT, namely the induction of hippocampal neurogenesis and BDNF. The experimental outcome in *Tph2*$^{-/-}$ and control mice revealed that serotonin signaling is a prerequisite in mediating the key neurobiological effects of ECS. The main finding is a diminished treatment-induced increase in cell survival and BDNF concentrations in the hippocampus of *Tph2*$^{-/-}$ mice. Interestingly, both biological systems are correlated in WT animals, but were uncoupled in the absence of serotonin. Serotonin has long been recognized for its role in the regulation of mood. Manipulations increasing serotonin levels lead to clinical improvement from depression that is associated with a delayed increase in adult neurogenesis [124,187]. Furthermore, serotonin neurotransmission is under the influence of BDNF [385], which is believed to contribute to the effects of antidepressants and ECT [287]. Further evidence supporting this theory that neurotrophins are relevant for antidepressant effects of ECT/ECS is that BDNF is a major player in survival and maturation of new neurons and synapses, and is increased following (dose-dependent [259]) ECS/ECT treatment in limbic structures in patients and rodents [287,448,648–650]. Accordingly, rodent ECS treatment changes numerous of neurotrophic pathway genes in hippocampus and cortex [285,651–653]. ECT induces changes in regional cerebral blood flow and regional glucose metabolism in regions related to MDD [275–277]. An up-surge in blood pressure after ECT / ECS treatment might result in a break in the continuity of the BBB leading to certain neuro-chemicals released from circulation to brain parenchyma, inducing increased BDNF levels and changes in angiogenesis and neurogenesis [245,278]. Furthermore in depressed patients, low serum BDNF levels are normalized by ECT [245,448,449,654,655]. In rodents, ECS experiments have revealed altered expression of various target genes for neuronal plasticity and neurogenesis, e.g. VGEF, NG2, *c-Fos, Egr1, Neuritin 1, BDNF, Gadd45b, Snap29, STEP61, Synapsin I, FGF-1* [245,269,279–283]. As mentioned, earlier experiments

using SSRIs clearly demonstrate that the serotonin system may be harnessed to increase neurogenesis and BDNF concentrations [124,271,287,656]. In the neuroendocrine model of depression, antidepressant-like effects of ECS require adult neurogenesis [266]. However, whether the strong increase in cell survival after ECS is directly mediated by increased BDNF or whether both systems require serotonin signaling independently remains undefined. In rats, Taliaz *et al.* [657] demonstrated an antidepressant-like effect of ECT. The effect was more dependent on ECT-induced significant reduction of BDNF expression in the ventral tegmental area (VTA) rather than elevated hippocampal BDNF expression. Earlier researches also pointed to this contrasting BDNF action in the hippocampus and the VTA [245,657]. In another study by Stelzhammer *et al.* in 2013, it was hypothesized that BDNF expression differs after acute vs. chronic ECT applications: Serum samples were taken after the 1st, 6th and 12th ECT treatment (in total, treatment was done for 4 weeks), and BDNF levels were significantly decreased with ongoing treatment, while its elevation seems to be an acute effect. Therefore different tissue isolation time points during the single ECT/ECS sessions treatment should be considered [441]. In humans, Ryan *et al.* 2018 measured BDNF plasma levels in depressed and healthy patients subjected to bi-weekly ECT treatment (min. 2 weeks). The study found neither a differences in plasma BDNF levels between the control and depressed groups, nor in patients following treatment with ECT, indicating no association between plasma BDNF levels and depression severity or the clinical response to ECT [658]. In our study, elevated BDNF levels were observed in brain tissue; plasma or serum BDNF levels were measured neither in WT nor *Tph2*$^{-/-}$ mice. In this context Balu *et al.* 2009 demonstrated the effects of ECS on BDNF levels in multiple rat brain regions. Single ECS treatment cause a 25 % increase of BDNF only in the amygdala, but ten days of ECS treatments resulted in robust doubling of BDNF protein levels in the hippocampus and amygdala, and still moderate but significant elevations in the frontal cortex were observed, supporting our results after 5 days of ECS treatment in mice [389].

The current finding of reduced BDNF levels in sham treated *Tph2*$^{-/-}$ mice as compared with WT is in apparent contradiction to our earlier report [312]. We speculate that *Tph2*$^{-/-}$ mice are highly sensitive to stress as a result of sham ECS [509], while all animals in the earlier study were virtually unhandled. ECT has been demonstrated to reduce cortisol induced inhibition of neuroplasticity [245,259,266,659], and as the *Tph2*$^{-/-}$ mice show already lower levels in baseline CORT and after treatment. It would be of interest to investigate

CRF, CORT and ACTH (plasma) levels in *Tph2*$^{-/-}$ mice at several timepoints during the ECS treatment paradigm to see if ECS is able to rebalance the altered CORT levels caused by the lifelong lack of brain serotonin. Antidepressant efficacy of ECS sessions can be examined by behavioral tests in rodents [648,660], e.g., elevated plus maze is used to analyze changes in anxiety-related behavior and has recently been translated to humans as "unconditioned approach–avoidance conflict" test [661]. Yet, as *Tph2*$^{-/-}$ mice do not show a typical depressive phenotype in these tests, the use of an inducible serotonin knockout would be more beneficial. Besides alleviating depressed mood, ECS therapy is used to improve despair-like behavior and to ameliorate symptoms of anxiety. In animal models, decreased thigmotaxis or increased open arm entries might indicate less anxious behavior. However, changes in behavior upon ECS may not be detectable in 'non-depressed' WT groups, and are time-dependent as shown in rats [648,660]. Our short-term analysis scheme of up to only 3 days after a 5-day ECS series may not have been enough to detect profound alterations, and the behavior was largely unaffected in WT mice. In the more susceptible *Tph2*$^{-/-}$ model, previous observations on behavior at baseline were confirmed: *Tph2*$^{-/-}$ mice are highly active and impulsive [98] accompanied by a reduced anxious phenotype that results in decreased thigmotaxis. Therefore, it might be difficult to detect further treatment effects on anxiety levels. However, in response to ECS, explorative behavior of *Tph2*$^{-/-}$ mice was reduced, and the highly active phenotype was attenuated. ECT has been hypothesized to enhance release of hormones from hypothalamus into CSF and blood through excitation of diencephalic structures, a so called neuroendocrine model of depression [662], and with our results in the *Tph2*$^{-/-}$ mice, we can definitely say, serotonin seems to be one of the ECT's / ECS' antidepressant attributes. To summarize, our results indicate that brain serotonin critically contributes to the physiological outcome of ECS, by possibly coupling adult neurogenesis with BDNF signaling. These findings add to our understanding of serotonin action and intertwined biological systems.

4.5 Behavior as biomarker

Besides stress, monitoring dissocial or altered general behavior of serotonin-depleted mice compared to control is of importance. To address the psychological challenge - if depression is a mankind specific mental disease, with diagnosis mainly based on appropriate communication (which mice are lacking), or if there is a comparable and visible depressive-like behavior in mice, I strived to find a suitable (supportive) biomarker. A behavioral approach was set to address deterioration in the ability to perform "Activities of daily living" (ADL) of rodents [502,503]. Several behaviors such as glucose preference test, nesting, the capability to hoard food, further burrow a hole or frightening things (marble burying test), elevated plus or O-mazes and open field tests can be used as biomarker to define a depressive-like state in rodents. The aim here was to determine whether alteration of serotonin in rodent CNS leads to comparable less structured ADL, as seen in depressive patients [24,25]. A typical ADL for mice is nest building behavior, as wild mice build constructs to provide thermoregulation, protection and shelter from elements and sexual competitors and provide a higher chance to survive for the offspring [504]. Often ADL-behaviors are getting more and more disrupted with a decreasing wellbeing of the animal, maybe even up to a level as a depression [505]. Here, different mouse strains with altered serotonin concentrations in the CNS were taken, with all of them showing impaired nesting behavior, when compared with their respective WT.

My results showed that *Tph2*$^{-/-}$ mice were incapable of building proper nests but were still able to completely shred the nesting material. Their *Tph2*$^{+/+}$ littermates nonetheless were able to build nests to some extend but not as perfect as the *C57BL/6N or J* companions, as they left some of the nestlets partially unused or made the impression of being anxious of the new material. *Tph2*$^{-/-}$ mice show a striking escalating aggression behavior, being associated with an elevation of testosterone level and with an escalation of compulsive behaviors [98,307,640,663] as seen in the impulsive nestlet-shredding; quite fast but without forming any nesting structure.

It has been shown in patients and rodents that anxiety is associated with reduced central SERT and serotonin availability in unmedicated patients with unipolar major depression [322,324,408,664], indicating a parallel behavior as seen in our *SERT*$^{-/-}$ mice, when subjected to the nesting paradigm, as they were mostly afraid of the nestlet and tried to avoid the “novel object” by sleeping in a position in a safe distance. Their CNS-hypo-serotonergic phenotype seems to affect their anxiety level to a certain extent,

resulting in not pursuing ADL. Adult, but not early adult *SERT*$^{-/-}$ mice exhibit increased anxiety [324]. Further physiological and phenotypic changes in *SERT*$^{-/-}$ knockouts are: atypical barrel-cortex formation as well as malfunctioning thalamo-cortical connections, resulting in impaired somatosensory feedback and locomotion impairments (Reviews [320,321]), making it maybe even impossible for the *SERT*$^{-/-}$ mice to progress with locomotion and fine motor skills requiring tasks such as nestlet shredding and nest building. Also with the reduction of 5-HT$_{1A}$-mediated temperature response in the *SERT*$^{-/-}$ mice, their thermoregulation might be that imbalanced and non-responsive, that a hypothermic state is not occurring at RT and therefore no nesting instinct was initiated within the experimental conditions when nesting was tested [325].

Furthermore nesting behavior is stated to maintain body temperature in resting times, it is stated that most animal facilities environment with 22°C are too cold compared to the body core temperature of 37°C in rodents [665].So, depending on the season also the MDC-animal facility rooms have 22 – 24 °C, and therefore the animals are driven towards nest building. To support the data gathered by the nesting assays, the body temperature of all tested transgenic mouse strains should be determined via rectal measurement, preferably before and right after the nesting. This might eliminate strain and gender differences based on altered core body temperatures of the different transgenic mouse lines. Remarkably, it has been shown by Gutknecht *et al.* in 2015, that only male *Tph2*$^{-/-}$ show a higher basal body temperature compared to *Tph2*$^{+/+}$, but with no body temperature difference in female *Tph2*$^{-/-}$ mice, when compared to WT [307].

An additional treatment with SSRI/E is thinkable and will help to specify the usefulness of nesting etc. as a supportive biomarker for depressive behavior and to verify the involvement of serotonin in it. Interestingly it has been shown that 5-HT$_{1A}$ receptor agonist-induced hypothermia is blunted also in *Tph2 knock-in* mice with reduced brain serotonin levels. Jacobsen *et al.* also suggest that the blunted hypothermic response is directly related to low extracellular serotonin levels in the brain [627]. Combined with my results from the nesting paradigm, where *Tph2*$^{-/-}$ mice were also impaired in nestbuilding, these mice lack a sensation for hypothermia, and therefore maybe coming with an absent activation of the 5-HT$_{1A}$ receptor. This could be tested further by subjecting SERT$^{-/-}$ and *Tph2*$^{-/-}$ to colder room conditions and thereby forcing them to build proper nests, in order to distinguish if the impaired nesting behavior is temperature-regulation or “depression-/motivation”-mediated.

Furthermore, it could be hypothesized that the illumination in the animal house was set too high with 400 Lux during light phase, driving WT animals to anxiety-like behavior forcing them to create protective nests [666,667], whereas the less anxious, partly aggressive *Tph2*$^{-/-}$ are not affected by the environmental surroundings.

In rodents, several behavior tests can be used to examine antidepressant efficacy, and explorative behavior. *Tph2*$^{-/-}$ mice are generally less anxious. In the open field test, *Tph2*$^{-/-}$ mice spent significantly more time in the center of the arena, an effect that was diminished by ECS treatment (Figure 46e). Latency to immobility was significantly shorter regardless of treatment. *Tph2*$^{-/-}$ mice revealed an increased immobility time that was also abolished upon ECS. Overall, ECS sessions attenuate the highly active phenotype of *Tph2*$^{-/-}$ mice as shown by shorter distances traveled. Following SSRI treatment, that already decreased anxiety levels at 5 days (increased time spent in the center) in WT, no changes were observed in *Tph2*$^{-/-}$ mice. However, *Tph2*$^{-/-}$ phenotype seems to increase anxiety at 20 days. Behavior tests overall can be used as an additional marker to describe a specific phenotype; or to define treatment effects, i.e. in transgenic animal models as compared with WT. However, for WT alone a phenotype needs to be induced first to test efficacy of drugs.

The results above show the nest keeping behavior was altered. Together with video/audio recordings that might provide information about a baseline dissocial behavior and “aspects of daily living” in the absence of serotonin, this ADL behavior may be a new “biomarker” experiment for rodents in depression research.

4.6 Conclusion

In summary, the results in my thesis add to the growing knowledge of serotonin signaling and its role in various brain functions such as adult neurogenesis, BDNF signalizing, and stress-induced responses, mechanisms contributing to the pathology of depression and to the understanding of antidepressant drug action. My data also underpin that generating a ‘unified theory’ to describe the pathology of depression is not possible. Results are too controversial, the research field of serotonin, and especially of depression is vague, the effects, mechanisms, and exogenous inputs are too manifold; e.g., mechanisms catalyzing depressive symptoms and behavior in response to stress differ already between the various neural circuits in the CNS, some of them are even already altered by depression itself. To define ‘THE” definition of depression is continued and needs a clearer separation, classification, and subdivision

of the single types of these global burden psychiatric disorders, currently gathered under the term 'depression'. The physiological and neurobiological causes with their pathological consequences are manifold and occur independently from each other; disorders have been described as polygenic, induced by many different genetic variants (reviewed in [495,668]). Nonetheless, they terminate in the same "bottleneck-depression phenotype", as experienced and often misunderstood by outsiders. With the extensive study of "monoamine hypothesis of depression" in humans, a vast number of single nucleotide polymorphisms (SNPs) in serotonin-associated genes are known by now (*VMAT, MAO, SERT* etc.). These SNPs often result in altered serotonin levels in the brain and are accordingly often linked to depressive phenotypes. Yet by the team of Richard Broder, some of the classical genetic polymorphisms associated with depression have been declared as false positive, due to low sample sizes and therefore should be reevaluated [376]. For the HPA-axis, 68 genetic SNPs were determined in a gene association study from 2017. Only angiotensin converting enzyme variants were nominally associated with depression. Overall, one has to always distinguish between human data and animal research. The transgenic *Tph2*$^{-/-}$ mouse model mostly used here, does not exhibit a respective 'depression model' phenotype *per se* [305,316,669], which was also previously reported for congenital serotonin deficient mice [670,671]. In addition, mice often derived from different origin strains, e.g., FVBN were backcrossed to C57BL/6, which also brings different types of mutations as reviewed in [316]. Furthermore, the literature is often narrowed down to cover minimal connections in a complex brain, that together lead to a such complex mental disease with multi-causes such as MDD. However, to define antidepressant mechanisms targeting biological processes as was done here is an important step, which yet will need further basic and field translational research to benefit patients. This thesis provides insight into serotonin-dependent, but also -independent possibilities for novel therapeutic targets, new pathways that antidepressant drugs may use. My data clarify that a deeper and more detailed analysis of single molecules is required, as well as an overall understanding of the complexity of the brain and organism is needed.

5 Material

Table 46 Chemicals and organic substances.

Substance/Chemical/Kit	Company/Country
Animal treatment	
Citalopram hydrochloride, Cirpramil	Lundbeck, Germany
Isoflurane	Abbott, USA
Ketavet (100 mg/ml)	Pfizer, Germany
Rompun 2 % (Xylazin)	Bayer, Germany
RPMI Media 1640	Thermo Fisher Scientific, USA)
Tianeptine sodium salt	Tocris, UK
ELISA	
ACTH (Human, Mouse)	IBL/TECAN, Germany
BDNF Emax ® ImmunoAssay System	Promega, Germany
Corticosterone (Human, Rat, Mouse)	IBL/TECAN, Germany
Histology	
4 % Paraformaldehyde solution	Otto Fisher GmBh; Germany
Boric acid	Sigma-Aldrich, USA
Bromodeoxyuridine BrdU	Sigma-Aldrich, USA
DAB Peroxidase (HRP) Substrate Kit (with Nickel), 3,3'-diaminobenzidine	Vector Laboratories, Germany
DABCO-1,4 diazabicyclo [2.2.2]octane	Sigma-Aldrich, Germany
Ethylenglycol	Roth, Germany
Glycerol	Roche, Germany
In Situ Cell Death Detection Kit, TMR red	Sigma-Aldrich, Germany
Neo-Clear® (xylene substitute) for microscopy	Merck, Germany
Neo-Mount®	Merck, Germany
Normal donkey serum	Sigma-Aldrich, Germany
PVA-polyvinyl alcohol	Sigma-Aldrich, Germany
Sodium chloride	Sigma-Aldric, Germany)
Sodium dihydrogenphosphate	Merck, Germany
Sodium hydrogenphosphate	Merck, Germany
Sodium hydroxide (NaOH)	Roth, Germany
Sucrose	Merck, Germany
Tissuetek® O.C.T Compound	Sakura, Japan
Triton X-100	Sigma-Aldrich, Germany
Trizma base	Sigma-Aldrich, Germany
Trizma HCl	Sigma-Aldrich, Germany
Tunnel Cell Death Staining Kit	Roche, Germany
Tween-20	Sigma-Aldrich, Germany
Vectashield® Mounting Medium with/out DAPI (Hard Set)	Vector Laboratories, USA
VECTASTAIN ABC HRP Kit (Peroxidase, Standard)	Vector Laboratories, USA
Xylene	Roth, Germany
Xylol	Roth, Germany

For PCR / Genotyping

10x Thermo Pol Buffer	New England Biolabs, USA
Agarose	Biozym, Germany
Bromphenol blue	Sigma-Aldrich, Germany
DNA-Ladder 100bp, 1000pb	New England Biolabs, USA
dNTP Mix (10 mM each)	Thermo Fisher, USA
Ethidium Bromide	Invitrogen, Germany; Sigma-Aldrich, Germany
Magnesium chloride ($MgCl_2$; 50mM)	Sigma-Aldrich, Germany
Proteinase K	Invitrogen, Germany
Proteinase K	Invitrogen, Germany
RNAse A	Promega, USA
Sucrose	Merck, Germany
Thermo Pol Taq DNA Polymerase (5.000 U/ml)	New England Biolabs, USA

cDNA Synthesis

DNase I recombinant, RNase-free	Sigma Aldrich, Germany
dNTP Mix (10 mM each)	Thermo Fisher, USA
M-MLV RT Reaction Buffer 5x	Promega, USA
Moloney Murine Leukemia Virus Reverse Transcriptase (M-MLV RT)	Promega, USA
Random Hexamers	Thermo Fischer, USA
RNAsin: Ribonuclease Inhibitor	Roboklon, Germany

qPCR

CXR Reference Dye	Promega, USA
GoTaq® qPCR Master Mix	Promega, USA
MicroAmp® Optical 384-Well Reaction Plate	Thermo Scientific, USA

Miscellaneous Chemicals

1,4-Dithiothreitol (DTT; 0.1M)	Invitrogen, Germany
Acetic acid (glacial)	Roth, Germany
Acetone	Roth, Germany
Agarose	Biozym, Germany
Aqua-Rothi Phenole	Roth, Germany
Bovine Serum Albumine (BSA)	Sigma-Aldrich, Germany
Bromphenol blue	Sigma-Aldrich, Germany
Chloroform	Merck, Germany
Deoxyribonucleotide (dNTP)	Bioline, Germany
Diethylpyrocarbonate (DEPC)	Serva, Sigma-Aldrich, Germany
Ethanol (EtOH)	Roth, Germany
Ethidium Bromide	Sigma-Aldrich, Germany
Hydrochloric acid (HCl)	Roth, Germany
Isopropanol	Roth, Germany
Lysis buffer (10x)	Biolegend, USA
Magnesium chloride	Roth, Germany
Magnesium chloride (MgCl2; 50mM)	Sigma-Aldrich, Germany
Maygrünwalds Eosin-Methylen blue solution modified	Merck, Germany
N-2-hydroxyethylpiperazine-N-2-ethane sulfonic acid (HEPES)	Thermo Fisher Scientific
Normal Donkey Serum (NDS)	Sigma-Aldrich, Germany
Paraformaldehyde (PFA)	Merck, Germany
Perchloric acid	Sigma-Aldrich, Germany
Phosphate buffered saline (PBS)	Sigma-Aldrich, Germany

Miscellaneous Chemicals	
Potassium Acetate	Merck, Germany
Potassium chloride (KCl)	Sigma-Aldrich, Germany
Phosphoric acid (H3PO4)	Sigma-Aldrich, Germany
Picric Acid (Aqueous solution)	AppliChem, Germany
Potassium dihydrogenphosphate	Merck, Germany
Potassium hydroxide	Fluka, Germany
Sodium acetate	Sigma-Aldrich, Germany
Sodium chloride	Sigma-Aldrich, Germany
Sodium citrate	Merck, Germany
Sodium deoxycholate	Merck, Germany
Sodium hydrogen carbonate	Merck, Germany
Tris(hydroxymethyl)aminomethane	Roth, Germany
Trizol®	Invitrogen, Germany

5.1 Antibodies

Table 47 Primary antibodies

Name	Ref – No	Company	Dilution
Anti Iba1, Rabbit Monoclonal	016-20001	Wako	1:100
Anti BrdU, rat Monoclonal	LS-C188215	LS Bio	1:500
Biotin-SP-conjugated AffiniPure Donkey anti rat	712-065-150	Jackson Immunosresearch	1:250
Anti-BrdU, Rat Monoclonal	LS-C337097-100	LS Bio	1:500
Anti-BrdU, Rat Monoclonal	OBT0030	Bio Rad	1:500
Anti-Calretinin, Goat Polyclonal	AB1550	Sigma Aldrich	1:250
Anti-NeuN mouse Monoclonal	clone A60	Merck	1:200
Anti-NeuN rabbit Monoclonal	ab177487	Abcam	1:200
Anti-Doublecortin (DCX), goat Polyclonal	sc-8066	Santa Cruz	1:250
Anti Sox2, goat Polyclonal	sc-17320	Santa Cruz	1:250
Anti GFP, goat Polyclonal	ab6673	Abcam	1:400
Anti-Caspase 9 rabbit Polyclonal	HPA001473	Sigma Aldrich	1:300
Anti-Caspase 3 rabbit Polyclonal	C8487	Sigma Aldrich	1:500
Anti-Mineralocorticoid Receptor Rabbit Polyclonal	AB64457	Abcam	1:500
Anti-Glucocorticoid Receptor Rabbit Polyclonal	AB3580	Abcam	1:500

Table 48 Secondary antibodies

Name	Ref – No	Company	Dilution
Biotin-SP-conjugated AffiniPure Donkey anti rat	712-065-150	Jackson Immunosresearch	1:250
Anti-goat IgG Alexa Fluor R 488 donkey	AB_2534102	Invitrogen	1:250
Anti-rabbit IgG Cy3 donkey	711-165-152	Jackson Immuno Research /Dianova,	1:250
Anti-rabbit IgG Cy5 goat	ab6564	Abcam	1:250
Anti-rabbit IgG Alexa Fluor R 488 goat	A-11008	Invitrogen	1:250
Anti-mouse IgG Cy3 donkey	715-165-151	Jackson Immuno Research /Dianova	1:250
Anti-rat IgG Cy3 donkey	712-165-153	Jackson Immuno Research	1:800

5.2 Oligonucleotides (Primers)

All oligonucleotides are synthetized by Biotez Berlin Buch GmbH and delivered in a lyophilized state. The primers were diluted in ddH20 to a concentration of 50 pmol/µl

at 55° for 15min in an orbital shaker at 150 rounds/min. Storage at -20°C. For (q)PCR reactions, primers diluted to a final concentration of 5 pmol/µl in ddH2O. Table 49 lists all oligonucleotides used for genotyping and quantitative RT-PCR).

Table 49 Primer / Oligonucleotides

Name	Target Gene	5‘ to 3‘	Sequence	Type
Actb fwd	b-Actin	Forward	TCC AGC CTT CCT TCT TGG GT	Housekeeping Gene
Actb rev		Reverse	GCA CTG TGT TGG CAT AGA GGT	Housekeeping Gene
r18s fwd	18S ribosomal RNA	Forward	TTG ATT AAG TCC CTG CCC TTT GT	Housekeeping Gene
R18s rev		Reverse	CGA TCC GAG GGC CTC ACT A	Housekeeping Gene
28SmusF new	28S ribosomal RNA	Forward	GGA TGG CGA GAA ATA CCA GA	Housekeeping Gene
28SmusR		Reverse	AGC GCA GTC CAT TAC TTG CT'	Housekeeping Gene
mRpb1 fwd	RNA-Polymerase II	Forward	GAC CGA AAG CAC ATG ACT GA	Housekeeping Gene
mRpb1 rev		Reverse	CAA TTC AAA TCA TCG CCA AA	Housekeeping Gene
TBPf2	Tata binding protein	Forward	CCC CAT CAC TCC TGC CAC ACC	Housekeeping Gene
TBPr2		Reverse	CGA AGT GCA ATG GTC TTT AGG TC	Housekeeping Gene
ACE_WT	ACE 2	Reverse	TAA TTC CTT GGG AGG CAG CAC T	Target gene
ACE_COM		Forward	AGT GGA GGG TAT TTG TCA GGG C	Target gene
ACE_MUT		Multiplex for +/-	TAA AGC GCA TGC TCC AGA CTG C	Target gene
SERT WT IMR8900	SERT	Reverse	CCT AGA TAC CAG GCC CAC AA	Target gene
SERT COM IMR8899		Forward	AAT GGT GAG GAG TGG TGG AG	Target gene
SERT MUT IMR7415		Multiplex for +/-	GCC AGA GGC CAC TTG TGT AG	Target gene
TPH54	Tryptophan hydroxylase 2 TPH2	Forward	CCA AAG AGC TAC TCG ACC TAC	Target gene
TPH34		Reverse	AGC TGA GGC AGA CAG AAA GG	Target gene
NEO3		Multiplex for +/-	CTG CGC TGA CAG CCG GAA CAC	Target gene
Nr3C2_MRB_fw	Mineralocorticoid-receptor Nr3C2	Forward	GGA CCA AAT TAC CCT CAT CCA	Target gene
Nr3C2_MRB_rv		Reverse	GTA TGT TTG TAC GAT CTC CAA CTC AAG	Target gene
Nr3C1_GRD_fw	Glucocorticoid-receptor Nr3C1	Forward	CGG GAC CAC CTC CCA AA	Target gene
Nr3C1_GRD_rv		Reverse	CCC CAT AAT GGC ATC CCG AA	Target gene
Mouse CRF VMPS-1367 Fwd	Corticotropin releasing hormone CRF	Forward	GCA GCT CCG ATA TCA TTT GT	Target gene
Mouse CRF VMPS-1367 Rev		Reverse	TGA CTC CCA TCT GCT TTT TC	Target gene
POMCfw1	Proopiomelanocortin POMC	Forward	CCA TAG ATG TGT GGA GCT GGT	Target gene
POMCrv		Reverse	AGC GAG AGG TCG AGT TTG CA	Target gene

5.3 Laboratory Equipment

Table 50 Equipment and expendable material.

Name	Company, location
Alpha Imager (UV)	Alpha Innotech, Germany
Anesthesia Unit	MDC workshop, Germany
Brushes Cosmotop Fine tip Size 1 - 3	Davinci, Germany
Burrowing Tube grey plastic Ø = 7 cm; L = 10 cm	Workshop Freie University, Germany
Centrifuge 5415C	Eppendorf, Hamburg
Centrifuge Sorvall RC 5C	Heraeus, Germany
Corning® Netwells® inserts for 12 well plate	Sigma, Germany
Cryostat CM 1850	Leica, Germany
Disposable Filtertips Safe Seal SurPhob 1250, 300, 20, 10 µl	Biozym Scientific GmbH, Germany
Disposable Micro tube 2, 1.5, 0.5 ml SafeSeal	Sarstedt, Germany
Disposable Pipet tips 1000, 200, 10 µl	Sarstedt, Germany
Disposable Pipettes CellstarR 1, 2, 5, 10, 25 ml	Pipettes Gilson, USA
Elektrophoresis Gel Chamber System	Biozym Scientific GmbH, Germany
Elektrophoresis Gel UV Imaging System C200	Azure Systems, USA
Falcon tubes TPPR	Trasadingen, Switzerland
FastPrep	MP Biomedicals, France
Fluorescent microscope	Keyence Corp., USA
Fluorescent microscope	Leica, Germany
Freezer -25 Bio Compact RF410	Gram Bioline Denmark
Freezer -80	Binder, USA
Gloves Latex/Nitrile Size Large Rotiprotect	Roth, Germany
Hoarding cage 40x22x15 cm with mesh chow tube (L= 43 cm Ø = 7 cm)	Workshop Freie University, Germany
Incubator for 60°C	Binder, USA
Individually ventilated cage systems IVC	Tecniplast, USA
Medorex tube pump	Medorex, Germany
Microplate Reader, Infinite M200	Tecan, Switzerland
Microwave 8020	Privileg, Germany
MiniCollect® EDTA-coated tubes	Greiner, Germany
Mulitpette M4 250 µl	Eppendorf, Germany
Multistep Pipets Xplorer, Range 1250, 300, 20, 10	Eppendorf, Germany
Nanodrop	Thermo Scientific, USA
Nestlets 5x5 cm	Ancare, USA
PCR tubes	Biozym Scientific GmbH, Germany
PCR-Thermocycler PEQ-Star	Peqlab - Germany
pH Meter	pH Level 1 WTW, Germany
Pipetboy Pipetpump for Disposable Pipets	Integra USA
Pipets Brand Transferpette, Volume 1000; 200; 20, 10, 2.5 µl	Brand, Germany
Power Supply Gel System CS 300V	Biozym Scientific GmbH, Germany
Real time PCR machine Quantstudio 5	Theromo Scientific USA
Superfrost Plus slides	Menzel Gläser, Germany
Surgical Tools	FST, Germany
Syringe Needles 13 – 26 Gauge	Braun, Germany
Syringes 50 – 1 ml Omnifix/Injekt	Braun, Germany
Thermoshaker Ts-100	Biosan, Lettland
Ultrasound Sonoplus	Bandelin electronic, Germany
Video camera Sony CCD IRIS / Sony Alpha 37	Sony, Japan
Well-plates TC Standard with lid; Size 96, 48, 24,12, 6	Sarstedt, Germany

5.4 Software

Table 51 List of software used for this thesis.

Software	Company
QuantStudio™ Design & Analysis Software v1.4.3	Thermo Scientific, USA
Inkscape v0.92	Free Software Foundation, Inc The GNU General Public License https://inkscape.org/de/
Statistica 8	Statsoft 2007 USA
Prism 6	Graphpad USA
Microsoft Office 365	Microsoft USA
GNU Image Manipulation Program – GIMP 2.10.8	Free Software Foundation, Inc The GNU General Public License https://www.gimp.org/
Pyhton v3.6	python.org
R v3.5.3 The Great Truth	r-project.org
Zotero v5.0.6	Zotero.org

6 Abbreviations

Abbreviation	Word
5-HIAA	5-hydroxyindoleacetic acid
5-HT	5-Hydroxytryptamine, serotonin
5-HTP	5-hydroxytryptophan
Ach	Acetylcholine
ACN	Accumbens nucleus
AD	Aldehyde dehydrogenase
ADCY	Adenylate cyclases
ADL	Activities of daily living
Amy	Amygdala
Approx..	approximately
ASRI	Allosteric serotonin reuptake inhibitors
AVP	Arginine vasopressin
BDNF	Brain derived neurotrophic factor
bFGF	Basic fibroblast growth factor
BH4	Tetrabiopterin
BLBP	Brain lipid binding protein
BOLD	Blood oxygen dependent level contrast
Bp	Base pair
BrdU	Bromdesoxyuridin
cAMP	cyclic AMP
Cc	Corpus callosum
Ce	Cerebellum
ChR2	Channel Rhodopsin 2
CIT	Citalopram
CPu	Caudate putamen
CRP	C-reactive protein
Cx	Cortex
DA	Dopamine
DAG	Diacylglycerol
ddH20	Double distilled water
Dex	Dexamethasone
DH	Dorsal horn spinal cord
dH20	Distilled water
DOPAC	3,4-dihydroxyphenylacetic acid
DR	Dorsal Raphé Nucleus
DRN	Dorsa raphé nucleus
DSM	Diagnostic and Statistical Manual of Mental Diseases
EC	Enteroendocrine cell
EC	Enterochromaffin cells
ENT	Entorhinal cortex
EPM	Elevated plus maze
Fcx	Frontal cortex
Fill to x Volume	Fill to desired Volume
FKBP5	FK-506 binding protein 5
FST	Forced swimming test
GABA	gamma-Aminobutyric acid
GDNF	Glial cell line-derived neurotrophic factor
GFAP	Glial fibrillary acidic protein
GI	Gastro-intestinal
GLAST	Glutamate aspartate transporter
GM-CSF	Granulocyte macrophage colony-stimulating factor
GNAI	Gi/o protein alpha subunit

Abbreviation	Word
GNAQ	Gq/11 protein alpha
GNAS	Guanine nucleotide binding protein alpha subunit S
HIOMT	N-acetyl-5-HT-O-methyl-transferase
Hip / HC	Hippocampus
HOMX	Hemoxygenase
HVA	, homovanillic acid
Hyp	Hypothalamus
i.p.	intraperitoneal
ICD	International Classification of Diseases and Related Health Problems
IFN α, γ	Interferon alpha or gamma
IGF	Insuline like growth factor
IL 1-10	Interleukine 1-10
Incl.	including
IP-10	Interferon gamma-induced protein 10
IP3	myoinositol- 1, 4, 5-trisphosphate
IPN	Interpeduncular nucleus
LC	Locus coeruleus
L-dopa	L-3,4-dihydroxyphenylalanine
LS	Lateral septum
LSD	Lyseric-acid-diethylamide
MAO	Monoamine oxidase
MBT	Marble burying test
MCP 1-4	Monocyte chemoattractant protein 1-4
MDD	Major depressive disorder
MDE	Mild depressive episode
MHPG	3-methoxy-4-hydroxyphenylglycol
Mip1α β	Macrophage inflammatory protein alpha / beta
M-MLV RT	Moloney Murine Leukemia Virus Reverse Transcriptase
MRN	Median raphé nucleus
MRT	Magnet resonance tomography
NA	Noradrenaline
NE	Norepinephrine
NeuN	Neuronal nuclear marker
Neuro D1	Neurogenic differentiation 1
NGF	Neuronal Growth Factor
NM	Normetanephrine
NSCs	Neuronal stem cells
NTS	Nucleus of the solitary tract
o/N	Over night
O_2	Oxygen
OB	Olfactory bulb
OCD	Obsessive-compulsive disorder
OD	Optical density
P5P	Pyridoxal-5-phosphate
p7	Postnatal day 7
PAG	Periaqueductal gray
PCPA	Para-chlorophenylalanine
PCR	Polymerase Chain Reaction
PET	Positron-emission-tomography
PLCB	Phospholipase C
Prox1	Prospero homeobox protein 1
PVN	Paraventricular hypothalamicnucleus
qPCR	Quantitative Polymerase Chain Reaction
RAAS	Renin-Angiotensin-Aldosterone-System
RGLs	Radial-glia-like-cells

Abbreviations

Abbreviation	Word
RO	Raphé obscurus nucleus
Rpa	Raphé pallidus
RPo	Saphe pontis nucleus
RT	Room temperature
Rt-PCR / qPCR	Real time Polymerase chain reaction
SAA	Serum amyloid A
SCN	Suprachiasmic nucleus
SERT or 5-HTT	Serotonin transporter
sFlt-1	Soluble fms-like tyrosine kinase-1
sICAM1	Soluble intercellular adhesion molecule 1
SN	Subtantia nigra
SNAT	5-HT-N-acetyl-transferase
SNP	Single nucleotide polymorphism
Sox2	SRY (sex determining region Y)-box 2
sVCAM1	Soluble vascular cell adhesion molecule 1
TARC,	Thymus and activation-regulated chemokine
Tbr2	Eomesodermin also known as T-box brain protein 2
Tha	Thalamus
TIA	tianeptine
Tie2	Angiopoetin receptor
TNF-α	Tumor necrosis factor alpha
TPH	Trypthophan-hydroxylase
Trp	L-tryptophan
TSH	thyroid-stimulating hormone
VEGF	Vascular Endothelial Growth Factor
VH	Ventral horn
VMAT	Vesicular monoamine transporter
v-SVZ	Ventricular-subventricular zone
VTA	Ventral tegmental area
YLD	Years lost to disability

7 Bibliography

1. Styron, W. *Darkness Visible: A Memoir of Madness*. (Open Road Media, 2010).
2. Ferrari, A. J. *et al.* Burden of depressive disorders by country, sex, age, and year: findings from the global burden of disease study 2010. *PLoS Med.* **10**, e1001547 (2013).
3. Smith, K. & De Torres, C. A World of Depression. *Nature* **515**, 180–181 (2014).
4. World Health Organization. WHO | Depression and Other Common Mental Disorders WHO/MSD/MER/2017.2. (2017).
5. Kennedy, P. Opinion | The Great God of Depression. *The New York Times* (2018).
6. Global, regional, and national incidence, prevalence, and years lived with disability for 310 diseases and injuries, 1990–2015: a systematic analysis for the Global Burden of Disease Study 2015. *Lancet* **388**, 1545–1602 (2016).
7. Krishnan, V. & Nestler, E. J. The molecular neurobiology of depression. *Nature* **455**, 894–902 (2008).
8. Nestler, E. J. *et al.* Neurobiology of depression. *Neuron* **34**, 13–25 (2002).
9. Vos, T. *et al.* Years lived with disability (YLDs) for 1160 sequelae of 289 diseases and injuries 1990-2010: a systematic analysis for the Global Burden of Disease Study 2010. *Lancet* **380**, 2163–2196 (2012).
10. Kessler, R. C. & Bromet, E. J. The epidemiology of depression across cultures. *Annu Rev Public Health* **34**, 119–138 (2013).
11. Radden, J. Is This Dame Melancholy?: Equating Today's Depression and Past Melancholia. *Philosophy, Psychiatry, & Psychology* **10**, 37–52 (2003).
12. Jackson, W. A. A short guide to humoral medicine. *Trends in Pharmacological Sciences* **22**, 487–489 (2001).
13. Marrazzi, A. S. & Hart, E. R. Relationship of hallucinogens to adrenergic cerebral neurohumors. *Science* **121**, 365–367 (1955).
14. Psychology from Islamic Perspective: Contributions of Early Muslim Scholars and Challenges to Contemporary Muslim Psychologists | SpringerLink. https://link.springer.com/article/10.1007%2Fs10943-004-4302-z.
15. Burton, R. *Burton's Anatomy of Melancholy, 1628*. (Demokritus Junior, 1621).
16. Lewis, A. J. Melancholia: A Historical Review: Part I. *Journal of Mental Science* **80**, 1–42 (1934).
17. Freud, S. Trauer und Melancholie. *Internationale Zeitschrift für Ärztliche Psychoanalyse* **4**, 288–301 (1917).
18. Horwitz, A. V. DSM - I and DSM - II. in *The Encyclopedia of Clinical Psychology* 1–6 (American Cancer Society, 2014). doi:10.1002/9781118625392.wbecp012.
19. Davison, K. Historical aspects of mood disorders. *Psychiatry* **5**, 115–118 (2006).
20. Spitzer, R. L., Endicott, J. & Robins, E. Research diagnostic criteria: rationale and reliability. *Arch. Gen. Psychiatry* **35**, 773–782 (1978).
21. Philipp, M., Maier, W. & Delmo, C. D. The concept of major depression. I. Descriptive comparison of six competing operational definitions including ICD-10 and DSM-III-R. *Eur Arch Psychiatry Clin Neurosci* **240**, 258–265 (1991).
22. Gruenberg, A. M., Goldstein, R. D. & Pincus, H. A. Classification of Depression: Research and Diagnostic Criteria: DSM-IV and ICD-10. in *Biology of Depression* 1–12 (John Wiley & Sons, Ltd, 2008). doi:10.1002/9783527619672.ch1.
23. ICD-10 Version:2015. https://icd.who.int/browse10/2015/en#/F32.
24. Hirschfeld, R. M. History and evolution of the monoamine hypothesis of depression. *J Clin Psychiatry* **61 Suppl 6**, 4–6 (2000).
25. Boku, S., Nakagawa, S., Toda, H. & Hishimoto, A. Neural basis of major depressive disorder: Beyond monoamine hypothesis. *Psychiatry Clin. Neurosci.* **72**, 3–12 (2018).
26. Duman, R. S., Malberg, J. & Thome, J. Neural plasticity to stress and antidepressant treatment. *Biol. Psychiatry* **46**, 1181–1191 (1999).
27. Manji, H. K. & Duman, R. S. Impairments of neuroplasticity and cellular resilience in severe mood disorders: implications for the development of novel therapeutics. *Psychopharmacol Bull* **35**, 5–49 (2001).
28. Pittenger, C. & Duman, R. S. Stress, Depression, and Neuroplasticity: A Convergence of Mechanisms. *Neuropsychopharmacology* **33**, 88–109 (2007).
29. Ludwig, C. & Schmidt, A. Das Verhalten der Gase, welche mit dem Blut durch den reizbaren Säugethiermuskel strömen. *Arbeiten aus der Physiologischen Anstalt zu Leipzig* 1–61 (1868).
30. Rapport, M. M., Green, A. A. & Page, I. H. Serum vasoconstrictor, serotonin; isolation and characterization. *J. Biol. Chem.* **176**, 1243–1251 (1948).
31. Erspamer, V. & Asero, B. Identification of enteramine, the specific hormone of the enterochromaffin cell system, as 5-hydroxytryptamine. *Nature* **169**, 800–801 (1952).
32. Twarog, B. M. & Page, I. H. Serotonin content of some mammalian tissues and urine and a method for its determination. *Am. J. Physiol.* **175**, 157–161 (1953).
33. Sjoerdsma, A. & Palfreyman, M. G. History of serotonin and serotinin disorders. *Ann. N. Y. Acad. Sci.* **600**, 1–7; discussion 7-8 (1990).

34. THE SYNTHESIS OF 5-HYDROXYTRYPTAMINE - Journal of the American Chemical Society (ACS Publications). https://pubs.acs.org/doi/abs/10.1021/ja01154a551.
35. Gaddum, J. H. Antagonism between lysergic acid diethylamide and 5-hydroxytryptamine. *J. Physiol. (Lond.)* **121**, 15P (1953).
36. Woolley, D. W. & Shaw, E. Some Neurophysiological Aspects of Serotonin. *Br Med J* **2**, 122–126 (1954).
37. Woolley, D. W., Van Winkle, E. & Shaw, E. A METHOD FOR INCREASING BRAIN SEROTONIN WITHOUT INCURRING SOME OF THE PERIPHERAL EFFECTS OF THE HORMONE. *Proc Natl Acad Sci U S A* **43**, 128–133 (1957).
38. Woolley, D. W. & Shaw, F. N. EVIDENCE FOR THE PARTICIPATION OF SEROTONIN IN MENTAL PROCESSES. *Annals of the New York Academy of Sciences* **66**, 649–667 (1957).
39. Woolley, D. W. & Shaw, E. A biochemical and pharmacological suggestion about certain mental disorders. *Science* **119**, 587–588 (1954).
40. Bogdanski, D. F., Pletscher, A., Brodie, B. B. & Undenfriend, S. Identification and assay of serotonin in brain. *J. Pharmacol. Exp. Ther.* **117**, 82–88 (1956).
41. Radwanski, E. R. & Last, R. L. Tryptophan biosynthesis and metabolism: biochemical and molecular genetics. *Plant Cell* **7**, 921–934 (1995).
42. Welford, R. W. D. *et al.* Serotonin biosynthesis as a predictive marker of serotonin pharmacodynamics and disease-induced dysregulation. *Sci Rep* **6**, (2016).
43. Miller, M. R., McClure, D. & Shiman, R. p-Chlorphenylalanine effect on phenylalanine hydroxylase in hepatoma cells in culture. *J. Biol. Chem.* **250**, 1132–1140 (1975).
44. Koe, B. K. & Weissman, A. p-Chlorophenylalanine: a specific depletor of brain serotonin. *J. Pharmacol. Exp. Ther.* **154**, 499–516 (1966).
45. Weber, L. J. p-Chlorophenylalanine depletion of gastrointestinal 5-hydroxytryptamine. *Biochem. Pharmacol.* **19**, 2169–2172 (1970).
46. Young, S. N. How to increase serotonin in the human brain without drugs. *J Psychiatry Neurosci* **32**, 394–399 (2007).
47. Gulati, K., Anand, R. & Ray, A. Chapter 16 - Nutraceuticals as Adaptogens: Their Role in Health and Disease. in *Nutraceuticals* (ed. Gupta, R. C.) 193–205 (Academic Press, 2016). doi:10.1016/B978-0-12-802147-7.00016-4.
48. Van Praag, H. M. & Lemus, C. Monoamine precursors in the treatment of psychiatric disorders. *Nutrition and the Brain* **7**, 89–138 (1986).
49. Fiumara, A. *et al.* Aromatic L-amino acid decarboxylase deficiency with hyperdopaminuria. Clinical and laboratory findings in response to different therapies. *Neuropediatrics* **33**, 203–208 (2002).
50. Human Metabolome Database: Showing Protein Aromatic-L-amino-acid decarboxylase (HMDBP00278). http://www.hmdb.ca/proteins/HMDBP00278.
51. Honig, G., Jongsma, M. E., Hart, M. C. G. van der & Tecott, L. H. Chronic Citalopram Administration Causes a Sustained Suppression of Serotonin Synthesis in the Mouse Forebrain. *PLOS ONE* **4**, e6797 (2009).
52. Meijer, W. G., Kema, I. P., Volmer, M., Willemse, P. H. & de Vries, E. G. Discriminating capacity of indole markers in the diagnosis of carcinoid tumors. *Clin. Chem.* **46**, 1588–1596 (2000).
53. Shih, J. C. & Chen, K. Regulation of MAO-A and MAO-B Gene Expression. https://www.ingentaconnect.com/content/ben/cmc/2004/00000011/00000015/art00004 (2004) doi:info:doi/10.2174/0929867043364757.
54. Walther, D. J. *et al.* Synthesis of Serotonin by a Second Tryptophan Hydroxylase Isoform. *Science* **299**, 76–76 (2003).
55. Walther, D. J. & Bader, M. A unique central tryptophan hydroxylase isoform. *Biochem. Pharmacol.* **66**, 1673–1680 (2003).
56. Laporta, J., Peters, T. L., Merriman, K. E., Vezina, C. M. & Hernandez, L. L. Serotonin (5-HT) Affects Expression of Liver Metabolic Enzymes and Mammary Gland Glucose Transporters during the Transition from Pregnancy to Lactation. *PLOS ONE* **8**, e57847 (2013).
57. Marshall, A. M., Hernandez, L. L. & Horseman, N. D. Serotonin and Serotonin Transport in the Regulation of Lactation. *J Mammary Gland Biol Neoplasia* **19**, 139–146 (2014).
58. Stull, M. A. *et al.* Mammary gland homeostasis employs serotonergic regulation of epithelial tight junctions. *PNAS* **104**, 16708–16713 (2007).
59. Matsuda, M. *et al.* Serotonin Regulates Mammary Gland Development via an Autocrine-Paracrine Loop. *Developmental Cell* **6**, 193–203 (2004).
60. Crane, J. D. *et al.* Inhibiting peripheral serotonin synthesis reduces obesity and metabolic dysfunction by promoting brown adipose tissue thermogenesis. *Nature Medicine* **21**, 166–172 (2015).
61. Kim, H. *et al.* Serotonin regulates pancreatic beta cell mass during pregnancy. *Nature Medicine* **16**, 804–808 (2010).
62. Bertrand, P. P. & Bertrand, R. L. Serotonin release and uptake in the gastrointestinal tract. *Auton Neurosci* **153**, 47–57 (2010).
63. Kendig, D. M. & Grider, J. R. Serotonin and Colonic Motility. *Neurogastroenterol Motil* **27**, 899–905 (2015).

64. Walther, D. J. *et al.* Serotonylation of Small GTPases Is a Signal Transduction Pathway that Triggers Platelet α-Granule Release. *Cell* **115**, 851–862 (2003).
65. Duerschmied, D. *et al.* Platelet serotonin promotes the recruitment of neutrophils to sites of acute inflammation in mice. *Blood* **121**, 1008–1015 (2013).
66. Vrints, C. J. M., Bult, H., Bosmans, J., Herman, A. G. & Snoeck, J. P. Paradoxical vasoconstriction as result of acetylcholine and serotonin in diseased human coronary arteries. *Eur Heart J* **13**, 824–831 (1992).
67. Nebigil, C. G. *et al.* Serotonin 2B receptor is required for heart development. *PNAS* **97**, 9508–9513 (2000).
68. Nebigil, C. G. & Maroteaux, L. A Novel Role for Serotonin in Heart. *Trends in Cardiovascular Medicine* **11**, 329–335 (2001).
69. Sari, Y. & Zhou, F. C. Serotonin and its transporter on proliferation of fetal heart cells. *International Journal of Developmental Neuroscience* **21**, 417–424 (2003).
70. Oberlander, T. F. Fetal Serotonin Signaling: Setting Pathways for Early Childhood Development and Behavior. *Journal of Adolescent Health* **51**, S9–S16 (2012).
71. Yadav, V. K. *et al.* A Serotonin-Dependent Mechanism Explains the Leptin Regulation of Bone Mass, Appetite, and Energy Expenditure. *Cell* **138**, 976–989 (2009).
72. Galli, C., Macaluso, G. & Passeri, G. Serotonin: a novel bone mass controller may have implications for alveolar bone. *J Negat Results Biomed* **12**, 12 (2013).
73. Margolis, K. G. *et al.* Pharmacological reduction of mucosal but not neuronal serotonin opposes inflammation in mouse intestine. *Gut* **63**, 928–937 (2014).
74. Catena-Dell'Osso, M., Rotella, F., Dell'Osso, A., Fagiolini, A. & Marazziti, D. Inflammation, serotonin and major depression. *Curr Drug Targets* **14**, 571–577 (2013).
75. Lesurtel, M. *et al.* Platelet-Derived Serotonin Mediates Liver Regeneration. *Science* **312**, 104–107 (2006).
76. Namkung, J., Kim, H. & Park, S. Peripheral Serotonin: a New Player in Systemic Energy Homeostasis. *Mol Cells* **38**, 1023–1028 (2015).
77. Sommer, C. Serotonin in pain and analgesia. *Mol Neurobiol* **30**, 117–125 (2004).
78. Cortes-Altamirano, J. L. *et al.* Review: 5-HT1, 5-HT2, 5-HT3 and 5-HT7 Receptors and their Role in the Modulation of Pain Response in the Central Nervous System. *Curr Neuropharmacol* **16**, 210–221 (2018).
79. Sommer, C. CHAPTER 3.11 - Serotonin in Pain and Pain Control. in *Handbook of Behavioral Neuroscience* (eds. Müller, C. P. & Jacobs, B. L.) vol. 21 457–471 (Elsevier, 2010).
80. Martin, A. M. *et al.* The Diverse Metabolic Roles of Peripheral Serotonin. *Endocrinology* **158**, 1049–1063 (2017).
81. Watanabe, H. *et al.* Peripheral Serotonin Enhances Lipid Metabolism by Accelerating Bile Acid Turnover. *Endocrinology* **151**, 4776–4786 (2010).
82. Hannon, J. & Hoyer, D. Molecular biology of 5-HT receptors. *Behav. Brain Res.* **195**, 198–213 (2008).
83. Fidalgo, S., Ivanov, D. K. & Wood, S. H. Serotonin: from top to bottom. *Biogerontology* **14**, 21–45 (2013).
84. Charnay, Y. & Leger, L. Brain serotonergic circuitries. *Dialogues Clin Neurosci* **12**, 471–487 (2010).
85. Tajeddinn, W. *et al.* Association of Platelet Serotonin Levels in Alzheimer's Disease with Clinical and Cerebrospinal Fluid Markers. *J. Alzheimers Dis.* **53**, 621–630 (2016).
86. Kaye, W. H. *et al.* Serotonin alterations in anorexia and bulimia nervosa: new insights from imaging studies. *Physiol. Behav.* **85**, 73–81 (2005).
87. Garvin, B. & Wiley, J. W. The role of serotonin in irritable bowel syndrome: implications for management. *Curr Gastroenterol Rep* **10**, 363–368 (2008).
88. Goadsby, P. J. Serotonin receptor ligands: treatments of acute migraine and cluster headache. *Handb Exp Pharmacol* 129–143 (2007).
89. Jhoo, J. H. *et al.* Availability of brain serotonin transporters in patients with restless legs syndrome. *Neurology* **74**, 513–518 (2010).
90. Jindal, R. D. Insomnia in patients with depression: some pathophysiological and treatment considerations. *CNS Drugs* **23**, 309–329 (2009).
91. Kinney, H. C., Richerson, G. B., Dymecki, S. M., Darnall, R. A. & Nattie, E. E. The Brainstem and Serotonin in the Sudden Infant Death Syndrome. *Annual Review of Pathology: Mechanisms of Disease* **4**, 517–550 (2009).
92. Sternbach, H. The serotonin syndrome. *Am J Psychiatry* **148**, 705–713 (1991).
93. Muller, C. L., Anacker, A. M. J. & Veenstra-VanderWeele, J. The serotonin system in autism spectrum disorder: From biomarker to animal models. *Neuroscience* **321**, 24–41 (2016).
94. Patrick, R. P. & Ames, B. N. Vitamin D and the omega-3 fatty acids control serotonin synthesis and action, part 2: relevance for ADHD, bipolar disorder, schizophrenia, and impulsive behavior. *FASEB J.* **29**, 2207–2222 (2015).
95. Eggers, A. E. A serotonin hypothesis of schizophrenia. *Med. Hypotheses* **80**, 791–794 (2013).
96. Marcinkiewcz, C. A. *et al.* Serotonin engages an anxiety and fear-promoting circuit in the extended amygdala. *Nature* **537**, 97–101 (2016).
97. Akimova, E., Lanzenberger, R. & Kasper, S. The serotonin-1A receptor in anxiety disorders. *Biol. Psychiatry* **66**, 627–635 (2009).

98. Mosienko, V. *et al.* Exaggerated aggression and decreased anxiety in mice deficient in brain serotonin. *Translational Psychiatry* **2**, e122 (2012).
99. Politis, M. & Niccolini, F. Serotonin in Parkinson's disease. *Behav. Brain Res.* **277**, 136–145 (2015).
100. Grahame-Smith, D. G. Serotonin in affective disorders. *Int Clin Psychopharmacol* **6 Suppl 4**, 5–13 (1992).
101. Grünblatt, E. *et al.* Combining genetic and epigenetic parameters of the serotonin transporter gene in obsessive-compulsive disorder. *J Psychiatr Res* **96**, 209–217 (2018).
102. Jacobs, B. L. & Azmitia, E. C. Structure and function of the brain serotonin system. *Physiological Reviews* **72**, 165–229 (1992).
103. Kiyasova, V. & Gaspar, P. Development of raphe serotonin neurons from specification to guidance. *Eur. J. Neurosci.* **34**, 1553–1562 (2011).
104. Vitalis, T., Ansorge, M. S. & Dayer, A. G. Serotonin homeostasis and serotonin receptors as actors of cortical construction: special attention to the 5-HT3A and 5-HT6 receptor subtypes. *Frontiers in Cellular Neuroscience* **7**, (2013).
105. Hornung, J.-P. The human raphe nuclei and the serotonergic system. *J. Chem. Neuroanat.* **26**, 331–343 (2003).
106. Muzerelle, A., Scotto-Lomassese, S., Bernard, J. F., Soiza-Reilly, M. & Gaspar, P. Conditional anterograde tracing reveals distinct targeting of individual serotonin cell groups (B5-B9) to the forebrain and brainstem. *Brain Struct Funct* **221**, 535–561 (2016).
107. Hensler, J. G. Serotonergic modulation of the limbic system. *Neurosci Biobehav Rev* **30**, 203–214 (2006).
108. Erickson, J. D., Schafer, M. K., Bonner, T. I., Eiden, L. E. & Weihe, E. Distinct pharmacological properties and distribution in neurons and endocrine cells of two isoforms of the human vesicular monoamine transporter. *Proc. Natl. Acad. Sci. U.S.A.* **93**, 5166–5171 (1996).
109. Hoffman, B. J., Hansson, S. R., Mezey, E. & Palkovits, M. Localization and dynamic regulation of biogenic amine transporters in the mammalian central nervous system. *Front Neuroendocrinol* **19**, 187–231 (1998).
110. Nizzo, M. C. *et al.* Brain cortex phospholipids liposomes effects on CSF HVA, 5-HIAA and on prolactin and somatotropin secretion in man. *J. Neural Transm.* **43**, 93–102 (1978).
111. Strüder, H. K. & Weicker, H. Physiology and pathophysiology of the serotonergic system and its implications on mental and physical performance. Part I. *Int J Sports Med* **22**, 467–481 (2001).
112. Turcotte-Cardin, V. *et al.* Loss of adult 5-HT1A autoreceptors results in a paradoxical anxiogenic response to antidepressant treatment. *The Journal of Neuroscience* 0352–18 (2018) doi:10.1523/JNEUROSCI.0352-18.2018.
113. Bockaert, J., Claeysen, S., Bécamel, C., Dumuis, A. & Marin, P. Neuronal 5-HT metabotropic receptors: fine-tuning of their structure, signaling, and roles in synaptic modulation. *Cell Tissue Res.* **326**, 553–572 (2006).
114. Albert, P. R., Le François, B. & Millar, A. M. Transcriptional dysregulation of 5-HT1A autoreceptors in mental illness. *Mol Brain* **4**, 21 (2011).
115. Wesołowska, A. In the search for selective ligands of 5-HT5, 5-HT6 and 5-HT7 serotonin receptors. *Pol J Pharmacol* **54**, 327–341 (2002).
116. Rebholz, H., Friedman, E. & Castello, J. Alterations of Expression of the Serotonin 5-HT4 Receptor in Brain Disorders. *Int J Mol Sci* **19**, (2018).
117. Sangkuhl, K., Klein, T. E. & Altman, R. B. Selective serotonin reuptake inhibitors pathway. *Pharmacogenet. Genomics* **19**, 907–909 (2009).
118. Lummis, S. C. R. 5-HT(3) receptors. *J. Biol. Chem.* **287**, 40239–40245 (2012).
119. Brindley, R. L., Bauer, M. B., Blakely, R. D. & Currie, K. P. M. An interplay between the serotonin transporter (SERT) and 5-HT receptors controls stimulus-secretion coupling in sympathoadrenal chromaffin cells. *Neuropharmacology* **110**, 438–448 (2016).
120. YE, R. & BLAKELY, R. D. NATURAL AND ENGINEERED CODING VARIATION IN ANTIDEPRESSANT-SENSITIVE SEROTONIN TRANSPORTERS. *Neuroscience* **197**, (2011).
121. Daws, L. C. & Gould, G. G. Ontogeny and Regulation of the Serotonin Transporter: Providing Insights into Human Disorders. *Pharmacol Ther* **131**, 61–79 (2011).
122. Quick, M. W. Regulating the conducting states of a mammalian serotonin transporter. *Neuron* **40**, 537–549 (2003).
123. Racagni, G. & Popoli, M. Cellular and molecular mechanisms in the long-term action of antidepressants. *Dialogues Clin Neurosci* **10**, 385–400 (2008).
124. Malberg, J. E., Eisch, A. J., Nestler, E. J. & Duman, R. S. Chronic antidepressant treatment increases neurogenesis in adult rat hippocampus. *The Journal of Neuroscience* **20**, 9104–9110 (2000).
125. Klempin, F. *et al.* Serotonin Is Required for Exercise-Induced Adult Hippocampal Neurogenesis. *J. Neurosci.* **33**, 8270–8275 (2013).
126. Alenina, N. & Klempin, F. The role of serotonin in adult hippocampal neurogenesis. *Behavioural Brain Research* **277**, 49–57 (2015).
127. Kempermann, G., Song, H. & Gage, F. H. Neurogenesis in the Adult Hippocampus. *Cold Spring Harb Perspect Biol* **7**, a018812 (2015).
128. Roy, N. S. *et al.* In vitro neurogenesis by progenitor cells isolated from the adult human hippocampus. *Nat. Med.* **6**, 271–277 (2000).

129. Spalding, K. L. *et al.* Dynamics of hippocampal neurogenesis in adult humans. *Cell* **153**, 1219–1227 (2013).
130. Gratzner, H. G. Monoclonal antibody to 5-bromo- and 5-iododeoxyuridine: A new reagent for detection of DNA replication. *Science* **218**, 474–475 (1982).
131. Zhang, J. & Jiao, J. Molecular Biomarkers for Embryonic and Adult Neural Stem Cell and Neurogenesis. *Biomed Res Int* **2015**, 727542 (2015).
132. Vadodaria, K. C. & Gage, F. H. SnapShot: Adult Hippocampal Neurogenesis. *Cell* **156**, 1114-1114.e1 (2014).
133. Toda, T., Parylak, S. L., Linker, S. B. & Gage, F. H. The role of adult hippocampal neurogenesis in brain health and disease. *Molecular Psychiatry* **24**, 67–87 (2019).
134. Kempermann, G. *Adult neurogenesis*. (Oxford University Press, 2011).
135. Lie, D. C., Song, H., Colamarino, S. A., Ming, G. & Gage, F. H. Neurogenesis in the adult brain: new strategies for central nervous system diseases. *Annu. Rev. Pharmacol. Toxicol.* **44**, 399–421 (2004).
136. Kempermann, G., Gast, D., Kronenberg, G., Yamaguchi, M. & Gage, F. H. Early determination and long-term persistence of adult-generated new neurons in the hippocampus of mice. *Development* **130**, 391–399 (2003).
137. Snyder, J. S. *et al.* Adult-born hippocampal neurons are more numerous, faster maturing, and more involved in behavior in rats than in mice. *J. Neurosci.* **29**, 14484–14495 (2009).
138. Sorrells, S. F. *et al.* Human hippocampal neurogenesis drops sharply in children to undetectable levels in adults. *Nature* **555**, 377–381 (2018).
139. Cajal, S. R. y. *Texture of the Nervous System of Man and the Vertebrates*. (Springer Science & Business Media, 1999).
140. Lorente De Nó, R. Studies on the structure of the cerebral cortex. II. Continuation of the study of the ammonic system. *Journal für Psychologie und Neurologie* **46**, 113–177 (1934).
141. Stepan, J., Dine, J. & Eder, M. Functional optical probing of the hippocampal trisynaptic circuit in vitro: network dynamics, filter properties, and polysynaptic induction of CA1 LTP. *Front Neurosci* **9**, (2015).
142. Lieberwirth, C., Pan, Y., Liu, Y., Zhang, Z. & Wang, Z. Hippocampal adult neurogenesis: Its regulation and potential role in spatial learning and memory. *Brain Res.* **1644**, 127–140 (2016).
143. Squire, L. R. Memory and the hippocampus: a synthesis from findings with rats, monkeys, and humans. *Psychol Rev* **99**, 195–231 (1992).
144. Alam, M. J. *et al.* Adult Neurogenesis Conserves Hippocampal Memory Capacity. *J. Neurosci.* (2018) doi:10.1523/JNEUROSCI.2976-17.2018.
145. Clelland, C. D. *et al.* A functional role for adult hippocampal neurogenesis in spatial pattern separation. *Science* **325**, 210–213 (2009).
146. D'Angelo, F. *et al.* Micropatterned hydrogenated amorphous carbon guides mesenchymal stem cells towards neuronal differentiation. *Eur Cell Mater* **20**, 231–244 (2010).
147. França, T. F. A., Bitencourt, A. M., Maximilla, N. R., Barros, D. M. & Monserrat, J. M. Hippocampal neurogenesis and pattern separation: A meta-analysis of behavioral data. *Hippocampus* **27**, 937–950 (2017).
148. Gandy, K. *et al.* Pattern Separation: A Potential Marker of Impaired Hippocampal Adult Neurogenesis in Major Depressive Disorder. *Front Neurosci* **11**, 571 (2017).
149. Akers, K. G. *et al.* Hippocampal neurogenesis regulates forgetting during adulthood and infancy. *Science* **344**, 598–602 (2014).
150. Yau, S., Li, A. & So, K.-F. Involvement of Adult Hippocampal Neurogenesis in Learning and Forgetting. *Neural Plast.* **2015**, 717958 (2015).
151. Biebl, M., Cooper, C. M., Winkler, J. & Kuhn, H. G. Analysis of neurogenesis and programmed cell death reveals a self-renewing capacity in the adult rat brain. *Neurosci. Lett.* **291**, 17–20 (2000).
152. Ryu, J. R. *et al.* Control of adult neurogenesis by programmed cell death in the mammalian brain. *Molecular Brain* **9**, 43 (2016).
153. Gould, null, Tanapat, null, Hastings, null & Shors, null. Neurogenesis in adulthood: a possible role in learning. *Trends Cogn. Sci. (Regul. Ed.)* **3**, 186–192 (1999).
154. Gage, F. H. Mammalian Neural Stem Cells. *Science* **287**, 1433–1438 (2000).
155. Fuchs, E. & Gould, E. In vivo neurogenesis in the adult brain: regulation and functional implications. *European Journal of Neuroscience* **12**, 2211–2214 (2000).
156. Duman, R. S., Malberg, J. & Nakagawa, S. Regulation of adult neurogenesis by psychotropic drugs and stress. *J. Pharmacol. Exp. Ther.* **299**, 401–407 (2001).
157. Kempermann, G., Kuhn, H. G. & Gage, F. H. More hippocampal neurons in adult mice living in an enriched environment. *Nature* **386**, 493–495 (1997).
158. van Praag, H., Christie, B. R., Sejnowski, T. J. & Gage, F. H. Running enhances neurogenesis, learning, and long-term potentiation in mice. *Proc. Natl. Acad. Sci. U.S.A.* **96**, 13427–13431 (1999).
159. Kuhn, H. G., Dickinson-Anson, H. & Gage, F. H. Neurogenesis in the dentate gyrus of the adult rat: age-related decrease of neuronal progenitor proliferation. *J. Neurosci.* **16**, 2027–2033 (1996).
160. Mathews, K. J. *et al.* Evidence for reduced neurogenesis in the aging human hippocampus despite stable stem cell markers. *Aging Cell* **16**, 1195–1199 (2017).

161. Parent, J. M. The role of seizure-induced neurogenesis in epileptogenesis and brain repair. *Epilepsy Res.* **50**, 179–189 (2002).
162. Kokaia, Z. & Lindvall, O. Neurogenesis after ischaemic brain insults. *Curr. Opin. Neurobiol.* **13**, 127–132 (2003).
163. Sahay, A. & Hen, R. Adult hippocampal neurogenesis in depression. *Nat. Neurosci.* **10**, 1110–1115 (2007).
164. Snyder, J. S., Soumier, A., Brewer, M., Pickel, J. & Cameron, H. A. Adult hippocampal neurogenesis buffers stress responses and depressive behavior. *Nature* **476**, 458–461 (2011).
165. Yau, S.-Y., Lau, B. W.-M. & So, K.-F. Adult hippocampal neurogenesis: a possible way how physical exercise counteracts stress. *Cell Transplant* **20**, 99–111 (2011).
166. Oleskevich, S. & Descarries, L. Quantified distribution of the serotonin innervation in adult rat hippocampus. *Neuroscience* **34**, 19–33 (1990).
167. Oleskevich, S., Descarries, L., Watkins, K. C., Séguéla, P. & Daszuta, A. Ultrastructural features of the serotonin innervation in adult rat hippocampus: an immunocytochemical description in single and serial thin sections. *Neuroscience* **42**, 777–791 (1991).
168. Maddaloni, G. *et al.* Development of Serotonergic Fibers in the Post-Natal Mouse Brain. *Front Cell Neurosci* **11**, 202 (2017).
169. Nozaki, K., Kubo, R. & Furukawa, Y. Serotonin modulates the excitatory synaptic transmission in the dentate granule cells. *J. Neurophysiol.* **115**, 2997–3007 (2016).
170. Brezun, J. M. & Daszuta, A. Depletion in serotonin decreases neurogenesis in the dentate gyrus and the subventricular zone of adult rats. *Neuroscience* **89**, 999–1002 (1999).
171. Brezun, J. M. & Daszuta, A. Serotonergic reinnervation reverses lesion-induced decreases in PSA-nCAM labeling and proliferation of hippocampal cells in adult rats. *Hippocampus* **10**, 37–46 (2000).
172. Jha, S., Rajendran, R., Davda, J. & Vaidya, V. A. Selective serotonin depletion does not regulate hippocampal neurogenesis in the adult rat brain: differential effects of p-chlorophenylalanine and 5,7-dihydroxytryptamine. *Brain Res.* **1075**, 48–59 (2006).
173. Amsterdam, J. D. & Berwish, N. Treatment of refractory depression with combination reserpine and tricyclic antidepressant therapy. *J Clin Psychopharmacol* **7**, 238–242 (1987).
174. Kenney, C., Hunter, C., Mejia, N. & Jankovic, J. Is history of depression a contraindication to treatment with tetrabenazine? *Clin Neuropharmacol* **29**, 259–264 (2006).
175. Shulman, K. I., Herrmann, N. & Walker, S. E. Current place of monoamine oxidase inhibitors in the treatment of depression. *CNS Drugs* **27**, 789–797 (2013).
176. Dos Santos, R. G. *et al.* Antidepressive, anxiolytic, and antiaddictive effects of ayahuasca, psilocybin and lysergic acid diethylamide (LSD): a systematic review of clinical trials published in the last 25 years. *Ther Adv Psychopharmacol* **6**, 193–213 (2016).
177. Palfreyman, M. G. & McDonald, I. A. Method for treating depression. (1983).
178. Stahl, S. M., Grady, M. M., Moret, C. & Briley, M. SNRIs: their pharmacology, clinical efficacy, and tolerability in comparison with other classes of antidepressants. *CNS Spectr* **10**, 732–747 (2005).
179. Hiemke, C. & Härtter, S. Pharmacokinetics of selective serotonin reuptake inhibitors. *Pharmacol. Ther.* **85**, 11–28 (2000).
180. G, K. & Af, W. Neurochemical profile of tianeptine, a new antidepressant drug. *Clin Neuropharmacol* **11 Suppl 2**, S43-50 (1987).
181. Gillman, P. K. Tricyclic antidepressant pharmacology and therapeutic drug interactions updated. *Br J Pharmacol* **151**, 737–748 (2007).
182. Banasr, M., Hery, M., Printemps, R. & Daszuta, A. Serotonin-induced increases in adult cell proliferation and neurogenesis are mediated through different and common 5-HT receptor subtypes in the dentate gyrus and the subventricular zone. *Neuropsychopharmacology* **29**, 450–460 (2004).
183. Santarelli, L. *et al.* Requirement of Hippocampal Neurogenesis for the Behavioral Effects of Antidepressants. *Science* **301**, 805–809 (2003).
184. Radley, J. J. & Jacobs, B. L. 5-HT1A receptor antagonist administration decreases cell proliferation in the dentate gyrus. *Brain Research* **955**, 264–267 (2002).
185. Barnes, N. M. & Sharp, T. A review of central 5-HT receptors and their function. *Neuropharmacology* **38**, 1083–1152 (1999).
186. Diaz, S. L. *et al.* Paradoxical increase in survival of newborn neurons in the dentate gyrus of mice with constitutive depletion of serotonin. *Eur. J. Neurosci.* **38**, 2650–2658 (2013).
187. Klempin. Oppositional effects of serotonin receptors 5-HT1a, 2, and 2c in the regulation of adult hippocampal neurogenesis. *Frontiers in Molecular Neuroscience* (2010) doi:10.3389/fnmol.2010.00014.
188. Imoto, Y. *et al.* Role of the 5-HT4 receptor in chronic fluoxetine treatment-induced neurogenic activity and granule cell dematuration in the dentate gyrus. *Mol Brain* **8**, 29 (2015).
189. Kobayashi, K. *et al.* Reversal of hippocampal neuronal maturation by serotonergic antidepressants. *Proc. Natl. Acad. Sci. U.S.A.* **107**, 8434–8439 (2010).

190. Briley, M. & Moret, C. Neurobiological mechanisms involved in antidepressant therapies. *Clin Neuropharmacol* **16**, 387–400 (1993).
191. Zanos, P. *et al.* NMDAR inhibition-independent antidepressant actions of ketamine metabolites. *Nature* **533**, 481–486 (2016).
192. Wang, J.-W., David, D. J., Monckton, J. E., Battaglia, F. & Hen, R. Chronic fluoxetine stimulates maturation and synaptic plasticity of adult-born hippocampal granule cells. *J. Neurosci.* **28**, 1374–1384 (2008).
193. Encinas, J. M., Vaahtokari, A. & Enikolopov, G. Fluoxetine targets early progenitor cells in the adult brain. *Proc. Natl. Acad. Sci. U.S.A.* **103**, 8233–8238 (2006).
194. Guelfi, J. D., Dulcire, C., Moine, P. L. & Tafani, A. Clinical Safety and Efficacy of Tianeptine in 1,858 Depressed Patients Treated in General Practice. *NPS* **25**, 140–148 (1992).
195. Benfield, P., Heel, R. C. & Lewis, S. P. Fluoxetine. *Drugs* **32**, 481–508 (1986).
196. *Arzneiverordnungs-Report 2017*. (Springer-Verlag, 2017).
197. Cipriani, A. *et al.* Sertraline versus other antidepressive agents for depression. *Cochrane Database Syst Rev* CD006117 (2009) doi:10.1002/14651858.CD006117.pub2.
198. Henry, L. K. *et al.* Tyr-95 and Ile-172 in transmembrane segments 1 and 3 of human serotonin transporters interact to establish high affinity recognition of antidepressants. *J. Biol. Chem.* **281**, 2012–2023 (2006).
199. Taha, E. A., Salama, N. N. & Wang, S. Micelle Enhanced Fluorimetric and Thin Layer Chromatography Densitometric Methods for the Determination of (±) Citalopram and its S - Enantiomer Escitalopram. *Analytical Chemistry Insights* **4**, ACI.S2274 (2009).
200. Chen, F. *et al.* Characterization of an allosteric citalopram-binding site at the serotonin transporter. *J. Neurochem.* **92**, 21–28 (2005).
201. Chen, F., Larsen, M. B., Sánchez, C. & Wiborg, O. The S-enantiomer of R,S-citalopram, increases inhibitor binding to the human serotonin transporter by an allosteric mechanism. Comparison with other serotonin transporter inhibitors. *Eur Neuropsychopharmacol* **15**, 193–198 (2005).
202. Neubauer, H. A., Hansen, C. G. & Wiborg, O. Dissection of an allosteric mechanism on the serotonin transporter: a cross-species study. *Mol. Pharmacol.* **69**, 1242–1250 (2006).
203. Mennini, T., Mocaer, E. & Garattini, S. Tianeptine, a selective enhancer of serotonin uptake in rat brain. *Naunyn-Schmiedeberg's Arch Pharmacol* **336**, 478–482 (1987).
204. Fattaccini, C. M., Bolaños-Jimenez, F., Gozlan, H. & Hamon, M. Tianeptine stimulates uptake of 5-hydroxytryptamine in vivo in the rat brain. *Neuropharmacology* **29**, 1–8 (1990).
205. Watanabe, Y., Sakai, R. R., McEwen, B. S. & Mendelson, S. Stress and antidepressant effects on hippocampal and cortical 5-HT1A and 5-HT2 receptors and transport sites for serotonin. *Brain Research* **615**, 87–94 (1993).
206. Kasper, S. & McEwen, B. S. Neurobiological and clinical effects of the antidepressant tianeptine. *CNS Drugs* **22**, 15–26 (2008).
207. Costa e Silva, J. A. *et al.* Placebo-controlled study of tianeptine in major depressive episodes. *Neuropsychobiology* **35**, 24–29 (1997).
208. Lôo, H. *et al.* Efficacy and safety of tianeptine in the treatment of depressive disorders in comparison with fluoxetine. *J Affect Disord* **56**, 109–118 (1999).
209. Novotny, V. & Faltus, F. Tianeptine and fluoxetine in major depression: a 6-week randomised double-blind study. *Hum Psychopharmacol* **17**, 299–303 (2002).
210. Waintraub, L., Septien, L. & Azoulay, P. Efficacy and safety of tianeptine in major depression: evidence from a 3-month controlled clinical trial versus paroxetine. *CNS Drugs* **16**, 65–75 (2002).
211. Bonierbale, M., Lançon, C. & Tignol, J. The ELIXIR study: evaluation of sexual dysfunction in 4557 depressed patients in France. *Curr Med Res Opin* **19**, 114–124 (2003).
212. Ridout, F. & Hindmarch, I. Effects of tianeptine and mianserin on car driving skills. *Psychopharmacology (Berl.)* **154**, 356–361 (2001).
213. Wilde, M. I. & Benfield, P. Tianeptine. A review of its pharmacodynamic and pharmacokinetic properties, and therapeutic efficacy in depression and coexisting anxiety and depression. *Drugs* **49**, 411–439 (1995).
214. Curzon, G., Kennett, G. A., Sarna, G. S. & Whitton, P. S. The Effects of Tianeptine and other Antidepressants on a Rat Model of Depression. *British Journal of Psychiatry* **160**, 51–55 (1992).
215. Thiébot, M.-H., Martin, P. & Puech, A. J. Animal Behavioural Studies in the Evaluation of Antidepressant Drugs. *The British Journal of Psychiatry* **160**, 44–50 (1992).
216. Kelly, J. P. & Leonard, B. E. The effect of tianeptine and sertraline in three animal models of depression. *Neuropharmacology* **33**, 1011–1016 (1994).
217. Wagstaff, A. J., Ormrod, D. & Spencer, C. M. Tianeptine: a review of its use in depressive disorders. *CNS Drugs* **15**, 231–259 (2001).
218. McEwen, B. S., Magarinos, A. M. & Reagan, L. P. Structural plasticity and tianeptine: cellular and molecular targets. *Eur. Psychiatry* **17 Suppl 3**, 318–330 (2002).

219. McEwen, B. S. *et al.* The neurobiological properties of Tianeptine (Stablon): from monoamine hypothesis to glutamatergic modulation. *Mol Psychiatry* **15**, 237–249 (2010).
220. Bergink, V., van Megen, H. J. G. M. & Westenberg, H. G. M. Glutamate and anxiety. *Eur Neuropsychopharmacol* **14**, 175–183 (2004).
221. Lowy, M. T., Wittenberg, L. & Yamamoto, B. K. Effect of acute stress on hippocampal glutamate levels and spectrin proteolysis in young and aged rats. *J. Neurochem.* **65**, 268–274 (1995).
222. Paul, I. A. & Skolnick, P. Glutamate and depression: clinical and preclinical studies. *Ann. N. Y. Acad. Sci.* **1003**, 250–272 (2003).
223. Sanacora, G., Rothman, D. L., Mason, G. & Krystal, J. H. Clinical studies implementing glutamate neurotransmission in mood disorders. *Ann. N. Y. Acad. Sci.* **1003**, 292–308 (2003).
224. Skolnick, P., Legutko, B., Li, X. & Bymaster, F. P. Current perspectives on the development of non-biogenic amine-based antidepressants. *Pharmacol. Res.* **43**, 411–423 (2001).
225. Zarate, C. A. *et al.* Regulation of cellular plasticity cascades in the pathophysiology and treatment of mood disorders: role of the glutamatergic system. *Ann. N. Y. Acad. Sci.* **1003**, 273–291 (2003).
226. Reznikov, L. R. *et al.* Acute stress-mediated increases in extracellular glutamate levels in the rat amygdala: differential effects of antidepressant treatment. *Eur. J. Neurosci.* **25**, 3109–3114 (2007).
227. Czéh, B. *et al.* Stress-induced changes in cerebral metabolites, hippocampal volume, and cell proliferation are prevented by antidepressant treatment with tianeptine. *PNAS* **98**, 12796–12801 (2001).
228. Lucassen, P. J., Fuchs, E. & Czéh, B. Antidepressant treatment with tianeptine reduces apoptosis in the hippocampal dentate gyrus and temporal cortex. *Biological Psychiatry* **55**, 789–796 (2004).
229. Zoladz, P. R., Muñoz, C. & Diamond, D. M. Beneficial Effects of Tianeptine on Hippocampus-Dependent Long-Term Memory and Stress-Induced Alterations of Brain Structure and Function. *Pharmaceuticals* **3**, 3143–3166 (2010).
230. Sapolsky, R. M. Depression, antidepressants, and the shrinking hippocampus. *PNAS* **98**, 12320–12322 (2001).
231. Pollano, A., Zalosnik, M. I., Durando, P. E. & Suárez, M. M. Differential effects of tianeptine on the dorsal hippocampal volume of rats submitted to maternal separation followed by chronic unpredictable stress in adulthood. *Stress* **19**, 599–608 (2016).
232. Vouimba, R.-M., Muñoz, C. & Diamond, D. M. Differential effects of predator stress and the antidepressant tianeptine on physiological plasticity in the hippocampus and basolateral amygdala. *Stress* **9**, 29–40 (2006).
233. Pillai, A. G., Anilkumar, S. & Chattarji, S. The same antidepressant elicits contrasting patterns of synaptic changes in the amygdala vs hippocampus. *Neuropsychopharmacology* **37**, 2702–2711 (2012).
234. McEwen, B. S. & Chattarji, S. Molecular mechanisms of neuroplasticity and pharmacological implications: the example of tianeptine. *Eur Neuropsychopharmacol* **14 Suppl 5**, S497-502 (2004).
235. Rogóz, Z., Skuza, G., Dlaboga, D., Maj, J. & Dziedzicka-Wasylewska, M. Effect of repeated treatment with tianeptine and fluoxetine on the central alpha(1)-adrenergic system. *Neuropharmacology* **41**, 360–368 (2001).
236. Rzesnitzek, L. & Lang, S. 'Electroshock Therapy' in the Third Reich. *Med Hist* **61**, 66–88 (2017).
237. Friedlander, H. *The origins of Nazi genocide: from euthanasia to the final solution*. (Univ. of North Carolina Press, 2008).
238. Sienaert, P., Dhossche, D. M., Vancampfort, D., De Hert, M. & Gazdag, G. A clinical review of the treatment of catatonia. *Front Psychiatry* **5**, 181 (2014).
239. Tharyan, P. & Adams, C. E. Electroconvulsive therapy for schizophrenia. *Cochrane Database Syst Rev* CD000076 (2005) doi:10.1002/14651858.CD000076.pub2.
240. Malhi, G. S., Tanious, M. & Berk, M. Mania: diagnosis and treatment recommendations. *Curr Psychiatry Rep* **14**, 676–686 (2012).
241. Lunde, M. E., Lee, E. K. & Rasmussen, K. G. Electroconvulsive therapy in patients with epilepsy. *Epilepsy & Behavior* **9**, 355–359 (2006).
242. Dierckx, B., Heijnen, W. T., van den Broek, W. W. & Birkenhäger, T. K. Efficacy of electroconvulsive therapy in bipolar versus unipolar major depression: a meta-analysis. *Bipolar Disord* **14**, 146–150 (2012).
243. Group, T. U. E. R. Efficacy and safety of electroconvulsive therapy in depressive disorders: a systematic review and meta-analysis. *The Lancet* **361**, 799–808 (2003).
244. *Kaplan & Sadock's comprehensive textbook of psychiatry*. (Lippincott Williams & Wilkins, 2009).
245. Singh, A. & Kar, S. K. How Electroconvulsive Therapy Works?: Understanding the Neurobiological Mechanisms. *Clin Psychopharmacol Neurosci* **15**, 210–221 (2017).
246. Ottosson, J. O. Experimental studies of the mode of action of electroconvulsive therapy: Introduction. *Acta Psychiatr Scand Suppl* **35**, 5–6 (1960).
247. Bolwig, T. G. How Does Electroconvulsive Therapy Work? Theories on its Mechanism. *Can J Psychiatry* **56**, 13–18 (2011).
248. McNally, K. A. & Blumenfeld, H. Focal network involvement in generalized seizures: new insights from electroconvulsive therapy. *Epilepsy Behav* **5**, 3–12 (2004).
249. Mahar, I., Bambico, F. R., Mechawar, N. & Nobrega, J. N. Stress, serotonin, and hippocampal neurogenesis in relation to depression and antidepressant effects. *Neuroscience & Biobehavioral Reviews* **38**, 173–192 (2014).

250. Fink, M. & Ottosson, J. O. A theory of convulsive therapy in endogenous depression: significance of hypothalamic functions. *Psychiatry Res* **2**, 49–61 (1980).
251. Bolwig, T. G., Woldbye, D. P. & Mikkelsen, J. D. Electroconvulsive therapy as an anticonvulsant: a possible role of neuropeptide Y (NPY). *J ECT* **15**, 93–101 (1999).
252. Allen, J. P., Denney, D., Kendall, J. W. & Blachly, P. H. Corticotropin release during ECT in man. *Am J Psychiatry* **131**, 1225–1228 (1974).
253. Herman, J. P. *et al.* Chronic electroconvulsive shock treatment elicits up-regulation of CRF and AVP mRNA in select populations of neuroendocrine neurons. *Brain Res.* **501**, 235–246 (1989).
254. Yuuki, N. *et al.* HPA axis normalization, estimated by DEX/CRH test, but less alteration on cerebral glucose metabolism in depressed patients receiving ECT after medication treatment failures. *Acta Psychiatr Scand* **112**, 257–265 (2005).
255. Smith, J. E., Williams, K., Burkett, S., Glue, P. & Nutt, D. J. Oxytocin and vasopressin responses to ECT. *Psychiatry Res* **32**, 201–202 (1990).
256. Sørensen, P. S., Hammer, M. & Bolwig, T. G. Vasopressin release during electroconvulsive therapy. *Psychoneuroendocrinology* **7**, 303–308 (1982).
257. Ohman, R., Walinder, J., Balldin, J. & Wallin, L. Prolactin response to electroconvulsive therapy. *Lancet* **2**, 936–937 (1976).
258. Devanand, D. P. *et al.* Effects of electroconvulsive therapy on plasma vasopressin and oxytocin. *Biol. Psychiatry* **44**, 610–616 (1998).
259. Hellsten, J. *et al.* Electroconvulsive seizures increase hippocampal neurogenesis after chronic corticosterone treatment. *Eur. J. Neurosci.* **16**, 283–290 (2002).
260. Sheline, Y. I., Gado, M. H. & Kraemer, H. C. Untreated depression and hippocampal volume loss. *Am J Psychiatry* **160**, 1516–1518 (2003).
261. Videbech, P. & Ravnkilde, B. Hippocampal volume and depression: a meta-analysis of MRI studies. *Am J Psychiatry* **161**, 1957–1966 (2004).
262. Czéh, B. & Lucassen, P. J. What causes the hippocampal volume decrease in depression? Are neurogenesis, glial changes and apoptosis implicated? *Eur Arch Psychiatry Clin Neurosci* **257**, 250–260 (2007).
263. Bremner, J. D. *et al.* Hippocampal Volume Reduction in Major Depression. *American Journal of Psychiatry* **157**, 115–118 (2000).
264. Nordanskog, P. *et al.* Increase in hippocampal volume after electroconvulsive therapy in patients with depression: a volumetric magnetic resonance imaging study. *J ECT* **26**, 62–67 (2010).
265. Olesen, M. V., Wörtwein, G., Folke, J. & Pakkenberg, B. Electroconvulsive stimulation results in long-term survival of newly generated hippocampal neurons in rats. *Hippocampus* **27**, 52–60 (2017).
266. Schloesser, R. J. *et al.* Antidepressant-like Effects of Electroconvulsive Seizures Require Adult Neurogenesis in a Neuroendocrine Model of Depression. *Brain Stimul* **8**, 862–867 (2015).
267. Madsen, T. M. *et al.* Increased neurogenesis in a model of electroconvulsive therapy. *Biological Psychiatry* **47**, 1043–1049 (2000).
268. Scott, B. W., Wojtowicz, J. M. & Burnham, W. M. Neurogenesis in the dentate gyrus of the rat following electroconvulsive shock seizures. *Exp. Neurol.* **165**, 231–236 (2000).
269. Wennström, M., Hellsten, J. & Tingström, A. Electroconvulsive seizures induce proliferation of NG2-expressing glial cells in adult rat amygdala. *Biol. Psychiatry* **55**, 464–471 (2004).
270. Inta, D. *et al.* Electroconvulsive therapy induces neurogenesis in frontal rat brain areas. *PLoS ONE* **8**, e69869 (2013).
271. Perera, T. D. *et al.* Antidepressant-Induced Neurogenesis in the Hippocampus of Adult Nonhuman Primates. *Journal of Neuroscience* **27**, 4894–4901 (2007).
272. Jonckheere, J. *et al.* Short- and long-term efficacy of electroconvulsive stimulation in animal models of depression: The essential role of neuronal survival. *Brain Stimul* **11**, 1336–1347 (2018).
273. Chen, F., Madsen, T. M., Wegener, G. & Nyengaard, J. R. Repeated electroconvulsive seizures increase the total number of synapses in adult male rat hippocampus. *Eur Neuropsychopharmacol* **19**, 329–338 (2009).
274. Schoenfeld, T. J., McCausland, H. C., Morris, H. D., Padmanaban, V. & Cameron, H. A. Stress and Loss of Adult Neurogenesis Differentially Reduce Hippocampal Volume. *Biol. Psychiatry* **82**, 914–923 (2017).
275. Bonne, O. *et al.* Increased cerebral blood flow in depressed patients responding to electroconvulsive therapy. *J. Nucl. Med.* **37**, 1075–1080 (1996).
276. Yatham, L. N., Clark, C. C. & Zis, A. P. A preliminary study of the effects of electroconvulsive therapy on regional brain glucose metabolism in patients with major depression. *J ECT* **16**, 171–176 (2000).
277. Suwa, T. *et al.* Corticolimbic balance shift of regional glucose metabolism in depressed patients treated with ECT. *J Affect Disord* **136**, 1039–1046 (2012).
278. Andrade, C. & Bolwig, T. G. Electroconvulsive therapy, hypertensive surge, blood-brain barrier breach, and amnesia: exploring the evidence for a connection. *J ECT* **30**, 160–164 (2014).
279. Dyrvig, M., Christiansen, S. H., Woldbye, D. P. D. & Lichota, J. Temporal gene expression profile after acute electroconvulsive stimulation in the rat. *Gene* **539**, 8–14 (2014).

280. Barreto, G. *et al.* Gadd45a promotes epigenetic gene activation by repair-mediated DNA demethylation. *Nature* **445**, 671–675 (2007).
281. Ma, D. K. *et al.* Neuronal activity-induced Gadd45b promotes epigenetic DNA demethylation and adult neurogenesis. *Science* **323**, 1074–1077 (2009).
282. Jun, H., Mohammed Qasim Hussaini, S., Cho, C. H., Welby, J. & Jang, M.-H. Gadd45b Mediates Electroconvulsive Shock Induced Proliferation of Hippocampal Neural Stem Cells. *Brain Stimul* **8**, 1021–1024 (2015).
283. Minelli, A. *et al.* Vascular Endothelial Growth Factor (VEGF) serum concentration during electroconvulsive therapy (ECT) in treatment resistant depressed patients. *Prog. Neuropsychopharmacol. Biol. Psychiatry* **35**, 1322–1325 (2011).
284. Rotheneichner, P. *et al.* Hippocampal neurogenesis and antidepressive therapy: shocking relations. *Neural Plast.* **2014**, 723915 (2014).
285. Altar, C. A. *et al.* Electroconvulsive seizures regulate gene expression of distinct neurotrophic signaling pathways. *J. Neurosci.* **24**, 2667–2677 (2004).
286. Ito, M. *et al.* Effects of repeated electroconvulsive seizure on cell proliferation in the rat hippocampus. *Synapse* **64**, 814–821 (2010).
287. Nibuya, M., Morinobu, S. & Duman, R. S. Regulation of BDNF and trkB mRNA in rat brain by chronic electroconvulsive seizure and antidepressant drug treatments. *J. Neurosci.* **15**, 7539–7547 (1995).
288. Altar, C. A., Whitehead, R. E., Chen, R., Wörtwein, G. & Madsen, T. M. Effects of electroconvulsive seizures and antidepressant drugs on brain-derived neurotrophic factor protein in rat brain. *Biol. Psychiatry* **54**, 703–709 (2003).
289. Narboux-Nême, N. *et al.* Severe serotonin depletion after conditional deletion of the vesicular monoamine transporter 2 gene in serotonin neurons: neural and behavioral consequences. *Neuropsychopharmacology* **36**, 2538–2550 (2011).
290. Hainer, C. *et al.* Beyond Gene Inactivation: Evolution of Tools for Analysis of Serotonergic Circuitry. *ACS Chem Neurosci* **6**, 1116–1129 (2015).
291. Kalueff, A. V., Olivier, J. D. A., Nonkes, L. J. P. & Homberg, J. R. Conserved role for the serotonin transporter gene in rat and mouse neurobehavioral endophenotypes. *Neurosci Biobehav Rev* **34**, 373–386 (2010).
292. Zhuang, X., Masson, J., Gingrich, J. A., Rayport, S. & Hen, R. Targeted gene expression in dopamine and serotonin neurons of the mouse brain. *J. Neurosci. Methods* **143**, 27–32 (2005).
293. Bortolato, M. *et al.* Monoamine oxidase A and A/B knockout mice display autistic-like features. *Int. J. Neuropsychopharmacol.* **16**, 869–888 (2013).
294. Scott, A. L., Bortolato, M., Chen, K. & Shih, J. C. Novel monoamine oxidase A knock out mice with human-like spontaneous mutation. *Neuroreport* **19**, 739–743 (2008).
295. Cheng, L. *et al.* Lmx1b, Pet-1, and Nkx2.2 coordinately specify serotonergic neurotransmitter phenotype. *J. Neurosci.* **23**, 9961–9967 (2003).
296. Zhao, S. *et al.* Cell type–specific channelrhodopsin-2 transgenic mice for optogenetic dissection of neural circuitry function. *Nat. Methods* **8**, 745–752 (2011).
297. Scott, M. M. *et al.* A genetic approach to access serotonin neurons for in vivo and in vitro studies. *Proc. Natl. Acad. Sci. U.S.A.* **102**, 16472–16477 (2005).
298. Kistner, A. *et al.* Doxycycline-mediated quantitative and tissue-specific control of gene expression in transgenic mice. *Proc. Natl. Acad. Sci. U.S.A.* **93**, 10933–10938 (1996).
299. Weber, T. *et al.* Tetracycline inducible gene manipulation in serotonergic neurons. *PLoS ONE* **7**, e38193 (2012).
300. Bader, M. Mouse knockout models of hypertension. *Methods Mol. Med.* **108**, 17–32 (2005).
301. Pelosi, B., Pratelli, M., Migliarini, S., Pacini, G. & Pasqualetti, M. Generation of a Tph2 Conditional Knockout Mouse Line for Time- and Tissue-Specific Depletion of Brain Serotonin. *PLoS ONE* **10**, e0136422 (2015).
302. Alenina, N. *et al.* Growth retardation and altered autonomic control in mice lacking brain serotonin. *Proc. Natl. Acad. Sci. U.S.A.* **106**, 10332–10337 (2009).
303. Jahanshahi, A. *et al.* Altered expression of neuronal tryptophan hydroxylase-2 mRNA in the dorsal and median raphe nuclei of three genetically modified mouse models relevant to depression and anxiety. *J. Chem. Neuroanat.* **41**, 227–233 (2011).
304. Lesch, K.-P., Araragi, N., Waider, J., van den Hove, D. & Gutknecht, L. Targeting brain serotonin synthesis: insights into neurodevelopmental disorders with long-term outcomes related to negative emotionality, aggression and antisocial behaviour. *Philos. Trans. R. Soc. Lond., B, Biol. Sci.* **367**, 2426–2443 (2012).
305. Fernandez, S. P. & Gaspar, P. Investigating anxiety and depressive-like phenotypes in genetic mouse models of serotonin depletion. *Neuropharmacology* **62**, 144–154 (2012).
306. Savelieva, K. V. *et al.* Genetic disruption of both tryptophan hydroxylase genes dramatically reduces serotonin and affects behavior in models sensitive to antidepressants. *PLoS ONE* **3**, e3301 (2008).
307. Gutknecht, L. *et al.* Interaction of brain 5-HT synthesis deficiency, chronic stress and sex differentially impact emotional behavior in Tph2 knockout mice. *Psychopharmacology (Berl.)* **232**, 2429–2441 (2015).
308. Placidi, G. P. *et al.* Aggressivity, suicide attempts, and depression: relationship to cerebrospinal fluid monoamine metabolite levels. *Biol. Psychiatry* **50**, 783–791 (2001).
309. Kästner, N. *et al.* Brain serotonin deficiency affects female aggression. *Sci Rep* **9**, 1366 (2019).

310. Solarewicz, J. Z., Angoa-Perez, M., Kuhn, D. M. & Mateika, J. H. The sleep-wake cycle and motor activity, but not temperature, are disrupted over the light-dark cycle in mice genetically depleted of serotonin. *Am. J. Physiol. Regul. Integr. Comp. Physiol.* **308**, R10-17 (2015).
311. Hainer, C. The Role of Brain Serotonin in Female Reproduction and Adult Neurogenesis. (Humboldt University Berlin, 2018).
312. Kronenberg, G. *et al.* Increased brain-derived neurotrophic factor (BDNF) protein concentrations in mice lacking brain serotonin. *Eur Arch Psychiatry Clin Neurosci* 1–4 (2015) doi:10.1007/s00406-015-0611-3.
313. Gutknecht, L. *et al.* Deficiency of brain 5-HT synthesis but serotonergic neuron formation in Tph2 knockout mice. *J Neural Transm (Vienna)* **115**, 1127–1132 (2008).
314. Waider, J. *et al.* GABA concentration and GABAergic neuron populations in limbic areas are differentially altered by brain serotonin deficiency in Tph2 knockout mice. *Histochem. Cell Biol.* **139**, 267–281 (2013).
315. Kriegebaum, C. *et al.* Brain-specific conditional and time-specific inducible Tph2 knockout mice possess normal serotonergic gene expression in the absence of serotonin during adult life. *Neurochem. Int.* **57**, 512–517 (2010).
316. Mosienko, V. *et al.* Life without brain serotonin: Reevaluation of serotonin function with mice deficient in brain serotonin synthesis. *Behav. Brain Res.* (2014) doi:10.1016/j.bbr.2014.06.005.
317. Bengel, D. *et al.* Altered brain serotonin homeostasis and locomotor insensitivity to 3, 4-methylenedioxymethamphetamine ('Ecstasy') in serotonin transporter-deficient mice. *Mol. Pharmacol.* **53**, 649–655 (1998).
318. Rumajogee, P. *et al.* Adaption of the serotoninergic neuronal phenotype in the absence of 5-HT autoreceptors or the 5-HT transporter: involvement of BDNF and cAMP. *Eur. J. Neurosci.* **19**, 937–944 (2004).
319. Lira, A. *et al.* Altered depression-related behaviors and functional changes in the dorsal raphe nucleus of serotonin transporter-deficient mice. *Biol. Psychiatry* **54**, 960–971 (2003).
320. van Kleef, E. S., Gaspar, P. & Bonnin, A. Insights into the complex influence of 5-HT signaling on thalamocortical axonal system development. *Eur J Neurosci* **35**, 1563–1572 (2012).
321. Luo, X., Persico, A. M. & Lauder, J. M. Serotonergic regulation of somatosensory cortical development: lessons from genetic mouse models. *Dev. Neurosci.* **25**, 173–183 (2003).
322. Sakakibara, Y. *et al.* Developmental alterations in anxiety and cognitive behavior in serotonin transporter mutant mice. *Psychopharmacology (Berl.)* **231**, 4119–4133 (2014).
323. Schmitt, A. *et al.* Adult neurogenesis in serotonin transporter deficient mice. *J Neural Transm (Vienna)* **114**, 1107–1119 (2007).
324. Holmes, A., Yang, R. J., Lesch, K.-P., Crawley, J. N. & Murphy, D. L. Mice lacking the serotonin transporter exhibit 5-HT(1A) receptor-mediated abnormalities in tests for anxiety-like behavior. *Neuropsychopharmacology* **28**, 2077–2088 (2003).
325. Li, Q. *et al.* Reduction of 5-hydroxytryptamine (5-HT)(1A)-mediated temperature and neuroendocrine responses and 5-HT(1A) binding sites in 5-HT transporter knockout mice. *J. Pharmacol. Exp. Ther.* **291**, 999–1007 (1999).
326. Mitchell, N. C., Gould, G. G., Koek, W. & Daws, L. C. Ontogeny of SERT Expression and Antidepressant-like Response to Escitalopram in Wild-Type and SERT Mutant Mice. *J. Pharmacol. Exp. Ther.* **358**, 271–281 (2016).
327. Nackenoff, A. G., Moussa-Tooks, A. B., McMeekin, A. M., Veenstra-VanderWeele, J. & Blakely, R. D. Essential Contributions of Serotonin Transporter Inhibition to the Acute and Chronic Actions of Fluoxetine and Citalopram in the SERT Met172 Mouse. *Neuropsychopharmacology* **41**, 1733–1741 (2016).
328. Jiang, X., Wang, J., Luo, T. & Li, Q. Impaired hypothalamic-pituitary-adrenal axis and its feedback regulation in serotonin transporter knockout mice. *Psychoneuroendocrinology* **34**, 317–331 (2009).
329. Kalueff, A. V., Ren-Patterson, R. F. & Murphy, D. L. The developing use of heterozygous mutant mouse models in brain monoamine transporter research. *Trends Pharmacol. Sci.* **28**, 122–127 (2007).
330. Li, Q. Cellular and molecular alterations in mice with deficient and reduced serotonin transporters. *Mol. Neurobiol.* **34**, 51–66 (2006).
331. Caspi, A. *et al.* Influence of life stress on depression: moderation by a polymorphism in the 5-HTT gene. *Science* **301**, 386–389 (2003).
332. Zalsman, G. *et al.* Association of a triallelic serotonin transporter gene promoter region (5-HTTLPR) polymorphism with stressful life events and severity of depression. *Am J Psychiatry* **163**, 1588–1593 (2006).
333. Roy, A., Hu, X.-Z., Janal, M. N. & Goldman, D. Interaction between childhood trauma and serotonin transporter gene variation in suicide. *Neuropsychopharmacology* **32**, 2046–2052 (2007).
334. McEwen, B. S. & Olié, J. P. Neurobiology of mood, anxiety, and emotions as revealed by studies of a unique antidepressant: tianeptine. *Mol. Psychiatry* **10**, 525–537 (2005).
335. Kraus, C., Castrén, E., Kasper, S. & Lanzenberger, R. Serotonin and neuroplasticity - Links between molecular, functional and structural pathophysiology in depression. *Neurosci Biobehav Rev* **77**, 317–326 (2017).
336. Liu, B., Liu, J., Wang, M., Zhang, Y. & Li, L. From Serotonin to Neuroplasticity: Evolvement of Theories for Major Depressive Disorder. *Front Cell Neurosci* **11**, (2017).

337. Hamburger, V. & Levi-Montalcini, R. Proliferation, differentiation and degeneration in the spinal ganglia of the chick embryo under normal and experimental conditions. *J. Exp. Zool.* **111**, 457–501 (1949).
338. Cohen, S., Levi-Montalcini, R. & Hamburger, V. A NERVE GROWTH-STIMULATING FACTOR ISOLATED FROM SARCOM AS 37 AND 180. *Proc. Natl. Acad. Sci. U.S.A.* **40**, 1014–1018 (1954).
339. Levi-Montalcini, R. The nerve growth factor: its mode of action on sensory and sympathetic nerve cells. *Harvey Lect.* **60**, 217–259 (1966).
340. Barde, Y. A., Edgar, D. & Thoenen, H. Purification of a new neurotrophic factor from mammalian brain. *EMBO J.* **1**, 549–553 (1982).
341. Lu, B. BDNF and Activity-Dependent Synaptic Modulation. *Learn. Mem.* **10**, 86–98 (2003).
342. Foltran, R. B. & Diaz, S. L. BDNF isoforms: a round trip ticket between neurogenesis and serotonin? *J. Neurochem.* **138**, 204–221 (2016).
343. Bibel, M. & Barde, Y. A. Neurotrophins: key regulators of cell fate and cell shape in the vertebrate nervous system. *Genes Dev.* **14**, 2919–2937 (2000).
344. Lewin, G. R. & Barde, Y.-A. Physiology of the Neurotrophins. *Annual Review of Neuroscience* **19**, 289–317 (1996).
345. Lee, B.-H., Kim, H., Park, S.-H. & Kim, Y.-K. Decreased plasma BDNF level in depressive patients. *J Affect Disord* **101**, 239–244 (2007).
346. Kim, Y.-K. *et al.* Low plasma BDNF is associated with suicidal behavior in major depression. *Prog. Neuropsychopharmacol. Biol. Psychiatry* **31**, 78–85 (2007).
347. Maisonpierre, P. C. *et al.* Human and rat brain-derived neurotrophic factor and neurotrophin-3: gene structures, distributions, and chromosomal localizations. *Genomics* **10**, 558–568 (1991).
348. Aid, T., Kazantseva, A., Piirsoo, M., Palm, K. & Timmusk, T. Mouse and rat BDNF gene structure and expression revisited. *J. Neurosci. Res.* **85**, 525–535 (2007).
349. Greenberg, M. E., Xu, B., Lu, B. & Hempstead, B. L. New Insights in the Biology of BDNF Synthesis and Release: Implications in CNS Function. *Journal of Neuroscience* **29**, 12764–12767 (2009).
350. Tao, X., West, A. E., Chen, W. G., Corfas, G. & Greenberg, M. E. A calcium-responsive transcription factor, CaRF, that regulates neuronal activity-dependent expression of BDNF. *Neuron* **33**, 383–395 (2002).
351. Hong, E. J., McCord, A. E. & Greenberg, M. E. A biological function for the neuronal activity-dependent component of Bdnf transcription in the development of cortical inhibition. *Neuron* **60**, 610–624 (2008).
352. Pang, P. T. *et al.* Cleavage of proBDNF by tPA/plasmin is essential for long-term hippocampal plasticity. *Science* **306**, 487–491 (2004).
353. Hwang, J. J., Park, M.-H., Choi, S.-Y. & Koh, J.-Y. Activation of the Trk signaling pathway by extracellular zinc. Role of metalloproteinases. *J. Biol. Chem.* **280**, 11995–12001 (2005).
354. Mizoguchi, H. *et al.* Matrix metalloproteinase-9 contributes to kindled seizure development in pentylenetetrazole-treated mice by converting pro-BDNF to mature BDNF in the hippocampus. *J. Neurosci.* **31**, 12963–12971 (2011).
355. Teng, H. K. *et al.* ProBDNF Induces Neuronal Apoptosis via Activation of a Receptor Complex of p75NTR and Sortilin. *J. Neurosci.* **25**, 5455–5463 (2005).
356. Woo, N. H. *et al.* Activation of p75NTR by proBDNF facilitates hippocampal long-term depression. *Nat. Neurosci.* **8**, 1069–1077 (2005).
357. Mowla, S. J. *et al.* Biosynthesis and post-translational processing of the precursor to brain-derived neurotrophic factor. *J. Biol. Chem.* **276**, 12660–12666 (2001).
358. Farhadi, H. F. *et al.* Neurotrophin-3 sorts to the constitutive secretory pathway of hippocampal neurons and is diverted to the regulated secretory pathway by coexpression with brain-derived neurotrophic factor. *J. Neurosci.* **20**, 4059–4068 (2000).
359. Chao, M. V. & Hempstead, B. L. p75 and Trk: a two-receptor system. *Trends Neurosci.* **18**, 321–326 (1995).
360. Kowiański, P. *et al.* BDNF: A Key Factor with Multipotent Impact on Brain Signaling and Synaptic Plasticity. *Cell Mol Neurobiol* **38**, 579–593 (2018).
361. Musumeci, G. & Minichiello, L. BDNF-TrkB signalling in fear learning: from genetics to neural networks. *Rev Neurosci* **22**, 303–315 (2011).
362. Bekinschtein, P., Cammarota, M. & Medina, J. H. BDNF and memory processing. *Neuropharmacology* **76**, 677–683 (2014).
363. Katoh-Semba, R. *et al.* Riluzole enhances expression of brain-derived neurotrophic factor with consequent proliferation of granule precursor cells in the rat hippocampus. *FASEB J.* **16**, 1328–1330 (2002).
364. Lee, J., Duan, W. & Mattson, M. P. Evidence that brain-derived neurotrophic factor is required for basal neurogenesis and mediates, in part, the enhancement of neurogenesis by dietary restriction in the hippocampus of adult mice. *Journal of neurochemistry* **82**, 1367–1375 (2002).
365. Russo-Neustadt, A., Beard, R. C. & Cotman, C. W. Exercise, antidepressant medications, and enhanced brain derived neurotrophic factor expression. *Neuropsychopharmacology* **21**, 679–682 (1999).
366. Rossi, C. *et al.* Brain-derived neurotrophic factor (BDNF) is required for the enhancement of hippocampal neurogenesis following environmental enrichment. *Eur. J. Neurosci.* **24**, 1850–1856 (2006).

367. Bamji, S. X. *et al.* The p75 neurotrophin receptor mediates neuronal apoptosis and is essential for naturally occurring sympathetic neuron death. *J. Cell Biol.* **140**, 911–923 (1998).
368. Lang, U. E. *et al.* Association of a functional BDNF polymorphism and anxiety-related personality traits. *Psychopharmacology* **180**, 95–99 (2005).
369. Tsai, S.-J., Cheng, C.-Y., Yu, Y. W.-Y., Chen, T.-J. & Hong, C.-J. Association study of a brain-derived neurotrophic-factor genetic polymorphism and major depressive disorders, symptomatology, and antidepressant response. *American Journal of Medical Genetics Part B: Neuropsychiatric Genetics* **123B**, 19–22 (2003).
370. Aydemir, O., Deveci, A. & Taneli, F. The effect of chronic antidepressant treatment on serum brain-derived neurotrophic factor levels in depressed patients: a preliminary study. *Prog. Neuropsychopharmacol. Biol. Psychiatry* **29**, 261–265 (2005).
371. Brunoni, A. R., Lopes, M. & Fregni, F. A systematic review and meta-analysis of clinical studies on major depression and BDNF levels: implications for the role of neuroplasticity in depression. *Int. J. Neuropsychopharmacol.* **11**, 1169–1180 (2008).
372. Buchmann, A. F. *et al.* BDNF Val 66 Met and 5-HTTLPR genotype moderate the impact of early psychosocial adversity on plasma brain-derived neurotrophic factor and depressive symptoms: a prospective study. *Eur Neuropsychopharmacol* **23**, 902–909 (2013).
373. Gervasoni, N. *et al.* Partial normalization of serum brain-derived neurotrophic factor in remitted patients after a major depressive episode. *Neuropsychobiology* **51**, 234–238 (2005).
374. Karege, F., Vaudan, G., Schwald, M., Perroud, N. & La Harpe, R. Neurotrophin levels in postmortem brains of suicide victims and the effects of antemortem diagnosis and psychotropic drugs. *Brain Res. Mol. Brain Res.* **136**, 29–37 (2005).
375. Sen, S., Duman, R. & Sanacora, G. Serum brain-derived neurotrophic factor, depression, and antidepressant medications: meta-analyses and implications. *Biol. Psychiatry* **64**, 527–532 (2008).
376. Border, R. *et al.* No Support for Historical Candidate Gene or Candidate Gene-by-Interaction Hypotheses for Major Depression Across Multiple Large Samples. *AJP* **176**, 376–387 (2019).
377. Surtees, P. G. *et al.* No association between the BDNF Val66Met polymorphism and mood status in a non-clinical community sample of 7389 older adults. *Journal of Psychiatric Research* **41**, 404–409 (2007).
378. Verhagen, M. *et al.* Meta-analysis of the *BDNF* Val66Met polymorphism in major depressive disorder: effects of gender and ethnicity. *Molecular Psychiatry* **15**, 260–271 (2010).
379. Yu, H. & Chen, Z. The role of BDNF in depression on the basis of its location in the neural circuitry. *Acta Pharmacol. Sin.* **32**, 3–11 (2011).
380. Martinowich, K. & Lu, B. Interaction between BDNF and Serotonin: Role in Mood Disorders. *Neuropsychopharmacology* **33**, 73–83 (2007).
381. Larsen, M. H., Rosenbrock, H., Sams-Dodd, F. & Mikkelsen, J. D. Expression of brain derived neurotrophic factor, activity-regulated cytoskeleton protein mRNA, and enhancement of adult hippocampal neurogenesis in rats after sub-chronic and chronic treatment with the triple monoamine re-uptake inhibitor tesofensine. *Eur. J. Pharmacol.* **555**, 115–121 (2007).
382. Sairanen, M. Brain-Derived Neurotrophic Factor and Antidepressant Drugs Have Different But Coordinated Effects on Neuronal Turnover, Proliferation, and Survival in the Adult Dentate Gyrus. *Journal of Neuroscience* **25**, 1089–1094 (2005).
383. Scharfman, H. *et al.* Increased neurogenesis and the ectopic granule cells after intrahippocampal BDNF infusion in adult rats. *Experimental Neurology* **192**, 348–356 (2005).
384. Luo, L. *et al.* Macranthol promotes hippocampal neuronal proliferation in mice via BDNF-TrkB-PI3K/Akt signaling pathway. *Eur. J. Pharmacol.* **762**, 357–363 (2015).
385. Benmansour, S. *et al.* Influence of brain-derived neurotrophic factor (BDNF) on serotonin neurotransmission in the hippocampus of adult rodents. *Eur. J. Pharmacol.* **587**, 90–98 (2008).
386. Daftary, S. S., Calderon, G. & Rios, M. Essential role of brain-derived neurotrophic factor in the regulation of serotonin transmission in the basolateral amygdala. *Neuroscience* **224**, 125–134 (2012).
387. Deltheil, T. *et al.* Behavioral and serotonergic consequences of decreasing or increasing hippocampus brain-derived neurotrophic factor protein levels in mice. *Neuropharmacology* **55**, 1006–1014 (2008).
388. Deltheil, T. *et al.* Consequences of changes in BDNF levels on serotonin neurotransmission, 5-HT transporter expression and function: studies in adult mice hippocampus. *Pharmacol. Biochem. Behav.* **90**, 174–183 (2008).
389. Balu, D. T. *et al.* Differential regulation of central BDNF protein levels by antidepressant and non-antidepressant drug treatments. *Brain Res.* **1211**, 37–43 (2008).
390. Thomas, K. L. H. & Ellingrod, V. L. Pharmacogenetics of selective serotonin reuptake inhibitors and associated adverse drug reactions. *Pharmacotherapy* **29**, 822–831 (2009).
391. Drago, A., De Ronchi, D. & Serretti, A. Pharmacogenetics of antidepressant response: an update. *Hum. Genomics* **3**, 257–274 (2009).
392. Gass, P. & Riva, M. A. CREB, neurogenesis and depression. *Bioessays* **29**, 957–961 (2007).

393. Nibuya, M., Nestler, E. J. & Duman, R. S. Chronic antidepressant administration increases the expression of cAMP response element binding protein (CREB) in rat hippocampus. *J. Neurosci.* **16**, 2365–2372 (1996).
394. Selye, H. A syndrome produced by diverse nocuous agents. 1936. *J Neuropsychiatry Clin Neurosci* **10**, 230–231 (1998).
395. de Guia, R. M., Rose, A. J. & Herzig, S. Glucocorticoid hormones and energy homeostasis. *Hormone Molecular Biology and Clinical Investigation* **19**, (2014).
396. Maniam, J., Antoniadis, C. & Morris, M. J. Early-Life Stress, HPA Axis Adaptation, and Mechanisms Contributing to Later Health Outcomes. *Front Endocrinol (Lausanne)* **5**, 73 (2014).
397. Clewell, T. Mourning beyond melancholia: Freud's psychoanalysis of loss. *J Am Psychoanal Assoc* **52**, 43–67 (2004).
398. Holmes, T. H. & Rahe, R. H. The Social Readjustment Rating Scale. *J Psychosom Res* **11**, 213–218 (1967).
399. Kendler, K. S., Karkowski, L. M. & Prescott, C. A. Causal relationship between stressful life events and the onset of major depression. *Am J Psychiatry* **156**, 837–841 (1999).
400. Mayer, S. E. *et al.* The psychology of HPA axis activation: Examining subjective emotional distress and control in a phobic fear exposure model. *Psychoneuroendocrinology* **82**, 189–198 (2017).
401. Munck, A., Guyre, P. M. & Holbrook, N. J. Physiological functions of glucocorticoids in stress and their relation to pharmacological actions. *Endocr. Rev.* **5**, 25–44 (1984).
402. Bethin, K. E., Vogt, S. K. & Muglia, L. J. Interleukin-6 is an essential, corticotropin-releasing hormone-independent stimulator of the adrenal axis during immune system activation. *Proc Natl Acad Sci U S A* **97**, 9317–9322 (2000).
403. Bernardini, R. *et al.* Interactions between tumor necrosis factor-alpha, hypothalamic corticotropin-releasing hormone, and adrenocorticotropin secretion in the rat. *Endocrinology* **126**, 2876–2881 (1990).
404. Aguilar, M. T. *et al.* Study of the diagnostic value of the dexamethasone suppression test in endogenous depression. *Journal of Affective Disorders* **6**, 33–42 (1984).
405. Carroll, B. J. The Dexamethasone Suppression Test for Melancholia. *The British Journal of Psychiatry* **140**, 292–304 (1982).
406. Stetler, C. & Miller, G. E. Depression and Hypothalamic-Pituitary-Adrenal Activation: A Quantitative Summary of Four Decades of Research. *Psychosomatic Medicine* **73**, 114 (2011).
407. Rush, A. J. *et al.* Dexamethasone response, thyrotropin-releasing hormone stimulation, rapid eye movement latency, and subtypes of depression. *Biological Psychiatry* **41**, 915–928 (1997).
408. Reimold, M. *et al.* Central serotonin transporter levels are associated with stress hormone response and anxiety. *Psychopharmacology* **213**, 563–572 (2011).
409. Han, F. *et al.* Changes in the expression of corticotrophin-releasing hormone, mineralocorticoid receptor and glucocorticoid receptor mRNAs in the hypothalamic paraventricular nucleus induced by fornix transection and adrenalectomy. *J. Neuroendocrinol.* **19**, 229–238 (2007).
410. Gomez-Sanchez, E. & Gomez-Sanchez, C. E. The Multifaceted Mineralocorticoid Receptor. *Compr Physiol* **4**, 965–994 (2014).
411. De Kloet, E. R. Hormones and the stressed brain. *Ann. N. Y. Acad. Sci.* **1018**, 1–15 (2004).
412. Gesing, A. *et al.* Psychological stress increases hippocampal mineralocorticoid receptor levels: involvement of corticotropin-releasing hormone. *J. Neurosci.* **21**, 4822–4829 (2001).
413. de Kloet, E. R. *et al.* Stress and Depression: a Crucial Role of the Mineralocorticoid Receptor. *J. Neuroendocrinol.* **28**, (2016).
414. Cole, M. A. *et al.* Selective blockade of the mineralocorticoid receptor impairs hypothalamic-pituitary-adrenal axis expression of habituation. *J. Neuroendocrinol.* **12**, 1034–1042 (2000).
415. Pace, T. W. W. & Spencer, R. L. Disruption of mineralocorticoid receptor function increases corticosterone responding to a mild, but not moderate, psychological stressor. *Am. J. Physiol. Endocrinol. Metab.* **288**, E1082-1088 (2005).
416. McEWEN, B. S. Corticosteroids and Hippocampal Plasticity. *Annals of the New York Academy of Sciences* **746**, 134–142 (1994).
417. Bamberger, C. M., Bamberger, A.-M., Wald, M., Chrousos, G. P. & Schulte, H. M. Inhibition of mineralocorticoid activity by the β-isoform of the human glucocorticoid receptor. *The Journal of Steroid Biochemistry and Molecular Biology* **60**, 43–50 (1997).
418. Tytherleigh, M. Y., Vedhara, K. & Lightman, S. L. Mineralocorticoid and glucocorticoid receptors and their differential effects on memory performance in people with Addison's disease. *Psychoneuroendocrinology* **29**, 712–723 (2004).
419. Brinks, V., H. van der Mark, M., de Kloet, E. R. & S. Oitzl, M. Differential MR/GR Activation in Mice Results in Emotional States Beneficial or Impairing for Cognition. *Neural Plast* **2007**, (2007).
420. Young, E. A., Lopez, J. F., Murphy-Weinberg, V., Watson, S. J. & Akil, H. Mineralocorticoid Receptor Function in Major Depression. *Arch Gen Psychiatry* **60**, 24–28 (2003).
421. DeRijk, R. H., de Kloet, E. R., Zitman, F. G. & van Leeuwen, N. Mineralocorticoid receptor gene variants as determinants of HPA axis regulation and behavior. *Endocr Dev* **20**, 137–148 (2011).
422. Qi, X.-R. *et al.* Aberrant stress hormone receptor balance in the human prefrontal cortex and hypothalamic paraventricular nucleus of depressed patients. *Psychoneuroendocrinology* **38**, 863–870 (2013).

423. Biomarkers Definitions Working Group. Biomarkers and surrogate endpoints: preferred definitions and conceptual framework. *Clin. Pharmacol. Ther.* **69**, 89–95 (2001).
424. Williams, J. B. Standardizing the Hamilton Depression Rating Scale: past, present, and future. *Eur Arch Psychiatry Clin Neurosci* **251 Suppl 2**, II6-12 (2001).
425. Montgomery, S. A. & Asberg, M. A new depression scale designed to be sensitive to change. *Br J Psychiatry* **134**, 382–389 (1979).
426. Spitzer, R. L., Kroenke, K. & Williams, J. B. Validation and utility of a self-report version of PRIME-MD: the PHQ primary care study. Primary Care Evaluation of Mental Disorders. Patient Health Questionnaire. *JAMA* **282**, 1737–1744 (1999).
427. Gaynes, B. N. *et al.* What did STAR*D teach us? Results from a large-scale, practical, clinical trial for patients with depression. *Psychiatr Serv* **60**, 1439–1445 (2009).
428. Strawbridge, R., Young, A. H. & Cleare, A. J. Biomarkers for depression: recent insights, current challenges and future prospects. *Neuropsychiatr Dis Treat* **13**, 1245–1262 (2017).
429. Jeon, S. & Kim, Y.-K. Molecular Neurobiology and Promising New Treatment in Depression. *International Journal of Molecular Sciences* **17**, 381 (2016).
430. Haapakoski, R., Mathieu, J., Ebmeier, K. P., Alenius, H. & Kivimäki, M. Cumulative meta-analysis of interleukins 6 and 1β, tumour necrosis factor α and C-reactive protein in patients with major depressive disorder. *Brain Behav. Immun.* **49**, 206–215 (2015).
431. Howren, M. B., Lamkin, D. M. & Suls, J. Associations of depression with C-reactive protein, IL-1, and IL-6: a meta-analysis. *Psychosom Med* **71**, 171–186 (2009).
432. Liu, Y., Ho, R. C.-M. & Mak, A. Interleukin (IL)-6, tumour necrosis factor alpha (TNF-α) and soluble interleukin-2 receptors (sIL-2R) are elevated in patients with major depressive disorder: a meta-analysis and meta-regression. *J Affect Disord* **139**, 230–239 (2012).
433. Farooq, R. K., Asghar, K., Kanwal, S. & Zulqernain, A. Role of inflammatory cytokines in depression: Focus on interleukin-1β. *Biomed Rep* **6**, 15–20 (2017).
434. Köhler, C. A. *et al.* Peripheral cytokine and chemokine alterations in depression: a meta-analysis of 82 studies. *Acta Psychiatr Scand* **135**, 373–387 (2017).
435. Wachholz, S. *et al.* Interleukin-4 is a participant in the regulation of depressive-like behavior. *Behav. Brain Res.* **326**, 165–172 (2017).
436. Laumet, G. *et al.* Resolution of inflammation-induced depression requires T lymphocytes and endogenous brain interleukin-10 signaling. *Neuropsychopharmacology* **43**, 2597–2605 (2018).
437. Gazal, M. *et al.* Association of interleukin-10 levels with age of onset and duration of illness in patients with major depressive disorder. *Braz J Psychiatry* **37**, 296–302 (2015).
438. Dahl, J. *et al.* The plasma levels of various cytokines are increased during ongoing depression and are reduced to normal levels after recovery. *Psychoneuroendocrinology* **45**, 77–86 (2014).
439. Eyre, H. A. *et al.* A meta-analysis of chemokines in major depression. *Prog. Neuropsychopharmacol. Biol. Psychiatry* **68**, 1–8 (2016).
440. Simon, N. M. *et al.* A detailed examination of cytokine abnormalities in Major Depressive Disorder. *Eur Neuropsychopharmacol* **18**, 230–233 (2008).
441. Stelzhammer, V. *et al.* Electroconvulsive therapy exerts mainly acute molecular changes in serum of major depressive disorder patients. *Eur Neuropsychopharmacol* **23**, 1199–1207 (2013).
442. Liu, Y., Ho, R. C.-M. & Mak, A. The role of interleukin (IL)-17 in anxiety and depression of patients with rheumatoid arthritis. *Int J Rheum Dis* **15**, 183–187 (2012).
443. Ogłodek, E. A. & Just, M. J. The association between inflammatory markers (iNOS, HO-1, IL-33, MIP-1β) and depression with and without posttraumatic stress disorder. *Pharmacol Rep* **70**, 1065–1072 (2018).
444. Milenkovic, V. M. *et al.* Macrophage-Derived Chemokine: A Putative Marker of Pharmacological Therapy Response in Major Depression? *Neuroimmunomodulation* **24**, 106–112 (2017).
445. Janelidze, S. *et al.* Altered chemokine levels in the cerebrospinal fluid and plasma of suicide attempters. *Psychoneuroendocrinology* **38**, 853–862 (2013).
446. Dimopoulos, N. *et al.* Elevation of plasma concentration of adhesion molecules in late-life depression. *Int J Geriatr Psychiatry* **21**, 965–971 (2006).
447. Wong, M.-L., Dong, C., Maestre-Mesa, J. & Licinio, J. Polymorphisms in inflammation-related genes are associated with susceptibility to major depression and antidepressant response. *Mol. Psychiatry* **13**, 800–812 (2008).
448. Brunoni, A. R., Baeken, C., Machado-Vieira, R., Gattaz, W. F. & Vanderhasselt, M.-A. BDNF blood levels after electroconvulsive therapy in patients with mood disorders: a systematic review and meta-analysis. *World J. Biol. Psychiatry* **15**, 411–418 (2014).
449. Molendijk, M. L. *et al.* Serum BDNF concentrations as peripheral manifestations of depression: evidence from a systematic review and meta-analyses on 179 associations (N=9484). *Mol. Psychiatry* **19**, 791–800 (2014).

450. Bocchio-Chiavetto, L. *et al.* Serum and plasma BDNF levels in major depression: a replication study and meta-analyses. *World J. Biol. Psychiatry* **11**, 763–773 (2010).
451. Pisoni, A. *et al.* Growth Factor Proteins and Treatment-Resistant Depression: A Place on the Path to Precision. *Front Psychiatry* **9**, 386 (2018).
452. Zhou, L. *et al.* Upregulation of blood proBDNF and its receptors in major depression. *J Affect Disord* **150**, 776–784 (2013).
453. Qiao, H., An, S.-C., Xu, C. & Ma, X.-M. Role of proBDNF and BDNF in dendritic spine plasticity and depressive-like behaviors induced by an animal model of depression. *Brain Res.* **1663**, 29–37 (2017).
454. Warner-Schmidt, J. L. & Duman, R. S. VEGF as a potential target for therapeutic intervention in depression. *Curr Opin Pharmacol* **8**, 14–19 (2008).
455. Carvalho, A. F. *et al.* Peripheral vascular endothelial growth factor as a novel depression biomarker: A meta-analysis. *Psychoneuroendocrinology* **62**, 18–26 (2015).
456. Lee, B.-H. & Kim, Y.-K. Increased plasma VEGF levels in major depressive or manic episodes in patients with mood disorders. *J Affect Disord* **136**, 181–184 (2012).
457. Tseng, P.-T., Cheng, Y.-S., Chen, Y.-W., Wu, C.-K. & Lin, P.-Y. Increased levels of vascular endothelial growth factor in patients with major depressive disorder: A meta-analysis. *Eur Neuropsychopharmacol* **25**, 1622–1630 (2015).
458. Chen, Y.-W. *et al.* Significantly lower nerve growth factor levels in patients with major depressive disorder than in healthy subjects: a meta-analysis and systematic review. *Neuropsychiatr Dis Treat* **11**, 925–933 (2015).
459. Ogłodek, E. A., Just, M. J., Szromek, A. R. & Araszkiewicz, A. Melatonin and neurotrophins NT-3, BDNF, NGF in patients with varying levels of depression severity. *Pharmacol Rep* **68**, 945–951 (2016).
460. Lin, P.-Y. & Tseng, P.-T. Decreased glial cell line-derived neurotrophic factor levels in patients with depression: a meta-analytic study. *J Psychiatr Res* **63**, 20–27 (2015).
461. Szczęsny, E. *et al.* Possible contribution of IGF-1 to depressive disorder. *Pharmacol Rep* **65**, 1622–1631 (2013).
462. Tu, K.-Y. *et al.* Significantly Higher Peripheral Insulin-Like Growth Factor-1 Levels in Patients With Major Depressive Disorder or Bipolar Disorder Than in Healthy Controls: A Meta-Analysis and Review Under Guideline of PRISMA. *Medicine (Baltimore)* **95**, e2411 (2016).
463. Wu, C.-K., Tseng, P.-T., Chen, Y.-W., Tu, K.-Y. & Lin, P.-Y. Significantly higher peripheral fibroblast growth factor-2 levels in patients with major depressive disorder: A preliminary meta-analysis under MOOSE guidelines. *Medicine (Baltimore)* **95**, e4563 (2016).
464. He, S. *et al.* Decreased serum fibroblast growth factor - 2 levels in pre- and post-treatment patients with major depressive disorder. *Neurosci. Lett.* **579**, 168–172 (2014).
465. Coplan, J. D., Gopinath, S., Abdallah, C. G. & Berry, B. R. A neurobiological hypothesis of treatment-resistant depression - mechanisms for selective serotonin reuptake inhibitor non-efficacy. *Front Behav Neurosci* **8**, 189 (2014).
466. Nutt, D. J. The role of dopamine and norepinephrine in depression and antidepressant treatment. *J Clin Psychiatry* **67 Suppl 6**, 3–8 (2006).
467. Belujon, P. & Grace, A. A. Dopamine System Dysregulation in Major Depressive Disorders. *Int. J. Neuropsychopharmacol.* **20**, 1036–1046 (2017).
468. Felger, J. C. The Role of Dopamine in Inflammation-Associated Depression: Mechanisms and Therapeutic Implications. *Curr Top Behav Neurosci* **31**, 199–219 (2017).
469. Salamone, J. D. *et al.* The pharmacology of effort-related choice behavior: Dopamine, depression, and individual differences. *Behav. Processes* **127**, 3–17 (2016).
470. Möhler, H. The GABA system in anxiety and depression and its therapeutic potential. *Neuropharmacology* **62**, 42–53 (2012).
471. Pierscionek, T., Adekunte, O., Watson, S., Ferrier, I. N. & Alabi, A. Role of corticosteroids in the antidepressant response. *ChronoPhysiology and Therapy* 87 (2014) doi:10.2147/CPT.S67272.
472. Juruena, M. F., Bocharova, M., Agustini, B. & Young, A. H. Atypical depression and non-atypical depression: Is HPA axis function a biomarker? A systematic review. *J Affect Disord* **233**, 45–67 (2018).
473. Ising, M. *et al.* FKBP5 Gene Expression Predicts Antidepressant Treatment Outcome in Depression. *Int J Mol Sci* **20**, (2019).
474. Choi, K. W. *et al.* Increased adrenocorticotropic hormone (ACTH) levels predict severity of depression after six months of follow-up in outpatients with major depressive disorder. *Psychiatry Res* **270**, 246–252 (2018).
475. Bao, A.-M. & Swaab, D. F. Corticotropin-releasing hormone and arginine vasopressin in depression focus on the human postmortem hypothalamus. *Vitam. Horm.* **82**, 339–365 (2010).
476. Peixoto, C. *et al.* Dehydroepiandrosterone (DHEA) for Depression: A Systematic Review and Meta-Analysis. *CNS Neurol Disord Drug Targets* **17**, 706–711 (2018).
477. Holsboer, F. & Ising, M. Stress hormone regulation: biological role and translation into therapy. *Annu Rev Psychol* **61**, 81–109, C1-11 (2010).
478. Buttenschøn, H. N. *et al.* Association analyses of depression and genes in the hypothalamus-pituitary-adrenal axis. *Acta Neuropsychiatr* **29**, 59–64 (2017).

479. Hage, M. P. & Azar, S. T. The Link between Thyroid Function and Depression. *J Thyroid Res* **2012**, 590648 (2012).
480. Häfner, S. *et al.* Sleep disturbances and depressed mood: a harmful combination associated with increased leptin levels in women with normal weight. *Biol Psychol* **89**, 163–169 (2012).
481. Lu, X.-Y. The leptin hypothesis of depression: a potential link between mood disorders and obesity? *Curr Opin Pharmacol* **7**, 648–652 (2007).
482. Kan, C. *et al.* A systematic review and meta-analysis of the association between depression and insulin resistance. *Diabetes Care* **36**, 480–489 (2013).
483. Wittekind, D. A. & Kluge, M. Ghrelin in psychiatric disorders - A review. *Psychoneuroendocrinology* **52**, 176–194 (2015).
484. Inoue, M. *et al.* Serum Levels of Albumin-β-Amyloid Complex in Patients with Depression. *Am J Geriatr Psychiatry* **24**, 764–772 (2016).
485. Lustman, P. J. *et al.* Depression and poor glycemic control: a meta-analytic review of the literature. *Diabetes Care* **23**, 934–942 (2000).
486. Liu, X. *et al.* Plasma lipidomics reveals potential lipid markers of major depressive disorder. *Anal Bioanal Chem* **408**, 6497–6507 (2016).
487. Wysokiński, A., Strzelecki, D. & Kłoszewska, I. Levels of triglycerides, cholesterol, LDL, HDL and glucose in patients with schizophrenia, unipolar depression and bipolar disorder. *Diabetes Metab Syndr* **9**, 168–176 (2015).
488. Qiao, H. *et al.* Dendritic Spines in Depression: What We Learned from Animal Models. *Neural Plast.* **2016**, 8056370 (2016).
489. Brand, S. J., Möller, M. & Harvey, B. H. A Review of Biomarkers in Mood and Psychotic Disorders: A Dissection of Clinical vs. Preclinical Correlates. *Curr Neuropharmacol* **13**, 324–368 (2015).
490. Sheline, Y. I. Neuroimaging studies of mood disorder effects on the brain. *Biol. Psychiatry* **54**, 338–352 (2003).
491. Wise, T., Cleare, A. J., Herane, A., Young, A. H. & Arnone, D. Diagnostic and therapeutic utility of neuroimaging in depression: an overview. *Neuropsychiatr Dis Treat* **10**, 1509–1522 (2014).
492. Fu, C. H. Y., Steiner, H. & Costafreda, S. G. Predictive neural biomarkers of clinical response in depression: a meta-analysis of functional and structural neuroimaging studies of pharmacological and psychological therapies. *Neurobiol. Dis.* **52**, 75–83 (2013).
493. Colla, M. *et al.* Hippocampal volume reduction and HPA-system activity in major depression. *Journal of Psychiatric Research* **41**, 553–560 (2007).
494. Major Depressive Disorder Working Group of the Psychiatric GWAS Consortium *et al.* A mega-analysis of genome-wide association studies for major depressive disorder. *Mol. Psychiatry* **18**, 497–511 (2013).
495. Sullivan, P. F. & Geschwind, D. H. Defining the Genetic, Genomic, Cellular, and Diagnostic Architectures of Psychiatric Disorders. *Cell* **177**, 162–183 (2019).
496. Needham, B. L. *et al.* Depression, anxiety and telomere length in young adults: evidence from the National Health and Nutrition Examination Survey. *Mol. Psychiatry* **20**, 520–528 (2015).
497. Criado-Marrero, M. *et al.* Hsp90 and FKBP51: complex regulators of psychiatric diseases. *Philos. Trans. R. Soc. Lond., B, Biol. Sci.* **373**, (2018).
498. Dunn, E. C. *et al.* Genetic determinants of depression: recent findings and future directions. *Harv Rev Psychiatry* **23**, 1–18 (2015).
499. Martinowich, K., Manji, H. & Lu, B. New insights into BDNF function in depression and anxiety. *Nat. Neurosci.* **10**, 1089–1093 (2007).
500. Hashimoto, K. Brain-derived neurotrophic factor as a biomarker for mood disorders: an historical overview and future directions. *Psychiatry Clin. Neurosci.* **64**, 341–357 (2010).
501. Jabbi, M. *et al.* Convergent genetic modulation of the endocrine stress response involves polymorphic variations of 5-HTT, COMT and MAOA. *Mol. Psychiatry* **12**, 483–490 (2007).
502. Deacon, R. M. Assessing nest building in mice. *Nat. Protocols* **1**, 1117–1119 (2006).
503. Deacon, R. Assessing Burrowing, Nest Construction, and Hoarding in Mice. *Journal of Visualized Experiments* (2012) doi:10.3791/2607.
504. Latham, N. & Mason, G. From house mouse to mouse house: the behavioural biology of free-living Mus musculus and its implications in the laboratory. *Applied Animal Behaviour Science* **86**, 261–289 (2004).
505. Jirkof, P. Burrowing and nest building behavior as indicators of well-being in mice. *J. Neurosci. Methods* **234**, 139–146 (2014).
506. Klempin, F. *et al.* Depletion of angiotensin-converting enzyme 2 reduces brain serotonin and impairs the running-induced neurogenic response. *Cell. Mol. Life Sci.* **75**, 3625–3634 (2018).
507. Brede, M. & Hein, L. Knockout Models of the Renin-Angiotensin System. in *Angiotensin Vol. I* 207–227 (Springer, Berlin, Heidelberg, 2004). doi:10.1007/978-3-642-18495-6_9.
508. Crackower, M. A. *et al.* Angiotensin-converting enzyme 2 is an essential regulator of heart function. *Nature* **417**, 822–828 (2002).
509. Weber, T. *et al.* Genetic fate mapping of type-1 stem cell-dependent increase in newborn hippocampal neurons after electroconvulsive seizures. *Hippocampus* **23**, 1321–1330 (2013).

510. Kronenberg, G. *et al.* Brain serotonin critically contributes to the biological effects of electroconvulsive seizures. *Eur Arch Psychiatry Clin Neurosci* (2018) doi:10.1007/s00406-018-0924-0.
511. Gong, S. *et al.* Dynamics and Correlation of Serum Cortisol and Corticosterone under Different Physiological or Stressful Conditions in Mice. *PLoS One* **10**, (2015).
512. Hellweg, R., Zueger, M., Fink, K., Hörtnagl, H. & Gass, P. Olfactory bulbectomy in mice leads to increased BDNF levels and decreased serotonin turnover in depression-related brain areas. *Neurobiol. Dis.* **25**, 1–7 (2007).
513. Hellweg, R., Arnim, C. A. F. von, Büchner, M., Huber, R. & Riepe, M. W. Neuroprotection and neuronal dysfunction upon repetitive inhibition of oxidative phosphorylation. *Experimental Neurology* **183**, 346–354 (2003).
514. Livak, K. J. & Schmittgen, T. D. Analysis of relative gene expression data using real-time quantitative PCR and the 2(-Delta Delta C(T)) Method. *Methods* **25**, 402–408 (2001).
515. Pellow, S., Chopin, P., File, S. E. & Briley, M. Validation of open:closed arm entries in an elevated plus-maze as a measure of anxiety in the rat. *J. Neurosci. Methods* **14**, 149–167 (1985).
516. Fuss, J. *et al.* Deletion of Running-Induced Hippocampal Neurogenesis by Irradiation Prevents Development of an Anxious Phenotype in Mice. *PLOS ONE* **5**, e12769 (2010).
517. Richter, S. H. *et al.* Effect of Population Heterogenization on the Reproducibility of Mouse Behavior: A Multi-Laboratory Study. *PLOS ONE* **6**, e16461 (2011).
518. Zueger, M. *et al.* Olfactory bulbectomy in mice induces alterations in exploratory behavior. *Neurosci. Lett.* **374**, 142–146 (2005).
519. Chourbaji, S., Zacher, C., Sanchis-Segura, C., Spanagel, R. & Gass, P. Social and structural housing conditions influence the development of a depressive-like phenotype in the learned helplessness paradigm in male mice. *Behav. Brain Res.* **164**, 100–106 (2005).
520. Castagné, V., Moser, P., Roux, S. & Porsolt, R. D. Rodent Models of Depression: Forced Swim and Tail Suspension Behavioral Despair Tests in Rats and Mice. *Current Protocols in Pharmacology* **49**, 5.8.1-5.8.14 (2010).
521. Byers, S. L., Wiles, M. V., Dunn, S. L. & Taft, R. A. Mouse Estrous Cycle Identification Tool and Images. *PLOS ONE* **7**, e35538 (2012).
522. Ghasemi, A. & Zahediasl, S. Normality Tests for Statistical Analysis: A Guide for Non-Statisticians. *Int J Endocrinol Metab* **10**, 486–489 (2012).
523. Kempermann, G., Jessberger, S., Steiner, B. & Kronenberg, G. Milestones of neuronal development in the adult hippocampus. *Trends Neurosci.* **27**, 447–452 (2004).
524. Allen Brain Atlas 2018. http://connectivity.brain-map.org/ (2018).
525. Franklin, K. B. J. & Paxinos, G. *The mouse brain in stereotaxic coordinates*. (Elsevier, AP, 2008).
526. Goel, N., Workman, J. L., Lee, T. T., Innala, L. & Viau, V. Sex differences in the HPA axis. *Compr Physiol* **4**, 1121–1155 (2014).
527. Oyola, M. G. & Handa, R. J. Hypothalamic-pituitary-adrenal and hypothalamic-pituitary-gonadal axes: sex differences in regulation of stress responsivity. *Stress* **20**, 476–494 (2017).
528. Goel, N., Plyler, K. S., Daniels, D. & Bale, T. L. Androgenic Influence on Serotonergic Activation of the HPA Stress Axis. *Endocrinology* **152**, 2001–2010 (2011).
529. Lowry, P. 60 YEARS OF POMC: Purification and biological characterisation of melanotrophins and corticotrophins. *J. Mol. Endocrinol.* **56**, T1–T12 (2016).
530. Haim, S., Shakhar, G., Rossene, E., Taylor, A. N. & Ben-Eliyahu, S. Serum levels of sex hormones and corticosterone throughout 4- and 5-day estrous cycles in Fischer 344 rats and their simulation in ovariectomized females. *J Endocrinol Invest* **26**, 1013–1022 (2003).
531. Pariante, C. M. & Lightman, S. L. The HPA axis in major depression: classical theories and new developments. *Trends in Neurosciences* **31**, 464–468 (2008).
532. Murphy, D. L. *et al.* Experimental gene interaction studies with SERT mutant mice as models for human polygenic and epistatic traits and disorders. *Genes, Brain and Behavior* **2**, 350–364 (2003).
533. Kim, J.-I. *et al.* Sexual activity counteracts the suppressive effects of chronic stress on adult hippocampal neurogenesis and recognition memory. *Brain Research* **1538**, 26–40 (2013).
534. Song, N.-N. *et al.* Reducing central serotonin in adulthood promotes hippocampal neurogenesis. *Scientific Reports* **6**, 20338 (2016).
535. Mombereau, C., Gur, T. L., Onksen, J. & Blendy, J. A. Differential effects of acute and repeated citalopram in mouse models of anxiety and depression. *Int J Neuropsychopharmacol* **13**, 321–334 (2010).
536. Mekada, K. *et al.* Genetic differences among C57BL/6 substrains. *Experimental Animals* **58**, 141–149 (2009).
537. Kole, M. H. P., Swan, L. & Fuchs, E. The antidepressant tianeptine persistently modulates glutamate receptor currents of the hippocampal CA3 commissural associational synapse in chronically stressed rats. *European Journal of Neuroscience* **16**, 807–816 (2002).
538. Fuchs, E. *et al.* Synaptic plasticity and tianeptine: structural regulation1To be presented at ECNP Barcelona, 5-9 October 2002, during the symposium "A new pharmacology of depression: the concept of synaptic plasticity." *European Psychiatry* **17**, 311–317 (2002).

539. Wang, L.-P., Kempermann, G. & Kettenmann, H. A subpopulation of precursor cells in the mouse dentate gyrus receives synaptic GABAergic input. *Molecular and Cellular Neuroscience* **29**, 181–189 (2005).
540. Fritze, S., Spanagel, R. & Noori, H. R. Adaptive dynamics of the 5-HT systems following chronic administration of selective serotonin reuptake inhibitors: a meta-analysis. *J. Neurochem.* **142**, 747–755 (2017).
541. Piñeyro, G., Deveault, L., de Montigny, C. & Blier, P. Effect of prolonged administration of tianeptine on 5-HT neurotransmission: an electrophysiological study in the rat hippocampus and dorsal raphe. *Naunyn Schmiedebergs Arch. Pharmacol.* **351**, 119–125 (1995).
542. K, F. O. Kinetics of citalopram in test animals; drug exposure in safety studies. *Prog Neuropsychopharmacol Biol Psychiatry* **6**, 297–309 (1982).
543. Samuels, B. A. *et al.* The Behavioral Effects of the Antidepressant Tianeptine Require the Mu-Opioid Receptor. *Neuropsychopharmacology* **42**, 2052–2063 (2017).
544. Grahn, R. E., Maswood, S., McQueen, M. B., Watkins, L. R. & Maier, S. F. Opioid-dependent effects of inescapable shock on escape behavior and conditioned fear responding are mediated by the dorsal raphe nucleus. *Behavioural Brain Research* **99**, 153–167 (1999).
545. Kalyuzhny, A. E., Arvidsson, U., Wu, W. & Wessendorf, M. W. μ-Opioid and δ-Opioid Receptors Are Expressed in Brainstem Antinociceptive Circuits: Studies Using Immunocytochemistry and Retrograde Tract-Tracing. *J. Neurosci.* **16**, 6490–6503 (1996).
546. Tao, R. & Auerbach, S. B. Involvement of the dorsal raphe but not median raphe nucleus in morphine-induced increases in serotonin release in the rat forebrain. *Neuroscience* **68**, 553–561 (1995).
547. Tao, R. & Auerbach, S. B. Increased Extracellular Serotonin in Rat Brain After Systemic or Intraraphe Administration of Morphine. *Journal of Neurochemistry* **63**, 517–524 (1994).
548. Tao, R. & Auerbach, S. B. Anesthetics block morphine-induced increases in serotonin release in rat CNS. *Synapse* **18**, 307–314 (1994).
549. Tao, R. & Auerbach, S. B. Opioid receptor subtypes differentially modulate serotonin efflux in the rat central nervous system. *J. Pharmacol. Exp. Ther.* **303**, 549–556 (2002).
550. Gassaway, M. M., Rives, M.-L., Kruegel, A. C., Javitch, J. A. & Sames, D. The atypical antidepressant and neurorestorative agent tianeptine is a μ-opioid receptor agonist. *Transl Psychiatry* **4**, e411 (2014).
551. Cominski, T. P., Ansonoff, M. A., Turchin, C. E. & Pintar, J. E. Loss of the mu opioid receptor induces strain-specific alterations in hippocampal neurogenesis and spatial learning. *Neuroscience* **278**, 11–19 (2014).
552. Sánchez, C. The pharmacology of citalopram enantiomers: the antagonism by R-citalopram on the effect of S-citalopram. *Basic Clin. Pharmacol. Toxicol.* **99**, 91–95 (2006).
553. Ruhé, H. G., Mason, N. S. & Schene, A. H. Mood is indirectly related to serotonin, norepinephrine and dopamine levels in humans: a meta-analysis of monoamine depletion studies. *Mol. Psychiatry* **12**, 331–359 (2007).
554. Stewart, M. G. *et al.* Stress suppresses and learning induces plasticity in CA3 of rat hippocampus: a three-dimensional ultrastructural study of thorny excrescences and their postsynaptic densities. *Neuroscience* **131**, 43–54 (2005).
555. Murray, F., Smith, D. W. & Hutson, P. H. Chronic low dose corticosterone exposure decreased hippocampal cell proliferation, volume and induced anxiety and depression like behaviours in mice. *Eur. J. Pharmacol.* **583**, 115–127 (2008).
556. Lee, T., Jarome, T., Li, S.-J., Kim, J. J. & Helmstetter, F. J. Chronic stress selectively reduces hippocampal volume in rats: a longitudinal magnetic resonance imaging study. *Neuroreport* **20**, 1554–1558 (2009).
557. Liu, W. *et al.* Tianeptine reverses stress-induced asymmetrical hippocampal volume and N-acetylaspartate loss in rats: an in vivo study. *Psychiatry Res* **194**, 385–392 (2011).
558. Luo, Y. *et al.* Dynamic study of the hippocampal volume by structural MRI in a rat model of depression. *Neurol. Sci.* **35**, 1777–1783 (2014).
559. Asan, E., Steinke, M. & Lesch, K.-P. Serotonergic innervation of the amygdala: targets, receptors, and implications for stress and anxiety. *Histochem Cell Biol* **139**, 785–813 (2013).
560. Puig, M. V. & Gulledge, A. T. Serotonin and Prefrontal Cortex Function: Neurons, Networks, and Circuits. *Mol Neurobiol* **44**, 449–464 (2011).
561. Roozendaal, B. *et al.* Memory retrieval impairment induced by hippocampal CA3 lesions is blocked by adrenocortical suppression. *Nature Neuroscience* **4**, 1169 (2001).
562. Jankord, R. & Herman, J. P. Limbic regulation of hypothalamo-pituitary-adrenocortical function during acute and chronic stress. *Ann. N. Y. Acad. Sci.* **1148**, 64–73 (2008).
563. Gould, E., Cameron, H. A., Daniels, D. C., Woolley, C. S. & McEwen, B. S. Adrenal hormones suppress cell division in the adult rat dentate gyrus. *J. Neurosci.* **12**, 3642–3650 (1992).
564. McEwen, B. S. Stress and hippocampal plasticity. *Annu. Rev. Neurosci.* **22**, 105–122 (1999).
565. Gould, E. & Tanapat, P. Stress and hippocampal neurogenesis. *Biol. Psychiatry* **46**, 1472–1479 (1999).
566. Vincent, M. Y., Donner, N. C., Smith, D. G., Lowry, C. A. & Jacobson, L. Dorsal raphé nucleus glucocorticoid receptors inhibit tph2 gene expression in male C57BL/6J mice. *Neurosci. Lett.* **665**, 48–53 (2018).

567. Petrik, D., Lagace, D. C. & Eisch, A. J. The neurogenesis hypothesis of affective and anxiety disorders: are we mistaking the scaffolding for the building? *Neuropharmacology* **62**, 21–34 (2012).
568. Abbott, C. C. *et al.* Hippocampal structural and functional changes associated with electroconvulsive therapy response. *Transl Psychiatry* **4**, e483 (2014).
569. Kronmüller, K.-T. *et al.* Hippocampal volume in first episode and recurrent depression. *Psychiatry Research: Neuroimaging* **174**, 62–66 (2009).
570. Boldrini, M. *et al.* Human Hippocampal Neurogenesis Persists throughout Aging. *Cell Stem Cell* **22**, 589-599.e5 (2018).
571. Deisseroth, K. Optogenetics and Psychiatry: Applications, Challenges, and Opportunities. *Biological Psychiatry* **71**, 1030–1032 (2012).
572. Svenningsson, P. *et al.* Involvement of AMPA receptor phosphorylation in antidepressant actions with special reference to tianeptine: AMPA receptor phosphorylation and tianeptine. *European Journal of Neuroscience* **26**, 3509–3517 (2007).
573. Invernizzi, R., Pozzi, L., Garattini, S. & Samanin, R. Tianeptine increases the extracellular concentrations of dopamine in the nucleus accumbens by a serotonin-independent mechanism. *Neuropharmacology* **31**, 221–227 (1992).
574. Qi, H. *et al.* Antidepressants reverse the attenuation of the neurotrophic MEK/MAPK cascade in frontal cortex by elevated platform stress; reversal of effects on LTP is associated with GluA1 phosphorylation. *Neuropharmacology* **56**, 37–46 (2009).
575. Mattson, M. P. Glutamate and neurotrophic factors in neuronal plasticity and disease. *Ann. N. Y. Acad. Sci.* **1144**, 97–112 (2008).
576. Porcher, C. *et al.* Positive feedback regulation between gamma-aminobutyric acid type A (GABA(A)) receptor signaling and brain-derived neurotrophic factor (BDNF) release in developing neurons. *J. Biol. Chem.* **286**, 21667–21677 (2011).
577. Jansson, L. C. *et al.* Brain-derived neurotrophic factor increases the motility of a particular N-methyl-D-aspartate /GABA-responsive subset of neural progenitor cells. *Neuroscience* **224**, 223–234 (2012).
578. García-García, A. L. *et al.* Regulation of serotonin (5-HT) function by a VGLUT1 dependent glutamate pathway. *Neuropharmacology* **70**, 190–199 (2013).
579. Fuchs, E. & Flügge, G. Adult Neuroplasticity: More Than 40 Years of Research. *Neural Plast* **2014**, (2014).
580. O'Connor, S. & Agius, M. A systematic review of structural and functional MRI differences between psychotic and nonpsychotic depression. *Psychiatr Danub* **27 Suppl 1**, S235-239 (2015).
581. Rajkowska, G. Cell pathology in mood disorders. *Semin Clin Neuropsychiatry* **7**, 281–292 (2002).
582. Jacobsen, J. P. R. & Mørk, A. The effect of escitalopram, desipramine, electroconvulsive seizures and lithium on brain-derived neurotrophic factor mRNA and protein expression in the rat brain and the correlation to 5-HT and 5-HIAA levels. *Brain Res.* **1024**, 183–192 (2004).
583. Gass, P. *et al.* Genetic disruption of mineralocorticoid receptor leads to impaired neurogenesis and granule cell degeneration in the hippocampus of adult mice. *EMBO Rep* **1**, 447–451 (2000).
584. Castrén, E. & Rantamäki, T. The role of BDNF and its receptors in depression and antidepressant drug action: Reactivation of developmental plasticity. *Dev Neurobiol* **70**, 289–297 (2010).
585. Larsen, M. H., Mikkelsen, J. D., Hay-Schmidt, A. & Sandi, C. Regulation of brain-derived neurotrophic factor (BDNF) in the chronic unpredictable stress rat model and the effects of chronic antidepressant treatment. *J Psychiatr Res* **44**, 808–816 (2010).
586. Murakami, S., Imbe, H., Morikawa, Y., Kubo, C. & Senba, E. Chronic stress, as well as acute stress, reduces BDNF mRNA expression in the rat hippocampus but less robustly. *Neuroscience Research* **53**, 129–139 (2005).
587. Taliaz, D. *et al.* Resilience to Chronic Stress Is Mediated by Hippocampal Brain-Derived Neurotrophic Factor. *J. Neurosci.* **31**, 4475–4483 (2011).
588. Wulsin, A. C., Herman, J. P. & Solomon, M. B. Mifepristone decreases depression-like behavior and modulates neuroendocrine and central hypothalamic-pituitary-adrenocortical axis responsiveness to stress. *Psychoneuroendocrinology* **35**, 1100–1112 (2010).
589. Mondelli, V. *et al.* Abnormal cortisol levels during the day and cortisol awakening response in first-episode psychosis: the role of stress and of antipsychotic treatment. *Schizophr. Res.* **116**, 234–242 (2010).
590. Groves, J. O. Is it time to reassess the BDNF hypothesis of depression? *Mol. Psychiatry* **12**, 1079–1088 (2007).
591. Egan, M. F. *et al.* The BDNF val66met polymorphism affects activity-dependent secretion of BDNF and human memory and hippocampal function. *Cell* **112**, 257–269 (2003).
592. Cao, B. *et al.* Reduced hippocampus volume and memory performance in bipolar disorder patients carrying the BDNF val66met met allele. *J Affect Disord* **198**, 198–205 (2016).
593. Chepenik, L. G. *et al.* Effects of the brain-derived neurotrophic growth factor val66met variation on hippocampus morphology in bipolar disorder. *Neuropsychopharmacology* **34**, 944–951 (2009).
594. Alfonso, J. *et al.* Regulation of hippocampal gene expression is conserved in two species subjected to different stressors and antidepressant treatments. *Biol. Psychiatry* **59**, 244–251 (2006).
595. Reagan, L. P. *et al.* Tianeptine increases brain-derived neurotrophic factor expression in the rat amygdala. *Eur. J. Pharmacol.* **565**, 68–75 (2007).

596. Je, H. S. *et al.* Role of pro-brain-derived neurotrophic factor (proBDNF) to mature BDNF conversion in activity-dependent competition at developing neuromuscular synapses. *Proc. Natl. Acad. Sci. U.S.A.* **109**, 15924–15929 (2012).
597. Carlino, D. *et al.* Low serum truncated-BDNF isoform correlates with higher cognitive impairment in schizophrenia. *J Psychiatr Res* **45**, 273–279 (2011).
598. Duman, R. S., Malberg, J., Nakagawa, S. & D'Sa, C. Neuronal plasticity and survival in mood disorders. *Biological Psychiatry* **48**, 732–739 (2000).
599. Katz, R. J., Roth, K. A. & Carroll, B. J. Acute and chronic stress effects on open field activity in the rat: implications for a model of depression. *Neurosci Biobehav Rev* **5**, 247–251 (1981).
600. Kennedy, C. L. M., Carter, S. D., Mifsud, K. R. & Reul, J. M. H. M. Unexpected effects of metyrapone on corticosteroid receptor interaction with the genome and subsequent gene transcription in the hippocampus of male rats. *J. Neuroendocrinol.* **32**, e12820 (2020).
601. Willner, P. Validity, reliability and utility of the chronic mild stress model of depression: a 10-year review and evaluation. *Psychopharmacology* **134**, 319–329 (1997).
602. Scott, L. V. & Dinan, T. G. Vasopressin and the regulation of hypothalamic-pituitary-adrenal axis function: Implications for the pathophysiology of depression. *Life Sciences* **62**, 1985–1998 (1998).
603. Chan, J. S. *et al.* Synergistical effects of ovine corticotropin-releasing factor (CRF) and arginine vasopressin (AVP) on the release of pro-opiomelanocortin (POMC) related peptides by pituitary adenoma of a patient with Nelson's syndrome in vitro. *Clin Invest Med* **7**, 205–208 (1984).
604. Castro, M. G. Effects of corticotrophin-releasing factor and arginine-vasopressin on proopiomelanocortin (POMC) mRNA levels, release and storage of adrenocorticotrophin from mouse anterior pituitary cells. *Comparative Biochemistry and Physiology Part A: Physiology* **104**, 105–112 (1993).
605. Jørgensen, H., Riis, M., Knigge, U., Kjær, A. & Warberg, J. Serotonin Receptors Involved in Vasopressin and Oxytocin Secretion. *Journal of Neuroendocrinology* **15**, 242–249 (2003).
606. Pérgola, P. E., Sved, A. F., Voogt, J. L. & Alper, R. H. Effect of Serotonin on Vasopressin Release: A Comparison to Corticosterone, Prolactin and Renin. *NEN* **57**, 550–558 (1993).
607. Cowley, M. A. *et al.* Leptin activates anorexigenic POMC neurons through a neural network in the arcuate nucleus. *Nature* **411**, 480–484 (2001).
608. Romanova, I. V. *et al.* The Leptin, Dopamine and Serotonin Receptors in Hypothalamic POMC-Neurons of Normal and Obese Rodents. *Neurochem Res* **43**, 821–837 (2018).
609. Jensen, J. B. *et al.* Acute and long-term treatments with the selective serotonin reuptake inhibitor citalopram modulate the HPA axis activity at different levels in male rats. *J. Neuroendocrinol.* **11**, 465–471 (1999).
610. Hesketh, S., Jessop, D. S., Hogg, S. & Harbuz, M. S. Differential actions of acute and chronic citalopram on the rodent hypothalamic–pituitary–adrenal axis response to acute restraint stress. *Journal of Endocrinology* **185**, 373–382 (2005).
611. Davis, J. N., Courtney, C. L., Superak, H. & Taylor, D. K. Behavioral, clinical and pathological effects of multiple daily intraperitoneal injections on female mice. *Lab Animal* **43**, 131–139 (2014).
612. Zennaro, M.-C. *et al.* Human Mineralocorticoid Receptor Genomic Structure and Identification of Expressed Isoforms. *J. Biol. Chem.* **270**, 21016–21020 (1995).
613. Arriza, J. L., Simerly, R. B., Swanson, L. W. & Evans, R. M. The neuronal mineralocorticoid eeceptor as a mediator of glucocorticoid response. *Neuron* **1**, 887–900 (1988).
614. Cerqueira, J. J., Mailliet, F., Almeida, O. F. X., Jay, T. M. & Sousa, N. The Prefrontal Cortex as a Key Target of the Maladaptive Response to Stress. *J. Neurosci.* **27**, 2781–2787 (2007).
615. Almeida, O. F. *et al.* Subtle shifts in the ratio between pro- and antiapoptotic molecules after activation of corticosteroid receptors decide neuronal fate. *FASEB J.* **14**, 779–790 (2000).
616. Crochemore, C. *et al.* Direct targeting of hippocampal neurons for apoptosis by glucocorticoids is reversible by mineralocorticoid receptor activation. *Mol. Psychiatry* **10**, 790–798 (2005).
617. Schwabe, L., Tegenthoff, M., Höffken, O. & Wolf, O. T. Mineralocorticoid receptor blockade prevents stress-induced modulation of multiple memory systems in the human brain. *Biol. Psychiatry* **74**, 801–808 (2013).
618. Schwabe, L., Höffken, O., Tegenthoff, M. & Wolf, O. T. Stress-induced enhancement of response inhibition depends on mineralocorticoid receptor activation. *Psychoneuroendocrinology* **38**, 2319–2326 (2013).
619. Munier, M. *et al.* Regulation of mineralocorticoid receptor expression during neuronal differentiation of murine embryonic stem cells. *Endocrinology* **151**, 2244–2254 (2010).
620. Vázquez, D. M. *et al.* Alpha, beta, and gamma mineralocorticoid receptor messenger ribonucleic acid splice variants: differential expression and rapid regulation in the developing hippocampus. *Endocrinology* **139**, 3165–3177 (1998).
621. Nishimura, M., Naito, S. & Yokoi, T. Tissue-specific mRNA Expression Profiles of Human Nuclear Receptor Subfamilies. *Drug Metabolism and Pharmacokinetics* **19**, 135–149 (2004).
622. Riester, A. *et al.* ACTH-Dependent Regulation of MicroRNA As Endogenous Modulators of Glucocorticoid Receptor Expression in the Adrenal Gland. *Endocrinology* **153**, 212–222 (2012).
623. Bamberger, C. M., Bamberger, A. M., Castro, M. de & Chrousos, G. P. Glucocorticoid receptor beta, a potential endogenous inhibitor of glucocorticoid action in humans. *J Clin Invest* **95**, 2435–2441 (1995).

624. Pujols, L. *et al.* Expression of glucocorticoid receptor α- and β-isoforms in human cells and tissues. *American Journal of Physiology - Cell Physiology* **283**, C1324–C1331 (2002).
625. Burnstein, K. L., Bellingham, D. L., Jewell, C. M., Powell-Oliver, F. E. & Cidlowski, J. A. Autoregulation of glucocorticoid receptor gene expression. *Steroids* **56**, 52–58 (1991).
626. Oakley, R. H., Jewell, C. M., Yudt, M. R., Bofetiado, D. M. & Cidlowski, J. A. The Dominant Negative Activity of the Human Glucocorticoid Receptor β Isoform SPECIFICITY AND MECHANISMS OF ACTION. *J. Biol. Chem.* **274**, 27857–27866 (1999).
627. Jacobsen, J. P. R. *et al.* Deficient serotonin neurotransmission and depression-like serotonin biomarker alterations in tryptophan hydroxylase 2 (Tph2) loss-of-function mice. *Molecular Psychiatry* **17**, 694–704 (2012).
628. Joels, M. & Kloet, E. de. Effects of glucocorticoids and norepinephrine on the excitability in the hippocampus. *Science* **245**, 1502–1505 (1989).
629. Kao, C.-Y., Stalla, G., Stalla, J., Wotjak, C. T. & Anderzhanova, E. Norepinephrine and corticosterone in the medial prefrontal cortex and hippocampus predict PTSD-like symptoms in mice. *European Journal of Neuroscience* **41**, 1139–1148 (2015).
630. Mitchell, J. B., Betito, K., Rowe, W., Boksa, P. & Meaney, M. J. Serotonergic regulation of type II corticosteroid receptor binding in hippocampal cell cultures: evidence for the importance of serotonin-induced changes in cAMP levels. *Neuroscience* **48**, 631–639 (1992).
631. Viau, V., Sharma, S., Plotsky, P. M. & Meaney, M. J. Increased plasma ACTH responses to stress in nonhandled compared with handled rats require basal levels of corticosterone and are associated with increased levels of ACTH secretagogues in the median eminence. *J. Neurosci.* **13**, 1097–1105 (1993).
632. Liu, D. *et al.* Maternal Care, Hippocampal Glucocorticoid Receptors, and Hypothalamic-Pituitary-Adrenal Responses to Stress. *Science* **277**, 1659–1662 (1997).
633. Liu, Caldji, Sharma, Plotsky, & Meaney. Influence of Neonatal Rearing Conditions on Stress-Induced Adrenocorticotropin Responses and Norepinepherine Release in the Hypothalamic Paraventricular Nucleus: Early life events, noradrenaline and HPA responses to stress. *Journal of Neuroendocrinology* **12**, 5–12 (2008).
634. Beis, D. PHENOTYPICAL ANALYSIS OF ANIMAL-MODELS WITH GENETIC CHANGES OF TRYPTOPHAN HYDROXYLASE 2 (TPH2) EXPRESSION. (Humboldt University Berlin, 2014).
635. Chung, K. & Deisseroth, K. CLARITY for mapping the nervous system. *Nat Meth* **10**, 508–513 (2013).
636. Bethea, C. L., Pecins-Thompson, M., Schutzer, W. E., Gundlah, C. & Lu, Z. N. Ovarian steroids and serotonin neural function. *Mol Neurobiol* **18**, 87–123 (1998).
637. Rubinow, D. R., Schmidt, P. J. & Roca, C. A. Estrogen–serotonin interactions: implications for affective regulation. *Biological Psychiatry* **44**, 839–850 (1998).
638. Hall, E. & Steiner, M. Serotonin and Female Psychopathology. *Womens Health (Lond Engl)* **9**, 85–97 (2013).
639. Goel, N. & Bale, T. L. Sex differences in the serotonergic influence on the hypothalamic-pituitary-adrenal stress axis. *Endocrinology* **151**, 1784–1794 (2010).
640. Pratelli, M. & Pasqualetti, M. Serotonergic neurotransmission manipulation for the understanding of brain development and function: Learning from Tph2 genetic models. *Biochimie* **161**, 3–14 (2019).
641. Heydendael, W. & Jacobson, L. Widespread hypothalamic–pituitary–adrenocortical axis-relevant and mood-relevant effects of chronic fluoxetine treatment on glucocorticoid receptor gene expression in mice. *European Journal of Neuroscience* **31**, 892–902 (2010).
642. Heydendael, W. & Jacobson, L. Glucocorticoid status affects antidepressant regulation of locus coeruleus tyrosine hydroxylase and dorsal raphé tryptophan hydroxylase gene expression. *Brain Res* **1288**, 69–78 (2009).
643. Marsden, H. M. & Bronson, F. H. THE SYNCHRONY OF OESTRUS IN MICE: RELATIVE ROLES OF THE MALE AND FEMALE ENVIRONMENTS. *Journal of Endocrinology* **32**, 313–319 (1965).
644. Szafarczyk, A., Malaval, F., Laurent, A., Gibaud, R. & Assenmacher, I. Further Evidence for a Central Stimulatory Action of Catecholamines on Adrenocorticotropin Release in the Rat. *Endocrinology* **121**, 883–892 (1987).
645. Soiza-Reilly, M., Goodfellow, N. M., Lambe, E. K. & Commons, K. G. Enhanced 5-HT1A receptor-dependent feedback control over dorsal raphe serotonin neurons in the SERT knockout mouse. *Neuropharmacology* **89**, 185–192 (2015).
646. Masand, P. S. Tolerability and adherence issues in antidepressant therapy. *Clin Ther* **25**, 2289–2304 (2003).
647. Ferguson, J. M. SSRI Antidepressant Medications: Adverse Effects and Tolerability. *Prim Care Companion J Clin Psychiatry* **3**, 22–27 (2001).
648. Li, B., Suemaru, K., Cui, R. & Araki, H. Repeated electroconvulsive stimuli have long-lasting effects on hippocampal BDNF and decrease immobility time in the rat forced swim test. *Life Sci.* **80**, 1539–1543 (2007).
649. Jorgensen, O. S. & Bolwig, T. G. Synaptic proteins after electroconvulsive stimulation. *Science* **205**, 705–707 (1979).
650. Bolwig, T. G. & Jørgensen, O. S. Synaptic proteins after electroconvulsive stimulation: reversibility and regional differences in the brain. *Acta Psychiatr Scand* **62**, 486–493 (1980).
651. Elfving, B. & Wegener, G. Electroconvulsive seizures stimulate the vegf pathway via mTORC1. *Synapse* **66**, 340–345 (2012).

652. Newton, S. S. *et al.* Gene profile of electroconvulsive seizures: induction of neurotrophic and angiogenic factors. *J. Neurosci.* **23**, 10841–10851 (2003).
653. Ploski, J. E., Newton, S. S. & Duman, R. S. Electroconvulsive seizure-induced gene expression profile of the hippocampus dentate gyrus granule cell layer. *J. Neurochem.* **99**, 1122–1132 (2006).
654. Polyakova, M. *et al.* Brain-Derived Neurotrophic Factor and Antidepressive Effect of Electroconvulsive Therapy: Systematic Review and Meta-Analyses of the Preclinical and Clinical Literature. *PLoS One* **10**, (2015).
655. Marano, C. M. *et al.* Increased plasma concentration of brain-derived neurotrophic factor with electroconvulsive therapy: a pilot study in patients with major depression. *J Clin Psychiatry* **68**, 512–517 (2007).
656. Alboni, S. *et al.* Hippocampus-related effects of fluoxetine treatment under stressful vs enriched conditions. *Mol. Psychiatry* **22**, 483 (2017).
657. Taliaz, D., Nagaraj, V., Haramati, S., Chen, A. & Zangen, A. Altered brain-derived neurotrophic factor expression in the ventral tegmental area, but not in the hippocampus, is essential for antidepressant-like effects of electroconvulsive therapy. *Biol. Psychiatry* **74**, 305–312 (2013).
658. Ryan, K. M., Dunne, R. & McLoughlin, D. M. BDNF plasma levels and genotype in depression and the response to electroconvulsive therapy. *Brain Stimul* **11**, 1123–1131 (2018).
659. Wennström, M., Hellsten, J., Ekstrand, J., Lindgren, H. & Tingström, A. Corticosterone-induced inhibition of gliogenesis in rat hippocampus is counteracted by electroconvulsive seizures. *Biol. Psychiatry* **59**, 178–186 (2006).
660. O'Donovan, S., Kennedy, M., Guinan, B., O'Mara, S. & McLoughlin, D. M. A comparison of brief pulse and ultrabrief pulse electroconvulsive stimulation on rodent brain and behaviour. *Prog. Neuropsychopharmacol. Biol. Psychiatry* **37**, 147–152 (2012).
661. Biedermann, S. V. *et al.* An elevated plus-maze in mixed reality for studying human anxiety-related behavior. *BMC Biol.* **15**, 125 (2017).
662. Haskett, R. F. Electroconvulsive therapy's mechanism of action: neuroendocrine hypotheses. *J ECT* **30**, 107–110 (2014).
663. Angoa-Pérez, M. *et al.* Genetic depletion of brain 5HT reveals a common molecular pathway mediating compulsivity and impulsivity. *Journal of Neurochemistry* **121**, 974–984 (2012).
664. Reimold, M. *et al.* Anxiety is associated with reduced central serotonin transporter availability in unmedicated patients with unipolar major depression: a [11 C]DASB PET study. *Molecular Psychiatry* **13**, 606–613 (2008).
665. Gaskill, B. N. *et al.* Impact of nesting material on mouse body temperature and physiology. *Physiol. Behav.* **110–111**, 87–95 (2013).
666. Ross, S., Nagy, Z. M., Kessler, C. & Scott, J. P. Effects of illumination on wall-leaving behavior and activity in three inbred mouse strains. *Journal of Comparative and Physiological Psychology* **62**, 338–340 (1966).
667. Kapogiannatou, A., Paronis, E., Paschidis, K., Polissidis, A. & Kostomitsopoulos, N. G. Effect of light colour temperature and intensity on the behaviour of male C57CL/6J mice. *Applied Animal Behaviour Science* **184**, 135–140 (2016).
668. Hoffman, G. E., Schrode, N., Flaherty, E. & Brennand, K. J. New considerations for hiPSC-based models of neuropsychiatric disorders. *Mol. Psychiatry* **24**, 49–66 (2019).
669. Angoa-Pérez, M. *et al.* Mice genetically depleted of brain serotonin do not display a depression-like behavioral phenotype. *ACS Chem Neurosci* **5**, 908–919 (2014).
670. Sachs, B. D. *et al.* The effects of congenital brain serotonin deficiency on responses to chronic fluoxetine. *Transl Psychiatry* **3**, e291 (2013).
671. Beaulieu, J.-M. *et al.* Role of GSK3 beta in behavioral abnormalities induced by serotonin deficiency. *Proc. Natl. Acad. Sci. U.S.A.* **105**, 1333–1338 (2008).

8 List of Tables

9 Table of Figures

10 Acknowledgments

Der größte Dank gilt PD Dr. Friederike Klempin, Dr. Sven Schmitt, Theresa Thuß und Birgit Herrmann, die mich in der Zeit des Schaffens unentwegt unterstützten und nie aufgaben.

Ein besonderer extra-Dank an Rike für ihre unermüdliche Betreuungsleistung. Ich wünsche Dir alles Gute und hoffe, dass Du baldigst in einer Professur zu sehen bist! Das Leben ist eine Kamera!

Ein großer Dank an Prof. Dr. Michael Bader, welcher mir Vertrauen entgegenbrachte und mich schützend in seine Arbeitsgruppe aufnahm. Er war mir damit oft ein gutes wissenschaftliches und auch menschliches Vorbild.

Dank geht an die Mitglieder meiner Promotionskommission: Prof. Dr. Rüdiger Krahe, Prof. Dr. Golo Kronenberg, Prof. Dr. Michael Bader, Prof. Dr. Thomas Sommer und Dr. Katharina Stumpenhorst, die trotz knappem Zeitbudgets meine wissenschaftliche Arbeit evaluierten .

Danke an Dr. Natascha Alenina, ohne sie ich nie in das tolle Labor gekommen wäre, und das Bereitstellen transgener Tiere für meine Versuche.

Um niemanden zu vernachlässigen, und da die Liste aller relevanten Personen unseres Labors den Rahmen sprengen würde, möchte ich dem Kollektiv des Bader–Geschwaders von 2013 bis 2020 herzlichst für die schöne und liebgewonnene Zeit danken!

Danke an meine *undergrads* und Bachelor-Studenten Samuel Chen, Varvara Karpenko und Erika Koch, die mein oft populär-wissenschaftliches Gerede ertrugen und auch nur teils meine Autorität in Frage stellten.

Dank an Claus Peter Nowak vom Institutes für Epidemiologie in Berlin, welcher sich die Zeit nahm, mir den Hintergrund der komplexen Welt der Statistik näher zu bringen.

Ohne die Finanzierungsquellen des Berliner Instituts für Gesundheitsforschung (BIH), dem Deutschen Akademischen Austauschdienst (DAAD), der Helmholtzgemeintschaft und ihrer Helmholtz Graduate School/Research School, sowie dem Institut für Mikrobiologie der FAU in Erlangen, wäre diese Arbeit, Konferenzreisen, Weiterbildungen im Rahmen des BIH PhD Grant Projects nicht durchführbar gewesen. Danke für das entgegengebrachte Vertrauen.

Danke an die Helmholtz Juniors und Doktorandenvertretungen, mit denen ich zusammen arbeiten durfte, um die prekären Vertragskonditionen des wissenschaftlichen Mittelbaus mit etwas mehr Perspektive und Gleichberechtigung versehen zu können. Auch hierfür Dank an den Präsidenten der Helmholtz Gemeinschaft Prof. Dr. Ottmar Wiestler, welcher sich für die Belange Junger Nachwuchswissenschaftler, trotz vollen Zeitplans engagierte

Ein Dankeschön an Annette, Michaela und Tina aus dem PhD Office für ihre Zusammenarbeit im Rahmen der Helmholtz-Juniors, PhD-Reps und ihre Unermüdlichkeit, die Stimmen der PhD Studenten hörbar zu machen. Macht weiter so!

Besonderer Dank geht auch an Dr. Sandra Krull aus dem Postdoc-office, für ermöglichte Chancen, Coaching und als exzellentes Beispiel für eine sehr gute Teamführung. Ich habe in der kurzen Zeit bei euch im Team unendlich viel gelernt.

Großen Dank an Yvonne Blieske und Marion Rädisch für die Verdeutlichung der Notwendigkeit einer essentiellen psychotherapeutischen Behandlung bei depressiven Verhalten und des Stellenwertes einer eigenen Identität.

Hochachtung geht auch an meine Freunde und Familie, welche es mit mir in dieser Zeit aushielten, besonders: Alisa, Büchi Eni, David, Heike, Lars, Matze, Nika, Pietzke, Sebi, Tobi, Uwe und natürlich Mama, Papa und JuliaP

Zu guter Letzt und vielleicht gar das wichtigste - „Voice for the Voiceless“ – großer Dank an alle welche tagtäglich den Wissenschaftsbetrieb und Infrastruktur aufrechterhalten, aber selten ein Danke erhalten. An die Damen und Herren :

- der BVG (nicht der S-Bahn) für ihre Beständigkeit des täglichen oft reibungsfreien Transports;

- der Mensa des Campus Buch fürs Nähren, der zentralen Dienste am Institut für ein reibungsarmes System;

- von Sci-Hub und den Open-Science Bewegungen für den Erhalt des gemeinschaftlichen wissenschaftlichen Gedankens;

- des Resourcenmanagements (BSR, Wasserbetriebe, Umweltbehörden etc.), ohne die der Klimawandel schon abgeschlossen wäre;

- der Tierpflege und des Tierschutzes, die dafür sorgen, dass auch die Würde der Tiere für unantastbar gilt

- den zahlreichen Musiker und Bands, welche mir in dieser Zeit des Schaffens als Muse dienten \m/